Polarized Light Vision in Crabs

SAMUEL PHILIP SMITHERS

School of Biological Sciences
University of Bristol

A dissertation submitted to the University of Bristol in accordance with the requirements of the Degree of Philosophy in the Faculty of Life Sciences.

June 2019

Word count: ~ 45,000

Abstract

Many animals are sensitive to the polarization of light and use this visual information for a variety of behavioural tasks such as navigation, communication and habitat localisation. One group in particular, decapod crustaceans, are sensitive to the polarization of light across their whole visual field and use this information for object-based visually guided behaviours.

The studies within this thesis investigated how crabs use polarization information, in combination with intensity, to detect objects and control visually guided behaviours. This thesis had three main aims. The first was to establish how polarization and intensity information are processed within the visual system of fiddler crabs to enhance object detection. Through a series of behavioural experiments, using a novel type of visual display technology that allowed polarization and intensity properties of visual stimuli to be adjusted independently and simultaneously, it was discovered that for a loom detection task, crabs process polarization and intensity information independently and in parallel. The second aim was to determine whether null points of polarization discrimination, which are inherent within the crab's visual system, affect the ability of fiddler crabs to use their polarization vision to detect targets viewed against the sky. The findings of this study suggest that the null points did effect the detectability of polarization contrasts produced by targets viewed against the sky. Finally, a study was conducted to test whether fiddler crabs can detect second-order motion, which is defined by higher-order image properties such as flicker. It was discovered that fiddler crabs are able to detect second-order motion in both intensity and polarization. It is suggested that the presence of this motion may enhance the detection of certain predators. In addition to these three main studies, a fourth study attempted to test whether contrast sensitivity in dark adapted ghost crabs was affected by restrictions, imposed by circadian cycle, that limit the maximum light sensitivity achievable during the day. This caveat study found circadian cycle does not have a negative effect on the ability of dark adapted crabs to detect intensity and polarization contrasts during the day.

Overall, the findings from this thesis shed light on the various ways that polarization vision can enhance object detection by providing a greater range of detectable contrast information for the receiver.

Dedication

*99% of this thesis is dedicated to my parents, for their love, sacrifice and unwavering belief in me. The remaining 1% is dedicated to the headmistress who once told my parents I was "ineducable".**

*Yes, "ineducable" is a real word.

Acknowledgments

I wish to start by thanking my supervisors Nick Roberts, Martin How and Andy Radford for their guidance, imparted knowledge, and enthusiasm throughout my PhD. I am especially grateful to Nick for sharing his extensive knowledge of physics and allowing me the independence and freedom to take my PhD in my own direction. I may have made the odd mistake as a result but I've learned far more from my errors than I have my successes. I must also express my sincerest gratitude to Martin for helping me find my feet at the very start of my PhD, for continuous guidance throughout, and for the immensely helpful discussions in the run up to submission.

Particular appreciation goes to Nick Scott-Samuel whose expertise and guidance helped make the study reported in chapter 4 a success. I am also extremely grateful to Megan Porter at the University of Hawaii for hosting me in her lab while I conducted the experiments for chapter 5 (and what turned out to be the preliminary experiments for chapter 3). Things might not have worked out the way I had planned but the time spent in your lab was one of the most worthwhile (and memorable) periods of my PhD. My thanks also go to the rest of the Porter Lab and a special mention to Marisa McDonald, Rachel Sommer and Jess Schaefer for kindly allowing a "sassy British man" into their home. You, and everyone I had the privilege of meeting, made me feel so welcome and at home during my stay on the most isolated archipelago on Earth.

To José Ignacio Navas Triano (Tato) and IFAPA, Centro de Agua del Pino, Consejería de Agricultura, Pesca y Desarrollo Rural, I send my gratitude for your help and support whilst at my field site in Spain. I also thank my field assistants Seb Lloyd, Maisie Brett, Ally Irwin and fellow PhD student, Emelie Brodrick, for the valuable help with "crabmin", both in the "lab" and on the mudflats.

To the Ecology of Vision lab, past and present, it has been a pleasure and privilege to work alongside you, namely David Wilby, Emelie Brodrick, Ilse Daly, Kate Feller, Alex Tibbs, Rochelle Meah, Ally Irwin, Vun Wen Jie (VJ), Mike Bok and Shelby Temple. I thank you for your advice, support, tolerance and friendship over the course of my PhD.

These acknowledgements would not be complete without expressing appreciation to my friends, both here in Bristol and across the world, particularly Nathan Masters, Sarah Richdon, Peter Rosso, Gerardo Arias-Robledo, Amy Ockenden, Sara Mynott, Jared Wilson-Aggarwal, Jess Schaefer, Stevie Kennedy-Gold (I did have this) and members, past and present, of the University of Bristol Expedition Society (UBES), for support, laughter, adventures and above all helping me maintain some shred of sanity.

A disproportionate amount of gratitude must be expressed to Tom Timberlake and Sam Huguet for sharing with me the highs and lows of the last four years. Your friendship has greatly enriched my life and I have no doubt it will continue to do so for many years to come.

Additional thanks go to VJ, Tom, Kate, Maisie, Stevie and Sam for the fantastic paintings, drawing, clay sculpture and wood engraving that decorate the title pages for each chapter.

Finally, to my brother and sister, and most importantly to my parents. My life could have taken a very different turn if it were not for your love, encouragement and support. Your struggles, hard work, and unwavering belief are paying off. Thank you so much.

Author’s Declaration

I declare that the work in this dissertation was carried out in accordance with the requirements of the University's Regulations and Code of Practice for Research Degree Programmes and that it has not been submitted for any other academic award. Except where indicated by specific reference in the text, the work is the candidate's own work. Work done in collaboration with, or with the assistance of, others, is indicated as such. Any views expressed in the dissertation are those of the author.

SIGNED: ..... DATE:.....

Contents

List of Figures

List of Tables

List of Abbreviations

Below is a list of the most common abbreviations used throughout the thesis. This list is not exhaustive, but all abbreviations and symbols are defined within the text.

AoP	angle of polarization
BLG2	bistratified lobula giant type 2
DoLP	degree of linear polarization
DoP	degree of polarization
DRA	dorsal rim area
ERG	electroretinogram
IP screen/model	intensity-polarization screen/model
IQR	interquartile range
LCD	liquid crystal display
LRT	likelihood ratio test
M2	monopolar cell 2
M3	monopolar cell 3
M4	monopolar cell 4
N	sample size
PD	polarization distance
PVA-LCD	patterned vertical alignment liquid crystal display
RGB	red, green and blue colour space
SD	standard deviation; $\sqrt{\frac{\sum(x-\overline{x})^2}{sample\ size-1}}$, where x is each value in the data set and $\overline{x}$ is the mean
SEM	standard error of the mean; $\frac{standard\ deviation}{\sqrt{sample\ size}}$
S_0	first Stokes parameter (intensity)
S_1	second Stokes parameter (linear polarization, vertical vs. horizontal)
S_2	third Stokes parameter (linear polarization, +45° vs. -45°)
UV	ultraviolet light
WC	Weber contrast

It gradually became increasingly common throughout my PhD to catch myself thinking,

"What I do isn't normal"

Chapter 1

Introduction

The fiddler crab *Afruca tangeri*
Clay sculpture by Vun Wen Jie

"Imagine the vast unseen world that must be inches from our faces and minds, hidden until one of us learns to look in just the right way."

Sönke Johnsen- The Optics of Life (2012)

The polarization of light provides a valuable source of information that many animals use for tasks such as habitat localisation, navigation, communication and contrast enhancement (Horváth, 2014). In recent years, advancements in technology and experimental techniques have led to numerous breakthroughs in our understanding of how animals detect and use the polarization of light for a number of different visually guided behaviours. This thesis focuses on one particular group of decapod crustaceans, crabs. Before focusing on this group however, it is necessary to first provide a general background to the topic of polarization vision. This introduction will begin by defining what polarized light is and how it is produced in nature, before providing a brief overview of the various different functions of polarization vision. The second half of the introduction provides a detailed description of the morphology of the compound eye of crabs and explains the foundations of their polarization sensitivity. Lastly, this introduction will introduce the reader to fiddler crabs, which form the focus of most of this thesis, and ghost crabs, before finally providing a brief overview of each chapter.

1.1 Background

The term light generally refers to the region of the electromagnetic spectrum between 300 - 700 nm that encompasses the ultraviolet (UV) range (300 - 400 nm) and human-visible range (400 - 700 nm) (Johnsen, 2012). Light consists of an oscillating electric and magnetic field (though only the electric field is important for biological systems and will be considered here) traveling through space as a transverse wave, i.e. it oscillates at right angles to the direction of travel (Johnsen, 2012; Foster et al., 2018). It can also be considered to act like a particle as a beam of light consists of discrete quantised packets of energy called photons (Johnsen, 2012; Foster et al., 2018). A beam of light is defined by three main properties: intensity, which is the number of photons or amplitude of the waves, wavelength (commonly referred to as colour), which is related the frequency and the energy of the light, and polarization, which describes how the light wave moves through space.

A great number of animal species are sensitive to light between 300 - 700 nm. In its simplest form an eye is sensitive to changes in the intensity of light. If an animal is able to use the detection of light to form an image then its light sensitivity can be called vision (Nilsson, 2009; Land & Nilsson, 2012). Many animals, including humans, are able to distinguish between different wavelengths of light and this ability is called colour vision. Although it is (almost) invisible to humans, the exception being the phenomenon known as Haidinger's brushes (von Haidinger, 1844; Temple et al., 2015), many animals are sensitive to the third property of light, polarization. It is these animals that form the focus of this thesis.

1.1.1 What is the polarization of light?

The polarization of light can be described by three properties: the angle of polarization, degree of polarization, and ellipticity. The angle of polarization (AoP) is the predominant axis of the

distribution of the waves from a source of light (Figure 1.1a) (Foster et al., 2018). The AoP can vary between 0º and 180º. The degree of polarization (DoP) (also referred to as the percentage polarization) is the ratio of the mean intensity of the polarized portion of the beam to its total (mean) intensity (Foster et al., 2018). The DoP may be considered a measure of the proportion (or percentage) of light waves within a beam that are oscillating along the same predominant axis (Figure 1.1b). The DoP is a value between 0 and 1 (or 0% to 100%). Unpolarized light, which is composed of multiple waves with a uniform distribution, has a DoP value of 0 while fully linearly polarized light, in which all waves are oscillating in the same plane, has a DoP of 1.

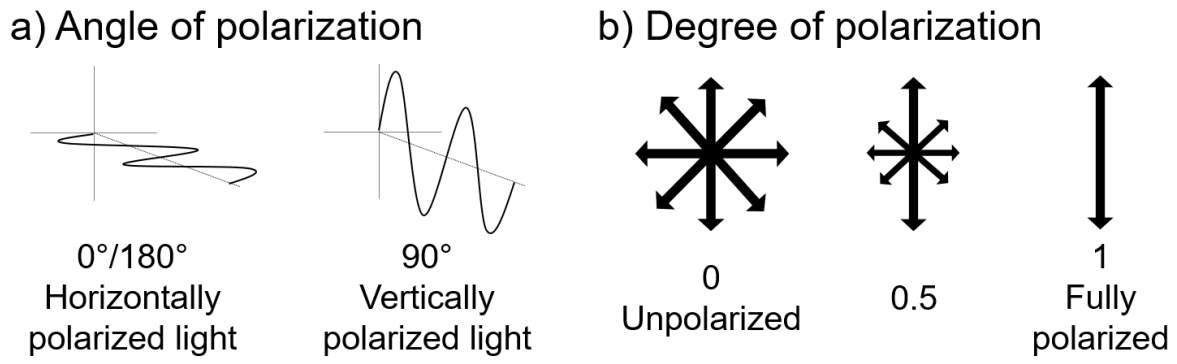

Figure 1.1: Schematic demonstrating the concept of the angle of polarization (AoP) and the degree of polarization (DoP). **a)** Example of linearly polarized light oscillating in the horizontal plane (left) or vertical plane (right). **b)** Depiction of the DoP. Each arrow represents the AoP of a group of transverse waves coming out of the page. The length and thickness of the arrow represents the number of waves (or photons) oscillating in the same plane. Light is unpolarized if an equal number of waves are oscillating uniformly throughout the full 180° range (left; DoP = 0). If a higher proportion of waves are oscillating in a single plane than any other orientation then the light is said to be partially polarized. In the example here half of the waves are oscillating in a single plane while the other half are oscillating uniformly throughout the rest of the 180° range (middle; DoP = 0.5). If all of the waves are oscillating in a single plane the light is fully polarized (right; DoP = 1).

Ellipticity is a more complex property of polarization. An elliptically polarized wave can be thought of as consisting of two linearly polarized waves with perpendicular electric fields which are out of phase with each other. The ellipticity of a beam of light is therefore a measure of the phase relationship and the relative amplitudes of these two perpendicular components

(Figure 1.2 and Figure 1.3) (Johnsen, 2012; Foster et al., 2018). The axis of the wave with highest amplitude is referred to as the major axis while the perpendicular axis is the minor axis. The major axis of the ellipse defines the AoP. Linear and circular polarization may be considered special cases of elliptically polarized light. For linearly polarized light the ellipse collapses and the wave oscillates only along the major axis. Alternatively linearly polarized light may be thought of as oscillating at 45^{o} to two in-phase components with the same amplitude (as is the case in Figure 1.3) (Johnsen, 2012; Foster et al., 2018). For circularly polarized light, the two perpendicular components have the same amplitude but are out of phase by one-quarter of a wavelength (Figure 1.2c) so when plotted the distribution of the resultant electric field of the light beam maps out as a circle (Figure 1.3). Because the electric field can rotate clockwise or anti-clockwise, circularly and elliptically polarized light exhibit chirality or handedness (Johnsen, 2012; Foster et al., 2018). Elliptical polarization is, however, rare in nature and does not affect how light is detected by most polarization sensitive animals (with the notable exception of some species of mantis shrimp that produce and are sensitive to circularly polarized light) (Chiou et al., 2008a; Roberts et al., 2009; Gagnon et al., 2015; Templin et al., 2017). To most polarization sensitive animals circularly polarized light appears the same as unpolarized light (How & Marshall, 2014). This is encapsulated by the measurement of the degree of linear polarization (DoLP) which disregards the elliptical component. Therefore, the only properties of polarization that are relevant to the majority of polarization sensitive animals are the AoP and DoLP.

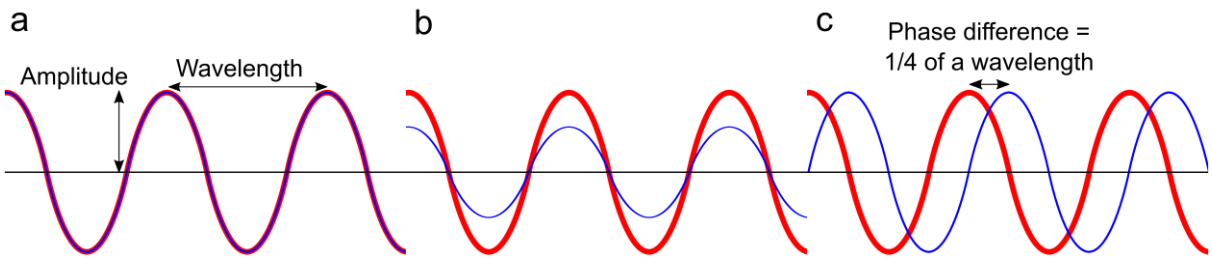

Figure 1.2: Wave amplitude and phase. **a)** The red and blue waves are in phase and both have the same amplitude. **b)** The red and blue waves are in phase but blue has a lower amplitude than red. **c)** The red and blue waves both have the same amplitude but are out of phase by one quarter of a wavelength.

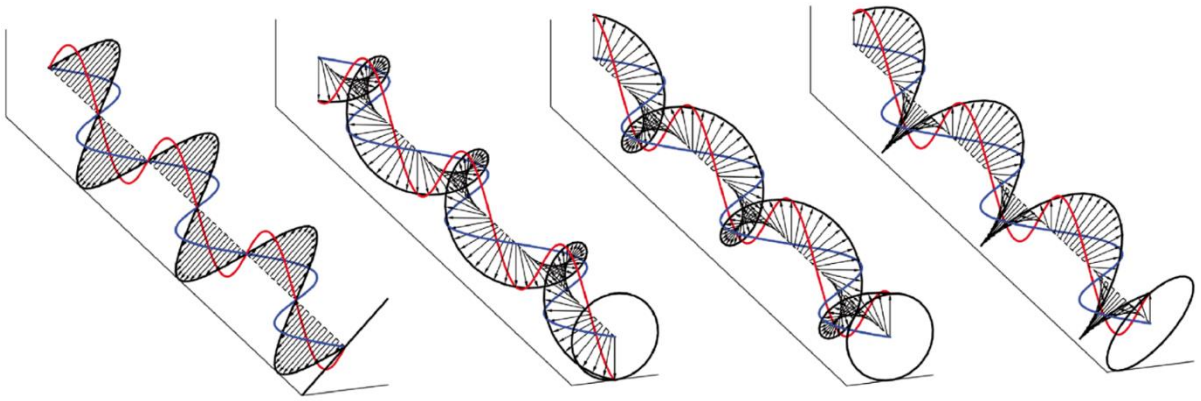

Figure 1.3: Visualisation of circularly and elliptically polarized light. Linearly, circularly and elliptically polarized light can be thought of as being made up of two perpendicular components (red and blue). The ellipticity of a beam of light is dictated by the relative phase (distance between peaks) between these two components. In linearly polarized light the phase difference is zero (or an integer multiple of a half wavelength) (left). In left-handed (left-centre) and right-handed (right-centre) circularly polarized light the phase difference is a quarter of a wavelength. A phase difference anywhere between 0 and a quarter of a wavelength results in elliptically polarized light (right). In these example cases, the amplitudes of the two components' are identical. Figure from Foster et al. (2018).

1.1.2 Sources of polarization in nature

There are two main non-biological mechanisms that produce polarized light in nature. The first is Rayleigh scattering; this is when unpolarized light is scattered by sub-wavelength particles (i.e. particles that are smaller than the wavelength of light) (Rayleigh, 1899). The second is specular reflection of unpolarized light off dielectric surfaces such as water (Johnsen, 2012).

Scattering

Light from the sun is unpolarized, but as it travels through Earth's atmosphere it becomes partially polarized, primarily as a result of Rayleigh scattering (the same phenomenon that makes the sky blue) (Rayleigh, 1899; Coulson, 1988) (Figure 1.4a). Rayleigh scattering occurs when light encounters particles that are smaller than its wavelength (Rayleigh, 1899). The AoP of the scattered light is always perpendicular to the initial path (Strutt, 1871; Coulson, 1988) and this means the AoP of light from an area of clear sky is perpendicular to a line between the sun and that area. The polarization pattern of the sky therefore appears as concentric circles around the sun (Figure 1.4b) (Coulson, 1988). The DoP is highest in a band 90º to the azimuth of the sun (Coulson, 1988; Cronin et al., 2006; Cronin & Marshall, 2011). At sunrise and sunset the maximum DoP therefore occurs in a band that appears directly overhead spanning from north to south. On a clear day the maximum DoP tends to be between 0.6 - 0.75, but it can occasionally get higher than this on very clear days (Brines & Gould, 1982; Horváth & Wehner, 1999; Cronin et al., 2006). While on clear days, Rayleigh scattering closely describes the celestial polarization pattern (Suhai & Horváth, 2004), Rayleigh single scattering does not explain the existence of the four unpolarized points (neutral points) that appear above and below the sun and anti-sun (Gál et al., 2001a; Horváth et al., 2002; Wang et al., 2016). These neutral points are considered to be polarization singularities (Berry et al., 2004), and although interesting, these neutral points are not generally thought to be biologically significant (Cronin & Marshall, 2011). The sun is not the only celestial body that produces a polarization pattern around it. Although it is at least a million times dimmer than during the day, a similar polarization pattern exists on moonlit nights as during the day (Gál et al., 2001b).

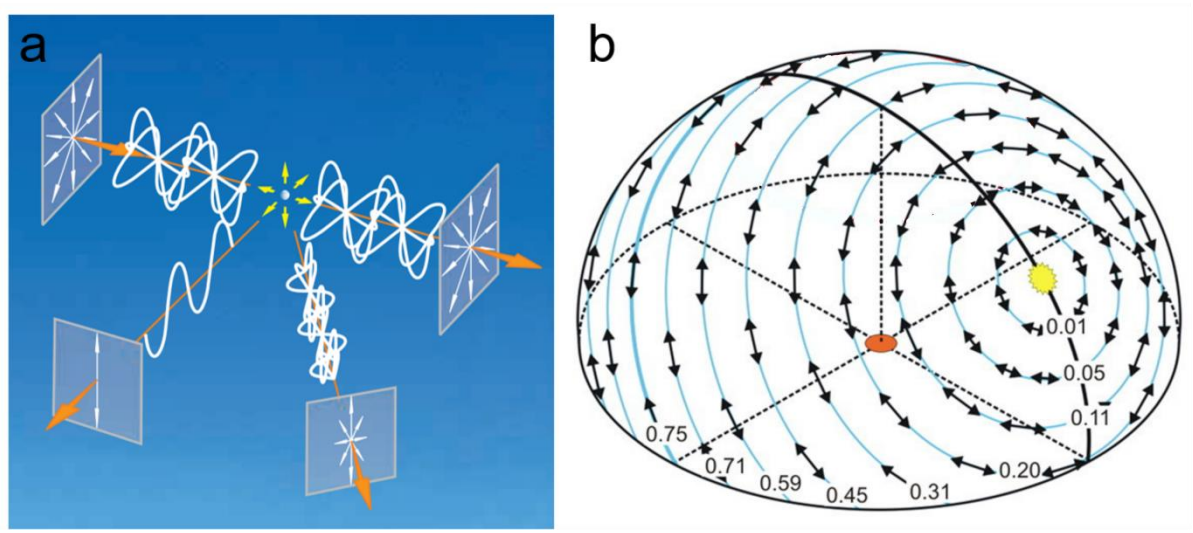

Figure 1.4: The polarization pattern of the sky produced by Rayleigh scattering. **a)** As unpolarized light from the sun (upper left panel) travels through the atmosphere it is scattered by molecules of oxygen and nitrogen. The DoP depends on the scattering angle with the highest DoP being when the scattering angle is 90° to the initial path (lower left panel) while light scattered at other angles will be less polarized (lower right panel). Light that reaches an observer without being scattered remains unpolarized (upper left panel). **b)** The polarization pattern of the sky created by Rayleigh single scattering. The AoP (indicated by the arrows) is seen from the ground as concentric circles around the sun. The values on the blue iso lines indicate DoP. The highest DoP occurs in a band 90° to the azimuth of the sun. (a) is adapted from Wehner (2001) and (b) is adapted from Pfeiffer et al. (2011).

Within aquatic environments the scattering of light within the water column is the main source of polarization (Wehner, 2001; Cronin & Marshall, 2011). The exception to this is Snell's window through which the main source is the polarization pattern of the sky (Sabbah & Shashar, 2007). Snell's window is a phenomenon that occurs at the water's surface where light from the entire hemisphere of the sky is refracted into a 96° window directly above an observer (Johnsen, 2012). Outside Snell's window, but still near the surface, the underwater polarization pattern remains highly dependent on the position of the sun (Cronin & Shashar, 2001; Sabbah & Shashar, 2007; Cronin & Marshall, 2011). In clear waters, the sun's position has been observed to influence the polarization field as deep as 200 m (Waterman, 1955, 2006; Powell et al., 2018). The underwater polarization pattern near the surface therefore varies with the time of day, season and geographical location (Waterman, 1954, 1955, 2006; Cronin & Shashar, 2001; Sabbah & Shashar, 2007; Powell et al., 2018). Throughout most of the day however the

AoP in habitats such as reefs is, on average, horizontal and only departs from this at dawn and dusk (Shashar et al., 2004). As you move into deeper water the influence of the sun's position on the underwater polarization field is reduced due to continuous scattering and absorption of light with a path orientated away from the zenith. Consequently, the polarization pattern is relatively stable throughout most of the ocean's depths penetrable by sunlight, and certainly below 200 m, with the AoP within a few degrees of horizontal (Wehner, 2001; Cronin & Marshall, 2011).

Specular reflection

The source of polarization that will probably be most familiar to humans is specular reflection. When unpolarized light is reflected from flat, or relatively flat, dielectric surfaces such as water it is partially linearly polarized with the AoP being parallel to the reflecting surface (Wehner, 2001; Johnsen, 2012; Horváth, 2014). A good example of this polarized light is the glare reflected from water and other flat surfaces such as roads and mudflats (Figure 1.5). Because the glare from these surfaces is horizontally polarized, humans use sunglasses containing a polarization filter to block out that glare. The DoP of the reflected light depends on the angle of incidence, with the maximum DoP being when the incident light is at Brewster's angle. Brewster's angle depends on the refractive index either side of an interface and for the water-air interface is 53° (Wehner, 2001; Johnsen, 2012).

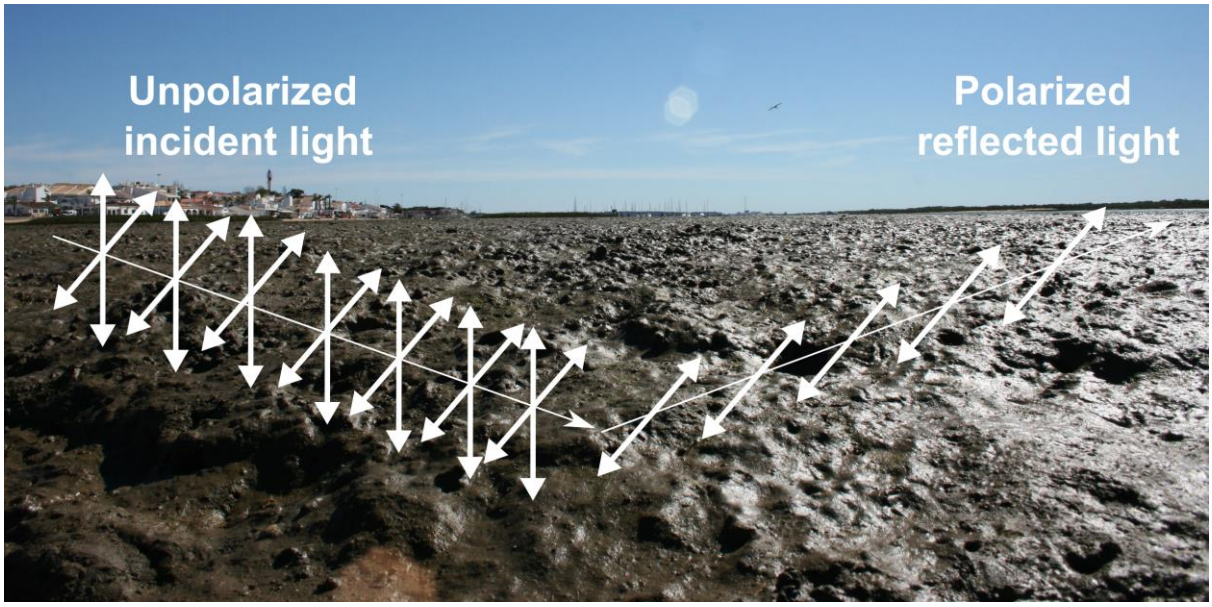

Figure 1.5: Simplified illustration of unpolarized incident light being reflected off a flat, non-metallic surface, such as a mudflat. The AoP of the reflected light is parallel to the surface.

1.2 Functions of polarization cues and signals

1.2.1 Habitat localisation

Many insects, including water bugs, dragonflies, and mayflies, that live and/or breed in and around water are attracted to the horizontally polarized light (often in the shorter wavelengths) that is reflected from the surface of ponds, lakes and other water bodies (Schwind, 1984; Kriska et al., 1998; Wildermuth, 1998; Egri et al., 2012). This phenomenon, often termed polarotaxis, is the reason why some water seeking species are attracted to man-made surfaces such as tarmac roads that reflect polarized light and are consequently mistaken for bodies of water (Kriska et al., 1998). Another example of the use of polarization sensitivity for habitat localisation is shore flight in *Daphnia*. Species such as *Daphnia pulex* consistently swim towards the area of water with the highest DoP (providing the AoP is horizontal) as this is indicative of deeper water and helps the animals avoid the higher predation risk associated with shallow, shoreline waters (Schwind, 1999). A particularly intriguing example of using polarization for habitat localisation has been demonstrated in the swallowtail butterfly, *Papilio*

aegeus. Kelber, (1999) demonstrated that *P. aegeus* detects polarization as 'false colours'. While this may seem problematic female *Papilio* use polarization, in combination with colour, to find suitable sites to lay their eggs. Behavioural experiments found that females looking for an oviposition site are attracted to green, horizontally polarized light; unsurprisingly this coincides with the fact that the safest place to lay their eggs, and thus the females preferred substrate, is under green horizontal leaves (Kelber, 1999; Kelber et al., 2001).

1.2.2 Spatial orientation

Ever since von Frisch (1949) first discovered that bees obtain compass cues from the polarization pattern of the sky, biologists have been fascinated by how animals use the celestial polarization pattern for navigation and orientation. Insects provide perhaps the most numerous and well-studied examples of the use of polarized light for navigation (reviewed by Waterman (1981), Wehner (2001, 2003), Hardie (2012), Dacke & el Jundi (2018) and Warren et al. (2019)). For instance, bees, crickets, locusts, desert ants and migrating butterflies are well known for their ability to navigate using the polarization pattern of the sky as a compass cue (von Frisch, 1949; Duelli & Wehner, 1973; Fent, 1986; Horváth & Wehner, 1999; Wehner, 2003; Reppert et al., 2004; Wehner & Müller, 2006; Henze & Labhart, 2007; Sakura et al., 2008, 2012; Evangelista et al., 2014). Spiders have also been shown to use polarization cues for navigation (Dacke et al., 1999, 2001; Ortega-Escobar, 2017). Among insects the polarization pattern of the sky is detected by a specialised region of the eye called the dorsal rim area (DRA) which looks up at the sky. The polarization sensitive photoreceptors in different regions of the DRA are aligned in such a way that they match the polarization pattern of the sky, thus the DRA functions as a matched filter for detecting the AoP of the sky's polarization pattern (Wehner, 1987, 1989; Bech et al., 2014). In a number of species

polarization information is often integrated with other celestial cues such as the spectral and intensity gradient of the sky (el Jundi et al., 2014a; Lebhardt & Ronacher, 2014)

One system in which the use of polarization cues for navigation has been particularly well studied is dung beetles. When a dung beetle finds a fresh pile of animal dropping it forms a ball of dung. Once completed, the beetle rolls its dung ball away in a random direction as quickly as possible to avoid competition from conspecifics and heterospecifics at the dung pile. The beetle utilises a variety of different celestial cues, such as the position of the sun (or moon) as well as the intensity and spectral gradient of the sky, in addition to the polarization pattern (Dacke et al., 2003a,b; el Jundi et al., 2014b; Dacke & el Jundi, 2018). Before starting their journey away from the dung pile, dung beetles perform a 'dance' atop their ball during which they take a snapshot of the visual cues in the sky; this mental snapshot acts as a template against which they compare and match their current view of the sky as they travel (Baird et al., 2012; el Jundi et al., 2016). This simple, but highly efficient, form of orientation is not limited to diurnal species. The crepuscular and nocturnal dung beetles *Scarabaeus zambesianus* and *Scarabaeus satyrus* respectively have been shown to orientate using the polarization pattern created by moonlight (Dacke et al., 2003a,b, 2011; el Jundi et al., 2015). Moreover, under a crescent moon, navigational accuracy exhibited by *S. satyrus* is equal to that measured for diurnal species that orient under the 100 million times brighter polarization pattern formed around the sun (Dacke et al., 2011). Nocturnal species have also been shown to use the Milky Way for navigation (Dacke et al., 2013). In recent years, several studies have investigated how diurnal and nocturnal dung beetles use and integrate the various different celestial cues. Experiments in which the different celestial cues were made to conflict with one another found that in diurnal species the polarization pattern is hierarchically subordinate to the position of the sun; suggesting that polarization cues, most likely in conjunction with the sky's intensity

gradient, function as a backup for when the sun is not visible (el Jundi et al., 2014b). Interestingly, the hierarchy of cues differs between diurnal and nocturnal species depending on the time of day (el Jundi et al., 2015). When the diurnal dung beetle *Scarabaeus lamarcki* and the nocturnal *S. satyrus* were tested during the day both species used the sun as their primary orientation cue. However, when they were tested at night, *S. lamarcki* preferentially used the moon (which is the dominant celestial body on moonlit nights) to orientate, while *S. satyrus* switched to using the lunar polarization pattern (el Jundi et al., 2015). The authors suggest that *S. satyrus* likely evolved to use the polarization pattern as their primary cue at night because it should be more reliable at low light intensities than the moon, which would appear as nothing more than a dimly illuminated disk, assuming of course it is not blocked by clouds. Indeed, under a crescent moon *S. satyrus* is able to consistently roll its ball in a straight line, even when the moon is obscured by clouds (el Jundi et al., 2015). More recently, the polarization pattern of the sky has been found to be the dominant orientation cue used by the forest living dung beetle *Sisyphus fasciculatus* (Khaldy et al., 2019). This was attributed to the fact that wide-field celestial cues are more reliable in cluttered environments such as forests (Khaldy et al., 2019).

Honey bees (*Apis mellifera*) arguably provide one of the most fascinating systems to study the use of polarization cues for navigation as they are not only capable of navigating purely using the polarization pattern of the sky but also communicate this information to other bees within the hive through the 'waggle dance' (Evangelista et al., 2014). Evangelista et al. (2014) trained honey bees to fly to a food source positioned at the end of a tunnel. In two of the conditions the tunnel was illuminated by light that was polarized either perpendicular or parallel to the axis of the tunnel, and in a third condition half of the tunnel was polarized perpendicular to its axis while the other half had parallel illumination. In each condition bees used a different dance

to communicate the direction of the food course to other bees within the hive, and in each case the direction and movements of the dance corresponded to the polarization information they had acquired whilst flying through the tunnel (Evangelista et al., 2014).

Compared to invertebrates, very little is known about the ability of vertebrates to use polarization as a source of information and the little that is known remains reasonably contentious, not least because of the uncertainties surrounding the mechanism of polarization sensitivity in vertebrates (Cameron & Pugh, 1991; Roberts et al., 2004; Roberts & Needham, 2007). Nonetheless, the topic has attracted some attention over the years. Migratory salmonids, for instance, are capable of orientating to a polarized light field (Hawryshyn & Bolger, 1990; Parkyn et al., 2003; Sabbah et al., 2013). Parkyn et al. (2003) used operant conditioning to train juvenile salmonids, rainbow trout (*Oncorhynchus mykiss*), steelhead (anadromous *O. mykiss*), and brook char (*Salvelinus fontinalis*), to orient relative to the AoP of a polarized light field under laboratory conditions. They found that when trained and untrained fishes were tested in a circular tank the trained fish orientated relative to the polarization field while the untrained fishes displayed no directional tendency (Parkyn et al., 2003). However, the ability of the fish to orientate to the polarized-light field was drastically reduced when the DoP was below 0.75 (Hawryshyn & Bolger, 1990; Parkyn et al., 2003). This raises questions regarding whether or not such orientation behaviour would be plausible under natural conditions, particularly given that navigation using the polarization field of the sky would be restricted to Snell's window (Shashar et al., 2004, 2011). In order to address this question, Parkyn et al. (2003) went on to test the fish outdoors under natural skylight and found rainbow trout trained under laboratory conditions showed very robust orientation behaviour under natural cues (Parkyn et al., 2003). These tests were conducted just before sunset when the DoP of the sky directly overhead is highest, thus it remains to be shown whether or not these fish can navigate using the

polarization pattern of the sky outside crepuscular time periods (Flamarique & Hawryshyn, 1997).

Among vertebrates, birds provide perhaps the most intriguing, yet highly controversial example of polarization-based navigation. Helbig (1990) was among the first to suggest that some migratory birds use celestial polarization cues. He found that migratory blackcaps (*Sylvia atricapilla*) are able to orientate themselves correctly in the direction of their migratory route in the absence of meaningful cues from the earth's magnetic field, providing they have a clear view of the evening sky. However, when the DoLP of the natural skylight was reduced using a polymer retarder film that converted linearly polarized light into circularly polarized light (which is indistinguishable from unpolarized light to all animals except some species of mantis shrimp) the birds became disoriented and also showed a decrease in their migratory restlessness (Helbig, 1990). A similar result was also found during experiments with yellow-faced honeyeaters (*Lichenostomus chrysops*), a species known to use the earth's magnetic field and the position of the sun for navigation (Munro & Wiltschko, 1993a,b). Munro and Wiltschko (1995) tested the directional migration preference of these birds in funnel cages and found that when the magnetic field was not available and the sun was concealed by cloud the birds were still able to orientate themselves in the preferred direction for migration. However, when the DoLP of the sky was reduced using a polymer retarder the birds became disorientated. More recently Muheim et al. (2016) suggested that in zebra finches (*Taeniopygia guttata*) the overhead polarization pattern of the sky may be involved in modulating the light-dependent magnetic compass used for orientation. The evidence for polarization sensitivity in birds is nonetheless still limited and the subject remains a topic of debate, not least because the mechanism behind it remains completely unknown.

1.2.3 Signalling and communication

Polarized light has been proposed as a means of communication in several taxa. In order for a particular morphological or behavioural trait to be called a 'signal' there needs to be evidence that it somehow increases the fitness of the sender (and is therefore under selection), and often also the receiver, by causing a change in the behaviour of the receiver (Endler, 2000; Caves et al., 2018). Compared to navigation, the use of polarization information for communication is less studied (Cronin, 2018; Marshall et al., 2019). Our relatively poor understanding of polarization signals may seem surprising given the amount of popular attention the topic attracts (the topic has been covered, to various degrees, by no fewer than four different books (Johnsen, 2012; Land & Nilsson, 2012; Cronin et al., 2014; Horváth, 2014)). The downside to the topics popular appeal is that when we discover polarization patterns on an animal we are often tempted to jump to conclusions about functionality (assuming a function exists at all) without evidence to support it. In order to demonstrate that a polarization pattern is a signal the following criteria must be met: (1) the visual system of the intended receiver must be capable of detecting the pattern; (2) the polarization pattern must be visible to the intended receiver when the animals interact; (3) the polarization pattern must be used in a behaviourally relevant context such as aggression, deterrence or mate selection; (4) detection of the polarization pattern by the receiver during such interactions must be associated with a clear response; and (5) the signal must occur in a natural setting and not just in an artificial lab environment (Cronin, 2018). Given the above criteria, and the difficulties associated with studying and working with polarization (Foster et al., 2018), our limited understanding of how animals use polarization for communication should be less surprising. Nonetheless, while we don't currently have absolute proof of the functionality of polarization for communication in nature, there are a number of examples that have very good circumstantial evidence.

One of the strongest cases for the use of polarization signals is in nymphalid butterflies, many of which exhibit polarized reflectance patterns on their wings (Sweeney et al., 2003; Douglas et al., 2007). Of the 144 species examined by Douglas el al. (2007), 75 exhibited polarized wing patterns. Sweeney et al. (2003) demonstrated that these polarized wing patterns are important for mate recognition in the forest living butterfly *Heliconius cydno* (Figure 1.6a). *Heliconius cydno* males were more likely to approach females viewed through windows that transmit polarized light than those viewed through windows that depolarized light. Their conclusions were further supported by the fact that *Heliconius melpomene*, which is closely related to *H. cydno* but does not have polarized wing patterns (Figure 1.6b), showed no differences in approach to females viewed through the same two types of windows (Sweeney et al., 2003). A large proportion of the species that possess these polarized patterns occupy dense forest habitats where polarized signals may have an adaptive communication value (Douglas et al., 2007). This is because the spectrum and intensity of the illumination in these dim habitats can vary dramatically (Endler, 1993), thus Douglas et al. (2007) argued that polarization signals are more likely to stand out in these dim environments making them a more effective and reliable signal than those based on colour or intensity.

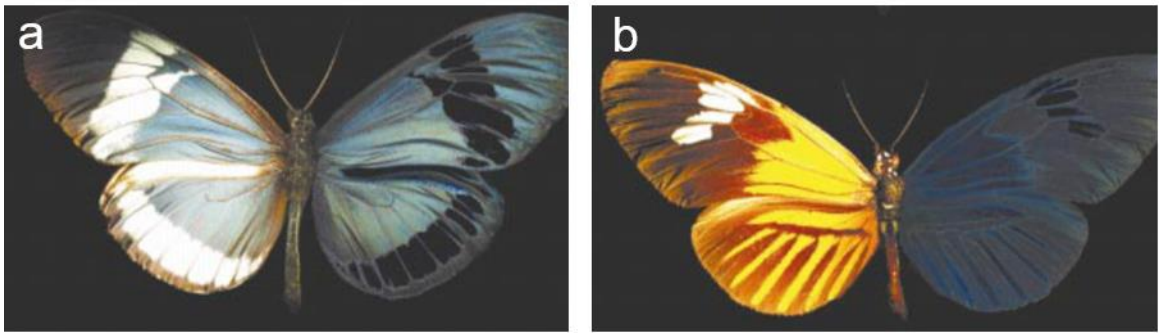

Figure 1.6: Polarization wing patterns of *Heliconius* butterflies. **a)** The iridescent polarization pattern on the wings of *Heliconius cydno* compared with **b)** *Heliconius melpomene malleti* that does not have polarization patterns on its wings. In both photos the left wing shows the original colour photo and the right wing shows the difference between a polarization photo taken at 0° and one taken at 90°. Figure adapted from Sweeney et al. (2003).

Other well-known examples of putative polarization signals are found among marine species, namely cephalopods and stomatopods (mantis shrimp) (Cronin, 2018; Marshall et al., 2019). Cuttlefish and squid have dynamic polarized patterns on their arms produced by modified iridophore cells that they are able to turn on and off (Figure 1.7a) (Shashar et al., 1996; Shashar & Hanlon, 1997; Hanlon & Mäthger, 2006; Chiou et al., 2007, 2008b; Mäthger et al., 2009b,a). The orientation of the arms does not affect the DoP or AoP (Chiou et al., 2007). Shashar et al. (1996) examined the function of the polarization patterns produced by the cuttlefish *Sepia officinalis*. When the cuttlefish were presented with an image of themselves reflected in a mirror their behavioural reaction was different depending on whether or not the polarization of the reflection was distorted, thus meeting some of the criteria of a true signal (Shashar et al., 1996). Cephalopods are colour blind (Messenger et al., 1973; Messenger, 1977; Marshall & Messenger, 1996; Mäthger et al., 2006) so their highly acute polarization vision may have evolved as an alternative to colour vision (Bernard & Wehner, 1977; Mäthger et al., 2009b; Temple et al., 2012). The actual message conveyed by these polarization signals is still unknown (Mäthger et al., 2009b,a; Marshall et al., 2019). However, the observation that species such as the squid *Loligo pealeii* display polarization patterns even when camouflaged (Hanlon & Mäthger, 2006) means that they, and other cephalopods, could signal in polarization at the same time as hiding from predators (Shashar et al., 1996). This is in line with the suggestion that polarization provides a ‘secret’ communication channel (Shashar et al., 1996); an idea that is tantalising to humans.

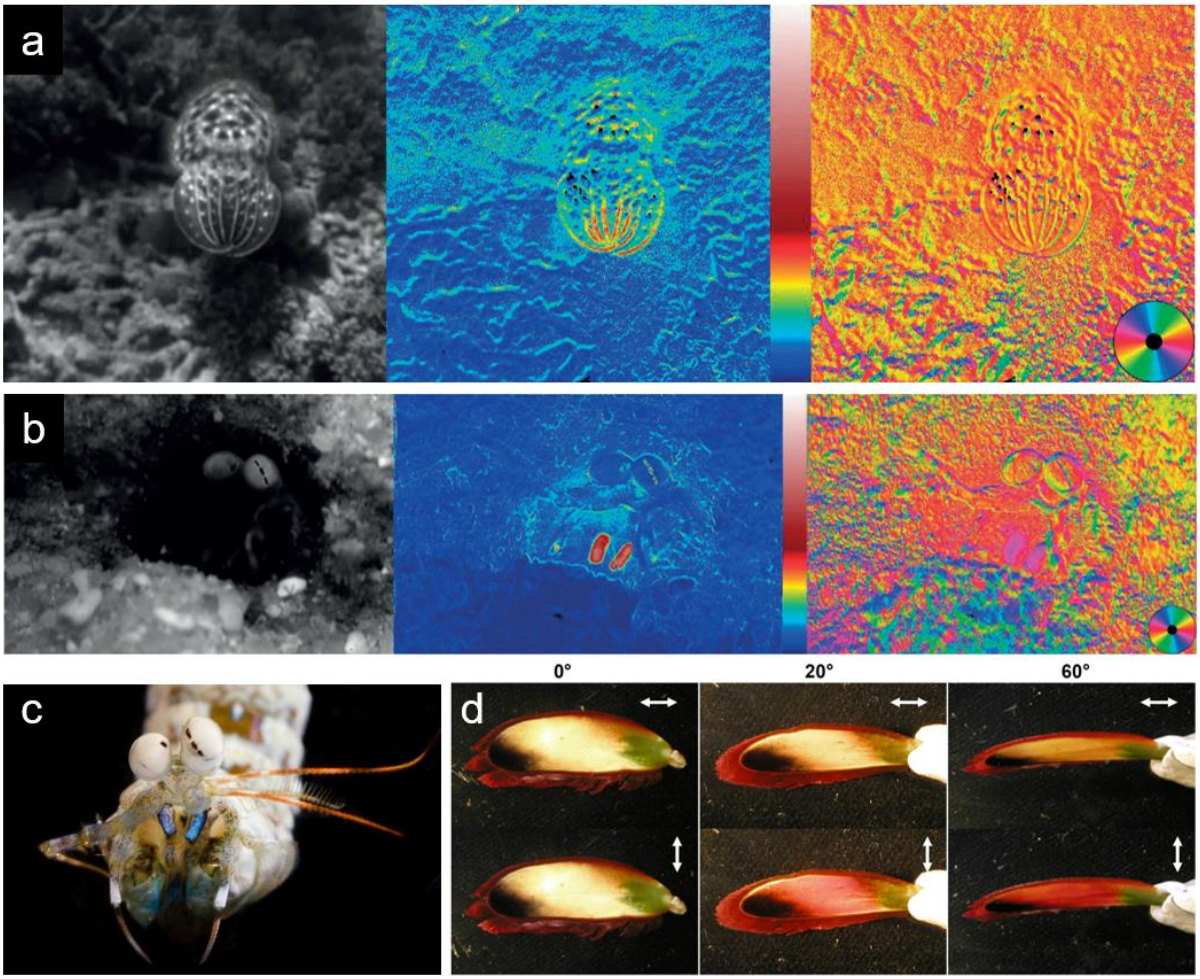

Figure 1.7: Polarization body patterns of cuttlefish and mantis shrimp. **a)** Intensity (left), DoP (middle), and AoP (right) images of the broad-club cuttlefish (*Sepia latimanus*) showing the highly polarized stripes on the arms. The DoP scale goes from 0 (blue) to 1 (white), with deep-red corresponding to a DoP of ~0.45. In the circular AoP scale orange/red is horizontal and cyan is vertical. **b)** Polarization images (order and colour scale as in (a)) of the mantis shrimp *Haptosquilla trispinosa* showing the highly horizontally polarized blue maxillipeds. **c)** Colour photo of *H. trispinosa* displaying the blue polarized maxillipeds. **d)** Photos of the antennal scale of the peacock mantis shrimp (*Odontodactylus scyllarus*) taken at different orientations (0°, 20° and 60°) through a horizontal (top row) and vertical (bottom row) polarizer. (a-b) from Marshall et al. (2019), (c) courtesy of Mike Bok, and (d) from Chiou et al. (2008a).

Arguably the most elaborate and diverse use of polarization signals can be found within stomatopod crustaceans, or mantis shrimp as they are more commonly known. The strongest case for polarization signals in mantis shrimp relates to the role played by the blue, horizontally polarized maxillipeds (appendages modified to function as mouthparts or for signalling) of *Haptosquilla trispinosa* in courtship (Figure 1.7b and Figure 1.7c). Chiou et al. (2011) found that while depriving *H. trispinosa* males of the horizontally polarized blue marking on their

first maxillipeds did not affect their overall mating success rate, it did have a negative impact on the cost of courtship. Compared to males with unaltered maxillipeds, males without polarized blue maxillipeds had to signal for longer to attract a female, mating duration was shorter, and females tended to be more aggressive towards the male (Chiou et al., 2011). These results strongly indicate that the polarized blue maxillipeds play a signalling role in mate selection. However, because the method used to remove the polarization component from the maxillipeds also destroyed the blue colour, it is impossible to know if it is the polarization, the blue colour, or both that is the important part of the signal. Interestingly, a number of other *Haptosquilla* species also have blue maxillipeds, but not all species possess the extra polarization element (How et al., 2014a). Based on the evolutionary transition from blue to blue and polarized maxillipeds, and an innate preference for horizontally polarized stimuli, the horizontally polarized component of the maxillipeds of *H. trispinosa* may have evolved to exploit a pre-existing sensory bias in the females (How et al., 2014a).

Several species of mantis shrimp have polarization markings on other areas of the body such as the antennal scales (the flap-like appendages that project laterally out from the base of the antennae), legs, carapace, telson, and uropods (Cronin et al., 2003; Chiou et al., 2008b, 2012; Cronin, 2018; Marshall et al., 2019). Although the exact function of these polarization markings are unknown, they are often displayed during agonistic displays, defence postures (such as those adopted during disputes over burrows) and courtship (Cronin et al., 2003; Cronin, 2018). Some of these polarization markings, such as the polarized antennal scales of *Odontodactylus scyllarus* (Figure 1.7d), are produced by oriented dichroic carotenoid molecules and thus generally appear bright red (Chiou et al., 2012), again making it difficult to disentangle the polarization and colour components of the signal. Nonetheless, the behaviours exhibited during these interactions do appear to indicate that the polarization

component is an important part of the signal. For instance, when a male *O. scyllarus* approaches a female from behind prior to mating, the female waves her laterally extended antennal scales (Cronin, 2018). Given that the DoP of light reflected from the scale changes depending on the angle from which they are viewed (Chiou et al., 2008b, 2012), waving the antennal scales in this way should create a flicking signal that is very obvious to the approaching male (Cronin, 2018).

Mantis shrimp are exceptional in that they are the only animals on the planet known to possess both circular polarization vision and circularly polarized colouration, raising the possibility that circularly polarized light is used as a communication signal (Chiou et al., 2008a; Gagnon et al., 2015; Templin et al., 2017). For example, *Gonodactylaceus falcatus* has left-handed circularly polarized markings that are most prevalent on the uropods of the tail, and ventral and frontal side of its legs (Gagnon et al., 2015). Gagnon et al. (2015) noted that during aggressive confrontations mantis shrimp shield themselves with their heavily armoured tail by curling their abdomen under their body, thus presenting the regions of the tail and legs where the circular polarization is strongest towards their aggressor. It is highly likely that the circularly polarized patterns function as a signal during these confrontations. Indeed, behavioural experiments found that *G. falcatus* avoided burrows that were illuminated from the inside with left-handed circularly polarized light; therefore suggesting that the circularly polarized markings on the legs and tail of *G. falcatus* serve as a highly conspicuous signal to communicate burrow occupancy to other mantis shrimp (Gagnon et al., 2015). In other species circularly polarized patterns may play a role in sexual selection. The keel on the median ridge of the telson of the mantis shrimp *Odontodactylus cultrifer* reflects and transmits circularly polarized light (Figure 1.8). When viewed from the right side, the polarization of the keel is right-handed, but when viewed from the left side it is left-handed (Chiou et al., 2008a; Cronin,

2018). While its function remains a mystery, the observation that the keel is sexually dimorphic (it is much larger in males than females) means it is highly likely that it is a sexual signal (Chiou et al., 2008a; Cronin, 2018). It is possible that circularly polarized signals may have evolved because unlike linearly polarized signals, which are visible to the excellent polarization vision of cephalopods (a predator of mantis shrimp), circularly polarized signals would not stand out to these predators. Circular polarization vision and signals may therefore represent the ultimate 'secret' communication channel.

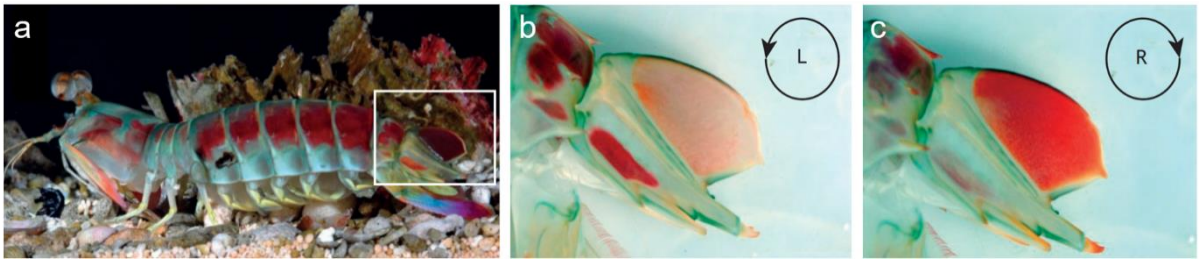

Figure 1.8: Circular polarization signals in mantis shrimp. **a)** The red colouration of the keel (indicated by the white box) of *Odontodactylus cultrifer* is circularly polarized as demonstrated by photographing the keel through, **b)** left-handed, and **c)** right-handed circularly polarizing filters. Figure adapted from Marshall et al. (2019).

The use of polarization for signalling has also been proposed for vertebrates, although as yet there exists no convincing evidence to support these claims. Calabrese et al. (2014) reported that swordtails (*Xiphophorus nigrensis*) show sexually dimorphic polarized reflectance in which males show a much greater polarization contrast both between their body and their background, and between different parts of their body. Calabrese et al. (2014) found that females displayed a strong preference for males exhibiting a high polarization contrast. However, polarization reflectance was manipulated by changing the polarization of the illumination light in a choice chamber making it difficult to determine whether it was the fish or background that elicited the difference in female preference. Furthermore, the study didn't

fully control for differences in intensity making it difficult to disentangle the relative importance of polarization and intensity (Calabrese et al., 2014; Marshall et al., 2019).

1.2.4 Contrast enhancement and object detection

The idea that polarization vision can enhance visual contrast, and therefore object detection, has been around for many years (Lythgoe & Hemmings, 1967) and is important for many different animals including fish (Bains, 1996; Kamermans & Hawryshyn, 2011; Flamarique, 2019), insects (Sharkey et al., 2015), cephalopods (Budelmann, 1995; Shashar & Cronin, 1996; Shashar et al., 1998, 2000; Pignatelli et al., 2011; Cartron et al., 2013a) and crustaceans (Glantz, 2001; Glantz & Schroeter, 2006; Tuthill & Johnsen, 2006; How et al., 2015). Over the last eight years, lab experiments using looming-stimuli (a two-dimensional shape that increases rapidly in size to mimic the direct approach of an object) presented on modified computer monitors, and field studies involving moving targets made from polarizing filters, have revealed much about how cephalopods (Pignatelli et al., 2011; Temple et al., 2012; Cartron et al., 2013a) and crustaceans (How et al., 2012, 2014a,b, 2015) use their polarization vision for contrast enhancement and object detection. For species that readily respond to looming stimuli this experimental approach is very powerful and has proven to be an effective method of investigating the characteristics and limitations of polarization vision in these species. For instance, How et al. (2012) used looming stimuli presented on modified computer monitors to show that the fiddler crab *Gelasimus vomeris* has highly acute polarization vision and is able to discriminate differences in the AoP as small as 3.2°. Even more impressively, using the same approach, Temple et al. (2012) found that the cuttlefish *Sepia plangon* can detect stimuli that differ from the AoP of the background by only 1°. Cartron et al. (2013b) used this approach to investigate if polarization vision in cuttlefish could enhance visual contrast in turbid waters. They found that the response to the stimuli in both intensity and polarization was the same in

clear water. However, as the water between the monitor and the cuttlefish became increasing more turbid, response to the intensity stimuli decreased faster than response to the polarized stimuli, indicating that polarization vision can enhance contrast and consequently improve object detection in turbid water (Cartron et al., 2013a).

Polarization vision has also been shown to enhance visual contrast in a number of crustacean species, and in crayfish it is thought to be involved in motion detection within low contrast environments (Glantz, 2001; Glantz & Schroeter, 2006). More recently, How et al. (2015) presented the first evidence from any animal that the detection of an approaching polarization contrast has a real behavioural consequence in nature. How et al. (2015) conducted field experiments with the fiddler crab *Leptuca stenodactylus* in which a pulley system was used to move different types of polarization targets towards crabs on the mudflat. Three target treatments were used: one rotated the AoP of transmitted light by 90° thus generating a strong contrast in the AoP; another depolarized the transmitted light thus generating a strong contrast in the DoLP (it did this by converting the linearly polarized light to circular, which crabs cannot discriminate from unpolarized light); the last treatment did not alter the polarization properties of the transmitted light and thus acted as a control (How et al., 2015). All of the targets were viewed against the horizontally polarized light reflected from the mudflats (Figure 1.9). The distance at which the crabs responded to each target was proportional to the target's polarization contrast. Crabs responded to the target with the contrast in AoP around 24% further away, and to the unpolarized target around 17% further away, than they did to the control (How et al., 2015). Whether crabs also use their polarization vision to detect targets viewed against the polarization pattern of the sky is investigated as part of this thesis (chapter 3).

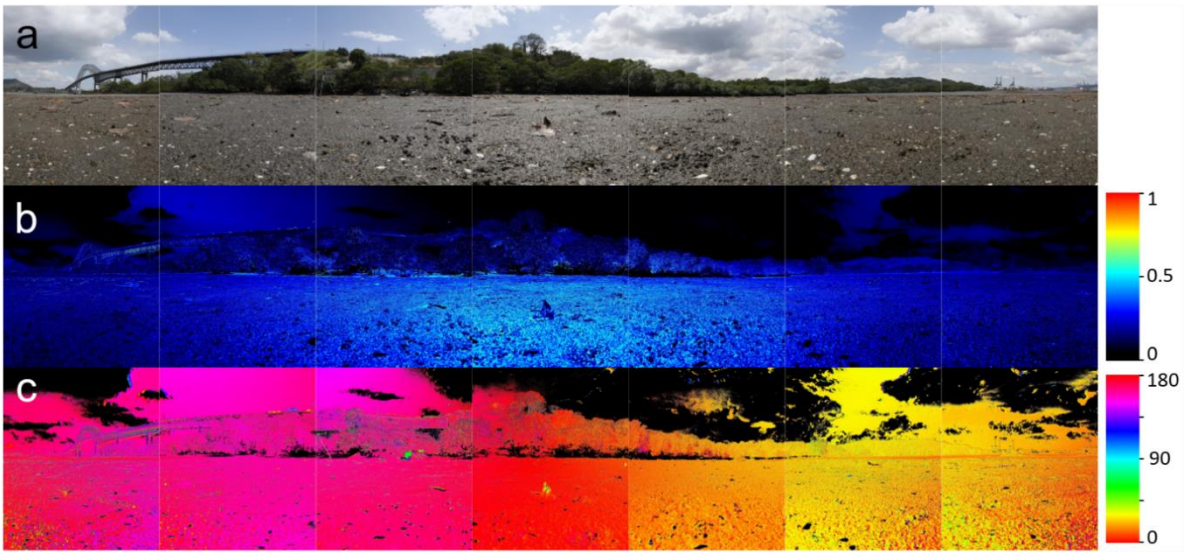

Figure 1.9: Image polarimetry showing polarized light reflected off a mudflat. **a)** Original photograph, **b)** DoP, and **c)** AoP. The AoP is parallel to the surface, which in this case is at or near horizontal (How, unpublished).

One idea that is particularly attractive is the suggestion that polarization vision may help animals to detect transparent prey (Shashar et al., 1998; Tuthill & Johnsen, 2006; Cartron et al., 2013b). This idea is based on the fact that many planktonic animals are strongly birefringent within some of their body tissues that would cause them to be highly conspicuous when viewed by an animal with polarization vision (Shashar et al., 1998). However, whether or not polarization vision really does enable animals to detect transparent prey in nature remains a topic of debate. Johnsen et al. (2011) for instance found that under natural *in situ* lighting conditions, the polarization contrast of transparent animals is no greater than their intensity contrast when viewed from a distance. The authors do nonetheless note that the polarization information is still advantageous and can be used to enhance overall visual contrast (Johnsen et al., 2011).

1.3 The dipolat visual system of crabs

Polarization sensitivity in crustaceans, and indeed all animals, depends on four main factors: 1) the visual pigment molecule, 2) the morphology of the retina, 3) neuronal wiring, and 4) how information relating to polarization is processed and interpreted by the brain.

The first of these requirements relates to the visual pigment molecule and is the foundation of polarization sensitivity. A single visual pigment molecule, such as rhodopsin, is intrinsically dichroic because they have a higher probability of absorbance for light that has an AoP parallel to the excitable long axis of the chromophore (Nilsson & Warrant, 1999; Roberts et al., 2011). A visual pigment molecule will therefore proportionally respond to a particular AoP, and thus a photoreceptor will only be polarization sensitive, if all of the visual pigment molecules within the cell membrane are preferentially aligned along a similar direction (Waterman, 1981; Nilsson & Warrant, 1999; Roberts et al., 2011). This leads to the second requirement of polarization vision, which relates to the structure of the retina.

There are three known arrangements of polarization sensitive photoreceptors that are able to provide contrast enhancement in image forming vision (Labhart, 2016).

- **Monopolat:** By aligning receptors across the eye in a single direction relative to the outside world, polarization contrasts can be converted into, and modulate existing, intensity contrasts. This is roughly analogous to the use of Polaroid sunglasses by humans, and has been demonstrated in butterflies and moths (Kelber et al., 2001; Belušič et al., 2017; Stewart et al., 2019). A key limitation of this system is its inability to discriminate between intensity and polarization, as both contribute to a single measure of scene contrast.

- **Dipolat:** A two-channel arrangement in which polarization receptors are typically oriented perpendicularly to each other. In such systems, an intensity-independent measure of polarization contrast can be produced through opponent processing between these two polarization sensitive channels (Bernard & Wehner, 1977; How & Marshall, 2014). Dipolatic receptor arrangements have been found in the image forming eyes of several taxa including: insects (Schneider & Langer, 1969; Laughlin & McGinness, 1978; Schwind, 1984), cephalopods (Moody & Parriss, 1961; Talbot & Marshall, 2011), and crustaceans (Waterman et al., 1969; Alkaladi & Zeil, 2014; Basnak et al., 2018). A key limitation of this anatomical arrangement is that such a system is vulnerable to null points of polarization discrimination (Bernard & Wehner, 1977; How et al., 2014b; How & Marshall, 2014; Basnak et al., 2018). How these null points affect target detection in fiddler crabs is investigated as part of this thesis in chapter 3.
- **Dynamic multipolat:** Stomatopod crustaceans make use of a complex anatomical arrangement of polarization sensitive photoreceptors. These species make use of a rotatable, four-channel linear polarization system (Marshall et al., 1991) that is capable of optimising visual contrast by aligning the axes of sensitivity relative to the contrasting scene (Daly et al., 2016). Combined with the ability to discriminate the ellipticity of polarization in the midband of the eye (Chiou et al., 2008a; Roberts et al., 2009; Gagnon et al., 2015; Templin et al., 2017), this system is complex and the visual processing mechanisms remain poorly understood.

The most common of these photoreceptor arrangements, which has been converged upon by at least two evolutionary lineages (arthropods and cephalopods) and forms the focus of this thesis, is the dipolat system, with two channels of polarization sensitivity arranged horizontally and vertically relative to the outside world. Decapod crustaceans represent an excellent model for

investigating a dipolat system and the use of polarization vision for contrast enhancement and object detection. It therefore this group that hereafter forms the focus of this thesis.

1.3.1 Structure of the crustacean apposition eye

Crustaceans have compound eyes which can be separated into two main forms; apposition eyes and superposition eyes. All of the species that form the focus of this thesis have apposition compound eyes (Land & Nilsson, 2012; Horváth, 2014) (Figure 1.10a). Apposition compound eyes are made up of repeated optical units called ommatidia. An individual ommatidium samples light from a specific region of space and effectively functions as a single 'pixel'. Each ommatidium consists of a corneal lens and crystalline cone that focus light onto a group of photoreceptors that form a single photoreceptive rhabdom (Figure 1.10b and Figure 1.10c) (Eguchi, 1965; Alkaladi et al., 2013; Alkaladi & Zeil, 2014). Crustaceans typically have eight retinular cells termed R1-R8 that contribute long, narrow tubes of membrane (microvilli) that form the light sensitive rhabdom (Stowe, 1977; Waterman, 1981; Marshall et al., 1991; Alkaladi et al., 2013; Alkaladi & Zeil, 2014). R1, R4 and R5 contribute horizontally orientated microvilli to the main rhabdom while R2, R3, R6 and R7 contribute vertically orientated microvilli (based on the commonly used R1 naming scheme; Figure 1.11) (Stowe, 1977; Waterman, 1981; Marshall et al., 1991; Alkaladi & Zeil, 2014). The orientation of microvilli from the different retinular cells gives the rhabdom a layered appearance. The distally located R8 contributes both horizontally and vertically orientated microvilli to the distal end of the rhabdom (Eguchi & Waterman, 1973). In the fiddler crab *Gelasimus vomeris* the R8 accounts for approximately 12% of the length of the whole rhabdom; the diameter of the main rhabdom is also around 50% wider than that of the R8 (Alkaladi & Zeil, 2014).

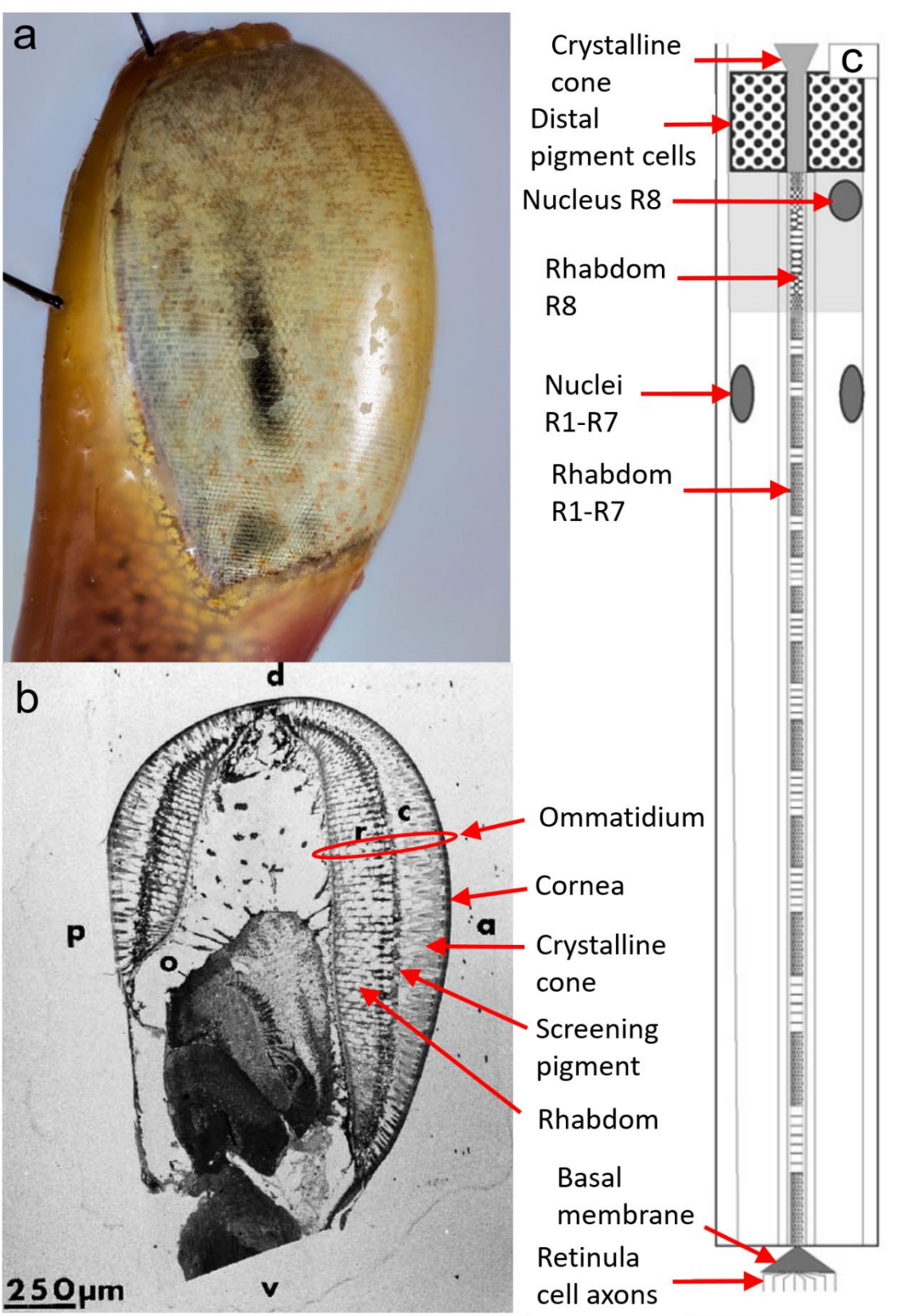

Figure 1.10: Structure of the crustacean apposition compound eye. **a)** The eye of the fiddler crab *Afruca tangeri* showing the dark pseudopupil. The pseudopupil indicates the ommatidia that are looking directly at the observer. **b)** Light micrograph of a longitudinal section through the dorsal part of an eye stalk of *Austruca lactea annulipes*. **c)** Schematic of a longitudinal section through an ommatidium of a fiddler crab. (a) courtesy of Emelie Brodrick, (b) is adapted from Zeil and Al-Mutairi (1996), and (c) is adapted from Alkaladi et al. (2013).

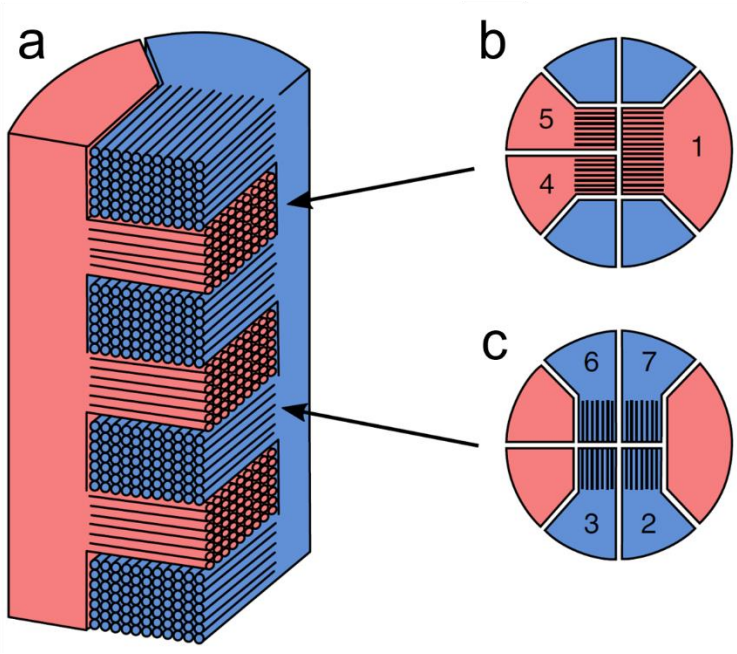

Figure 1.11: Structure of the main rhabdom of crustaceans. **a)** The main rhabdom consists of alternating bands of horizontal and vertical microvilli from the R1–7 photoreceptors. **b)** R1, R4 and R5 contribute horizontally orientated microvilli to the main rhabdom and, **c)** R2, R3, R6 and R7 contribute vertically orientated microvilli (based on the R1 naming scheme). Figure from Daly et al. (2016).

The fact that each individual retinular cell (with the exception of R8) only contributes either horizontally or vertically orientated microvilli to the rhabdom is fundamental to what makes crustaceans, and other arthropods, polarization sensitive. The cylindrical shape of the microvilli that constitute the rhabdom means that even if the visual pigments are randomly orientated, the membrane will have a dichroic ratio of 2, i.e. it will absorb two times more light when the AoP is parallel to the longitudinal axis of the membrane than when it is perpendicular to it (Roberts et al., 2011).

The dichroic nature of the microvilli that make up the rhabdom forms the foundation of polarization sensitivity in crustaceans and meets the first two requirements of polarization vision. However, on its own this is not enough to make an animal polarization sensitive; this is because the necessary neuronal connections must be in place to preserve the polarization information obtained from the different retinular cells. In crustaceans this function is carried

out by monopolar cells (Nässel & Waterman, 1977; Strausfeld & Nässel, 1981; Sabra & Glantz, 1985; Kleinlogel & Marshall, 2005).

1.3.2 Neural substrate underlying polarization vision in crustaceans

The third and fourth requirements for polarization vision relate to the neural wiring that encodes the polarization information from the photoreceptors and how this information is processed by the brain. The optic lobe of crustaceans consists of three main retinotopic neuropils, homologous to those found in insects, termed the lamina, medulla and the lobula (Strausfeld & Nässel, 1981). The photoreceptor terminals from R1-7 end at two different levels in the lamina, termed the external plexiform layers 1 and 2 (epl1 and epl2). There is conflicting species dependent evidence regarding the layer in which each set of receptors terminate (compare the findings of Nässel & Waterman (1977), Strausfeld & Nässel (1981) and Waterman (1981) with the findings of Sabra & Glantz (1985) and Kleinlogel & Marshall (2005)). In the crayfish *Procambarus clarkii*, and gonodactyloid stomatopods, the horizontal receptors (R1, R4 and R5) terminate in epl1 and have synaptic sites with monopolar cell 3 (M3) while the vertical receptors (R2, R3, R6 and R7) terminate in epl2 and have synaptic sites with M4 (Sabra & Glantz, 1985; Kleinlogel & Marshall, 2005). Together, opponent processed outputs from M3 and M4 may form an intensity-independent polarization channel. How this information is processed and whether or not it is integrated with intensity information, encoded by M2 which has synaptic terminals within epl1 and epl2 (Strausfeld & Nässel, 1981; Sztarker et al., 2009), is the subject of chapter 2.

1.4 Flat world crabs as a study system for polarization vision

All of the work within this thesis was conducted with the fiddler crab *Afruca tangeri* (previously *Uca tangeri* (Shih et al., 2016)) (chapters 2-4) and the horn-eyed ghost crab

Ocypode ceratophthalma (chapter 5), both of which are in the family Ocypodidae. Fiddler and ghost crabs are semi-terrestrial and can be found around the world, with the vast majority of species found in the tropics where they inhabit sand- and mudflats, or, as is often the case for ghost crabs, sandy beaches (Crane, 1975; Lucrezi & Schlacher, 2014). A few species of fiddler crab can even be found as far north as New England in the USA and as far south as Japan (Crane, 1975). Collectively fiddler and ghost crabs are often referred to as flat world crabs due to the local homogeneous topography of the sand- and mudflat environments in which these animals thrive.

Fiddler and ghost crabs both have apposition compound eyes (as detailed in section 1.3.1) located on characteristically long, vertically oriented eye stalks. Each eye spans almost the entire circumference of the eye stalk and provides the crab with a 360º panoramic view of the world (Zeil et al., 1986). The eyes of ghost crabs are considerably larger relative to body size than those of fiddler crabs. Both fiddler and ghost crabs have a narrow streak of high vertical resolution around the equator of the eye that can easily be seen by observing the shape of the pseudopupil (Zeil et al., 1986; Land & Layne, 1995; Zeil & Al-Mutairi, 1996; Smolka & Hemmi, 2009). In the fiddler crab *Leptuca pugilator* this vertical acute zone views the area of space approximately 15° above and below the visual horizon (Land & Layne, 1995). Horizontal resolution is more or less constant across the whole eye (Zeil et al., 1986; Land & Layne, 1995; Zeil & Al-Mutairi, 1996; Smolka & Hemmi, 2009).

One of the main features of a flat world is that any object that is larger than the viewer will appear above the visual horizon while anything that is smaller than the viewer will appear below it (Figure 1.12). Since the crab's predators are almost always larger than themselves, anything that appears above the crab's horizon is therefore a potential threat and is likely to

elicit an escape response (Land & Layne, 1995; Layne et al., 1997; Zeil & Hemmi, 2006). Furthermore, since stimulation of just one or two ommatidia is sufficient to elicit a response (Land & Layne, 1995; Zeil & Hemmi, 2006; Hemmi & Pfeil, 2010), the only feature that distinguishes a potential predator from other crabs is whether it appears above or below the crab's visual horizon (Land & Layne, 1995; Layne et al., 1997; Zeil & Hemmi, 2006). This has been demonstrated in experiments that found that crabs almost never displayed an escape response when presented with moving targets that appeared below their visual horizon, while those that appeared above it, even if only partially, consistently elicited an escape response (Layne et al., 1997; Layne, 1998). It is the position on the retina, i.e. whether an object is detected by ommatidia above or below the eye equator, and not the position relative to the horizon that distinguishes predators from nonthreatening conspecifics (or in the case of ghost crabs, potential prey that they may subsequently choose to attack) (Layne et al., 1997; Layne, 1998). It is therefore essential for the crabs to keep the equator of their eye aligned with the visual horizon, (Layne, 1998; Nalbach et al., 1989; Zeil et al., 1986).

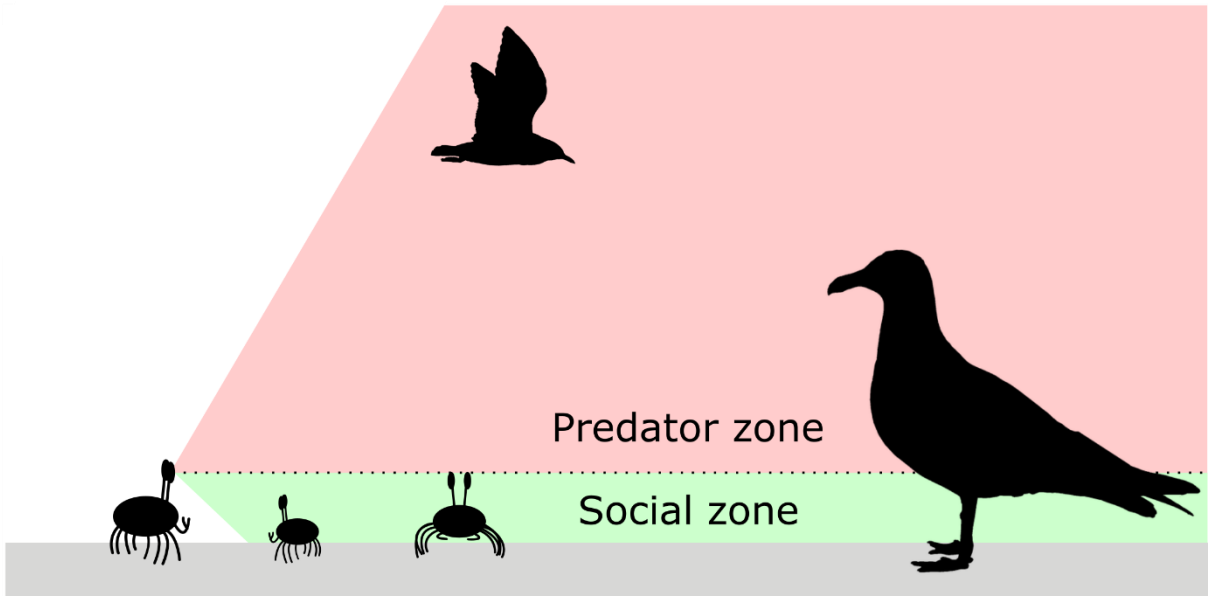

Figure 1.12: Anything below a crab's visual horizon is smaller than the crab, irrespective of distance, and so not a threat; anything that appears above a crab's visual horizon is larger and thus a potential threat. The social zone is usually only ever occupied by smaller or equally sized conspecifics (or in the case of ghost crabs, potential prey), while birds and other potential predators will always appear in the predator zone.

As described in section 1.1.2 and shown in Figure 1.9, polarization information is particularly prevalent in mudflat habitats because the damp, relatively flat surface reflects roughly horizontally polarized light creating a polarized background against which objects are viewed (Zeil & Hofmann, 2001; How & Marshall, 2014; How et al., 2015). Fiddler crabs, and other flat-world crabs, actively align their eyes with the visual horizon (Layne, 1998; Nalbach et al., 1989; Zeil et al., 1986) and therefore the horizontal/vertical arrangement of the photoreceptors functions as a matched filter for detecting polarization contrasts on the mudflats (Wehner, 1987; How et al., 2014b; How & Marshall, 2014). Their sensory ecology, in combination with their behavioural ecology (described below), therefore makes flat-world crabs, particularly fiddler crabs, an ideal system in which to study how polarization vision functions for contrast enhancement and target detection in an animal with a dipolat visual system.

1.4.1 Fiddler crabs (*Afruca tangeri*)

Afruca tangeri (Figure 1.13) is the largest species of fiddler crab with adults typically having a carapace width between 20-35 mm; although the largest male recorded was 47 mm across the carapace with a claw that measured 105 mm (Crane, 1975). *Afruca tangeri* is the only fiddler crab that occurs in Europe where it can be found on coastal sand- and mudflats, and estuaries along the south coast of Portugal and Spain (Crane, 1975). Here *A. tangeri* live in large colonies and are most active between March and late June during which time males display to attract females and ward off rival males (Wolfrath, 1993). Like all fiddler crabs, *A. tangeri* digs a burrow that it leaves at low tide to forage, usually feeding on organic particles within the sediment, or searching for mates at the surface. This species usually forages within the area immediately adjacent to its burrow. However, during the summer *A. tangeri* has been known to sometimes form large congregations (known as droves) that move down the beach to feed on the nutrient rich substrate around seagrass beds (Crane, 1975; Ens et al., 1993).

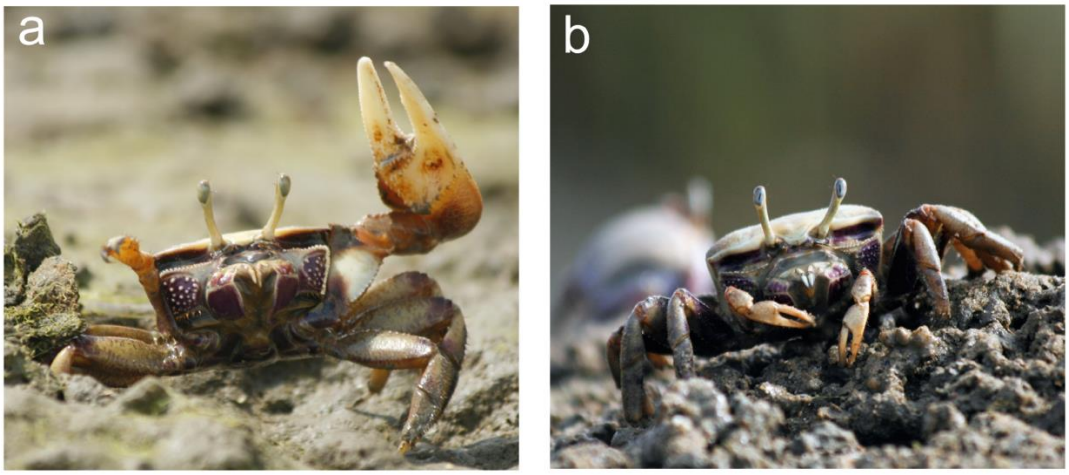

Figure 1.13: The fiddler crab *Afruca tangeri*. **a)** A male during his claw waving display and **b)** a female feeding.

Courtship displays

Fiddler crab males are well known for their enlarged claw that they use for fighting and courtship waving displays that they perform to attract females (Crane, 1975; Wolfrath, 1993; How & Hemmi, 2008a,b; How et al., 2009). In some species these courtship displays are known to incorporate auditory and seismic, as well as visual, elements (Crane, 1975; Salmon & Hyatt, 1979). The displays of many species involve waving the claw high above the crabs' body meaning that any nearby females would view the claw above the visual horizon, i.e. in the predator zone, and so the display may have evolved as a sensory trap, exploiting the females anti-predator freeze response (Christy, 1995; Land & Layne, 1995; How & Hemmi, 2008a). Males also use their enlarged claws for fighting with rivals (Jennions & Backwell, 1996; Muramatsu & Koga, 2016). It is not uncommon for males to lose their claw during these contests, in which case a male will grow a replacement claw. Regenerate claws are usually weaker than the original and so males with regenerate claws alter their behaviour accordingly and are more likely to use bluffs to win contests (Muramatsu & Koga, 2016).

Predation and anti-predator response in fiddler crabs

One of the main predators of fiddler crabs are birds; crabs are an especially important prey species for several wader and tern species (Zwarts, 1985; Koga et al., 1998, 2001; Iribarne & Martinez, 1999; Land, 1999). *Afruca tangeri* is preyed upon by several species of wader including the curlew (*Numenius arquata*), redshank (*Tringa tetanus*), whimbrel (*Numenius phaeopus*), common sandpiper (*Actitus hypoleucos*), kentish plover (*Charadrius alexandrines*) and grey plover (*Pluvialis squatarola*) (Zwarts, 1985), all of which occur in and around the field site where most of the work within this thesis was conducted. Some fiddler crab species, such as *L.* pugilator, are also food for other crabs such as the blue crab (*Callinectes sapidus*), which visually hunt fiddler crabs from the water's edge (Hughes & Seed, 1995; Tomsic et al., 2017).

Fiddler crabs have a well-defined multistage anti-predator response (reviewed by Hemmi (2005a) and Hemmi & Pfeil (2010)). It consists of three stages: *freeze*, *home run*, and as a last resort *burrow entry*. *Freezing*, which is when the crab ceases all activity and remains motionless, occurs as soon as the crab detects a moving object above its visual horizon. Often, stimulation of just one or two ommatidia is sufficient to elicit a freeze response (Land & Layne, 1995; Zeil & Hemmi, 2006; Hemmi & Pfeil, 2010). This behaviour helps the crab to assess predator-related visual cues, such as apparent size, retinal speed, and elevation, by removing any image motion induced by the crabs own movements (Hemmi, 2005a; Hemmi & Pfeil, 2010; Smolka et al., 2011). By remaining motionless, the crab will also render itself harder to detect. The next stage of the response is the *home run*, which is when the crab runs back to its burrow and either stops outside, or just inside, the entrance without fully entering the burrow. The *home run* is triggered by the retinal angular speed of the approaching, and thus expanding object, and often occurs shortly after the initial *freeze* response (Hemmi, 2005a; Hemmi &

Pfeil, 2010). It can also be triggered by flicker (Smolka et al., 2011, 2013) or even in response to escape behaviour exhibited by nearby conspecifics, even if the crab cannot see the stimulus that caused their neighbours to flee (Wong et al., 2005). The importance of visual flicker, and the possibility that it can generate a type of motion known as second-order motion, is investigated as part of this thesis in chapter 4. The *home run* greatly increases the crab's safety while keeping the cost of such a behaviour to a minimum as is it common for crabs to continue feeding just outside the entrance of their burrow. As with the *freeze* response, the *home run* allows the crab to gather more reliable information relating to the potential threat, but from a safer position. The third and final stage is *burrow entry*, in which the crab retreats down its burrow, at which point the risk of predation from most predators is eliminated. The decision to descend into the burrow is, however, very costly compared to the previous two stages. Firstly, once inside its burrow the crab is no longer able to feed. Secondly, the moment the crab enters the burrow it loses sight of the predator and therefore has no way of assessing when it is safe to leave the burrow again. As a result the crab will often end up waiting longer than is necessary before re-emerging (Hugie, 2004). The total amount of time that crabs remain hidden in their burrow is influenced by their size and sex. For instance, larger crabs tend to hide longer than smaller ones and in some species, such as *Leptuca beebei*, males hide longer than females (Jennions et al., 2003), most likely because their conspicuous enlarged claw leads to male biased predation by predators such as the great-tailed grackle (*Quiscalus mexicanus*) (Koga et al., 2001). However, reverse sexually biased predation has also been observed in the larger *L. pugilator* as ibises (*Eudocimus albus*) avoid males because of the increased handling time (Bildstein et al., 1989).

1.4.2 Ghost crabs (*Ocypode ceratophthalma*)

Ghost crabs, including *Ocypode ceratophthalma* (Figure 1.14a), are generally considered to be primarily nocturnal or crepuscular, however there is a great degree of variation between species and even between different populations of the same species (Lucrezi & Schlacher, 2014). The smaller juveniles are more likely to be active during the day than adults, perhaps to avoid predation by the larger cannibalistic adults (Daumer et al., 1963; Hughes, 1966). During the day *O. ceratophthalma* mostly hide at the bottom of deep burrows. In the collection sites used in this study it was common for many of the burrows above the high tide mark to be shaped like a corkscrew. These spiralling burrows, the entrance to which is usually marked by a large pyramid shaped mound of sand, are special 'copulation burrows' built by males for the purpose of attracting females and mating (Figure 1.14b) (Hughes, 1973). Ghost crabs are apex invertebrate consumers and are often used as ecological indicators for quickly assessing the impact of human disturbance on beach habitats (Barros, 2001; Neves & Bemvenuti, 2006; Lucrezi & Schlacher, 2009; Schlacher et al., 2011). They are opportunistic feeders that will readily consume organic particles within sediment (like fiddler crabs), scavenge carcasses, or actively pursue and kill a range of invertebrate and vertebrate prey (Wolcott, 1978; Lucrezi & Schlacher, 2014). Ghost crabs tend to forage over a much larger area then fiddler crabs and are not always associated with a burrow. It is not uncommon for *O. ceratophthalma* to dissociate from its burrow at the start of the its foraging period and dig a new one at the end of each night (Hughes, 1966).

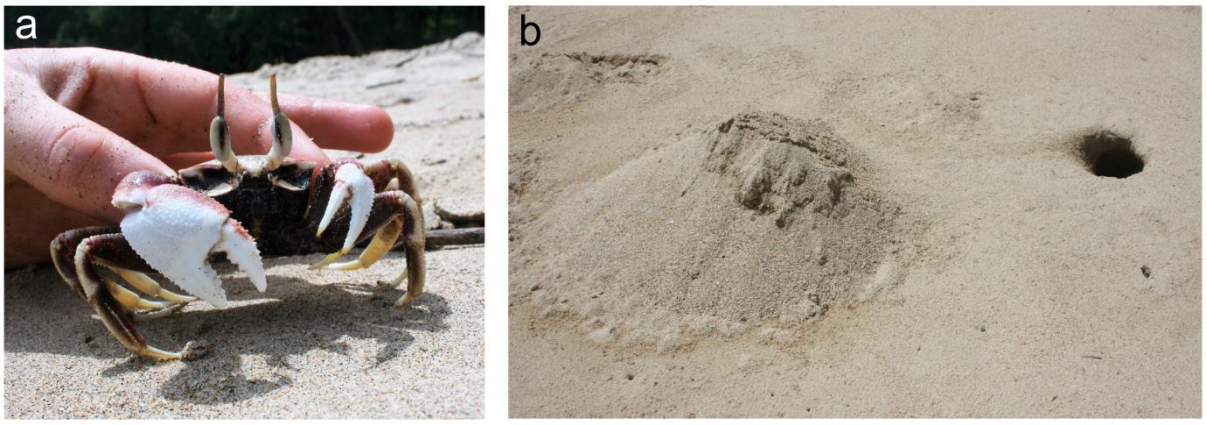

Figure 1.14: The horned, or horn-eyed, ghost crab *Ocypode ceratophthalma*. **a)** A male *O. ceratophthalma*. **b)** A copulation burrow with associated pyramid shaped mound of sand built by a male crab.

Predation and anti-predator response in ghost crabs

Like fiddler crabs, ghost crabs are also preyed upon by various shore birds including gulls, plovers, curlews and herons, along with some corvids and birds of prey (reviewed by Lucrezi & Schlacher (2014)). There are even reports of night time predation of ghost crabs by owls (Branco et al., 2010). They are also preyed upon by several lizard species (Blamires, 2004; Lucrezi & Schlacher, 2014) and by several mammal species including, in Hawaii, the small Indian mongoose (*Herpestes auropunctatus auropunctatus*) (La Rivers, 1948; Lucrezi & Schlacher, 2014).

The anti-predator response of ghost crabs is not as well characterised as the behaviour of fiddler crabs, partially because their nocturnal lifestyle makes them more difficult to observe. Escape response generally depends on the proximity of the crab to its burrow and the position of the potential predator relative to the crab and its burrow. When close to its burrow the escape response of *O. ceratophthalma* is similar to that of fiddler crabs, consisting of *freeze*, *home run*, and, if the threat continues to approach, *burrow entry* (S. Smithers, personal observations). While dissociated from a burrow, or if the potential predator is positioned between the crab

and its burrow, *O. ceratophthalma* will usually sprint away from the approaching threat or run into the surf before quickly burying itself in the soft sand (Hughes, 1966; S. Smithers, personal observations). While this may sound like a more risky strategy than that of fiddler crabs, it is worth noting that ghost crabs are the fastest crustacean on land (*Ocypode* means 'swift-footed') capable of reaching speeds of 4 miles per hour (approx. 6.5 km per hour) (Hafemann & Hubbard, 1969). Moreover, adults are capable of spotting an approaching human from over 100 m away (Hughes, 1966).

1.5 Overview of this thesis

The studies within this thesis investigated how fiddler and ghost crabs use their polarization vision for contrast enhancement and object detection. Lab experiments with fiddler crabs have shown that they have highly acute polarization vision (How et al., 2012, 2014b) and the field experiment described in section 1.2.4 demonstrated that the detection of an approaching polarization contrast leads to a behavioural response in the real world (How et al., 2015). There remains, however, a number of outstanding questions that are investigated in this thesis. While comparably less is known about polarization vision in ghost crabs, with what we do know limited to a handful of older studies (Schöne & Schöne, 1961; Daumer et al., 1963), this group offers an exciting opportunity to study polarization vision in a nocturnal species. In addition, ghost crabs are active predators and are therefore likely to use polarization vision for the detection of potential prey, as well as predators. The final data chapter of this thesis therefore sort to test whether ghost crabs could provide a new system for studying polarization vision.

- The first of these outstanding questions relates to how polarization information is processed within the visual system of crabs. It is unknown whether intensity and polarization information are combined together to provide crabs with a single, visual

representation of overall contrast, or processed separately to provide independent and parallel measures of polarization and intensity contrast. This longstanding question is investigated by the study reported in chapter 2.

- As discussed, field experiments have demonstrated that fiddler crabs use their polarization vision to enhance the detection of targets viewed against the surface of the mudflat. However, not all potential threats will be viewed against the mudflat. The study reported in chapter 3 addressed this gab in our knowledge by testing the ability of fiddler crabs to use their polarization vision to detect targets viewed against the polarization pattern of the sky. In particular, the study aimed to determine whether the crab's null points of polarization discrimination affected their ability to detect these aerial targets.
- Fiddler crabs respond to a combination of multiple visual cues that they use to assess the level of threat posed by a particular visual event. One cue in particular that is associated with a high level of threat is visual flicker, which is produced by the flapping wings of certain avian predators. Flicker is interesting because it can generate second-order motion, a form of motion that is not necessarily detectable by the same mechanisms used to detect first-order, or intensity-defined, motion. The study reported in chapter 4 tested whether fiddler crabs are able to detect second-order motion in both intensity and polarization.
- Chapter 5 is a standalone caveat chapter in which the study investigated how circadian cycle affected the ability of dark adapted ghost crabs to detect intensity and polarization contrasts at different times of day.
- Finally, chapter 6 provides a synopsis of the main findings reported in this thesis and highlights areas and directions for future research.

Chapter 2

Parallel processing of polarization and intensity information in fiddler crab vision

A one clawed fiddler crab, *Afruca tangeri*
Watercolour painting by Tom Timberlake

The first question that this thesis will address is how polarization information is processed within the visual system of crabs and whether or not it is integrated with intensity information early in visual processing. Understanding the processing circuits that underlie visually guided behaviours is essential if we are to fully comprehend how and why an animal responds to a visual stimulus in a particular way. This statement is especially true in regards to this thesis as the findings reported in this chapter are important for interpreting and understanding some of the results reported in later chapters. Parts of this chapter are published in the journal *Science Advances*, with me as first author and two co-authors (Nicholas W. Roberts and Martin J. How) (Smithers et al., 2019). The paper is recreated here with the addition of supplementary experiments, data, theory, and discussion.

2.1 Introduction

A number of animals are known to use the polarization of light for functional tasks that require the detection of a moving object, implying that polarization information is processed in a way that enhances visual contrast of the object against its background (Shashar & Cronin, 1996; Pignatelli et al., 2011; Cartron et al., 2013a; How et al., 2015; Sharkey et al., 2015). The start of section 1.3 gave an overview of the three known arrangements of polarization-sensitive photoreceptors that are able to provide contrast enhancement in image forming vision (Labhart, 2016). The most common of these photoreceptor arrangements, is the dipolat system; a two-channel arrangement in which photoreceptors are oriented perpendicular to each other. In such systems, an intensity-independent measure of polarization contrast may be produced through opponent processing between these two polarization sensitive channels (Bernard & Wehner, 1977; How & Marshall, 2014). In crustaceans, such as fiddler crabs that have a dipolat system, this visual information is relayed from each of the perpendicularly-oriented polarization-sensitive photoreceptors to the external plexiform layers (epl1 and epl2) of the lamina, where

they synapse with three types of translaminar neurons; two that preserve the two channels of polarization information and one that sums their inputs to produce a polarization-independent intensity channel (Strausfeld & Nässel, 1981; Sztarker et al., 2009) (Figure 2.1a). What is currently unknown, however, is how both polarization and intensity information are further processed, most likely within the medulla, to inform task-specific behaviours. Are these two forms of visual information processed separately to provide independent and parallel measures of polarization and intensity contrast; or are they combined to provide the animal with a single, visual representation of overall contrast?

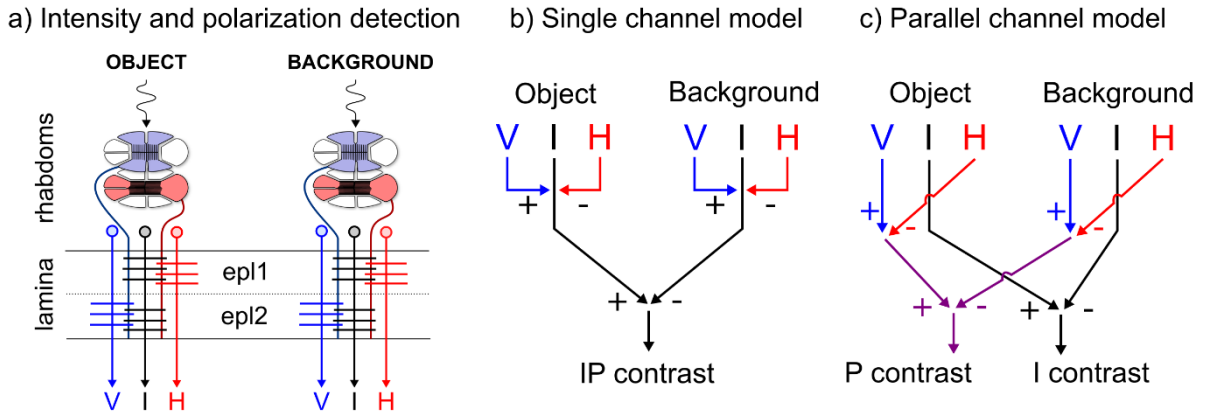

Figure 2.1: Hypothesised models of intensity and polarization channel integration in crustaceans. **a)** Horizontally and vertically oriented receptor cells project to the epl1 and epl2 layers of the lamina respectively where they synapse with three types of translaminar neuron (monopolar cells M2-M4), resulting in 3 channels of information per ommatidium; horizontal (H, M3) and vertical (V, M4) polarization, and intensity (I, M2) (Sabra & Glantz, 1985; Kleinlogel & Marshall, 2005) (redrawn from How & Marshall (2014)). **b)** Single channel model demonstrating a fusion of V, H and I into a single value (IP contrast). **c)** Parallel channel model in which the polarization (V and H) and intensity (I) channels combine separately into two parallel measures (P contrast and I contrast).

In dipolats, there is some evidence that could be consistent with animals integrating polarization and intensity information into a single contrast channel in specific behavioural contexts. For instance, the crayfish *Procambus clarkii* is known to respond to polarization contrasts almost identically to intensity contrasts (Glantz & Schroeter, 2006, 2007). Moreover, larval stage *Anax imperator* (the emperor dragonfly) shows an increase in responsiveness to

visual stimuli viewed through a naturalistic horizontally polarized light field, which was equivalent to an increase in the intensity contrast of 8% (Sharkey et al., 2015). A possible explanation for equivalence in response to either intensity or polarization contrasts is that the two polarization channels (V - vertical, and H - horizontal) combine with the intensity channel (I) (the three outputs from the lamina external plexiform layers, Figure 2.1a) via excitatory and inhibitory synapses (Figure 2.1b single channel model). However, such a single channel system would be subject to intensity/polarization cancellation points; situations where an animal would not be able to detect a visual contrast between an object and background despite differences in both intensity and polarization. In such cases, intensity and polarization channels would combine to cancel each other out.

Alternatively, polarization and intensity contrast within an image could be maintained and processed independently and in parallel, with these inputs being used in downstream processing circuits to mediate visually guided responses. This is somewhat analogous to our own intensity and colour vision, in which each dimension contributes its own measure of contrast in early visual processing (reviewed by Shapley (1990)). Here, this is referred to as the parallel channel model (Figure 2.1c). While the previously measured behaviours could result from either of these models, it has never been explicitly tested which one underlies the connectivity of a dipolatic visual system for a specific behavioural task.

There is a clear benefit for animals, and for crustaceans in particular, from using both intensity and polarization visual information independently. The mudflat environment in which fiddler crabs live is rich in polarization information, such as the polarization pattern of the sky and the predominantly horizontally polarized light reflected from damp areas of mudflat (Wehner, 2001; Zeil & Hofmann, 2001; How et al., 2015). Together, these different sources of polarized

light form a polarized background against which approaching targets (typically unpolarized) are viewed, thus creating a valuable source of visual contrast in addition to intensity cues. For instance, the main predators of fiddler crabs are birds that walk or fly over the mudflats (Zwarts, 1985; Koga et al., 1998; Iribarne & Martinez, 1999; Land, 1999). When viewed against the clear sky (Figure 2.2) or the mudflat (Figure 2.3), the intensity contrast between a bird and the background, e.g. whether it is positive (i.e. brighter than the background) or negative (i.e. darker than the background), will depend on the animal's colouration, the illumination conditions, and the viewing direction relative to the light source. In contrast, when polarization information is present, a bird will almost always be less polarized than the background and thus the opponent output of a dipolatic system, (measured as receptor contrast in Figure 2.2 and Figure 2.3) remains constant even if the intensity contrast varies spatially and/or temporally. Polarization contrast can therefore provide a more reliable source of information than intensity.

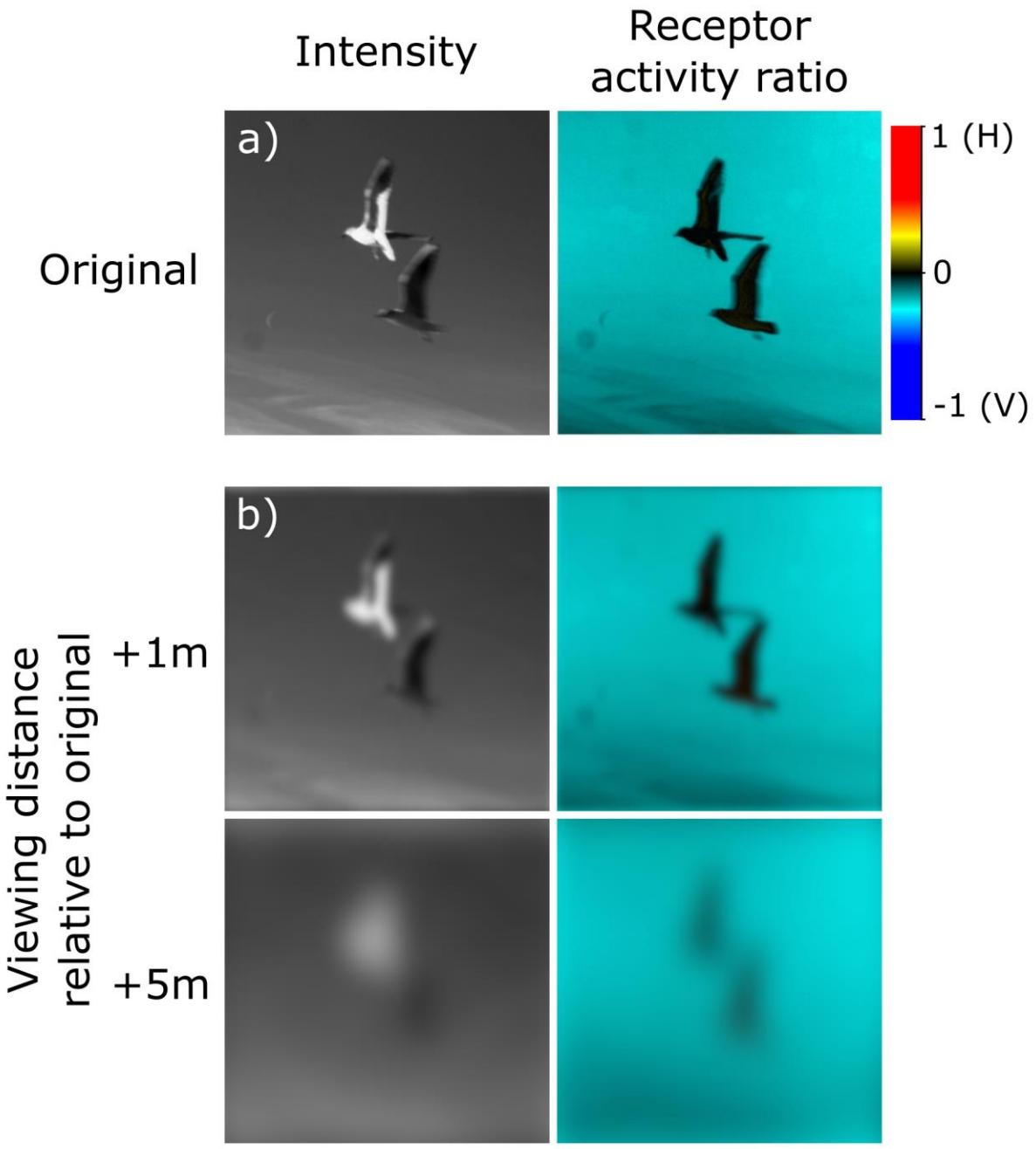

Figure 2.2: Images of two black headed gulls (*Chroicocephalus ridibundus*) viewed against a clear sky in **a)** intensity and polarization and **b)** the same images showing the visual features that are resolvable by the crabs at increasing viewing distance based on the visual resolution of the region of the eye in *Gelasimus vomeris* (data on *Afruca tangeri* was not available) viewing approximately 15°-20° above the horizon (Smolka & Hemmi, 2009; Caves & Johnsen, 2017). The polarization information is presented as a receptor activity ratio, i.e. the relative opponent output of the horizontally (H = 1) and vertically (V = -1) oriented photoreceptor channels calculated using a visual model (How & Marshall, 2014). Note how the intensity contrast of a predator can vary depending on the animal's coloration and illumination but the polarization contrast remains the same. See appendix A.3 for details on the polarization camera used to capture these images.

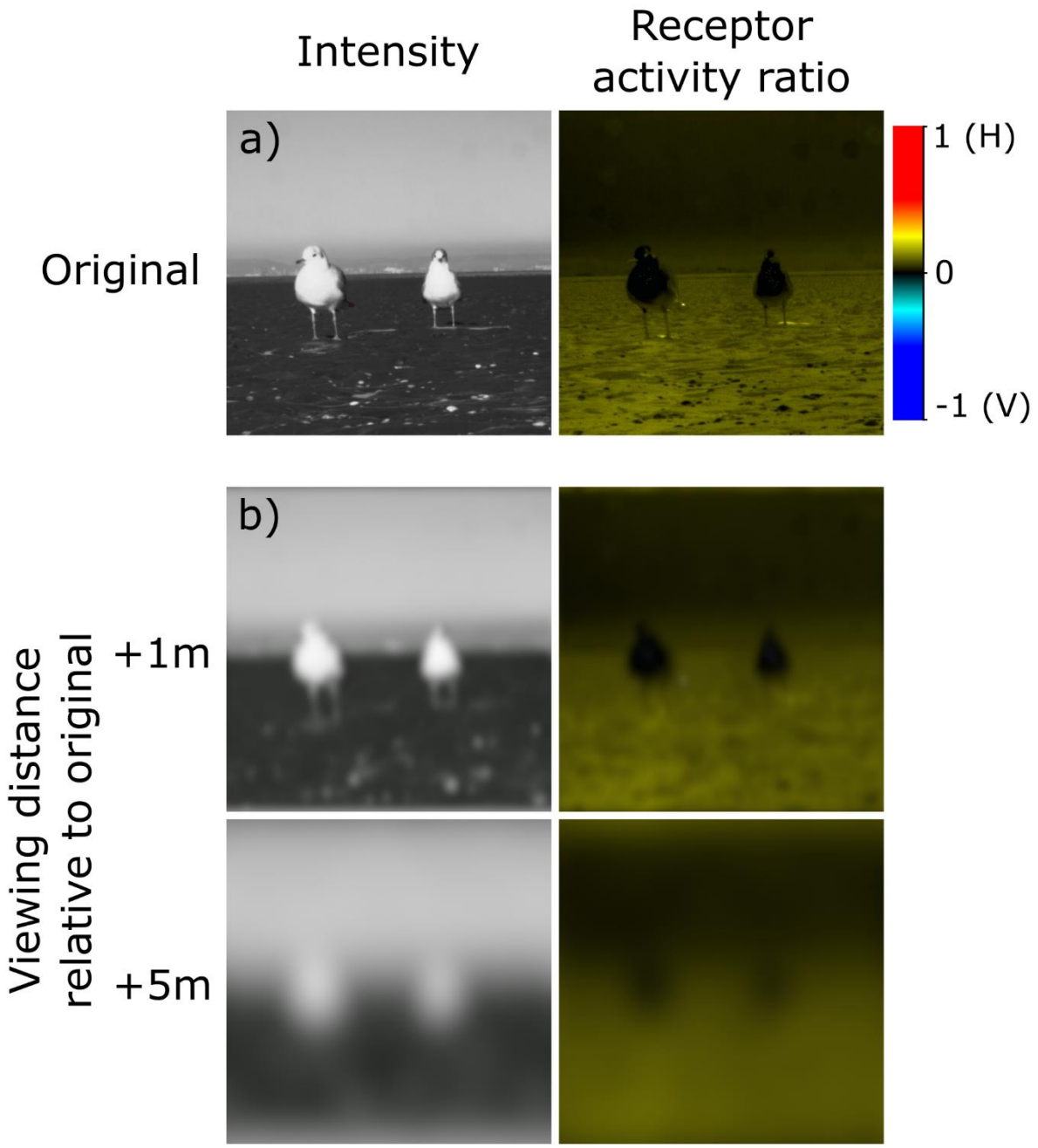

Figure 2.3: Images of two black headed gulls (*Chroicocephalus ridibundus*) viewed against a mudflat in (a) intensity and polarization and (b) the same images showing the visual features that are resolvable by the crabs at increasing viewing distance based on the visual resolution of the region of the eye in *Gelasimus vomeris* (data on *Afruca tangeri* was not available) viewing the horizon (Smolka & Hemmi, 2009; Caves & Johnsen, 2017). The polarization information is presented as a receptor activity ratio (see legend for Figure 2.2) (How & Marshall, 2014). See appendix A.3 for details on the polarization camera used to capture these images.

The aim of this study was to test whether a single channel or a parallel channel processing model functions in an animal with dipolat polarization vision. To this end a series of behavioural experiments was conducted with the fiddler crab *Afruca tangeri,* in which crabs were presented with a range of stimuli that differed in intensity and/or polarization, to test the predictions of the single- and parallel-channel response models.

2.2 Methods

2.2.1 Crab collection and preparation

Fiddler crabs (carapace width between 20 and 45 mm) were collected by hand from the mudflats of El Rompido, south west Spain (37.2207° N, 7.1238° W). Animal collection was carried out with the authorisation of Consejería de Medio Ambiente y Ordenación del Territorio de la Junta de Andalucía. Crabs were housed separately in plastic cups, with approximately 20 mm of fresh seawater and a folded strip of kitchen paper to provide a substrate (water and paper were changed daily). Crabs were kept for a maximum of five days under natural shade conditions and were fed with fish flake food (Purina, Friskies Multifloc) once a day. Prior to the experiment a wire harness consisting of a length of fishing wire that was looped at each end was glued to the crab's carapace. This allowed the crabs to be mounted above a treadmill for the experiments. The size (measured across the widest point of the carapace) and sex of each crab was recorded. After being tested the wire harness was removed and all crabs were released near the site of collection. A total of 436 crabs were tested across 11 experiments and each individual was only tested once.

2.2.2 Experimental setup

Each crab was loosely tethered on top of a 150 mm diameter Styrofoam treadmill (Figure 2.4a), suspended on a cushion of air supplied by a non-heating hair dryer (BaByliss 3Q), using a wire

hanger that was hooked through the harness glued to the crab's carapace and then introduced inside a metal guide positioned above the ball (How et al., 2012, 2014b). This allowed the crabs to walk freely while preventing translational or rotational movement. Stimuli were presented to the crabs using a custom-built intensity-polarization screen (IP screen) that allowed intensity and polarization contrasts (in the DoLP) to be adjusted independently (Figure 2.4b and Figure 2.4c). The screen consisted of two displays that were spatially and temporally synchronised: 1) a digital projector (CP-WX3030WN, Hitachi Ltd, Tokyo, Japan) that cast an intensity-based image onto a sheet of diffuser (#250 Half White Diffusion, Lee Filter, Andover, UK) on the rear surface of 2) a patterned vertical alignment liquid crystal display (PVA-LCD) panel dissembled from its outer casing (1905FP, Dell, Round Rock, USA) and with the outermost polarizer removed (Foster et al., 2018). Changes in pixel values addressed to the LCD panel caused alterations in the polarization of transmitted light, rather than intensity or hue. The model used in this experiment (and throughout this thesis) altered the DoLP across the majority of the 8-bit pixel scale, while keeping the AoP horizontal (Figure 2.4b and Figure 2.4c; note the AoP flips to near vertical at RGB values greater than ~180 thus all of the RGB values used in this study were well below this value). For all experiments, the background was set to a DoLP of 0.5. The IP screen was positioned directly in front of the crab, at a distance of 220 mm, and three other monitors (unmodified Dell 1905FP), two either side and one behind the crab, displayed a simulated visual horizon. A green filter with peak transmission at approximately 515 nm (#124, Lee Filters, Andover, UK) was positioned between the light source and the LCD panel of all the screens so that the output roughly corresponded with the peak sensitivity of the visual pigment within the R1-7 photoreceptors of the crabs (Lambda max = 530 nm) (Jordão et al., 2007).

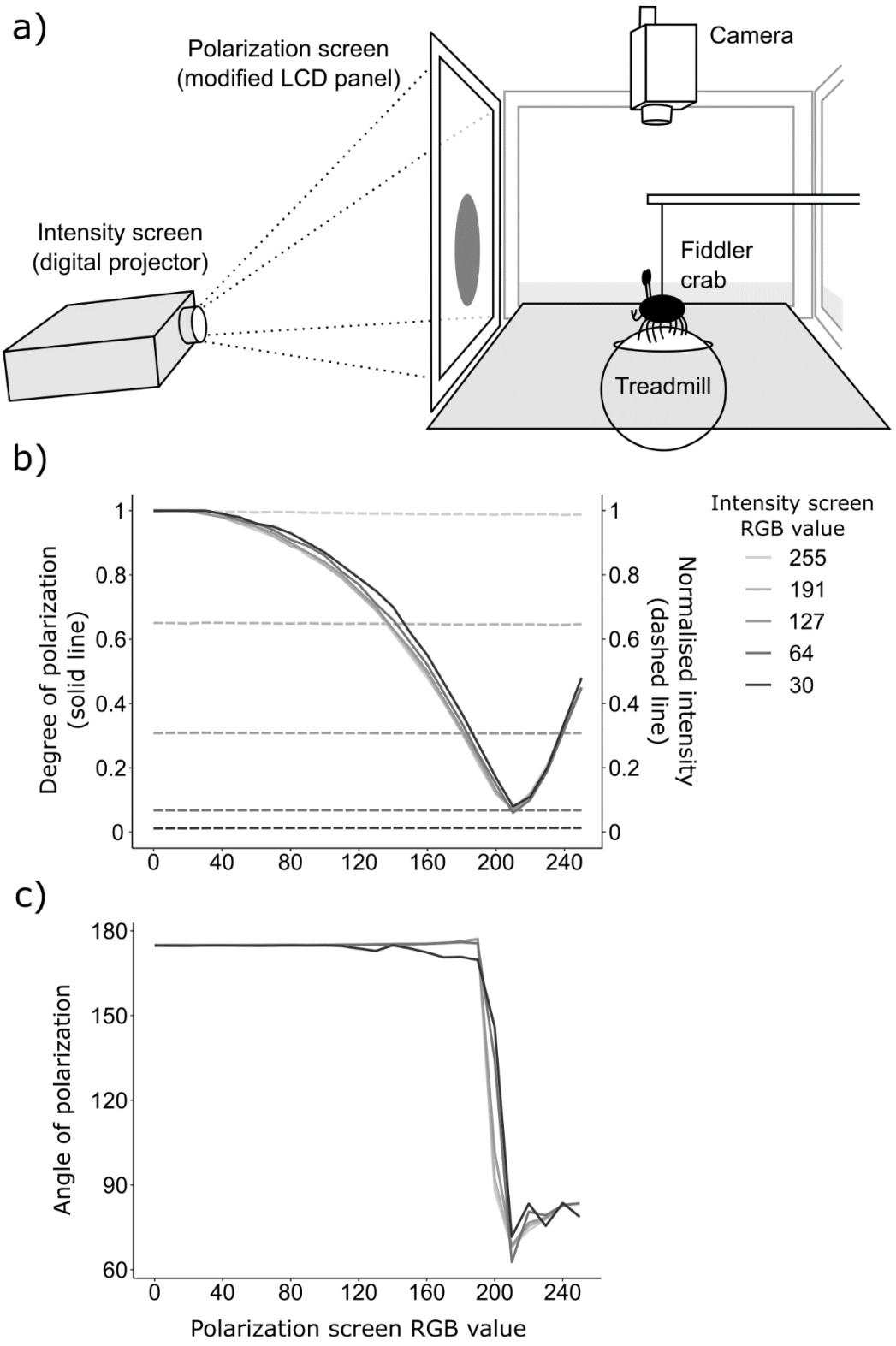

Figure 2.4: Experimental set up and properties of the intensity-polarization (IP) screen. **a)** Schematic of the treadmill apparatus and IP screen. Crabs were subjected to looming stimuli that varied independently in intensity (produced by the digital projector) and polarization (produced by the modified LCD panel). **b)** Degree of linear polarization (solid lines) and intensity (dashed lines), and **c)** angle of polarization measurements of the IP screen at different intensity and polarization screen RGB values (R=G=B).

A spectrometer (QE65000, Ocean Optics, Largo, USA) coupled to an optical fibre (P200-10-UV/VIS, Ocean Optics, Largo, USA) was used to measure the irradiance values of the IP screen. These were then used to calculate the Weber contrast of the stimulus/background combinations. Weber contrast was calculated as;

$$Weber\ contrast = \frac{I_O - I_B}{I_B}$$

where I_O is the intensity of the looming stimulus and I_B is the intensity of the background. A negative Weber contrast indicates the stimulus was darker than the background while a positive value indicates the stimulus was lighter than the background. Polarization properties were measured using a rotatable Glan-Thompson polarizer, with the polarizer at angles of 0°, 45°, 90° and -45°, coupled to the spectrometer (see appendix A.1 for details and calculations). The measured values were used to calculate the polarization distance (How & Marshall, 2014) between the stimulus and the background. The calculation of Weber contrast and polarization distance were based on the spectral sensitivity of the visual pigment within the R1-7 photoreceptors for *A. tangeri*. For this a pigment nomogram (Stavenga et al., 1993) was used to model the sensitivity of the visual pigment within the R1-7 photoreceptors given a lambda max of 530nm for *A. tangeri* (Jordão et al., 2007). Each spectrum was then multiplied by the pigment nomogram and the area under the resulting curve was used as a measure of perceived intensity (sometimes referred to as luminance); this was then used to calculate Weber contrast and polarization distance. It should be noted that this method does not account for other factors, many of which are unknown, such as the transmission of light through the ocular media or the effect of screening pigments. Calculating Weber contrast and polarization distance in this way was intended to provide the best possible approximation given the information available from the literature. Previous studies used the mean irradiance between 400-700nm to calculate

Weber contrast (e.g. Daly et al. (2017)) however both approaches yield very similar results (see appendix A.2).

2.2.3 Experimental procedure

The study consisted of 11 separate experiments (Table 2.1). Looming stimuli, consisting of expanding discs above the crab's visual horizon (to simulate an approaching predator), were presented to fiddler crabs using a fully automated protocol developed in Matlab (R2015a and R2016a, Mathworks, Natick, USA). After a 2 min acclimation period on the treadmill, each crab was presented with nine or ten stimuli (depending on the experiment) in a fully randomised order, with minimum between-stimulus intervals of 20 s plus a random pause of up to 20 s (any effect of habituation was controlled for in the statistical analysis and by the randomisation of the stimulus order). This pause was longer if the crab was stationary as Matlab was programmed to check that the crab was walking before initiating the next presentation. The looming stimulus expanded exponentially from a visual angle of 0° to 20° in a time of ~12 s. Behaviour and treadmill movement were recorded from above using a webcam (C270, Logitech, Lausanne, Switzerland). The crab's initial anti-predator freeze response was used as a proxy for the detection of the visual contrast in accordance with previous studies (How et al., 2012, 2014b). Response was scored automatically in Matlab at the end of each presentation using the two-dimensional motion detection algorithm (Zanker, 1996) which detected the motion of markings drawn on the polystyrene ball. The crab's response was scored within a 4 s window, 2 s before max loom size to 2 s after. As the crab's normal behaviour on the treadmill was to maintain a steady walk, a response to the stimulus was recorded if the animal stopped walking during the scoring window. Trials in which the crab was not walking at stimulus onset were rejected and the stimulus was appended to the end of the series for a repeat presentation (up to a maximum of five extra stimuli). Any effect of habituation was controlled for in the

statistical analysis (see below). Any remaining trials in which the crabs stopped before the scoring window were rejected post hoc. To limit the amount of time each crab spent on the treadmill, and thus any associated stress or motor fatigue the experiment was ended after 30 min.

Table 2.1: Description and sample size of the 11 experiments. WC = Weber contrast. PD = polarization distance.

Number	Experiment	Description	Sample size
1	I only	Varying intensity contrasts	46
2	P only	Varying polarization contrasts	44
3	I + fixed negative P (PD = -0.37)	Varying intensity contrasts with the addition of a fixed negative polarization contrast (PD = -0.37)	31
4	I (narrowed range) + fixed negative P (PD = -0.37)	Varying intensity contrasts (narrowed range) with the addition of a fixed negative polarization contrast (PD = -0.37)	30
5	P + fixed negative I (WC = -0.04)	Varying polarization contrasts with the addition of a fixed negative intensity contrast (WC = -0.04)	42
6	I + fixed positive P (PD = 0.43)	Varying intensity contrasts with the addition of a fixed positive polarization contrast (PD = 0.43)	30
7	I + fixed positive P (PD = 1.02)	Varying intensity contrasts with the addition of a fixed positive polarization contrast (PD = 1.02)	36
8	P + fixed positive I (WC = 0.04)	Varying polarization contrasts with the addition of a fixed positive intensity contrast (WC = 0.04)	44
9	P + fixed positive I (WC = 0.13)	Varying polarization contrasts with the addition of a fixed positive intensity contrast (WC = 0.13)	39
10	I only and I + P	Varying positive intensity contrasts on their own and the same intensity contrasts with the addition of a fixed negative polarization contrast	39
11	Combinations of I and P	Two negative intensity and polarization contrasts on their own and combinations of the two together	55

2.2.4 Statistical analysis

All statistical analysis was conducted in R (R Core Team, 2017). A mixed effects binary logistic regression was used to analyse the data from each experiment whereby the response variable was whether or not the crab responded. In specifying the maximum model, for the first set of experiments either Weber contrast (I only and I + fixed P) or polarization distance (P only and P + fixed I) was included as a continuous fixed effect. In the final two experiments both Weber contrast and polarization distance were included. Crab sex, size, and the presentation number (order) were included as additional fixed effects. The latter was included to control for any effect of habituation. Crab identification (to control for repeated measures) was included as a random effect. Model simplification was used to test for significant fixed effects. For this models were compared with one another using a likelihood ratio test (LRT) to sequentially remove non-significant effects. Finally, for the last experiment (combinations of I and P) experiment, pairwise McNemar tests were used to assess whether combined stimuli were more effective at eliciting responses than the most effective solo contrast.

2.3 Results

2.3.1 Predictions of single- and parallel channel models

Several predictions can be made about the probability of an individual responding to a controlled stimulus that comprises both intensity and polarization, depending on whether the information is processed with either a single or parallel channel model. If both forms of information are combined into a single measure of contrast then the addition of a fixed polarization contrast to a range of intensity contrasts (or *vice versa*) would cause a shift in the response minimum (Figure 2.5a, please refer to appendix A.4 for model calculations and explanation). Rather than falling to a minimum at the zero-contrast location on the x-axis, the curve would be shifted to the left or right (depending on the polarity of the combination),

revealing the contrast point where intensity and polarization cancel each other out. Alternatively, if polarization and intensity are processed in discrete and parallel channels then the model would predict an upwards shift in the response minimum (Figure 2.5b) as such a system would not suffer from cancellation points.

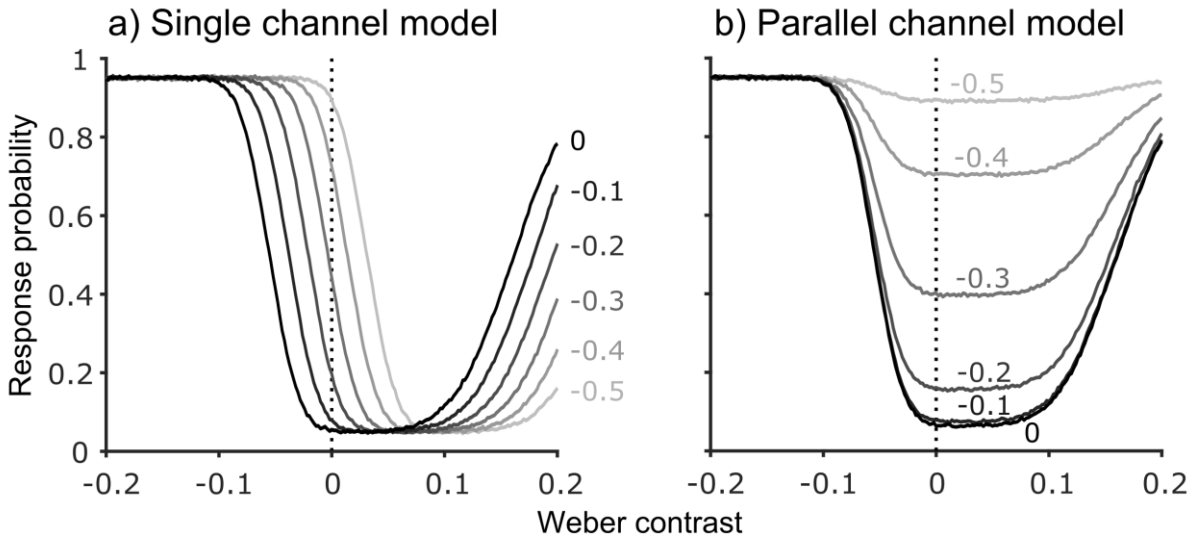

Figure 2.5: The predicted response probability of a simulated crab population (N=10,000) to a range of intensity contrasts, with the addition of a set of fixed polarization contrasts (polarization distance 0 to -0.5, grey lines in increasing lightness) using **a)** the single channel model and **b)** the parallel channel model (see appendix A.4 for model calculations and explanation).

2.3.2 Behavioural experiments

The predictions of the single and parallel channel models were tested using the series of behavioural experiments outlined in Table 2.1. Crabs responded strongly to both intensity-only and polarization-only looming stimuli, and response probability was positively correlated with the magnitude of the Weber contrast (Figure 2.6a; likelihood ratio test (LRT): $\chi^2_{(1)} = 55.5$, $P < 0.001$) and polarization distance (Figure 2.6b; LRT: $\chi^2_{(1)} = 19.12$, $P < 0.001$) respectively. In both cases, crabs responded to contrasts asymmetrically, with a greater response probability to negative Weber contrasts (i.e. when the stimulus was darker than the background) than to positive, and to negative polarization distances (i.e. less polarized than the horizontally

polarized background) than to positive. The shapes of the intensity-only and polarization-only response curves were similar (compare Figure 2.6a and Figure 2.6b).

To determine which shift in response probability occurs, the experiments were repeated with the addition of a fixed negative polarization or intensity contrast respectively (I + fixed negative P and P + fixed negative I). In both cases (Figure 2.6c and Figure 2.6d), the results showed an upwards shift in the response probability and there was no evidence for any cancellation points. This is supported by the fact that there was no longer a significant effect of Weber contrast (Figure 2.6c black dots; LRT: $\chi^2_{(1)} = 0.39$, $P = 0.533$). Similarly, the effect of polarization contrast was also reduced (Figure 2.6d; LRT: $\chi^2_{(1)} = 5.38$, $P = 0.02$). To confirm that a cancellation point had not been missed due to coarse sampling along the intensity contrast scale, the experiment from Figure 2.6c was repeated using a narrower intensity range with the same result (Figure 2.6c grey squares; LRT: $\chi^2_{(1)} = 0$, $P = 0.997$).

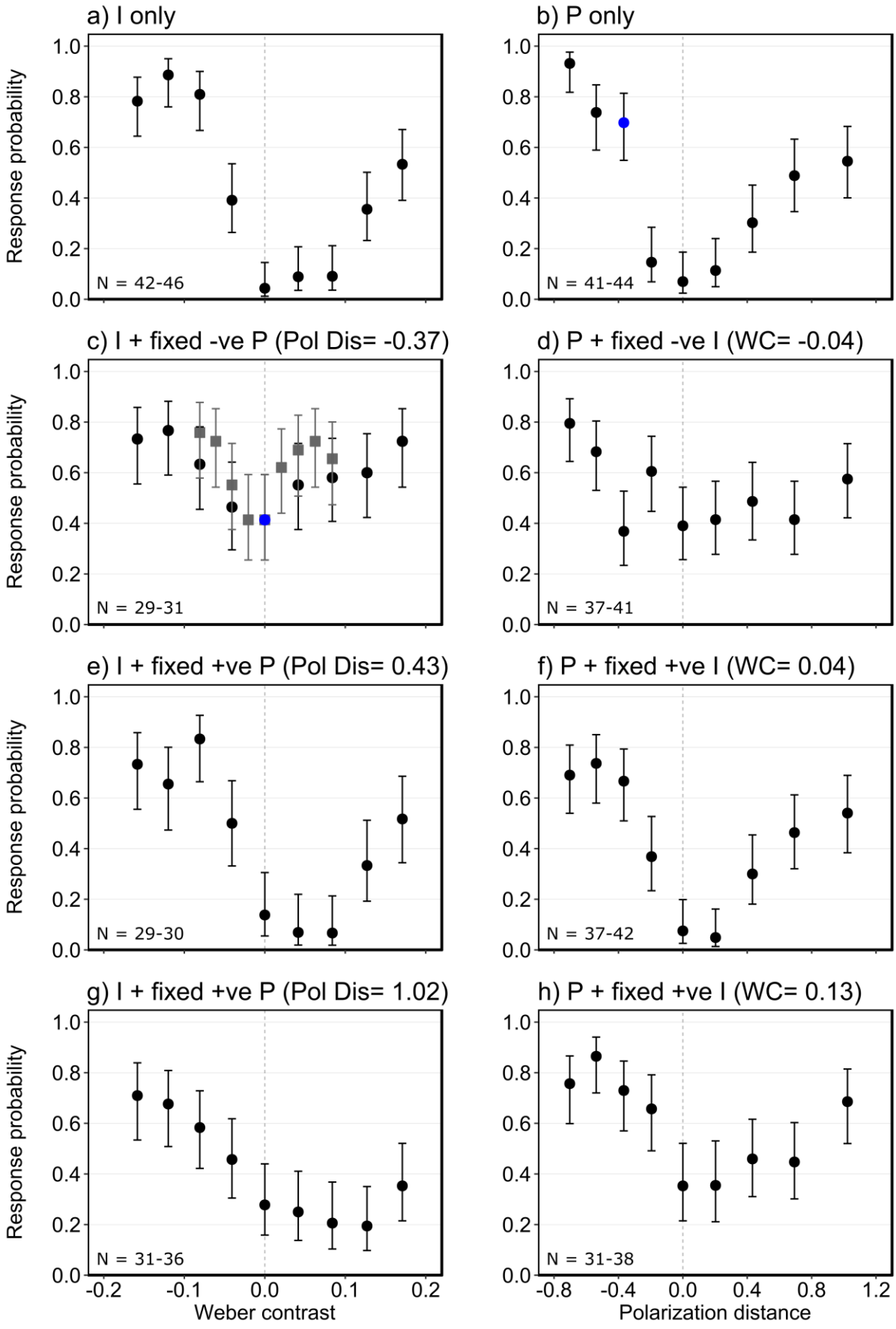

Figure 2.6 (legend on next page).

Figure 2.6 (previous page): Response probability (i.e. the proxy for detection of the visual contrast) of fiddler crabs to looming stimuli based on **a)** varying intensity contrasts, **b)** varying polarization contrasts, **c)** varying intensity contrasts with the addition of a negative polarization contrast, **d)** varying polarization contrasts with the addition of a negative intensity contrast, **e)** and **g)** varying intensity contrasts with the addition of a positive polarization contrast, and **f)** and **h)** varying polarization contrasts with the addition of a positive intensity contrast. Error bars are Wilson score intervals calculated using the sample size for each point (N) and the number of responses. Vertical dashed line is the location of zero contrast between stimulus intensity (for a, c, e, and g) or stimulus polarization (for b, d, f, and h) and the background. Note that data from two separate experiments are presented in (c), each with a different range of Weber contrasts. Note that the magnitude of response to any given stimulus depended on its contrast relative to that of the other stimuli tested within the same experiment rather than its absolute contrast. This is illustrated by comparing the response to the stimuli coloured blue in (b) and (c) both of which have the same polarization contrast (intensity contrast is zero). N is the number of animals that contributed to the response probability measured for each contrast.

To investigate if the addition of a positive contrast had the same effect, the intensity-only and polarization-only experiments were again repeated but this time with the addition of a fixed positive polarization or intensity contrast respectively (I + fixed positive P and P + fixed positive I). Although positive, the size of the fixed contrast was roughly the same as that used for the previous three experiment (i.e. Figure 2.6c and Figure 2.6d). The addition of the fixed positive polarization (Figure 2.6e) or intensity (Figure 2.6f) contrast had no effect on the overall level of response to the visual stimuli compared to the same stimuli in Figure 2.6a and Figure 2.6b respectively. Response probability remained highly dependent on the magnitude of the Weber contrast (Figure 2.6e; LRT: $\chi^2_{(1)} = 29.737$, $P < 0.001$) and polarization distance (Figure 2.6f; LRT: $\chi^2_{(1)} = 13.085$, $P < 0.001$). It was possible that the lack of an upwards shift in response probability following the addition of a fixed positive contrast could be attributed to the fact that the crabs were less responsive to positive contrasts compared to negative. Therefore, the I + fixed positive P and P + fixed positive I experiments were repeated using a greater positive weber contrast or polarization distance (Figure 2.6g and Figure 2.6h). In these experiments response probability continued to depend on the magnitude of the Weber contrast (Figure 2.6g; LRT: $\chi^2_{(1)} = 36.813$, $P < 0.001$) or polarization distance (Figure 2.6h; LRT: $\chi^2_{(1)} = 12.958$, $P < 0.001$). Nonetheless, Figure 2.6g does appear to show a small upwards shift in response probability with none of the stimuli eliciting a response probability below ~0.2. Likewise,

Figure 2.6h also shows an upwards shift in response to the stimuli with the lowest polarization contrast supporting the parallel channel model.

It is important to note that the response probability of a crab to any given stimulus depended on its contrast relative to that of the other stimuli tested within the same experiment rather than its absolute contrast. This makes it difficult to directly compare the magnitude of response probability between experiments (e.g. the contrast of the stimuli coloured blue in Figure 2.6b and Figure 2.6c are exactly the same). Therefore, to probe the interaction between the intensity and polarization channels further, multiple combinations of intensity and polarization contrasts were presented to crabs within single experiments. When, a near-threshold negative polarization contrast (P) was added to a series of negative intensity contrasts (I1-I4), it did not significantly boost response probability (Figure 2.7a; LRT: $\chi^2_{(1)} = 1.97$, $P = 0.161$ when data from the control (C; no intensity or polarization contrast) and P-only were excluded from the model). This is consistent with the results in Figure 2.6a and Figure 2.6c that show little or no change in response to the four darkest intensity stimuli (i.e. those with a negative Weber contrast) following the addition of the fixed negative polarization contrast (compare left side of Figure 2.6a with left side of Figure 2.6c). Furthermore, responses to combinations of two near-threshold intensity (Ia and Ib) and polarization (Pa and Pb) contrasts showed that, rather than interacting in an additive or multiplicative fashion to affect response probability, combined stimuli were no more effective at eliciting responses than the most contrasting channel on its own (Figure 2.7b).

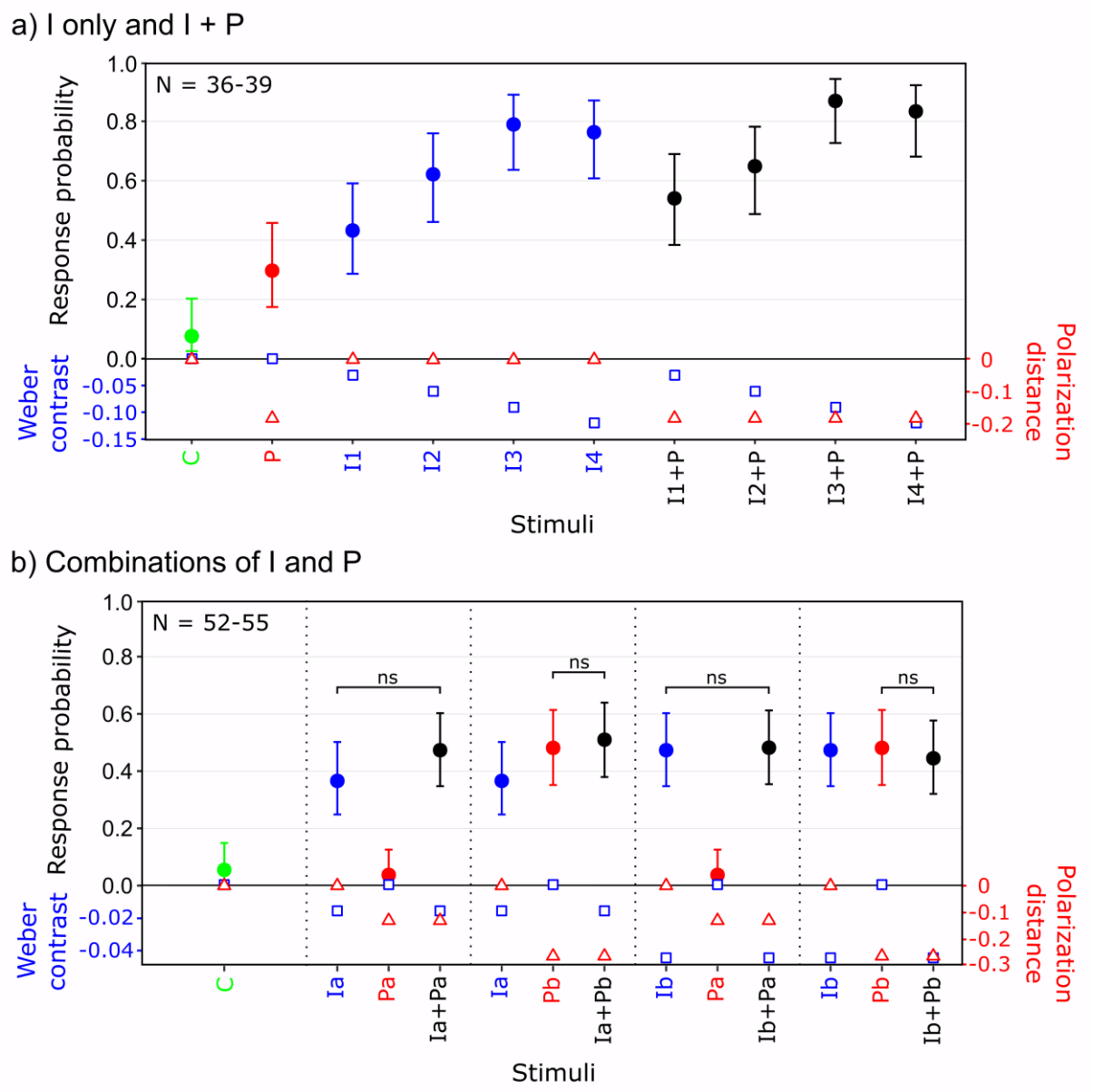

Figure 2.7. Interactions between intensity and polarization contrasts. **a)** Addition of a fixed polarization contrast (P) to a range of intensity only stimuli (I1-I4). **b)** Solo and combined effect of two intensity contrasts (Ia and Ib) and two polarization contrasts (Pa and Pb). Note that in (b), for clarity, each of the I- and P-only stimuli are plotted twice, once for each stimulus combination. C = control (no intensity or polarization contrast). Error bars are Wilson score intervals calculated using the sample size for each point (N) and the number of responses. Non-significance (ns) between the highest solo response probability and combined probability was determined using pairwise McNemar tests. Intensity and polarization contrast levels for each stimulus are plotted on the lower-most axes (Weber contrasts = blue squares; polarization distance = red triangles). N is the number of animals that contributed to the response probability measured for each contrast.

Several of the experiments showed evidence of habituation: I + fixed negative P (Figure 2.6c, black dots; LRT: $\chi^2_{(1)} = 12.71$, $P < 0.001$; grey squares; $\chi^2_{(1)} = 7.04$, $P = 0.008$), P + fixed negative I (Figure 2.6d; LRT: $\chi^2_{(1)} = 4.12$, $P = 0.043$), I + fixed positive P (Figure 2.6g; LRT:

$\chi^2_{(1)} = 13.659$, $P < 0.001$), P + fixed positive I (Figure 2.6f; LRT: $\chi^2_{(1)} = 4.45$ $P = 0.035$; Figure 2.6h; LRT: $\chi^2_{(1)} = 7.39$, $P = 0.007$), and the combinations of I and P (Figure 2.7b; LRT: $\chi^2_{(1)} = 7.45$, $P = 0.006$). This was controlled for by randomising stimulus order (meaning the effect of habituation would have been the same for all stimuli) and by including order within the statistical models. There was no effect of size or sex except for a weak significant effect of size for P + fixed positive I (Figure 2.6h; LRT: $\chi^2_{(1)} = 4.85$, $P = 0.028$) and sex for I + fixed positive P (Figure 2.6c black dots; LRT: $\chi^2_{(1)} = 4.05$, $P = 0.044$) and P + fixed positive I (Figure 2.6f; LRT: $\chi^2_{(1)} = 4.6745$ $P = 0.031$).

2.4 Discussion

2.4.1 Evidence for the parallel channel model

Overall, the findings of this study strongly support the suggestion that when detecting a moving object, fiddler crabs process polarization and intensity contrast separately and in parallel. They do not process these two visual dimensions as a single form of contrast as previously hypothesised for other crustaceans (Glantz & Schroeter, 2006, 2007). The key advantage of this method of processing polarization and intensity in a parallel system is that the separate channels of intensity and polarization provide a greater range of detectable contrast information for the receiver. Previous work has shown that crabs use polarization information for target detection within their natural habitat (How et al., 2015). Processing polarization and intensity in parallel channels would enhance the detection of a moving target by providing two alternative, non-conflicting, sources of information; overall increasing the chance of the crab spotting a potential threat. Such a parallel processing architecture does not suffer from the cancellation points inherent in the single channel model allowing the receiver to benefit from the more consistent polarization information (Figure 2.2), without it interfering with the perception of intensity. Meanwhile, the separate intensity channel will be particularly important

when polarization information is not available, for instance, when detecting a bird against a cloudy sky.

When considered in isolation it could be argued that Figure 2.6g is somewhat suggestive of the single channel model because the two stimuli with the greatest positive Weber contrast elicit a lower response than in Figure 2.6a suggesting that the addition of a strong positive polarization contrast may cancel out a positive intensity contrast. However, if a positive polarization contrast cancelled out a positive intensity contrast then it would also be evident in Figure 2.6h, which is not the case. Instead Figure 2.6h shows an upwards shift in the response curve following the addition of the fixed positive intensity contrast. It is also worth noting that the combination of a positive intensity contrast with such a high polarization contrast is unlikely to occur in nature and so does not represent a biologically relevant stimulus.

In the context of the animal's sensory ecology, the crab's initial anti-predator freeze response depends on whatever contrast is the most salient and above a certain response threshold, whether it be intensity or polarization. For instance, the addition of the fixed negative polarization contrast in Figure 2.6c only increased the response to the stimuli with the lowest Weber contrasts, indicating that in these cases it was the polarization contrast that was most salient while at higher Weber values the intensity contrast remained the most salient cue and so the addition of polarization appeared to have little effect. This is further supported by the findings of the second set of experiments (Figure 2.7), which show that when intensity and polarization contrasts were combined, the resulting response probability was the same as that to the most contrasting solo contrast, regardless of whether it was in intensity or polarization. It is apparent from the results that the polarity of the additional contrast (i.e. whether it was positive or negative) was very important. The addition of a fixed negative contrast had the

clearest enhancement affect. This is not surprising given that the crabs were more responsive to negative contrasts in both intensity and polarization. In comparison, when a fixed positive contrast was added, the additional weber contrast or polarization distance had to be much greater before it resulted in any upwards shift in the response curve.

2.4.2 Response to negative vs positive contrasts

An additional finding of interest is the similar asymmetry in the probability of response for the intensity only (Figure 2.6a) and polarization only (Figure 2.6b) experiments. The crabs were always more responsive to looms with a negative contrast (dark on light and less polarized on more polarized respectively). This asymmetric response to intensity contrasts has been well documented in other species from various taxa (Layne, 1998; Santer et al., 2005; Oliva et al., 2007; Yilmaz & Meister, 2013; Temizer et al., 2015). Layne (1998) for example, found that the fiddler crab *Leptuca pugilator* is more likely to respond to a dark target moving across a light background than to a light target moving across a dark background. The implication of this is that if a crab were approached by a bird with a weak positive intensity contrast, the polarization contrast would still be negative (Figure 2.2 and Figure 2.3) and so likely be the most salient cue in this instance. This further strengthens the argument that, when present, polarization can be a more reliable channel for detecting predators than intensity. The reliability of polarization information for target detection may also be an important driver behind the evolution of polarization vision in other species such as *Papilio* butterflies (Stewart et al., 2019).

Given that the intensity only and polarization only experiments both show a similar asymmetric response it could be argued that, when considered in isolation, this result suggests polarization and intensity contrasts are perceived similarly. For instance, it could be argued from Figure

2.6a and Figure 2.6b that negative polarization contrasts (i.e. less polarized than the horizontally polarized background; left side of Figure 2.6b) have a similar effect to negative intensity contrasts (left side of Figure 2.6a). If this were the case, given that in this study the AoP was always horizontal, it would imply that horizontally polarized light appears brighter than unpolarized light. However, the subsequent experiments reveal that this is absolutely not the case; instead polarization is processed in its own separate channel and is not detected as modulations of intensity. This is likely to have implication for other species of crustaceans that were thought to detect intensity and polarization similarly. For instance, previous work on crayfish concluded that *Procambarus clarkii* perceives a bright horizontally polarized stimulus as being equivalent to a darker unpolarized stimulus (Glantz & Schroeter, 2007). But as is evident from this study, just because an animal responds to a polarization contrast in a similar way to a given intensity contrast does not necessarily imply that they are detected in a similar way. It is therefore possible, perhaps even likely, that other crustaceans, such as crayfish, process intensity and polarization in a similar way to fiddler crabs and thus future research should aim to test this.

2.4.3 Neural substrate underlying the parallel channel model

If we consider the neural substrate, what evidence is there to support the parallel channel model? As described in section 1.3.2, in crabs the photoreceptor projections from the R1-7 terminate in the lamina where they synapse with monopolar cells within the external plexiform (epl1 and epl2). In the crayfish *Procambarus clarkii*, and gonodactyloid stomatopods, the horizontal receptors (R1, R4 and R5) terminate in epl1 and have synaptic sites with monopolar cell 3 (M3, coloured red in Figure 2.1a) while the vertical receptors (R2, R3, R6 and R7) terminate in epl2 and have synaptic sites with M4 (coloured blue in Figure 2.1a) (Sabra & Glantz, 1985; Kleinlogel & Marshall, 2005). Together, opponent processed outputs from M3

and M4 likely form an intensity-independent polarization channel. M2 has postsynaptic sites across both epl1 and epl2 with all seven photoreceptors (coloured black in Figure 2.1a) and is likely responsible for summing the inputs from both photoreceptor orientations to form a polarization-independent intensity channel (Strausfeld & Nässel, 1981; Sztarker et al., 2009). M2, M3 and M4 all terminate in the medulla (Strausfeld & Nässel, 1981; Sztarker et al., 2009), at which point, how the information is processed becomes less clear. In order for polarization contrasts to be determined, a mechanism of polarization opponency between the orthogonally orientated photoreceptors is first required (Bernard & Wehner, 1977; How & Marshall, 2014). This opponent mechanism almost certainly occurs within the crab's medulla where polarization opponent neurones (POL-neurons) likely receive antagonistic input from M3 and M4. The existence of POL-neurons has been studied in the medulla of crickets, locusts and cockroaches (Labhart, 1988; Loesel & Homberg, 2001; el Jundi et al., 2011; Homberg et al., 2011) and while comparably less is known about POL-neurons in crustaceans, polarization sensitive interneurons have been identified in the medulla of the crab *Scylla serrata* (Leggett, 1976) and tangential cells in the medulla of crayfish have been shown to exhibit polarization opponency (Glantz, 1996, 2001). Following this initial opponency between orthogonally orientated photoreceptors a measure of polarization contrast between different ommatidia (e.g. one viewing the object and the other the background) can be determined.

Speculation about the neural substrate involved with processing the separate intensity and polarization contrasts past this point is beyond the scope of this study. However, these results do suggest that the freeze response displayed by fiddler crabs during the first stage of their anti-predator response is likely controlled by a biphasic OR gate that receives two inputs, one from neurones relaying information on intensity contrast and the other information on polarization contrast. The OR gate would fire when one or both of these inputs is above a specific threshold.

Neural circuits that translate information about a looming stimulus into an escape response often rely on giant neurons and a relatively low number of synaptic connections to reduce processing time (Tomsic, 2016). A possible candidate involved in the control of the freeze response after the information has left the medulla is the bistratified lobula giant type 2 (BLG2) that has been well characterised in the crab *Neohelice granulate*, which has a similar life history to fiddler crabs (Medan et al., 2007; Tomsic, 2016). The BLG2 type neuron is most responsive when a loom is first detected, which coincides with the initial freeze response in *N. granulate*, but inactivates when the loom continues to expand (Tomsic, 2016).

Although not directly comparable, the separate channels for polarization and intensity may be thought of as being analogous to the well-studied M (magnocellular) and P (parvocellular) pathways of humans and old world monkeys that are generally considered to function as separate channels for intensity and colour information respectively (Shapley, 1990). Like the M and P pathways, the polarization and intensity channels start separately but likely converge at a later stage of visual processing to enable behavioural decision making. This therefore raises the possibility that they may be combined to form an image with separate layers of contrast information (Figure 2.8) analogous to how humans and other animals perceive intensity and colour information. In addition, there is some evidence to suggest that fiddler crabs are dichromatic (Horch et al., 2002; Detto, 2007; Detto & Backwell, 2009), presumably via an opponency between the short wavelength sensitive R8 receptor (which is not polarization sensitive) and the R1-7 receptors that are most sensitive to green wavelengths (Jordão et al., 2007). If this is the case, then future work might investigate whether intensity and polarization are integrated with potential colour channels.

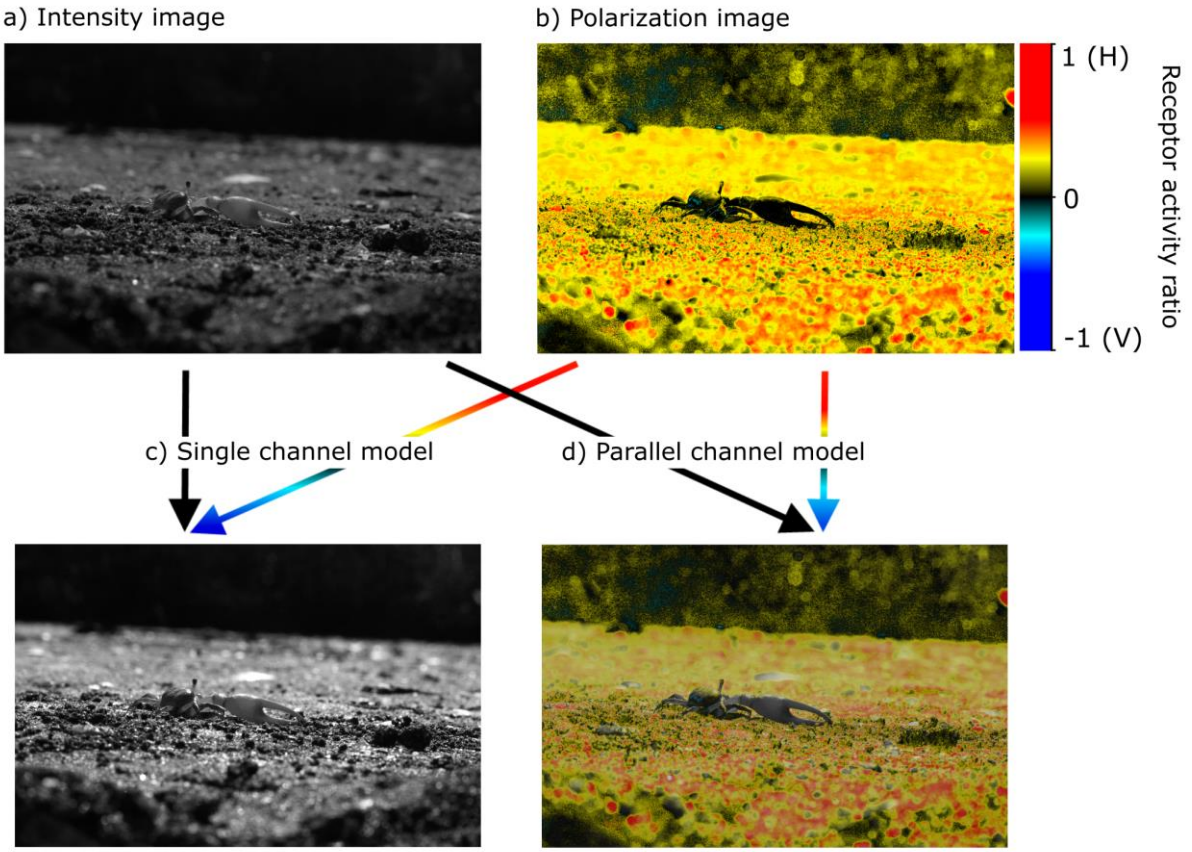

Figure 2.8. Image processing inspired by single and parallel channel models. An **a)** intensity and **b)** polarization image are combined, either to **c)** enhance intensity contrast through the single channel model, or **d)** as separate layers of contrast information using the parallel channel model.

2.4.4 Parallel processing of polarization and intensity in other animals

Parallel processing of intensity and polarization information has also been suggested for cuttlefish (Grable et al., 2002; Cartron et al., 2013b). In behavioural experiments Grable et al. (2002) compared how cuttlefish responded when placed on a checkerboard consisting of unpolarized black and white squares vs. one consisting of white paper overlaid by perpendicularly arranged square pieces of polarizing filter. The authors predicted that if polarization modulated intensity perception in cuttlefish then they would respond in the same way to both backgrounds. This was not the case suggesting that the cuttlefish did not detect the polarized background in the same way as the unpolarized intensity background (Grable et al., 2002). More recently, Cartron et al. (2013b) found that juvenile *Sepia officinalis* exhibit

differences in the maturation of polarization vs intensity contrast detection, again suggesting that polarization information is likely to be processed as a distinct channel of visual information. Further research is needed to test whether this is indeed the case. Given the close predator-prey relationship between many cephalopod and crustacean species, and that both have excellent polarization vision (How et al., 2012; Temple et al., 2012), it would be interesting to investigate whether there exist any parallels or differences in the way these two groups process polarization information.

2.5 Chapter summary

In summary, intensity and polarization information within a visual scene are processed independently in parallel channels within the visual system of fiddler crabs. Each form of visual information therefore contributes its own measure of visual contrast, which then feeds into processing circuits that mediate visually guided behaviour. This discovery proves that crabs, perhaps along with other crustaceans, do not simply detect polarization only as a modulation of the intensity information. Therefore, how these animals actually see polarization in terms of image forming is more complex and exciting than previously thought.

Chapter 3

The effect of null points of polarization discrimination on the detection of targets viewed against the sky

Testing fiddler crabs in their natural environment.

Oil painting on canvas by Kate Feller

One of the suggestions of the previous chapter was that polarization can provide a more consistent source of information about the approach of a potential predator than intensity. However, polarization information will not always be available or detectable by the crabs for a number of reasons. The study reported in this chapter investigated if the detection of polarization targets viewed against the sky is affected by null points of polarization discrimination that are intrinsic in the crab's dipolat visual system.

3.1 Introduction

The horizontal/vertical arrangements of the photoreceptors within the visual system of fiddler crabs is generally thought to function as a matched filter for detecting polarization contrasts against the mudflat (Wehner, 1987; Zeil & Hofmann, 2001; How et al., 2014b; How & Marshall, 2014). How et al. (2015) was the first to experimentally test in the field whether fiddler crabs use their polarization vision to enhance object detection. *Leptuca stenodactylus* were presented with an approaching target that differed from the background in either the AoP or DoLP. The crabs responded to the AoP and DoLP targets when they were 24% and 17% further away respectively than they did to a control target that did not change the polarization properties of the transmitted light (How et al., 2015). The study by How et al. (2015) neatly demonstrated that fiddler crabs use their polarization vision to enhance the detection of objects viewed against the mudflat under natural conditions. However, not all potential threats will be viewed against the surface of the mudflat. A key predator of many fiddler crab species are terns (such as *Gelochelidon nilotica*) that fly over mudflats in search of prey (Land, 1999; Smolka et al., 2011). In fact, the predation risk from these aerial predators is so high that some fiddler crabs species, such as *Gelasimus vomeris*, respond more often and sooner to flying terns than to any other bird (Smolka et al., 2011).

One of the suggestions from chapter 2 was that a bird viewed against the polarization pattern of the sky would appear less polarized than the background, in much the same way as a bird viewed against the mudflat. However, unlike reflections from the mudflat that are always roughly horizontally polarized (Zeil & Hofmann, 2001; How & Marshall, 2014), the polarization pattern of the sky is spatially and temporally variable, with both the DoLP and AoP depending on the area of sky being viewed and the time of day (Brines & Gould, 1982; Coulson, 1988; Horváth & Wehner, 1999; Cronin et al., 2006; Cronin & Marshall, 2011; Wang et al., 2016). A more detailed discussion of the polarization pattern of the sky can be found in section 1.1.2.

The variability of the sky's polarization pattern means that detecting unpolarized objects against the sky can be less reliable than detecting unpolarized objects against the mudflats. For instance, if we first consider the DoLP of the sky, a bird that is viewed against a patch of sky along a band that is 90º to the azimuth of the sun will present a higher polarization contrast in DoLP than a bird that is viewed against a patch of sky where the DoLP is lower, such as next to the sun. Secondly, because the AoP of light from a patch of clear sky is perpendicular to a line between the sun and the patch (Strutt, 1871; Coulson, 1988), meaning the AoP pattern forms concentric circles around the sun (see Figure 1.4b), certain solar positions will result in an AoP of around 45° or -45° across large parts of the sky (Brines & Gould, 1982). This has implications for fiddler crabs because the horizontal/vertical arrangement of their photoreceptors means that they have a null point of polarization discrimination at 45° and -45° (Bernard & Wehner, 1977; How et al., 2014b; How & Marshall, 2014; Basnak et al., 2018). For example, two stimuli with the same intensity, but one with an AoP of 45° and the other -45°, will be indistinguishable from one another, regardless of the DoLP of either stimulus, because the horizontal and vertical photoreceptors would be stimulated equally. Likewise, light

with an AoP of 45° or -45° will be indistinguishable from unpolarized light of the same intensity (Bernard & Wehner, 1977; How et al., 2014b; How & Marshall, 2014). Theoretically, an unpolarized bird viewed against the sky would not present a detectable polarization contrast if the AoP of the sky was ±45°, even if the DoLP of the patch of sky was high. In reality however, the extent to which these null points affect the ability of fiddler crabs to detect polarized and unpolarized objects depends on more than just the AoP of the background. For example, in lab experiments using looming stimuli, the fiddler crab *Uca heteropleura* was sensitive to differences in the DoLP of 0.23 when the AoP of the background and stimulus was -45° (How et al., 2014b). In comparison, when the AoP was horizontal the crabs were sensitive to a difference in DoLP of 0.08 (How et al., 2014b). The higher than expected sensitivity to the stimuli when the AoP was -45° was attributed to varying levels of eye alignment error that effectively moved the null points away from ±45° (How et al., 2014b). Given that in nature the AoP of any random patch of sky is unlikely to be exactly 45° or -45°, it remains to be tested if these null points have an ecologically important impact on the crabs in their natural environment.

The aim of this study was to test if fiddler crabs use their polarization vision to detect targets viewed against the polarization pattern of the sky and determine if the ability of the crabs to detect these targets is influenced by, i) the AoP of the sky (i.e. is response to an unpolarized or polarized target reduced when the AoP of the sky is near or at ±45°), and ii) the DoLP of the sky (i.e. is response to an unpolarized or polarized target reduced when the DoLP of the sky is lower)? To investigate this, a field experiment was conducted to determine the distance at which fiddler crabs first responded to a series of five different target treatments that approached the crab from above and were therefore viewed against the polarization pattern of the sky.

3.2 Methods

3.2.1 Crab collection and preparation

The study was carried out between the 4th and 14th May 2018. Fiddler crabs (*Afruca tangeri*) (carapace width between 22 - 31 mm) were collected by hand from mudflat sites in El Rompido (37.2207° N, 7.1238° W) on the south coast of Spain. Animal collection was carried out with the authorisation of Consejería de Medio Ambiente y Ordenación del Territorio de la Junta de Andalucía. Crabs were kept in the same way as in previous chapters, outside under shade for a maximum of five days and were fed with fish flake food (Purina, Friskies Multifloc) once a day. Prior to the experiment a wire harness, similar to that used in chapter 2, was glued to the crab's carapace so that it could be mounted above a treadmill. After being tested the wire harness was removed and all crabs were released. The field experiment was carried out close to the site of collection between the hours 09:30-13:30 (morning session) and 15:00-18:45 (afternoon session). A total of 50 crabs were tested (27 females and 23 males).

3.2.2 Experimental setup

The setup was inspired by previous studies (e.g. Hemmi (2005a), Hemmi & Pfeil (2010) and How et al. (2015)) that used a pulley system to investigate the response of fiddler crabs to visual targets in the field (Figure 3.1a and Figure 3.1b). The set up used a treadmill similar to that used in chapter 2, except it was adapted for use in the field. This field treadmill consisted of a 150 mm diameter Styrofoam ball floating in a bucket of water; the ball was held in position by four equally spaced ball transfer units screwed into a plastic platform placed over the bucket (Figure 3.1c). Crabs were tethered above the treadmill using a wire hanger that was hooked through the harness glued to the crab's carapace and then introduced inside a metal guide positioned above the ball. This allowed the crabs to walk freely in all directions while

preventing rotational movement, thus ensuring the crab was always facing the direction of the approaching target.

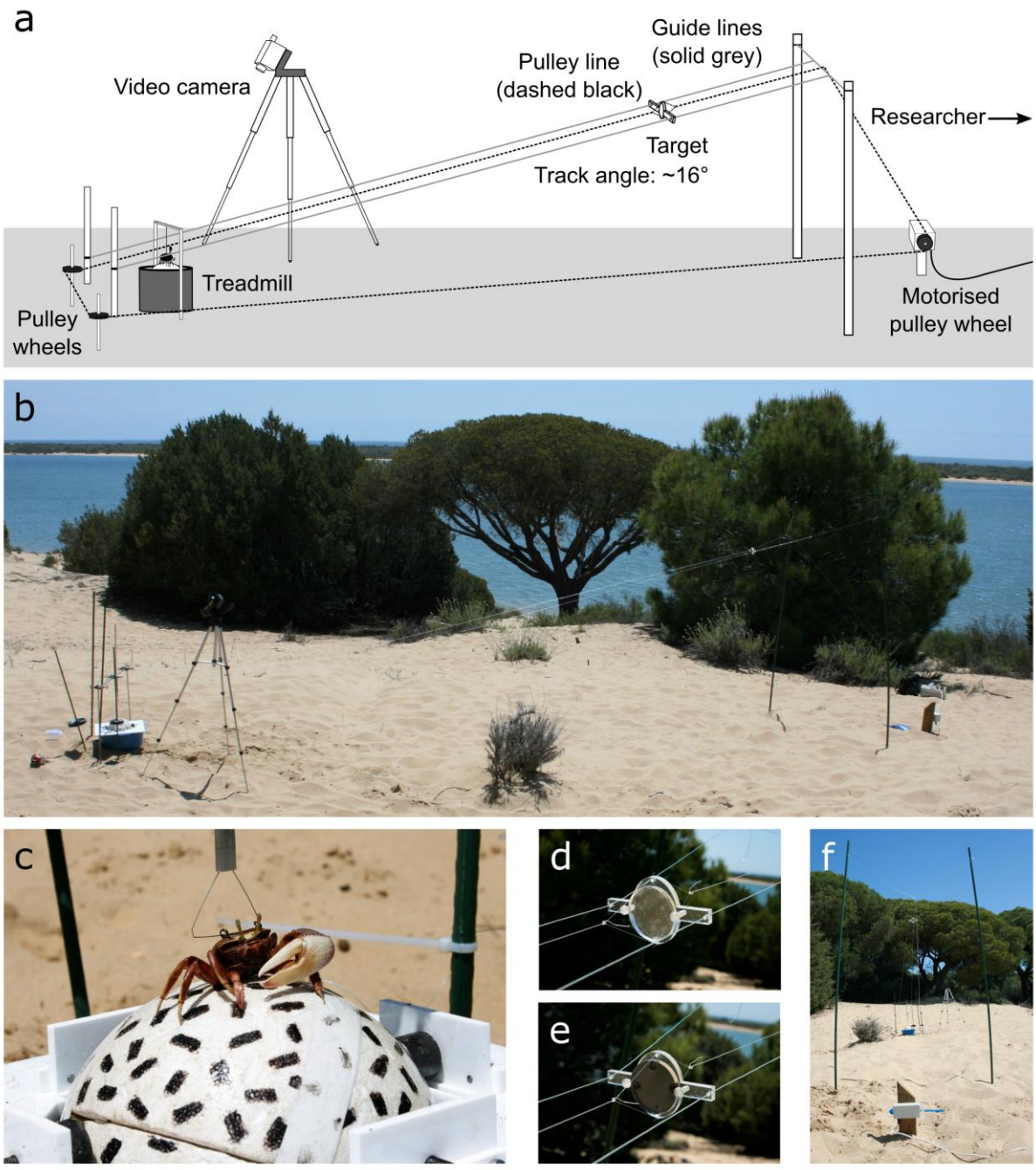

Figure 3.1: Experimental apparatus. **a)** Schematic and **b)** photo of the experimental set up built in the field. **c)** Field treadmill with fiddler crab held in position by the wire harness and hanger. **d)** Polarization (Pol-U) and **e)** intensity (Int) targets positioned in the target holder. **f)** Frontal view of the set up.

Each crab was shown five different target treatments in a random order. Each target was positioned in a 5 cm x 9 cm holder, made from 5 mm UV-visible transmitting Perspex. The arms of the holder were threaded on two parallel monofilament guidelines (0.5 mm Okuma ultramax line) (Figure 3.1d and Figure 3.1e). At one end these guidelines were tightly strung between two poles positioned behind the treadmill on either side at a height of approx. 30 cm. At the other end the guidelines were tied to the centre of a separate monofilament guideline suspended at a height of approx. 1.5 m between two poles set approx. 1.2 m apart and approx. 5 m from the position of the crab. The target was moved along the guidelines by a monofilament line attached to the front and back of the target holder and looped around two pulley wheels at the end next to the crab and a motorised wheel at the other end (Figure 3.1a, Figure 3.1b and Figure 3.1f). The target approached the crab from above at an angle of approx. 16° so that it was viewed against the sky. The speed and direction of the motorised wheel, and therefore the speed and direction of the target, was controlled by the researcher. The target moved at an average speed of approx. 33 cm/s. To ensure, as much as was possible, that the crabs viewed the targets against the patch of sky with the highest DoLP, and not into the sun, the position of the setup was changed between the morning and afternoon sessions. During the morning session the set up and the crab faced southwest while in the afternoon it was positioned to face southeast.

3.2.3 Target presentation

Five different target treatments (see section 3.2.5 for details) were presented in a random order to a total of 50 crabs. Each crab was positioned on the treadmill facing in the direction of the target. The crab was allowed a minimum of 2 min to acclimatise before the target began moving towards it, eventually stopping just in front of the crab's position. After each presentation the crab was transferred to a bucket of fresh sea water while the target was changed and reset to its

starting position. The behaviour of the crab, the rotation of one of the pulley wheels, and the last few seconds of the target's approach were recorded using a Sony HDR-SR11 Handycam.

3.2.4 Video analysis

A crab was recorded as having responded to the target's approach if it displayed any of the following behaviours: retracted limbs (legs and/or claws), flinching/walking away from the approaching target (e.g. stationary crabs started backing away from the target or walking crabs showed a change in direction away from the target), and sprinting away from target. In this study it was not possible to check that the crab was walking before initiating each target presentation. Consequently, although the freeze response was also recorded, this was not deemed to be a reliable or fair proxy for the detection of the target in this study because it was only applicable if the crab was walking when the target started moving. As such the freeze response was excluded from the analysis. Videos were blind scored in VLC media player 2.2.6 Umbrella. For each target presentation the following data were recorded: the time the target started moving (indicated by the rotation of the pulley wheel), the time it stopped in front of the crab, and the time the crab displayed any of the aforementioned behaviours. The speed of the moving target and the difference between the time of the first behavioural response and the time the target stopped in front of the crab were used to calculate how far away the target was from the crab when it first responded, i.e. response distance.

3.2.5 Target specifications

Four different target types were used to create the five treatments (two of the treatments used the same target as explained below). The four target types consisted of a control target, two polarization targets, and an intensity target. The control target (Co; Figure 3.2a) consisted of a 4 cm diameter circular piece of UV-visible transmitting Perspex (the same as that used to make

the target holder). The two polarization targets were identical to Co except one had a quarter-wave, and the other a half-wave, polymer retarder film (#88-252, Achromatic retarder 450-700 nm, Edmund Optics), which controlled the polarization properties of the transmitted light, attached to one side of the Perspex. The polymer retarder was the same as that used by How et al. (2015). The half-wave retarder was made from two layers of quarter-wave retarder.

Retarder film is a birefringent polymer sheet that modifies the polarization state, or phase, of transmitted light. Polymer retarders have a fast and slow axis that are perpendicular to one another. Light that is transmitted through a retarder may be thought to propagate through the fast axis more quickly than it does through the slow axis (Johnsen, 2012; Foster et al., 2018). Since the fast axis is always perpendicular to the slow axis it is common to describe the AoP in relation to the former, in which case it is referred to as the optic axis. In the case of a quarter-wave retarder, when the AoP of the incident light is parallel or perpendicular to either the fast or slow axes of the retarder, then the polarization state is unchanged as it passes through the retarder (Johnsen, 2012). When orientated in this way the target with the quarter-wave retarder functioned as an alignment control (Pol-C, Figure 3.2b; no polarization contrast). As detailed in section 1.1.1, linearly polarized light may be resolved into two perpendicular components. When the AoP of an incident beam of linearly polarized light is ±45° to both the fast and slow axes of the retarder, the component of the wave that passes through the slow axis is retarded one quarter of a wavelength out of phase from the other component that passes through the fast axis so that the linear polarized light is converted to circularly polarized light (see section 1.1.1 for details on circular polarization) (Johnsen, 2012). Since the visual system of crabs is insensitive to circularly polarized light, when AoP of the sky was at ±45° to the optic axis of the quarter-wave retarder, the target appears as unpolarized (Pol-U; Figure 3.2c; greatest contrast in DoLP). Considering either the fast or slow axis, if the angle of the retarder, θ, is, 0°

$< \theta < 45°$ or $45° < \theta < 90°$, to the AoP of the incident light, the light is converted to elliptically polarized light (Johnsen, 2012) and will appear partially polarized to the crabs. If the circular polarized light from the quarter-wave retarder passes through a second quarter-wave retarder (as is the case in a half-wave retarder) it is converted back into linearly polarized light, the AoP of which is 90° to the AoP of the light incident on the first retarder (Johnsen, 2012). Therefore, when the AoP of the sky was at ±45° to the optic axis of the target with the half-wave retarder, the target had an AoP that was perpendicular to the AoP of the sky (Pol-A; Figure 3.2d; greatest contrast in AoP). If the optic axis of either retarder was not aligned exactly ±45° to the AoP of the sky then the polarization contrast of the target would be reduced, (i.e. Pol-U would appear more polarized than intended and Pol-A would rotate the AoP by less than 90°). Pol-C therefore functioned as an alignment control. If, on average, the alignment of the optic axis relative to the AoP of the sky was poor then Pol-C and Pol-U would be predicted to elicit a similar response from the crabs.

Finally, the intensity target (Int; Figure 3.2e; greatest intensity contrast) was identical to Co except that a circular piece of black card was glued to it to block the transmission of light.

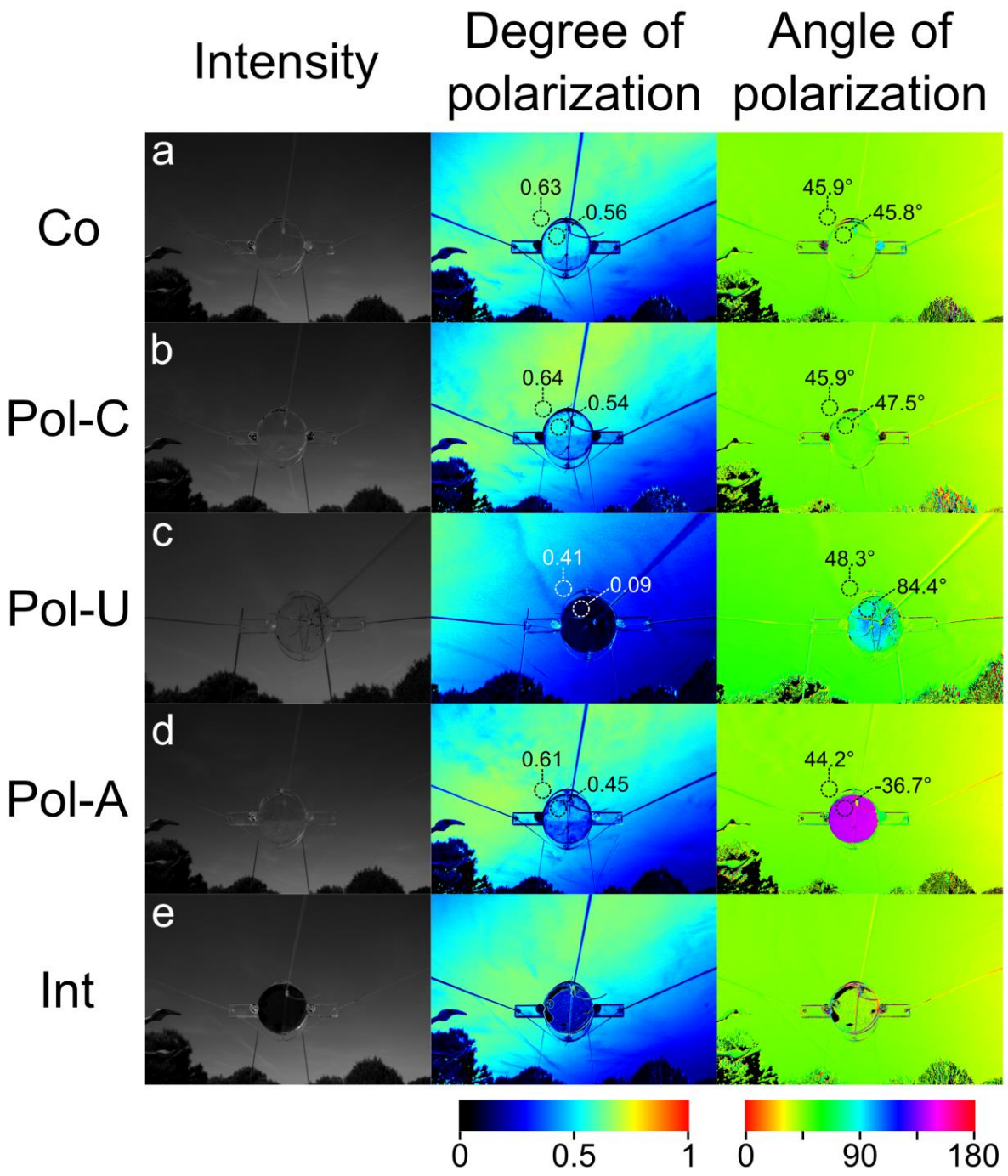

Figure 3.2: Polarization properties of the five target treatments (note that the same target was used for Pol-C and Pol-U). **a)** Co = control target (no intensity or polarization contrast). **b)** Pol-C = polarization control target; optic axis of the quarter-wave retarder aligned parallel to the AoP of the sky (low polarization contrast). **c)** Pol-U = unpolarized target; optic axis of the quarter-wave retarder aligned ±45º to the AoP of the sky (greatest contrast in DoLP). **d)** Pol-A = AoP target; optic axis of the half-wave retarder aligned ±45º to the AoP of the sky (greatest contrast in AoP). **e)** Int = intensity target (greatest intensity contrast).

The transmission of light through each of the targets was measured outside on a clear a day using a spectrometer (QE65000, Ocean Optics, Largo, USA) coupled to an optical fibre (P200-10-UV/VIS, Ocean Optics, Largo, USA; acceptance angle = 12.7°; full angle = 25.4°) with an SMA type connector. The optical fibre was directed towards a patch of clear blue sky, and held in position using a clamp stand. The irradiance of the patch of sky was then measured through the four target types, Co, Pol-C/Pol-U (quarter-wave retarder), Pol-A (half-wave retarder) and Int, along with the irradiance of the unobstructed sky (Figure 3.3a). The target was positioned directly against the end of the optical fibre so that the fibre only collected light that had been transmitted through the target. Each set of measurements was repeated 11 times with the order the measurements were taken randomised each time. For each set of measurements the irradiance spectra of the unobstructed sky was used as the reference to calculate the percentage of light transmitted through each of the targets. The percentage transmission was calculated as:

$$Percentage\ transmission = \frac{Irradiance\ through\ target}{Irradiance\ of\ unobstructed\ sky} \times 100$$

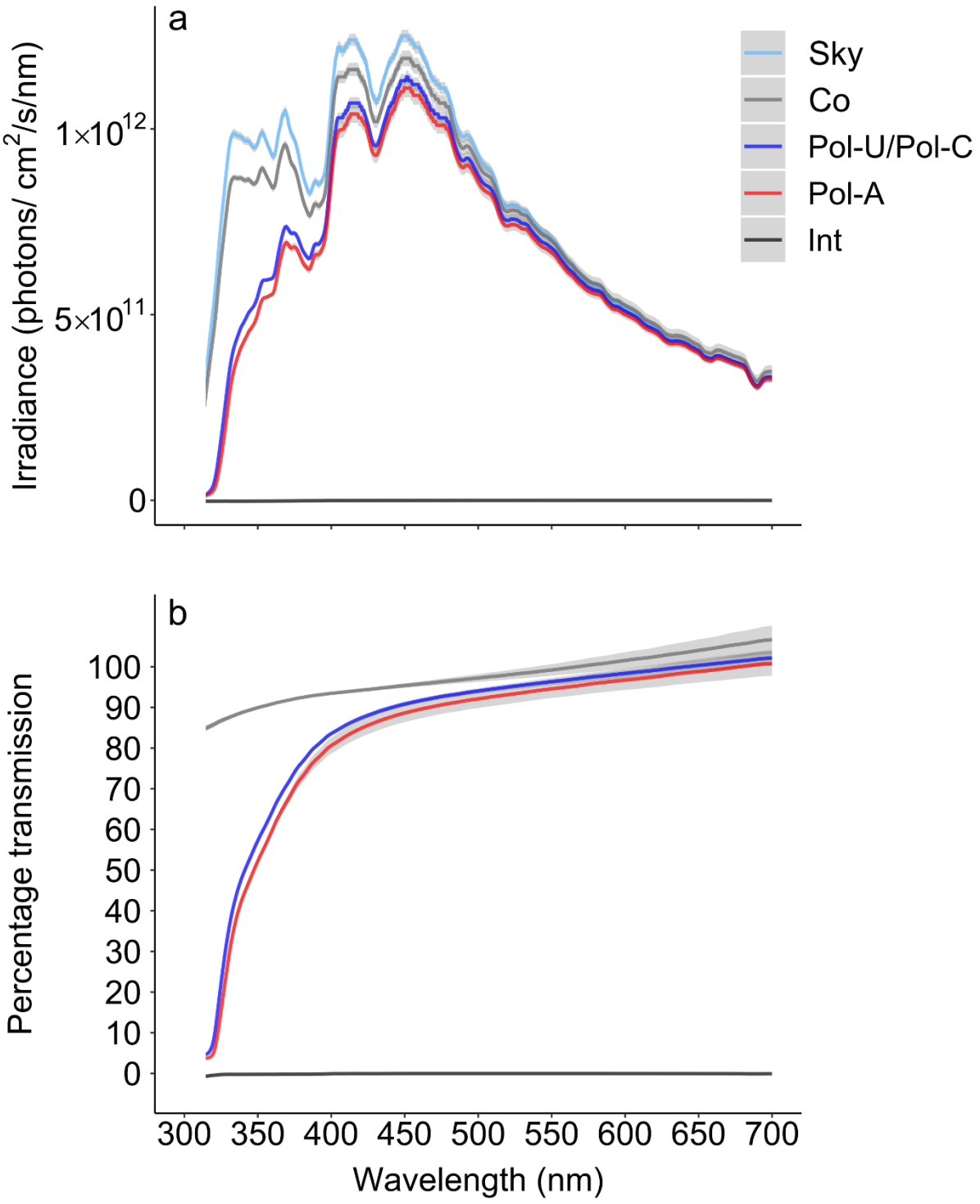

Figure 3.3: Transmission of light through the targets. **a)** The irradiance of a patch of clear sky compared to the irradiance of the same patch measured through the four targets (note that the same target was used for the Pol-C and Pol-U treatments). **b)** The percentage transmission through each target. The grey shaded area around each line in (a) and (b) shows the SD. For comparison, irradiance measurements taken in the field at different times of day are included in appendix A.5.

The quarter- and half-wave retarders were most efficient at transmitting wavelengths between 450-700 nm, but less efficient at transmitting wavelengths below 450 nm, with the biggest drop in transmission below 400 nm (Figure 3.3b). Consequently, the retarder film produced an intensity contrast that increased at ultraviolet wavelengths (UV). In *A. tangeri* the visual pigment within the R1-7 photoreceptors, which constitute the vast majority of the length of the rhabdom, has a lambda max of approx. 530 nm (Jordão et al., 2007). The R1-7 receptors would, at least theoretically, be sensitive to wavelengths within the UV and violet region of the spectrum (Stavenga et al., 1993; Govardovskii et al., 2000). Furthermore, sensitivity to short wavelengths has been shown in the shore crab *Carcinus maenas* (peak sensitivity approx. 440 nm) and the fiddler crab *Leptuca thayeri* (peak sensitivity approx. 430 nm) where it is associated with the small distally located R8 receptor (Martin & Mote, 1982; Horch et al., 2002). There is also behavioural evidence of UV sensitivity in the fiddler crab *Austruca mjoebergi* (Detto & Backwell, 2009). Therefore, to estimate if the difference in intensity between Co and the targets fitted with the retarder would have been detectable by the crabs the spectra from Figure 3.3a were used to calculate the Weber contrast between each target and the sky (see section 2.2.2 for details of calculating Weber contrast) based on the sensitivity of the visual pigment in the R1-7 photoreceptors of *A. tangeri* (Jordão et al., 2007) and the sensitivity of the R8 of *L. thayeri* (Horch et al., 2002) (Table 3.1). The UV contrast generated by the retarders and its potential implication are discussed in details within the discussion.

Table 3.1: Estimated Weber contrast between the four target types and the sky, and the difference in Weber contrast between each target and Co, after accounting for the sensitivity of the R1-7 receptors of *Afruca tangeri* (Jordão et al., 2007) and the R8 receptor of *Leptuca thayeri* (Horch et al., 2002).

Target	Weber contrast ± SD		Difference in Weber contrast between targets and Co ± SD	
	R1-7 Lambda max = 530nm	R8 Peak sensitivity = 430nm	R1-7 Lambda max = 530nm	R8 Peak sensitivity = 430nm
Co	-0.036 ± 0.009	-0.064 ± 0.003	na	na
Pol-C/Pol-U	-0.121 ± 0.006	-0.19 ± 0.005	-0.084 ± 0.01	-0.157 ± 0.006
Pol-A	-0.145 ± 0.019	-0.22 ± 0.017	-0.108 ± 0.022	-0.127 ± 0.019
In	-1 ± 0.0002	-1 ± 0.0002	-0.965 ± 0.009	-0.938 ± 0.003

3.2.6 Photographic polarimetry

Before testing each crab, photographic polarimetry was used to obtain measurements of the polarization properties of the patch of sky against which the targets would be viewed. The first target treatment to be presented to the crab was visible in these photos. The camera was positioned at the height and position of the crab so the target was approximately 5 m from the camera. A set of four photos were taken through a polarizing filter (SMC CIR-PL, Hoya), orientated at 0°, 45°, 90°, and -45°, fitted to a Canon EOS 400D DIGI digital camera with a Canon EFS 18-55mm lens. All camera settings were kept constant for each of the four photos. An infra-red remote trigger was used to avoid camera shake. In accordance with previous studies (e.g. How & Marshall (2014) and How et al. (2015)) the green channel (which best represents the spectral sensitivity of the R1-7 receptors) was extracted from these images and intensity differences between the four images were used to calculate the DoLP and AoP within the visual scene (Wolff, 1997; Foster et al., 2018). Examples of the polarization photos are provided in appendix A.6 and Figure 3.4. The DoLP and AoP of the sky were averaged across six points around the circumference of the target (Figure 3.4). The polarization properties of the sky during each target presentation were obtained from the polarization photo that was

taken closest to the time that each target was presented. In order to test if the crab's null points at ±45° had an effect on the response distance, the AoP of the sky was used to calculate the distance from the closest null point (i.e. 45° or -45°). For instance, if the AoP of the sky was 40°, then the distance from the crab's closest null point (i.e. 45°) would be 5°.

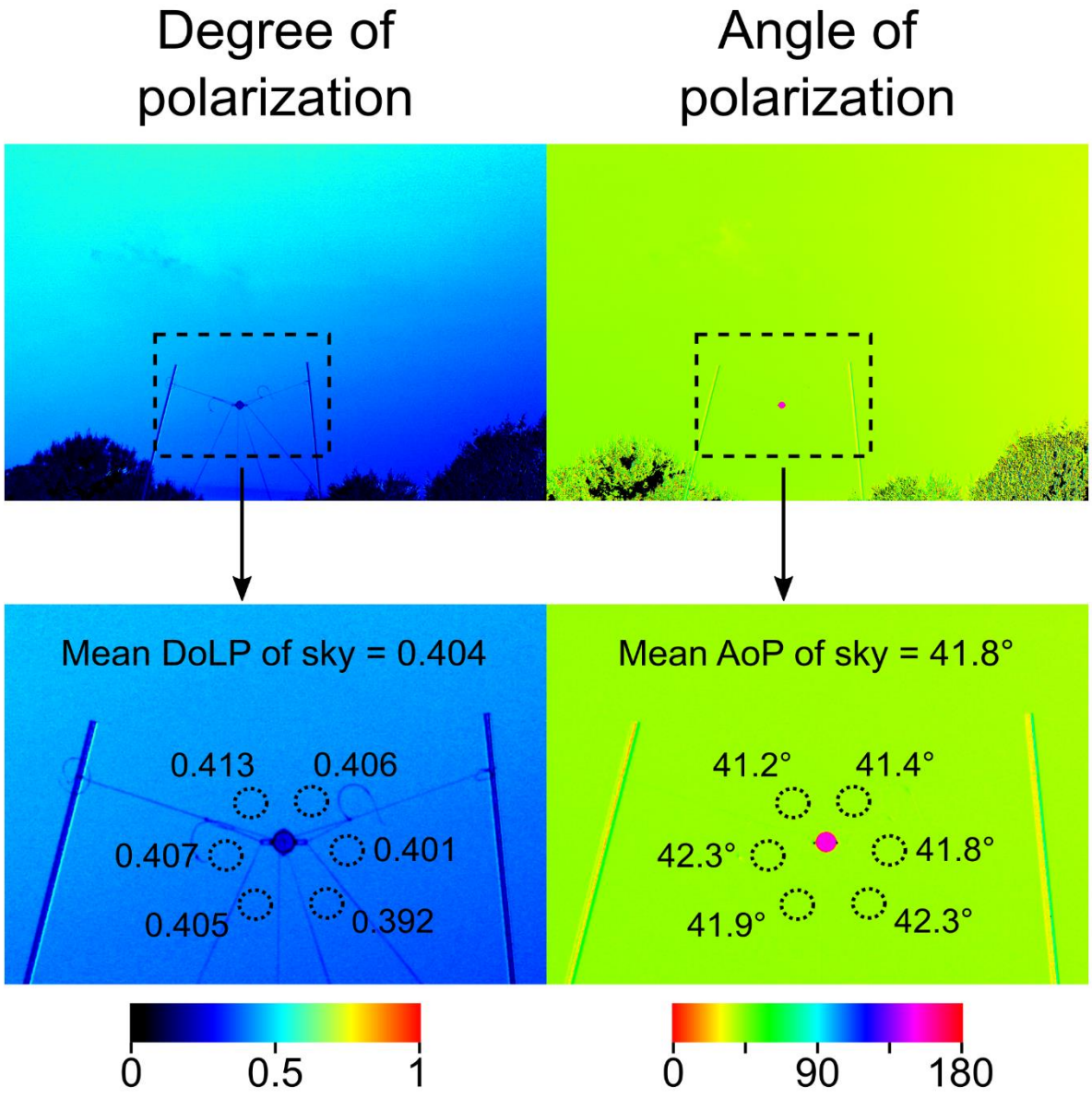

Figure 3.4: Example of a polarization image (showing Pol-A, i.e. greatest contrast in AoP) used to measure the DoLP (left) and AoP (right) of the patch of sky the targets were viewed against. The DoLP and AoP were sampled from six points around the circumference of the target (dashed circles) and used to calculate the mean DoLP and AoP of the background. A new set of polarization photos were taken at the start of each trial (i.e. each time a new crab was tested).

3.2.7 Modelling response to the UV contrast vs polarization contrast

The parallel channel model from chapter 2 was used to probe how the polarization and UV contrast properties of the treatments may have interacted to effect behavioural response of the animals. For each of the 50 presentations of each target treatment, the polarization properties of the sky were used to estimate the polarization distance (How & Marshall, 2014) between the sky and the target. The estimated values of polarization distance assumed that Pol-C did not change the polarization of transmitted light, Pol-U changed the DoLP of transmitted light to 0 but did not change the AoP, and Pol-A rotated the AoP by exactly 90° but did not change the DoLP. For the UV contrast the estimated Weber contrast detected by the R1-7 photoreceptors from Table 3.1 was used. Further details about model calculations and explanation can be found in appendix A.4.1.

The output from the parallel channel model is response probability, whereas the experiment in this study measured response distance. Therefore, the model was not intended to replicate or predict the results of the current study. The model was used to predict whether we would expect to see a difference in response level between Pol-C, Pol-U and Pol-A, and whether this difference would be masked by the estimated intensity contrast, if stimuli with the same polarization and intensity properties as the target treatments in this study were to be presented to crabs in lab experiments similar to those in chapter 2.

3.2.8 Statistical analysis

All statistical analysis was conducted in R (R Core Team, 2017). Linear mixed effects models, fitted using the lme4 package (Bates et al., 2015), were used to test whether there was a difference in response distance (i.e. how far away the target was when the crab first displayed one of the scored behaviours) between the different target treatments. Response distance was

used as the response variable. Target treatment, DoLP of the sky, the distance from closest null point, and an interaction between target and each of the other two factors, were included as fixed effects. Presentation order was also included as a fixed effect to test and control for any effect of habituation. Crab identification was included as a random effect factor to account for the repeated measures design (i.e. each crab saw all five treatments). Model simplification was used whereby models were fitted by maximum likelihood and compared using a likelihood ratio test (LRT) to sequentially remove non-significant interactions and effects.

For the results from the parallel channel model, Pearson's Chi-squared tests were used to test for differences in the predicted level of response to Pol-C, Pol-U and Pol-A when the model was run with polarization only, intensity only and both polarization and intensity. Planned pairwise comparisons were carried out using Pearson's Chi-squared tests. A Bonferroni correction was applied to control for multiple testing.

3.3 Results

3.3.1 Response distance to the targets

Response distance depended on an interaction between the target treatment and the distance from the closest null point (likelihood ratio test: target-distance from null point interaction: $\chi^2_{(4)} = 11.86$, $P = 0.018$; Figure 3.5 and Figure 3.6). In regards to target treatment, overall the crabs tended to respond to Pol-C, Pol-U and Pol-A further away than they did to Co, and to Int at a greater distance than they did to Pol-C, Pol-U, Pol-A and Co (Figure 3.5, insert). There appears to be no difference in response distance between Pol-C, Pol-U and Pol-A. On average, the crabs responded to Co when it was 46.26 cm ± 4.72 cm (mean ± SEM) away, while they responded to Pol-C at 79.66 cm ± 6.78 cm, Pol-U at 81.59 cm ± 7.43 cm, Pol-A at 78..18 cm ± 7.48 cm and Int at 103.06 cm ± 9.77 cm (i.e. 72.2 %, 76.4%, 69% and 122.8% further away than Co

respectively). In regards to the distance from the closest null point, there was a positive correlation between response distance and the distance from the closest null point for Pol-U and Int, but not for Co, Pol-C and Pol-A (Figure 3.6). The absolute value of the DoLP of the sky had no effect on response distance (LRT: $\chi^2_{(1)} = 0.03$, $P = 0.853$; Figure 3.7) regardless of the target treatment. The crabs did show signs of habituation (LRT: $\chi^2_{(1)} = 4.75$, $P = 0.029$), however the effect of habituation would have been the same for all targets due to the randomisation of target order.

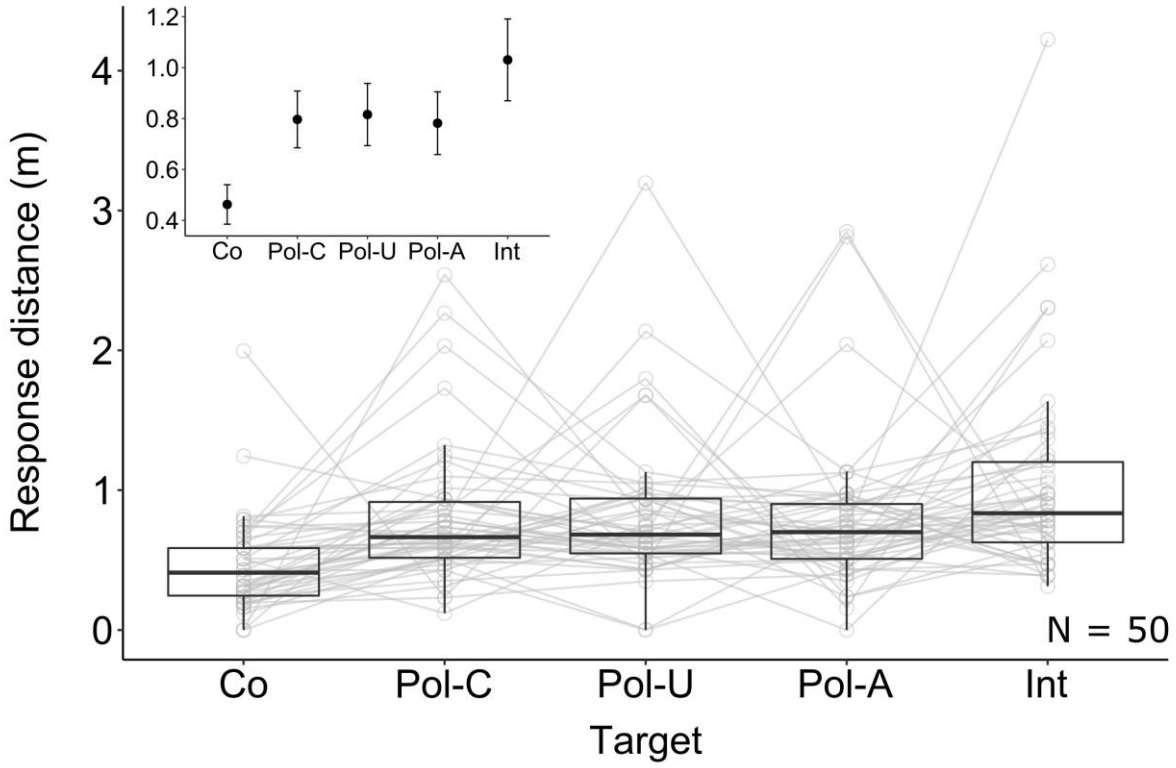

Figure 3.5: Detection distance of the five target treatments by fiddler crabs. Co = control target (no intensity or polarization contrast). Pol-C = polarization control target; optic axis of the quarter-wave retarder aligned parallel to the AoP of the sky (low polarization contrast). Pol-U = unpolarized target; optic axis of the quarter-wave retarder aligned ±45º to the AoP of the sky (greatest contrast in DoLP). Pol-A = AoP target; optic axis of the half-wave retarder aligned ±45º to the AoP of the sky (greatest contrast in AoP). Int = intensity target (greatest intensity contrast). The grey lines join data points from the same individual crab. Box plots show medians plus the interquartile range (IQR), whiskers are the lowest and highest values that are within 1.5 times the IQR from the upper and lower quartiles. Insert shows means with 95% confidence intervals.

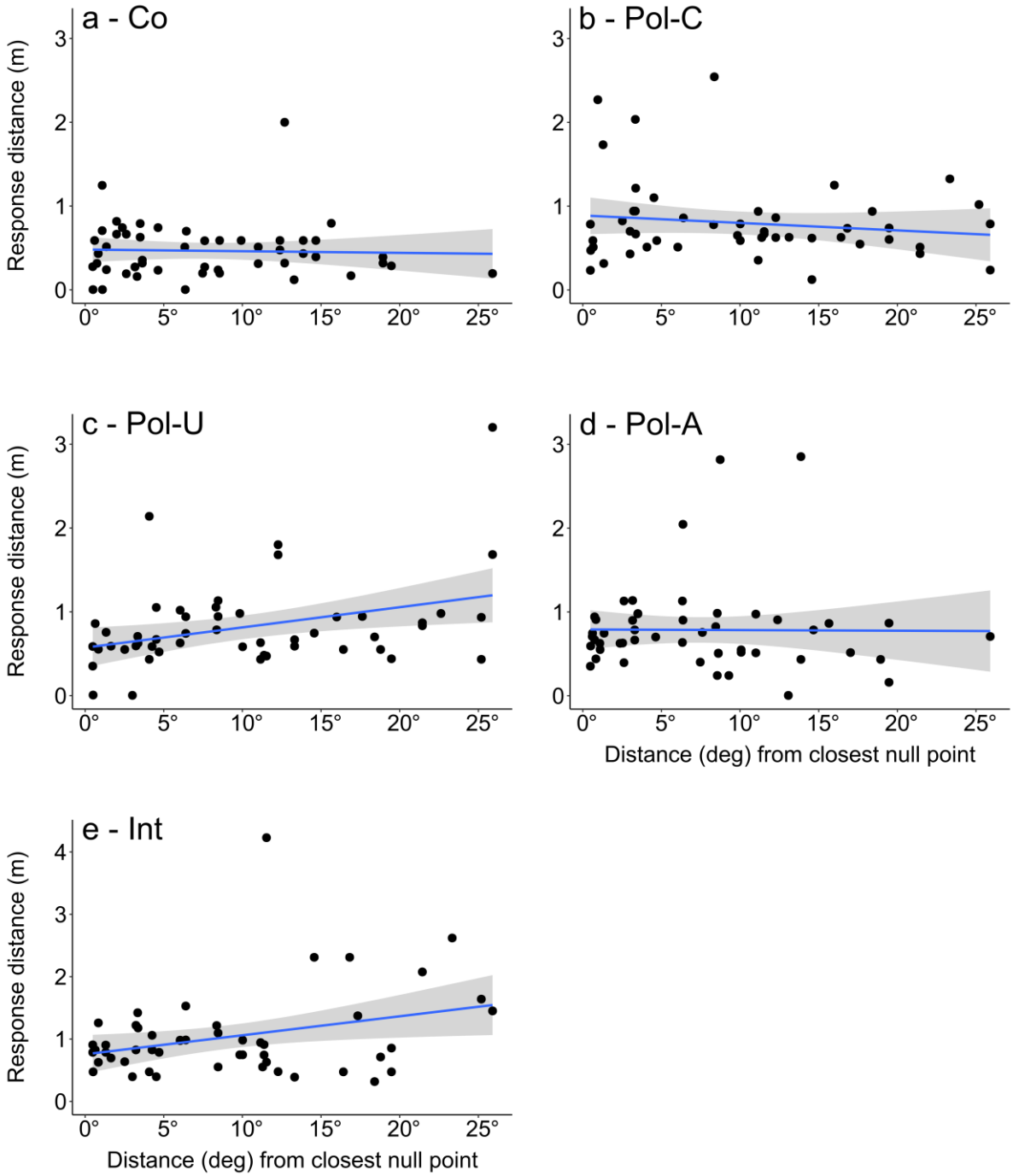

Figure 3.6: The effect of the crabs' null points of discrimination on the detection distance of the five target treatments. **a)** Co = control target (no intensity or polarization contrast). **b)** Pol-C = polarization control target; optic axis of the quarter-wave retarder aligned parallel to the AoP of the sky (low polarization contrast). **c)** Pol-U = unpolarized target; optic axis of the quarter-wave retarder aligned ±45º to the AoP of the sky (greatest contrast in DoLP). **d)** Pol-A = AoP target; optic axis of the half-wave retarder aligned ±45º to the AoP of the sky (greatest contrast in AoP). **e)** Int = intensity target (greatest intensity contrast). The x-axis is the difference between the AoP of the sky and the closest null point of discrimination (i.e. ±45°). Plots show linear regression line (blue line) and 95% confidence region (grey shaded area).

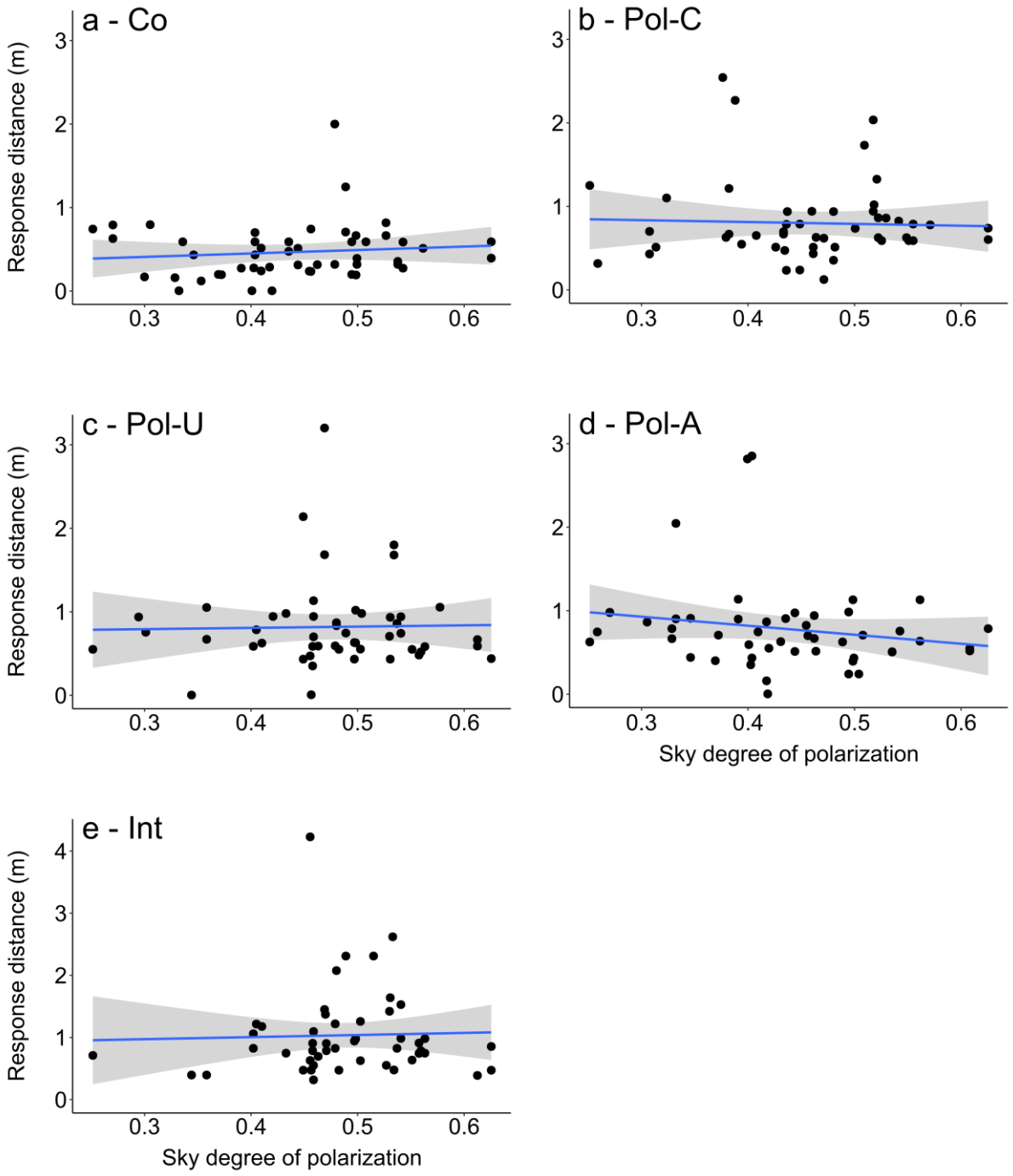

Figure 3.7: The effect of the DoLP of the sky on the crabs' detection distance of the five target treatments. **a)** Co = control target (no intensity or polarization contrast). **b)** Pol-C = polarization control target; optic axis of the quarter-wave retarder aligned parallel to the AoP of the sky (low polarization contrast). **c)** Pol-U = unpolarized target; optic axis of the quarter-wave retarder aligned ±45º to the AoP of the sky (greatest contrast in DoLP). **d)** Pol-A = AoP target; optic axis of the half-wave retarder aligned ±45º to the AoP of the sky (greatest contrast in AoP). **e)** Int = intensity target (greatest intensity contrast). Plots show linear regression line (blue line) and 95% confidence region (grey shaded area).

3.3.2 Polarization properties of the sky

Photographic polarimetry was used to obtain measurements of the polarization properties of the patch of sky against which the targets were viewed. The DoLP and AoP obtained from each polarization photo is shown in Figure 3.8. Across all 50 trials the DoLP of the patch of sky behind the target ranged between 0.25 - 0.63. The polarization properties of the sky during each target presentation were obtained from the polarization photo that was taken closest to the time that the target was presented (Figure 3.9). In approximately 20% of the presentations the AoP of the sky was within 15° to 10° from a null point of discrimination, in 22% the AoP was within 10° to 5° from a null point, and in 42% of the presentations the AoP was less than 5° from a null point (Figure 3.8).

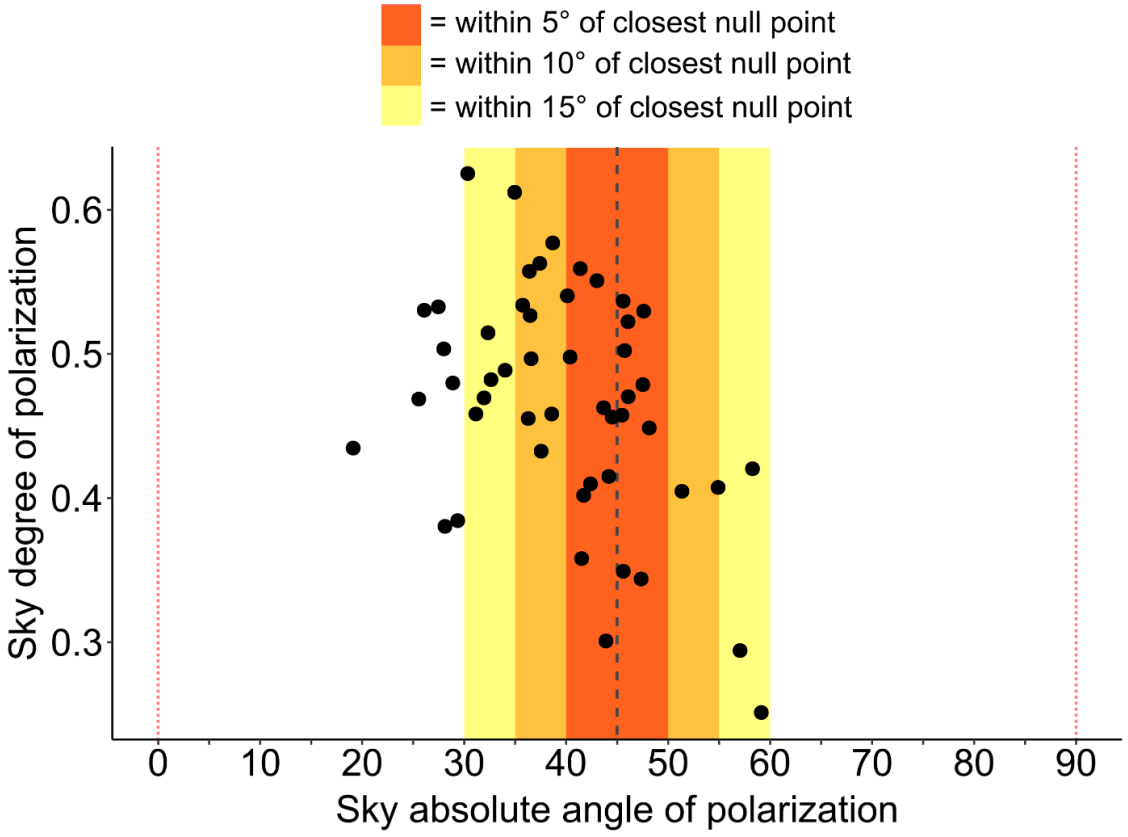

Figure 3.8: DoLP and absolute AoP of the patch of sky against which the targets were viewed obtained from polarization photos taken at the start of each of the 50 trials. The grey dashed lines represents the position of the crab's null points of discrimination at ±45°. The red dotted lines mark the angle furthest from the two null points, i.e. horizontally polarized light and vertically polarized light. The yellow shaded areas indicate photos in which the AoP of the sky was 15° to 10° from a null point, orange shaded areas indicated photo in which the AoP was 10° to 5° from a null point, and the red shaded areas indicate photo in which the AoP was less than 5° from a null point.

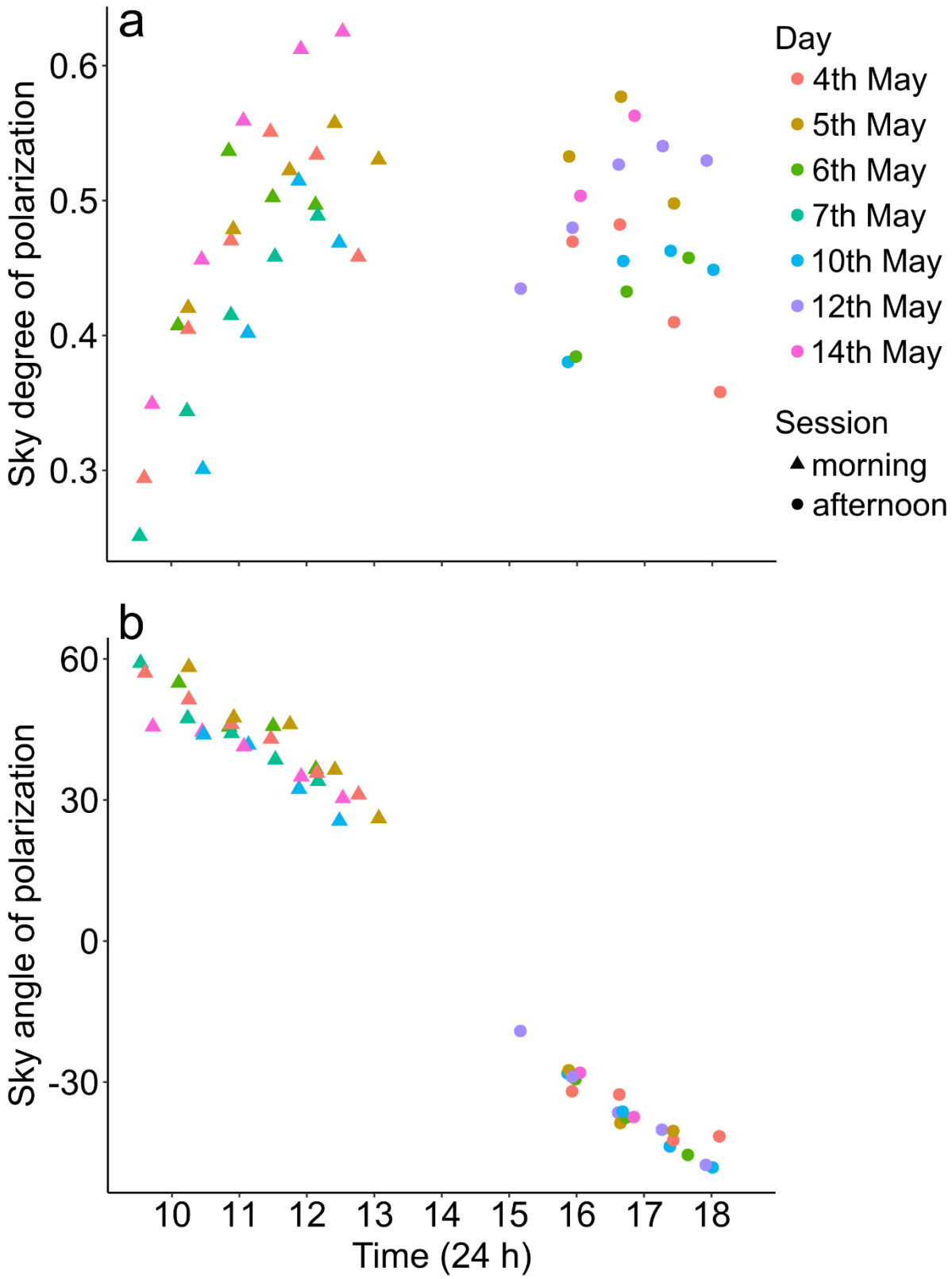

Figure 3.9: Polarization properties of the patch of sky against which the targets were viewed at different times of day on each day of the study. **a)** DoLP and **b)** AoP of the sky over time obtained from the polarization photos taken before the start of each trial.

3.3.3 Target alignment

The first target treatment presented to each crab was visible in the 50 polarization photos taken at the start of each trial. This allowed a rough estimate of the polarization properties of the targets to be ascertained and used to check how the actual polarization contrast between the target and the sky in each photo compared to the theoretical polarization contrast that would be predicted for the same target assuming perfect alignment. A summary of how the different target treatments affected the polarization properties of the transmitted light is provided in Table 3.2.

Table 3.2: Actual and theoretical percentage change in the DoLP and change in the AoP of light transmitted through the target treatments included in the polarization photos taken at the start of each trial. Note that it was not possible to ascertain the polarization properties of the target in two of the 50 photos.

Target	No. of photos	Mean % change in DoLP ± SD	Theoretical % change in DoLP	Mean change in AoP ± SD	Theoretical change in AoP
Co	10	15.46 ± 7.17	0	0.58° ± 0.75°	0°
Pol-C	8	15.91 ± 5.99	0	2.35° ± 1.2°	0°
Pol-U	10	75.74 ± 16.66	100	44.92° ± 17.23°	0°
Pol-A	9	32.76 ± 7.9	0	71.22° ± 11.42°	90°
Int	11	na	na	na	na

The polarization properties of the target and the sky from each photo were used to calculate the polarization distance (How & Marshall, 2014) and compare this to the theoretical polarization distance (i.e. the polarization distance if Co and Pol-C did not change the polarization of transmitted light, Pol-U changed the DoLP of transmitted light to 0 but did not change the AoP, and Pol-A rotated the AoP by exactly 90° but did not change the DoLP). The actual polarization distances of both Co and Pol-C were higher than predicted (Figure 3.10a and Figure 3.10b), however this can, at least in part, be attributed to the fact that both Co and Pol-C reduced the DoLP of transmitted light by ~15% (Table 3.2). Overall, the actual polarization distances of

Pol-U and Pol-A were lower than predicted (Figure 3.10c and Figure 3.10d). When taken alongside the result that Pol-A on average rotated the AoP by ~71° (rather than the full 90°) and Pol-U did not reduce the DoLP by 100% (Table 3.2) this implies that the optic axis of the retarder was not always positioned exactly ±45° to the AoP of the sky. It should however be noted that in the majority of the Pol-U photos the DoLP of the target was too low (<0.15) to accurately determine the AoP from this far away (the target was a 4cm object photographed from approximately 5m away). This has implications for the calculation of polarization distance because changes in the AoP, even when the DoLP is < 0.15 (but > ~0.05), can drastically effect the value of polarization distance. For example, in one of the Pol-U photos the DoLP was 0.53 for the sky and 0.12 for the target (difference of 0.41) and the AoP was 35.7° for the sky but -5.7° for the target (difference of 40°). This gives a polarization distance of 0.07. However, if the AoP of the target is changed to 35° ± 10° (as expected based on the photos of Pol-C) the calculated polarization distance increases to 0.21 ± 0.07. Figure 3.10b and Figure 3.10c should therefore be compared with extreme caution because in reality the actual polarization contrast generated by Pol-U would have been higher than the polarization distance calculated from the photos.

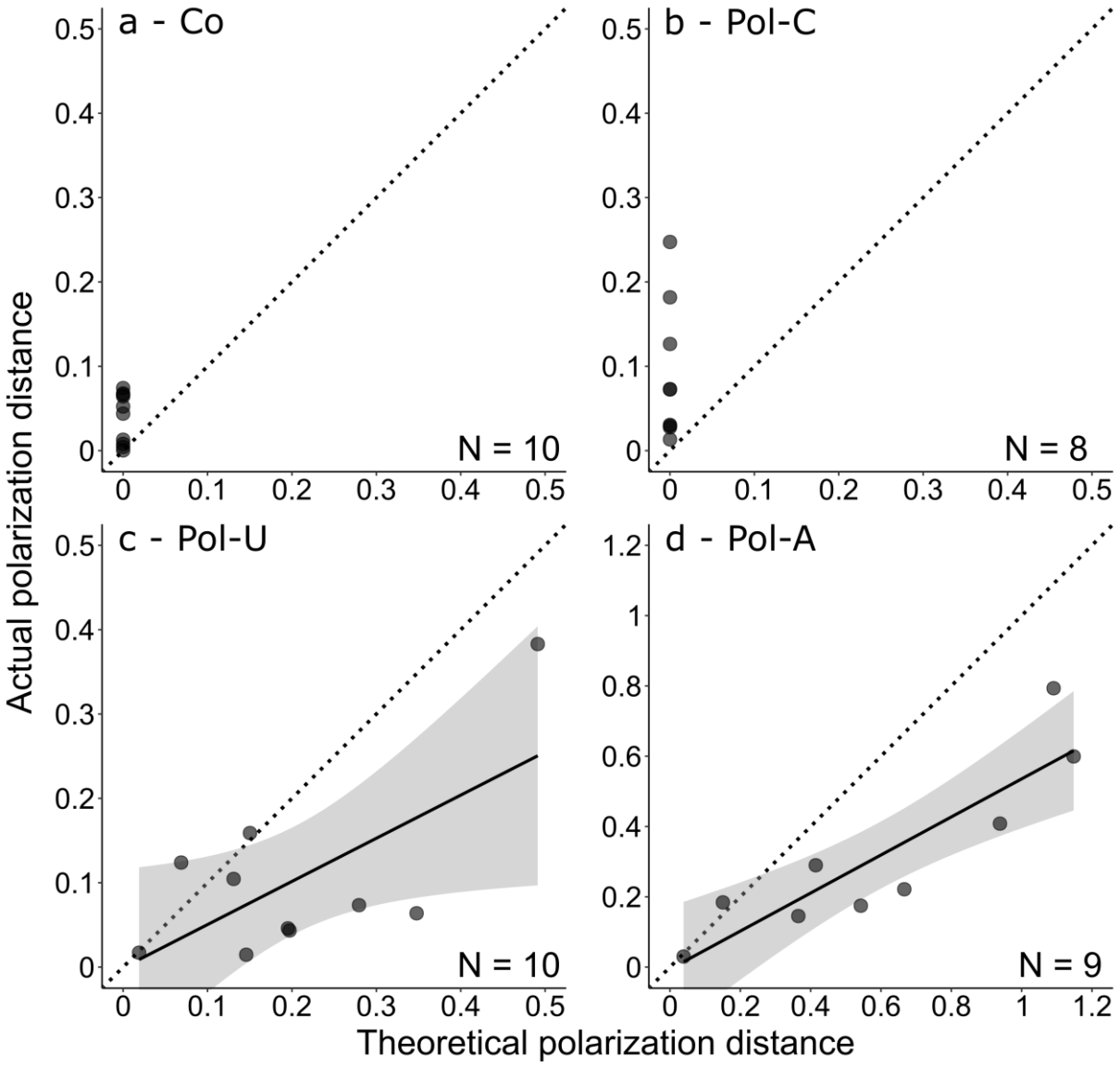

Figure 3.10: Actual absolute polarization distance between the target and the sky, calculated from the polarization photos taken at the start of each trial, against the theoretical absolute polarization distance. **a)** Co = control target (no intensity or polarization contrast). **b)** Pol-C = polarization control target; optic axis of the quarter-wave retarder aligned parallel to the AoP of the sky (low polarization contrast). **c)** Pol-U = unpolarized target; optic axis of the quarter-wave retarder aligned ±45º to the AoP of the sky (greatest contrast in DoLP). **d)** Pol-A = AoP target; optic axis of the half-wave retarder aligned ±45º to the AoP of the sky (greatest contrast in AoP). The calculation of the theoretical polarization distance is based on the assumption that Co and Pol-C did not change the polarization of transmitted light, Pol-U changed the DoLP of transmitted light to 0 but did not change the AoP, and Pol-A rotated the AoP by exactly 90° but did not change the DoLP. The dotted line indicates when the actual polarization distance was the same as the theoretical polarization distance and thus provides an indication of how well the optic axis of the retarder was aligned relative to the AoP of the sky. Points above the dotted line indicate that the actual polarization distance was greater than theoretically predicted, while points below the dotted indicate that the actual polarization distance was less than theoretically predicted. For simplicity polarization distance is given as an absolute value. The Int target is not included here since it blocked the transmission of light. Plots (c) and (d) show linear regression line and 95% confidence region.

3.3.4 Predictions of the parallel channel model

In the absence of the estimated UV contrast the parallel channel model predicted a difference in the level of response to Pol-C, Pol-U and Pol-A (Pearson's Chi-squared test: Polarization only; $\chi^2_{(2)} = 5123.5$, $P < 0.001$; Figure 3.11a) in a binary response assay. When the UV contrast was included in the model on its own the level of response was the same for all three treatments (Pearson's Chi-squared test: Intensity only; $\chi^2_{(2)} = 0.07$, $P = 1$). When both polarization distance and Weber contrast were included the level of response was the same as that to the UV contrast alone and there was no difference in response between the three treatments (Pearson's Chi-squared test: Polarization + intensity; $\chi^2_{(2)} = 0.16$, $P = 1$). This model does not however take into account that the polarization distance between the target and the sky would have been higher than theoretically predicted for Pol-C (Figure 3.10b) and potentially lower than predicted for Pol-U and Pol-A (Figure 3.10c and Figure 3.10d). Therefore, the estimated polarization distance for each target presentation was recalculated taking into account the values in Table 3.2. For these updated estimates Pol-C was assumed to reduce the DoLP of transmitted light by 16% and change the AoP by 2.35°, Pol-U reduced the DoLP by 76% and also changed the AoP by 2.35° (this value was used because the change in AoP calculated for Pol-U was unreliable due to the low DoLP), and Pol-A rotated the AoP by 71° and reduced the DoLP by 33%. When the parallel channel model was rerun without the UV contrast using these new estimations of polarization distance the model predicted no change in the level of response to Pol-C (Pearson's Chi-squared test: Polarization only, Pol-C from Figure 3.11a vs Pol-C from Figure 3.11b; $\chi^2_{(1)} = 1.68$, $P = 0.194$) but did predict a decrease in response to Pol-U (Pearson's Chi-squared test: Polarization only, Pol-U from Figure 3.11a vs Pol-U from Figure 3.11b; $\chi^2_{(1)} = 192.36$, $P < 0.001$) and Pol-A (Pearson's Chi-squared test: Polarization only, Pol-A from Figure 3.11a vs Pol-A from Figure 3.11b; $\chi^2_{(1)} = 1425.3$, $P < 0.001$). The model nevertheless still predicted a difference in the level of response between the three treatments in the absence

of the UV contrast (Pearson's Chi-squared test: Polarization only; $\chi^2_{(2)} = 1348.3$, $P < 0.001$; Figure 3.11b), but not when the UV contrast was present (Pearson's Chi-squared test: Intensity only; $\chi^2_{(2)} = 0.05$, $P = 1$; Polarization + intensity; $\chi^2_{(2)} = 0.01$, $P = 1$).

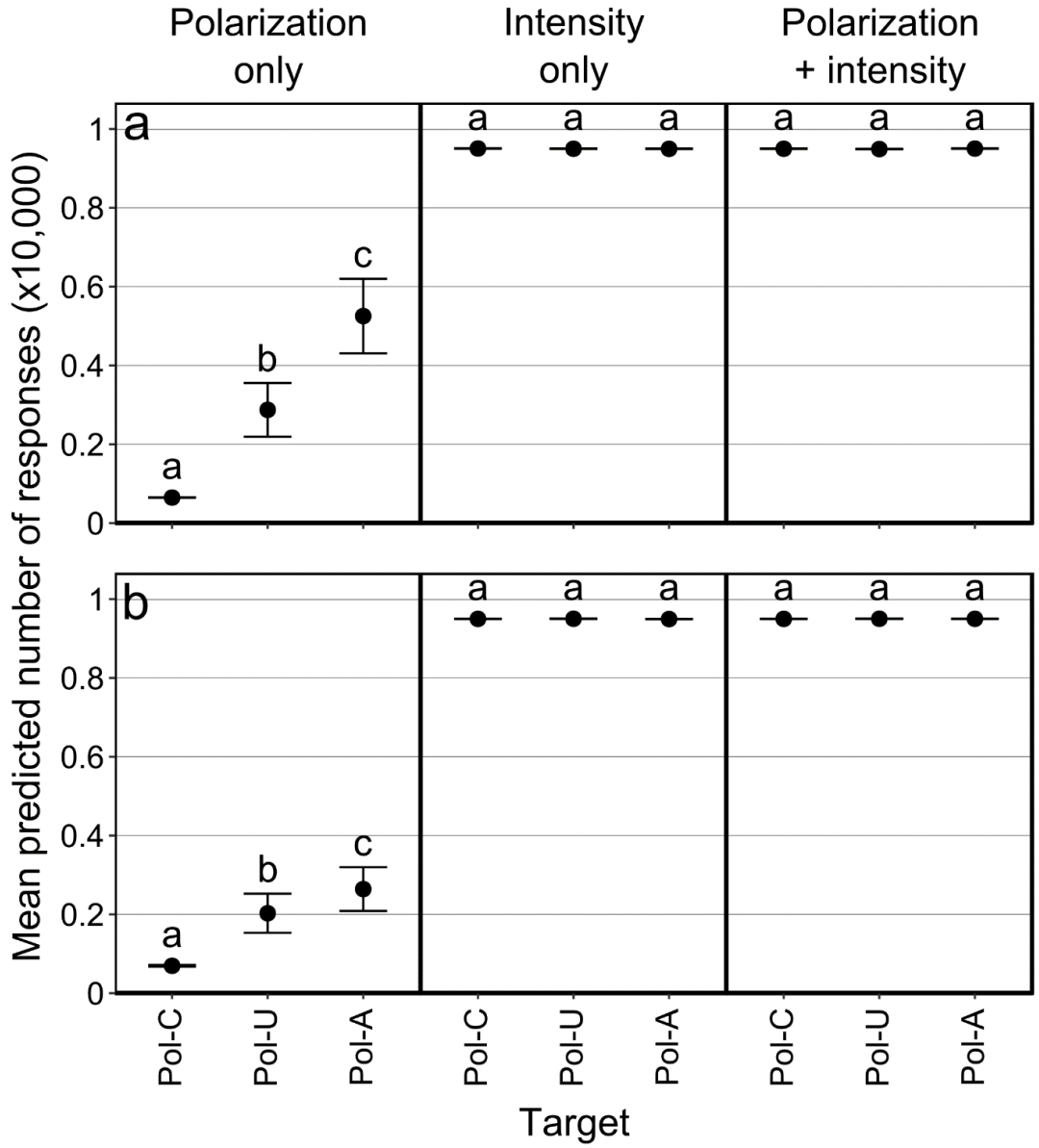

Figure 3.11: The mean number of responses of a simulated crab population (N=10,000) to Pol-C, Pol-U and Pol-A from each of the 50 trials using the parallel channel model from chapter 2. Response is based on the estimated polarization distance alone (left), the estimated Weber contrast alone (centre), and both the polarization distance and Weber contrast (right). **a)** The estimated polarization distance assuming that Pol-C did not change the polarization of transmitted light, Pol-U changed the DoLP of transmitted light to 0 but did not change the AoP, and Pol-A rotated the AoP by exactly 90° but did not change the DoLP. **b)** The estimated polarization distance taking into account the polarization properties in Table 3.2 (see text for details). Details about the model calculations and explanation can be found in the appendix A.4. Within each panel, points that do not have the same letter above them are statistically significant ($P < 0.001$) from one another based on planned pairwise Pearson's Chi-squared tests after applying a Bonferroni correction to control for multiple testing. Error bar show 95% confidence intervals.

3.4 Discussion

This study tested the distance at which fiddler crabs first responded to five different target treatments that approached from above and were therefore viewed against the polarization pattern of the sky. The crabs responded to Pol-C (which had a low polarization contrast), Pol-U (which had the greatest contrast in the DoLP), Pol-A (which had the greatest contrast in the AoP) and Int (which had the greatest intensity contrast) further away than they did to Co (which had the lowest intensity and polarization contrast). There was no difference in response distance between Pol-C, Pol-U and Pol-A, but the response distance to Pol-U and Int was affected by how close the AoP of the sky was to the crab's null points of discrimination at ±45°. The DoLP of the sky was not found to affect response distance to the targets.

3.4.1 Effect of target alignment on response

The polarization contrast generated by Pol-C was higher than theoretically predicted while the polarization contrast generated by Pol-U and Pol-A was lower than predicted (based on the polarization photos taken at the start of each trial). In the case of Pol-C and Pol-U this can be attributed to the optic axis of the retarder in Pol-C not being perfectly parallel or perpendicular to the AoP of the sky, and the optic axis of the retarder in Pol-U not being exactly ±45° to the AoP of the sky. Pol-C was also affected by the fact that the Perspex depolarized the transmitted light slightly (as evident by the result that the polarization distance generated by Co was also higher than expected). The target holder also had a tendency to bounce around slightly as it moved along the guidelines towards the crab, which would have further disrupted the alignment of the retarder relative to the sky's polarization pattern. As such, imperfect alignment of the optic axis of the retarder relative to the AoP of the background is likely to have contributed to the lack of a difference in response distance between Pol-C and Pol-U. Nonetheless, fiddler crabs are sensitive to even small differences in polarization contrasts (How et al., 2012, 2014b),

and so it is likely that Pol-U would still have been detectable from further away than Pol-C even if the difference in polarization contrast between the two treatments was less than expected. Indeed, the parallel channel model predicted a difference in the response probability to the estimated polarization contrasts generated by Pol-C and Pol-U even after accounting for the reduction in contrast caused by imperfect alignment of the optic axis of the retarder. This suggests that alignment alone is not enough to fully explain why there was no difference in response distance between Pol-C and Pol-U.

On average Pol-A was found to rotate the AoP of transmitted light by ~71°, rather than 90° as would be expected if the optic axis of the half-wave retarder was exactly ±45° to the AoP of the sky. Pol-A was also found to reduce the DoLP by ~33% on average. Relative to Pol-C and Pol-U, the predictions of the parallel channel model suggest that imperfect alignment of the optic axis of the half-wave retarder had more of an effect on the average polarization contrast generated by Pol-A. However, for Pol-A, alignment error alone is not enough to explain the reduction in the predicted response probability. This is because not aligning the optic axis of the half-wave retarder ±45° to the AoP of the sky had the potential to increase polarization distance (rather than just reducing it as it would have done for Pol-U) when the AoP of the sky was at, or close to, a null point. For instance, if the AoP of the sky was 45°, rotating the AoP by 71° would result in a greater polarization distance than if the AoP was rotated by the full 90°. Fiddler crabs are highly sensitive to changes in the AoP around the null points (How et al., 2012) so even a difference of a few degrees would theoretically be detectable by the crabs. This is supported by the fact that when the estimated values of polarization distance for all of the Pol-A presentations were recalculated after accounting for the alignment error and the depolarizing effect of the retarder, the mean absolute value of polarization distance actually increased slightly from 0.404 ± 0.328 (mean ± SD) to 0.425 ± 0.329. In order to understand the

reduction in the level of response to Pol-A predicted by the parallel channel model after accounting for the alignment error, it is necessary to consider the polarity of the polarization contrast. In some cases, when the AoP of the sky was at or close to ±45° (and thus indistinguishable from unpolarized light) and the AoP of light transmitted through the retarder was rotated by less than 90°, Pol-A would have appeared to the crab as being more polarized than the background. This could be the case whenever the AoP of the sky was closer to ±45° than the AoP of the target was; even if the actual DoLP of the target was lower than that of the sky. Consider the finding from chapter 2 that fiddler crabs are less responsive to positive polarization contrasts, then this could explain not only the reduction in the predicted response to Pol-A in Figure 3.11b, but also why the response distance to Pol-U and Pol-A were so similar (Figure 3.5).

3.4.2 The effect of the crabs' null points of discrimination

It was predicted that due to the crab's null points of discrimination, the closer the AoP of the sky was to ±45° the less sensitive the crabs would be to the Pol-U and Pol-A treatments (assuming Pol-A rotated the AoP by 90°). This is because at ±45° both the light from the background and the light transmitted through the targets would stimulate the horizontally and vertically oriented photoreceptors equally, meaning the target would be indistinguishable from the background in polarization (Bernard & Wehner, 1977; How et al., 2014b; How & Marshall, 2014). These null points were found to have had an effect on the detection of Pol-U as response distance increased the further the AoP of the sky was from ±45°. The null points also affected the response distance to Int. The latter result may be attributed to the fact that Int would have also presented a polarization contrast as it would have appeared unpolarized (i.e. there would have been no difference in the excitation of the vertical vs horizontal photoreceptors). The crabs' null points were not found to effect response to Pol-C, supporting the argument that Pol-

C and Pol-U were distinguishable from one another in polarization. Although the null points were not found to affect the response distance to Pol-A, this can be attributed to the fact that, as explained in the previous section, irrespective of the distance from the closest null point, Pol-A often generated a positive polarization contrast and so it is unlikely that this would have been high enough to enhance the detection of Pol-A.

Regardless of whether or not response distance increased with the distance from the null points, it is reasonable to suggest that when the AoP of the sky was close to a null point both Pol-U and Pol-A would have appeared less contrasting than they would have done if they had been viewed against a vertically or horizontally polarized background (as the targets in How et al. (2015) were). The effect of the null points is illustrated in Figure 3.12a, which shows the polarization information available to a crab viewing the targets shown in Figure 3.2 (in which the AoP of the sky is close to the crab's null point at 45°). The predicted reduction in the detectable polarization contrast due to the null points is particularly apparent for Pol-U which appears indistinguishable from Pol-C in Figure 3.12a. In contrast, if the orientation of the crab's photoreceptors was rotated by 45° (or if the AoP of the sky was horizontal) the detectable polarization contrast between the sky and Pol-U and Pol-A increases dramatically (Figure 3.12b). The only animal known to actively rotate its eyes, and thus the orientation of its photoreceptors, in order to resolve these null points and enhance polarization contrast is the mantis shrimp (Daly et al., 2016).

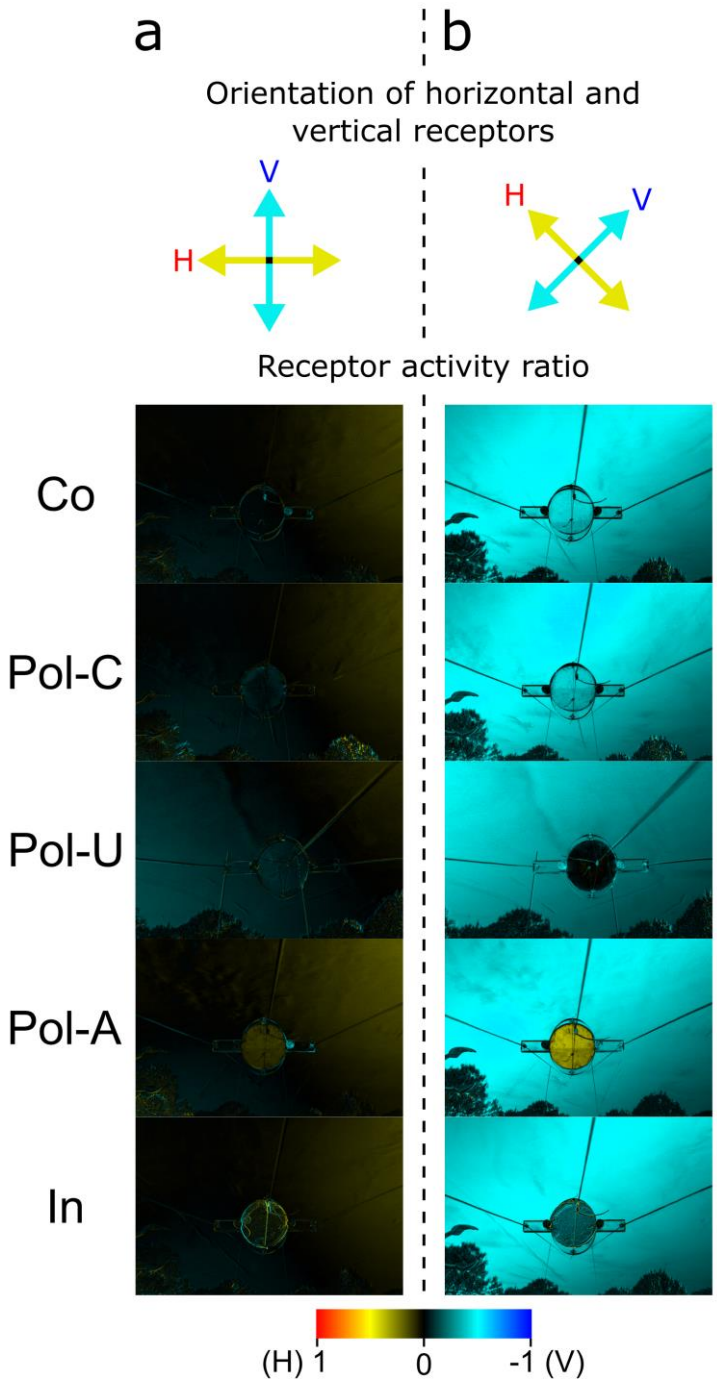

Figure 3.12: The five target treatments displayed as receptor activity ratio, i.e. the relative opponent output of the horizontally (H = 1) and vertically (V = -1) oriented photoreceptor channels calculated using a visual model (How and Marshall, 2014). **a)** The receptor activity ratio when the H and V receptors are oriented as they would be in nature (i.e. at 0° and 90° respectively), and **b)** the receptor activity ratio if the orientation of the photoreceptors was rotated by 45°. The original images were the same as those used to calculate the polarization properties shown in Figure 3.2. The AoP of the sky in each photo is close to the crab's null point at 45° (see Figure 3.2 for exact values). Co = control target (no intensity or polarization contrast). Pol-C = polarization control target; optic axis of the quarter-wave retarder aligned parallel to the AoP of the sky (low polarization contrast). Pol-U = unpolarized target; optic axis of the quarter-wave retarder aligned ±45º to the AoP of the sky (greatest contrast in DoLP). Pol-A = AoP target; optic axis of the half-wave retarder aligned ±45º to the AoP of the sky (greatest contrast in AoP). Int = intensity target (greatest intensity contrast).

3.4.3 Response to the UV intensity contrast

The estimated Weber contrast between the sky and the targets with the retarder was more than three times the lowest negative Weber contrast (i.e. -0.04) that the crabs responded to in chapter 2. Moreover, the difference in Weber contrast between the targets with the retarder and Co (the smallest difference for the R1-7 receptors was -0.084 for Pol-C/Pol-U; Table 3.1) was more than double the lowest negative intensity contrast the crabs responded to in chapter 2. Given that Co and Pol-C, on average, had very similar effects on the polarization properties of transmitted light (Table 3.2), it is plausible to suggest that the difference in response distance between Co and Pol-C was mostly due to the intensity contrast produced by the retarder.

The estimation of the Weber contrast was based on the peak sensitivity of the visual pigment within the R1-7 photoreceptors in *A. tangeri*. This does not however take into account the effect of screening pigments and how effectively UV wavelengths are transmitted through the ocular media. For instance, fiddler crabs possess a variety of ocular screening pigments that will affect the spectral distribution of light that actually reaches the photoreceptors (Cronin & Forward, 1988; Marshall et al., 1999; Zeil & Hemmi, 2006; Jordão et al., 2007). The distribution of these screening pigments varies across the eye and over time depending on the light adaption state of the eye (Cronin & Forward, 1988; Marshall et al., 1999; Zeil & Hemmi, 2006). *Afruca tangeri* has been shown to have orange/red screening pigments that modify the spectrum of light traveling down the rhabdom (Jordão et al., 2007). The actual spectral sensitivity of the R1-7 receptors is therefore sharpened and shifted towards longer wavelengths thus making the main rhabdom less sensitive to shorter wavelengths (Jordão et al., 2007). This means that the R1-7 receptors are probably less sensitive to the UV contrasts than Table 3.1 suggests, although they would most likely still be sensitive to the contrast generated by the retarder above 400nm.

It is also important to consider that crabs possess a second class of photoreceptor (R8) located at the distal end of the rhabdom (Alkaladi et al., 2013; Alkaladi & Zeil, 2014). Although no study to date has explicitly demonstrated the existence of a functional UV visual pigment in fiddler crabs, sensitivity to short wavelengths has been shown in the shore crab *C. maenas* and the fiddler crab *L. thayeri* (peak absorption around 440 nm and 430 nm respectively) where it is associated with the small R8 receptor (Martin & Mote, 1982; Horch et al., 2002). There is also limited behavioural evidence that UV colouration is important for mate selection in the fiddler crab *Au. mjoebergi* (Detto & Backwell, 2009). Based on the available evidence it is highly likely that the crabs would have been able to detect the intensity contrast produced by the retarder.

In the context of the findings from chapter 2, if the difference in intensity between the sky and the target was more contrasting than the difference in polarization, the crab's response may have depended solely on the intensity channel. If this were the case any difference in response distance that may have resulted from differences in polarization contrast between Pol-C, Pol-U and Pol-A would have been masked by the intensity contrast thus explaining why response distance to these three treatments was the same. This suggestion is supported by the predictions of the parallel channel model (Figure 3.11). It is however important to consider the finding that Pol-U and Int, both of which present a contrast in intensity and polarization, were detected sooner when the AoP of the sky was furthest from the null points. This finding suggests that either the polarization contrast was more salient than the intensity contrast when the AoP of the sky was furthest from ±45°, or that in this scenario there is an additive effect of intensity and polarization. While the latter might seem at odds with the findings of chapter 2, one should note that chapter 2 only looked at the crabs initial freeze response. This current study on the other hand excluded the freeze response (because the crab was not always walking when the

target started moving) and instead focused on other behavioural responses, such as sprinting. These different behaviours will be controlled by separate neuronal pathways to those controlling the initial freeze response and so intensity and polarization may be integrated differently.

3.4.4 Detection of polarization contrasts against the mudflat vs the sky

How et al. (2015) presented fiddler crabs with three different polarization targets that moved along the surface of the mudflat and were thus viewed against a horizontally polarized background. The polarization properties of these targets were manipulated in the same way, and using the same polymer retarder, as the targets in this study. In contrast to the findings of How et al. (2015), this study found no difference in response distance between Pol-C, Pol-U and Pol-A when they were viewed against the polarization pattern of the sky. This result has been attributed to the idea that due to the crabs null points, the intensity contrast produced by the retarder was on average more contrasting than the polarization contrast and so masked any difference in response distance that may otherwise have resulted from differences in polarization contrast between Pol-C, Pol-U and Pol-A. Since the targets in How, et al. (2015) were made from the same retarder film as that used in this study, and so would have also produced an intensity contrast, when the equivalent of Pol-C, Pol-U and Pol-A were viewed against the horizontally polarized mudflats in How et al. (2015) the polarization contrast must have been more salient than the UV contrast in this instance. This would explain why How et al. (2015) found a difference in response distance between the three polarization treatments while this study did not. However, until future work is conducted to explicitly test whether fiddler crabs can detect and respond to UV looming stimuli this suggestion remains purely speculative.

Overall, the findings of this study are consistent with the idea that the horizontal/vertical arrangements of the photoreceptors in fiddler crabs function as matched filters for detecting polarization contrasts on the mudflats (Wehner, 1987; Zeil & Hofmann, 2001; Alkaladi et al., 2013; How & Marshall, 2014; How et al., 2014b). In order to better understand the evolutionary drive behind such a matched filter it is important to consider the information that is conveyed by polarization and intensity, as well as the relative reliability of this information. When detecting objects against the sky, polarization can, at least under certain conditions, provide a more consistent source of information (chapter 2); although, as this chapter suggests, this will be restricted to objects viewed against specific regions of the sky. In other regions of the sky, where the crab's null points and/or the DoLP limit the detectability of polarization contrasts, the crabs must rely more heavily on intensity information. In either case, since objects viewed against the sky will always be above the crab's visual horizon, and therefore appear in the predator zone (Land & Layne, 1995; Layne et al., 1997; Zeil & Hemmi, 2006), both polarization and intensity will essentially convey the same information, i.e. the approach of a potential predator. For objects viewed against the mudflat on the other hand, below the crab's visual horizon, polarization has the potential to convey information that intensity does not. For instance, polarization vision may help crabs distinguish between non-threatening conspecifics that occupy neighbouring burrows and homeless competitors that may attempt to steal another crabs burrow (Zeil & Hofmann, 2001; How et al., 2015). This is because the DoLP of a crab's carapace will be highest when it is damp, thus indicating that it has regular access to ground water. In contrast, the carapace of a wandering crab with no access to ground water will be dry and will therefore appear unpolarized (Zeil & Hofmann, 2001; How et al., 2015). Additionally, other regions of a crab's body such as the enlarged major claw of males act like a scattering diffuser and so will appear less polarized than the background; this makes them highly

contrasting when viewed against the polarized glare from the mudflat and so polarization information is likely to be an important part of a males courtship display (How et al., 2015).

3.5 Chapter summary

In nature, as in this study, polarization cues and signals never appear in isolation of intensity information. Therefore, if the crab's null points of discrimination do, as suggested here, reduce the ability of fiddler crabs to use their polarization vision to detect targets viewed against the sky, the crabs would nevertheless still be able to detect objects based on other cues, such as intensity contrast and visual flicker (chapters 2 and 4; Smolka et al., 2011). Therefore, the redundancy in the different forms of information available to the crabs means the null points are unlikely to impose a meaningful fitness cost to the crabs in nature, nor does there seem to be any obvious selection pressure to evolve a visual system that eliminates them. When considered alongside the findings of chapter 2, this study supports the idea that by processing polarization and intensity in separate parallel channels crabs have evolved a system that is able to benefit from the advantages of both intensity and polarization vision whilst simultaneously mitigating the weaknesses of both.

Chapter 4

Detection of second-order motion in intensity and polarization

The fiddler crab *Afruca tangeri*
Acrylic painting by Maisie Brett

All of the experiments described within this thesis test the ability of crabs to detect the looming motion of an approaching target. In all of the experiments up until this point the looming stimulus generated first-order motion, which occurs when there is a difference in the mean intensity (or polarization) between the moving stimulus and the background (see definition below). The study in this chapter investigated the ability of fiddler crabs to respond to looming targets in which the motion was instead defined by second-order properties, such as flicker.

4.1 Introduction

When viewing a visual scene there are numerous image properties that animals use to detect movement of a stimulus within the scene. There are different forms of motion which depend on what image properties are being assessed, and not all forms of motion are necessarily detectable by the same mechanisms. As such, although motion detection in its broadest sense is almost ubiquitous among visual animals, it cannot be assumed that all animals are capable of seeing all forms of motion. First-order motion, also often referred to as Fourier motion, is defined by spatiotemporal correlations in intensity and is detectable by Reichardt-type motion detectors (Chubb & Sperling, 1988; Cavanagh & Mather, 1989; Scott-Samuel & Georgeson, 1999; Theobald et al., 2008; Nishida, 2011). Second-order (or non-Fourier) motion is defined by spatiotemporal correlations in higher-order image properties, such as texture, spatial frequency or flicker, which are not detectable by Reichardt-type detectors because there is no net directional Fourier motion energy (Chubb & Sperling, 1988; Lu & Sperling, 1995; Orger et al., 2000; Theobald et al., 2008; Nishida, 2011). In other words, first-order motion occurs when there is a difference in the mean intensity between a moving stimulus and the background, whilst second-order motion occurs when a stimulus has the same mean intensity as the background but differs from it in some second-order property (e.g. local contrast, texture or flicker).

Until relatively recently it was thought that the detection of second-order motion required a higher-level visual process that occurred in the visual cortex, thus restricting this ability to mammals (Zhou & Baker, 1990; Albright, 1992; Smith et al., 1998; Baker, 1999). However, Orger et al. (2000) reported that second-order motion can elicit optomotor behaviour in zebrafish larvae, which do not have a cortex, thus demonstrating that a higher-level visual process is not necessary. Since then a number of studies have shown that flies (Theobald et al., 2008, 2010; Aptekar et al., 2012; Lee & Nordstrom, 2012), and more recently the praying mantis (Nityananda et al., 2018), are also sensitive to second-order motion; proving that its detection is not confined to vertebrates. Mantids, for example, have been shown to use second-order motion in stereopsis (i.e. estimating distance based on the different images seen by each of the two eyes) and are capable of judging the distance of a moving stimulus even in the absence of coherent first-order motion (Nityananda et al., 2018).

With the exception of flies and mantids nothing is known about the detection of second-order motion in other arthropod groups, particularly more basal taxa such as the Crustacea. In addition, second-order features are not limited to intensity, but will also occur in polarization stimuli; the detection of which has never before been studied in any animal. Analogous to intensity modulation, a first-order polarization stimulus is defined by spatiotemporal correlations in the degree and/or angle of polarization (i.e. displacement of degree and/or angle of polarization differences). A second-order polarization stimulus is one defined by spatiotemporal correlations in second-order properties such as polarization flicker. In the context of the visual system of crabs and other crustaceans, first-order motion will be detected in polarization when there is a difference between the mean receptor activity ratio of the ommatidia viewing the stimulus and the mean receptor activity ratio of ommatidia viewing the

background; i.e. the polarization distance between the entire stimulus and the background is greater or less than zero. For second-order motion in polarization, the mean polarization distance between the stimulus and the background will be zero, but the stimulus will differ from the background in second-order properties.

One group of crustaceans in particular that might benefit from seeing second-order motion in both intensity and polarization is fiddler crabs. Fiddler crabs rely on their vision to detect objects and potential threats, whether it be a potential predator or mate, or a rival crab. As described in detail in section 1.4.1, fiddler crabs have a multi-stage anti-predator response (Hemmi, 2005b; Hemmi & Pfeil, 2010). The initial freeze response can be triggered when the approaching object is detected by only one or two ommatidia, meaning the animal has very little or no information regarding the movement of the target (Land & Layne, 1995; Zeil & Hemmi, 2006; Hemmi & Pfeil, 2010; Smolka et al., 2011). Subsequent stages of the response require more information about these properties. This is certainly the case for other crab species. For instance, when escaping from a predator, *Neohelice granulata*, which lives in similar habitats and have a comparable natural history to fiddler crabs, continuously adjust the speed and direction of their run depending on the motion of the approaching threat (Oliva et al., 2007; Oliva & Tomsic, 2012, 2016; Tomsic, 2016). Motion detection is therefore an integral part of a crab's anti-predator response. In fiddler crabs, subsequent stages of the response are controlled by a combination of multiple visual cues including retinal speed, elevation, position and movement direction relative to the crab, and flicker (Hemmi & Zeil, 2003; Hemmi, 2005b,a; Smolka et al., 2011, 2013).

Flicker, i.e. rapid changes in intensity (or polarization), which is produced by the flapping wings of some avian predators such as terns (Smolka et al., 2011, 2013), is particularly

interesting because it has the potential to generate second-order motion (Theobald et al., 2010). This therefore raises questions as to whether fiddler crabs, and other crab species, are able to see second-order motion and use it to detect potential threats. These animals also offer the exciting opportunity to study the detection of second-order motion in polarization for the first time in any animal. Furthermore, the findings of chapter 2 raises the possibility of a first-order/second-order distinction in polarized stimuli.

The purpose of this study was to determine whether fiddler crabs can detect second-order motion, not only in intensity, but also in polarization. To this end, behavioural experiments were conducted to test the response of *Afruca tangeri* to a series of different first- and second-order looming stimuli. Firstly, crabs were shown five different stimuli viewed against a static pseudorandom noise background designed to avoid spurious first-order artefacts (Smith & Ledgeway, 1997). Secondly, crabs were shown four different stimuli viewed against a dynamic random noise background.

4.2 Methods

4.2.1 Crab collection and preparation

Fiddler crabs (*A. tangeri*) (carapace width between 18 and 32 mm) were collected by hand from mudflat sites in El Rompido (37.2207° N, 7.1238° W) on the south coast of Spain. Animal collection was carried out with the authorisation of Consejería de Medio Ambiente y Ordenación del Territorio de la Junta de Andalucía. Crabs were housed separately in plastic cups with approximately 20 mm of fresh seawater and a folded strip of kitchen paper to provide a substrate (water and paper were changed daily). Crabs were kept for a maximum of five days and were fed with fish flake food once a day. Prior to the experiment, a wire harness was glued

to the crab's carapace in the same way as in previous chapters. After being tested the wire harness was removed and all crabs were released near the site they were collected from.

4.2.2 Experimental setup

The experiments used a similar treadmill setup to that described in chapter 2. Briefly, each crab was loosely tethered atop a 150 mm diameter Styrofoam treadmill suspended on a cushion of air. This allowed the crabs to walk freely whilst preventing translational or rotational movement. Visual stimuli were displayed on a patterned vertical alignment type liquid crystal display (PVA-LCD) computer monitor (1905FP, Dell, Round Rock, USA) positioned in front of the crab at a distance of about 200 mm (Figure 4.1). For the polarization experiment the LCD monitor was modified by removing the outer most polarizing filter so that intensity contrast was substituted for contrast in the DoLP (Foster et al., 2018). The polarization properties of this monitor were measured using the method detailed in appendix A.1. When operated in grey scale, instead of changing from black to white, the screens' display changed from fully polarized to nearly unpolarized (Figure A.11a). The AoP was always horizontal (Figure A.11b). A 40 x 40 x 40 cm white photographic tent (LT124, PhotoSEL), with a hole cut out for the treadmill and the front positioned against the LCD screen, blocked out any visual distractions that might have affected the behaviour of the crab.

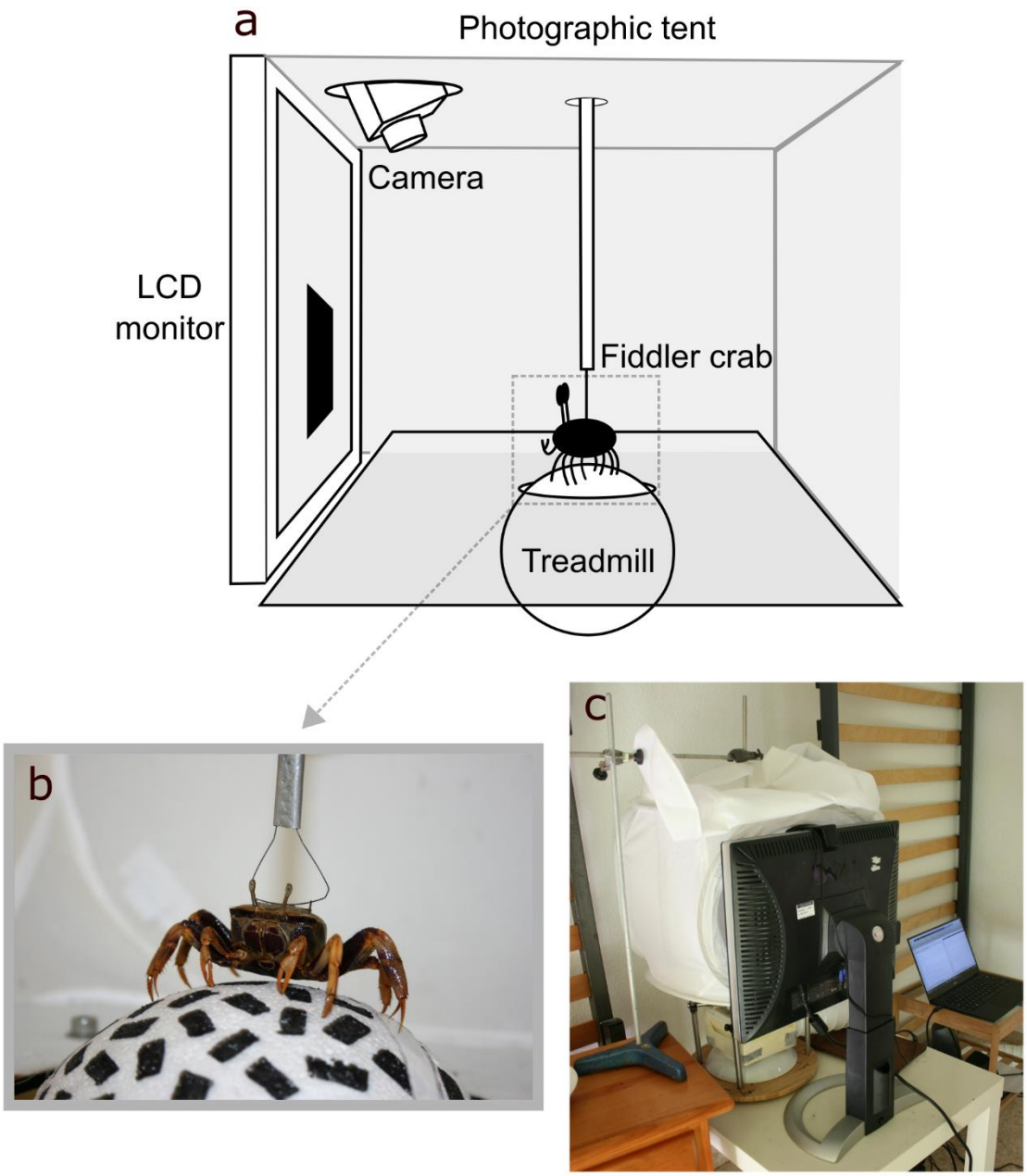

Figure 4.1: Experimental set up. **a)** Diagram showing the experimental apparatus and photographs of **b)** a fiddler crab tethered above the treadmill and **c)** the experiment set up.

4.2.3 Stimuli for static background experiments

The experiments were controlled by custom-written scripts in Matlab R2016a (MathWorks, Natick, USA) using the Psychophysics Toolbox extensions (Brainard, 1997; Pelli, 1997) to generate the visual stimuli and background. Stimuli were displayed against a pseudorandom noise background composed of 9 x 9 mm (angular size of 2.5° at the viewing distance of 200

mm) black (R = G = B = 0) and white (R = G = B = 255) squares in the intensity experiment, and unpolarized (DoLP = 0.1) and fully polarized (DoLP = 0.99) squares in the polarization experiment. Because clumping of squares with the same RGB value (which occurred when the pattern was random) could result in the generation of first-order artefacts in the second-order stimuli (Smith & Ledgeway, 1997), the pattern of squares was pseudorandom; each square could be directly next to no more than two squares of the same RGB value. The stimuli consisted of four different looming squares, and one non-looming square, that expanded for approximately 1.2 sec to a maximum size of 114 x 114 mm (150 mm from top left to bottom right) so that it occupied a maximum of 41.2º of the crab's visual field when fully expanded. Polarization stimuli that occupied a larger area of the visual field than this would suffer from intensity artefacts due to off-axis viewing angles (Foster et al., 2018). At stimulus onset the loom started by covering four background squares (layer 1) and a new layer of squares was added to the outer edge of the loom each time it expanded (see Figure 4.2 for details of loom expansion). This method of expansion was designed to ensure that the expanding edge of the loom only ever obscured complete background squares, i.e. it never obscured half a background square as to do so would generate first-order artefacts in the second-order stimuli. Once the loom reached its full size it remained on the screen for 2 s before disappearing.

A solid black or unpolarized loom, which differed from the background in mean intensity or DoLP, was used as the first-order (FO) stimulus in the intensity and polarization experiments respectively (see FO in Figure 4.2b and supplementary movie S1 via the link provided in appendix A.8). The first second-order motion stimulus (SO1) was calibrated using a spectrometer (USB2000, Ocean Optics, Largo, USA) coupled to an optical fibre (P200-10-UV/VIS, Ocean Optics, Largo, USA) to match the mean intensity (or mean DoLP in the polarization experiment (see appendix A.1 for details of polarization measurements and

calculations) of the background based on the spectral sensitivity of the R1-7 photoreceptors of the crabs (Lambda max = 530 nm (Jordão et al., 2007)), and thus was by definition second-order (see SO1 in Figure 4.2b and supplementary movie S2; appendix A.8). For the second second-order motion stimulus (SO2) each square within the loom was pseudorandomly assigned to be black or white every 83.3 ms (e.g. a black square could change to a white square or remain black) thus the resulting stimulus had an overall flicker rate of 6 Hz and was viewed against the static background (see SO2 in Figure 4.2b and supplementary movie S3; appendix A.8). The flicker rate of SO2 was measured using a photodiode coupled to an oscilloscope (LT354M, LeCroy, New York, USA). The flicker rate was well below the flicker fusion frequency of fiddler crabs (Falkowski and Hemmi, unpublished data). To confirm that the crabs were actually responding to the second-order motion cues and not just stationary flicker (i.e. the static change in intensity detected by only a few ommatidia) a flicker-only control stimulus (FC) was used. FC was the same as the SO2 except it did not loom; rather it appeared on the screen full size from the start of stimulus onset and so did not contain any motion cues (see FC in Figure 4.2b and supplementary movie S4; appendix A.8). Finally, a stimulus with the same pattern of squares as the background, which was therefore invisible, was used as the negative control (see control in Figure 4.2b and supplementary movie S5; appendix A.8).

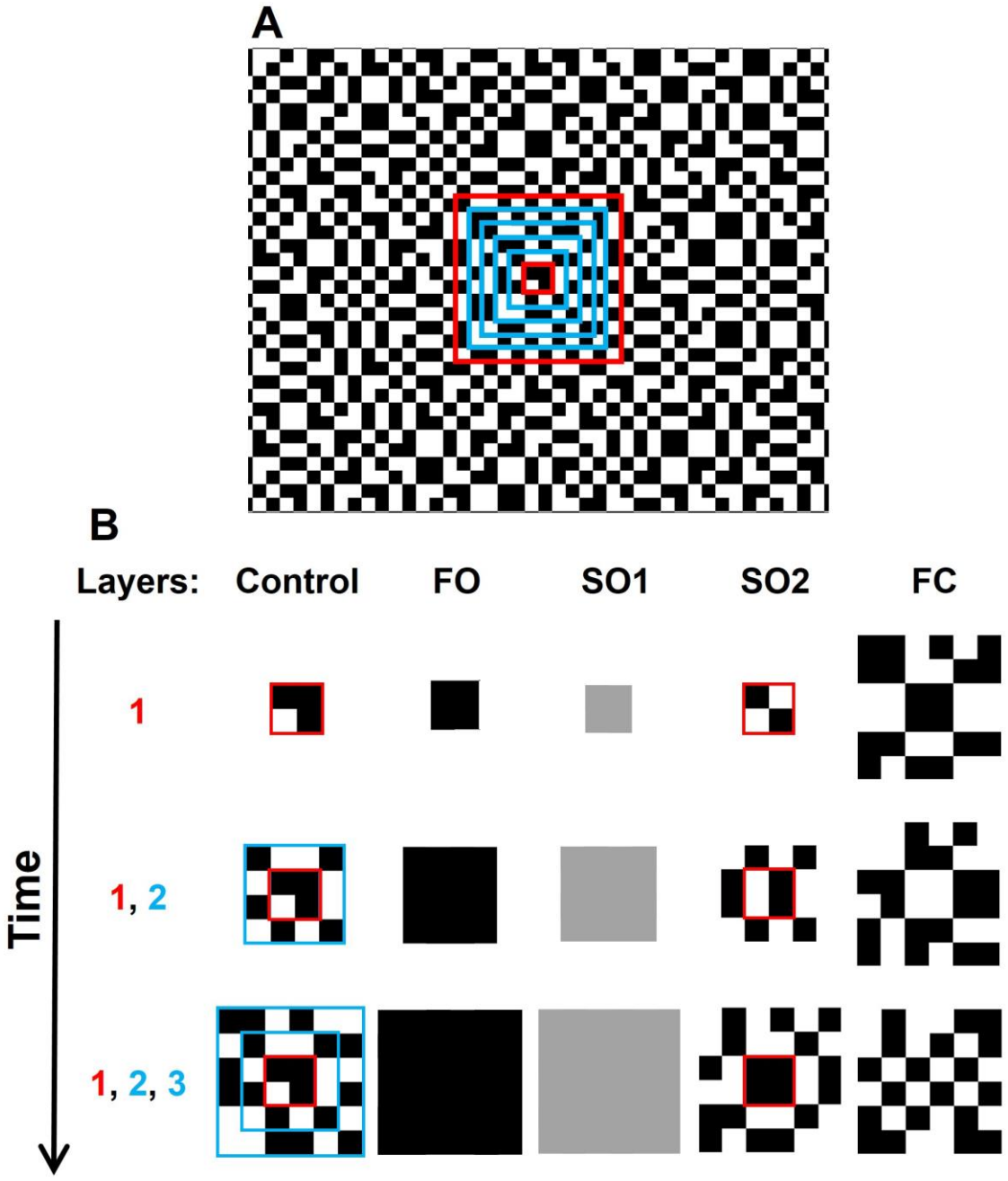

Figure 4.2: Stimuli from the static background experiments. **a)** Example of the pseudorandom noise background, used in the static background experiments, against which, **b)** the control, first-order (FO), two second-order (SO1 and SO2) and flicker-only control (FC) stimuli were displayed. In the polarization experiment intensity contrast was substituted for contrast in the DoLP. The start position of the loom is indicated by the smaller red box in (a). The light blue boxes indicate the position and size of loom at each subsequent stage during expansion until it reached full size (indicated by the larger red box in (a)). At stimulus onset the loom starts by covering four background squares (layer 1- indicated by the small red box in (a) and (b)) and a new layer of squares was added to the outer edge of the loom each time it expanded. For instance, layer 2 comprised of all of the squares that immediately surrounded layer 1 (i.e. the four squares in the centre), layer 3 comprised all of the squares that immediately surrounded layer 2, and so on until layer 6 (full size loom). Note how the pattern within each layer remains constant in the control but has changed by the time a new layer is added in SO2. For a better understanding of stimulus dynamics see supplementary movies S1-A5 (appendix A.8).

4.2.4 Stimuli for dynamic background experiments

For this set of experiments two second-order looms and two controls were displayed against a flickering random noise background similar to that used in the static background experiments. This time, the arrangement of the black and white, or polarized and unpolarized, squares was random rather than pseudorandom because the use of a dynamic background eliminated the generation of first-order artefacts that may have arisen due to clumping of squares in the static background. The second-order looms were similar to SO2 except that the background was also flickering. For one stimulus the background had a flicker rate of 3Hz and the loom a flicker rate of 6Hz (SO3; supplementary movie S6; appendix A.8) and for the other the background had a flicker rate of 6Hz and the loom a flicker rate of 3Hz (SO4; supplementary movie S7; appendix A.8). For the two controls both the background and the loom had a flicker rate of 3Hz (Control 1; supplementary movie S8; appendix A.8) or 6Hz (Control 2; supplementary movie S9; appendix A.8). For each stimulus presentation the background began flickering for a random duration between 30 s and 50 s before the onset of the loom and stopped flickering after a random duration between 10 s and 20 s after the loom disappeared.

4.2.5 Experimental procedure

A total of 120 crabs were tested in the two static background experiments (60 per experiment) and 133 crabs in the dynamic background experiments (63 and 70 in the intensity and polarization experiment respectively). The study used a fully automated protocol developed in Matlab R2016a (MathWorks, Natick, USA). The experimental procedure was similar to that described in chapter 2. Each crab was positioned on the treadmill facing the screen and allowed 3 min to acclimatise before being presented with the stimuli in a randomised order, with a minimum between-stimulus interval of 30 s (static background experiments) or 50 s (dynamic

background experiments) plus a random pause of up to 20 s (static background experiments) or 40 s (dynamic background experiments). Any effect of habituation was controlled for in the statistical analysis and by the randomisation of the stimulus order. The pause between each stimulus presentation was longer if the crab was stationary as Matlab was programmed to check whether the crab was walking before initiating the next presentation. For the static background experiments the pattern of the pseudorandom noise background was changed between each stimulus presentation. Crab behaviour and treadmill movement were recorded from above using a webcam (C270, Logitech, Lausanne, Switzerland). Behavioural response was scored automatically in Matlab at the end of each presentation using the two-dimensional motion detection algorithm (Zanker, 1996) which detected the motion of markings drawn on the polystyrene ball. Crab response was scored within a 3.2 s window, i.e. 1.2 s during loom expansion and 2 s after. The crab's pre-stimulus behaviour on the treadmill was usually to maintain a steady walk. A crab was therefore recorded as having responded to, and thus assumed to have detected, the stimulus if it stopped walking (i.e. displayed a freeze response), indicated by a cease in the motion of the marking on the ball within the defined scoring window. Trials in which the crab was not walking at stimulus onset were rejected and the stimulus was appended to the end of the series for a repeat presentation (up to a maximum of 5). The statistical analysis controlled for any effect that repeated exposure to the same stimulus may have had on the results. Any remaining trials in which the crabs stopped before the scoring window were rejected post hoc. Consequently, although each crab viewed all of the stimuli in each experiment, not all individuals contributed data to every stimulus tested hence the range of N values in each experiment.

4.2.6 Statistical analysis

All statistical analysis was conducted in R (R Core Team, 2017). Mixed effects binary logistic regression, fitted using the lme4 package (Bates et al., 2015), was used to analyse the data from each experiment using crab response as a binary response variable. Stimulus type, crab sex and size, and presentation number (order) were included as fixed effects. The latter was included to control for any effect of habituation. Crab identification was included as a random effect to account for the repeated measures design. Model simplification was used to test for significant fixed effects; models were compared with one another using a likelihood ratio test (LRT) to sequentially remove non-significant effects. Where stimulus type was found to be significant, post hoc pairwise comparisons were carried out using a Tukey's HSD test within the multicomp package (Hothorn et al., 2008).

4.3 Results

4.3.1 Static background experiments

In the intensity experiment the crabs responded to all of the experimental stimuli, including both second-order stimuli, more than the control (likelihood ratio test: $\chi^2_{(4)} = 63.4$, $P < 0.001$; Figure 4.3a). The crabs also showed a higher level of response to SO2 than to SO1 and FC. Similarly, there was also a difference in response probability between the different stimuli in the polarization experiment (LRT: $\chi^2_{(4)} = 45.34$, $P < 0.001$; Figure 4.3b). Response to the FO and SO2 stimuli was higher than the control and FC. Furthermore, response to the FO stimulus was also higher than response to SO1. There was no effect of crab sex or size, nor was there any evidence of habituation in either the intensity (LRT: sex: $\chi^2_{(1)} = 1.42$, $P = 0.233$; size: $\chi^2_{(1)} = 1.74$, $P = 0.19$; order: $\chi^2_{(1)} = 0.003$, $P = 0.954$) or polarization (LRT: sex: $\chi^2_{(1)} = 1.91$, $P = 0.17$; size: $\chi^2_{(1)} = 0.02$, $P = 0.89$; order: $\chi^2_{(1)} = 0.69$, $P = 0.405$) experiment.

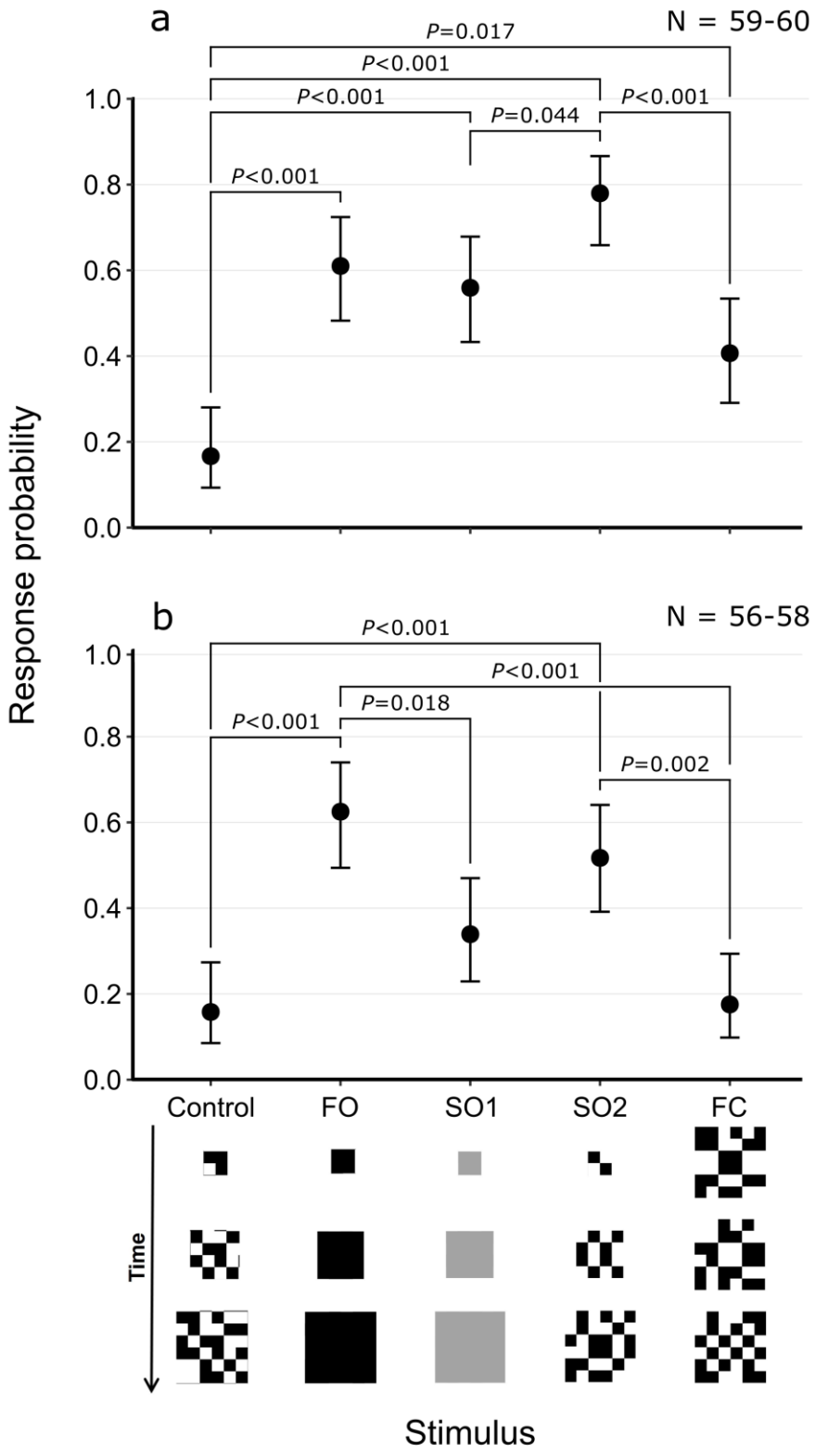

Figure 4.3: Response probability of fiddler crabs to the control, first-order motion (FO), two second-order motion (SO1 and SO2) and flicker-only control (FC) stimuli in the **a)** intensity and **b)** polarization static background experiments. Error bars represent Wilson score intervals calculated using the sample size for each point (N) and the number of responses. Statistical significance between the different stimuli was determined using a Tukey's HSD test, the results of which are only shown for pairs that were significantly different from one another.

4.3.2 Dynamic background experiments

The crabs did not respond to any of the stimuli presented against the dynamic random noise background in either the intensity (LRT: $\chi^2_{(3)} = 0.27$, $P = 0.965$; Figure 4.4a) or the polarization (LRT: $\chi^2_{(3)} = 1.06$, $P = 0.786$; Figure 4.4b) experiments. There was no effect of crab sex or size, nor was there any evidence of habituation in either the intensity (LRT: sex: $\chi^2_{(1)} = 0.34$, $P = 0.558$; size: $\chi^2_{(1)} = 0.03$, $P = 0.86$; order: $\chi^2_{(1)} = 0.01$, $P = 0.922$) or polarization (LRT: sex: $\chi^2_{(1)} = 1.1$, $P = 0.293$; size: $\chi^2_{(1)} = 0.02$, $P = 0.891$; order: $\chi^2_{(1)} = 2.31$, $P = 0.129$) experiment.

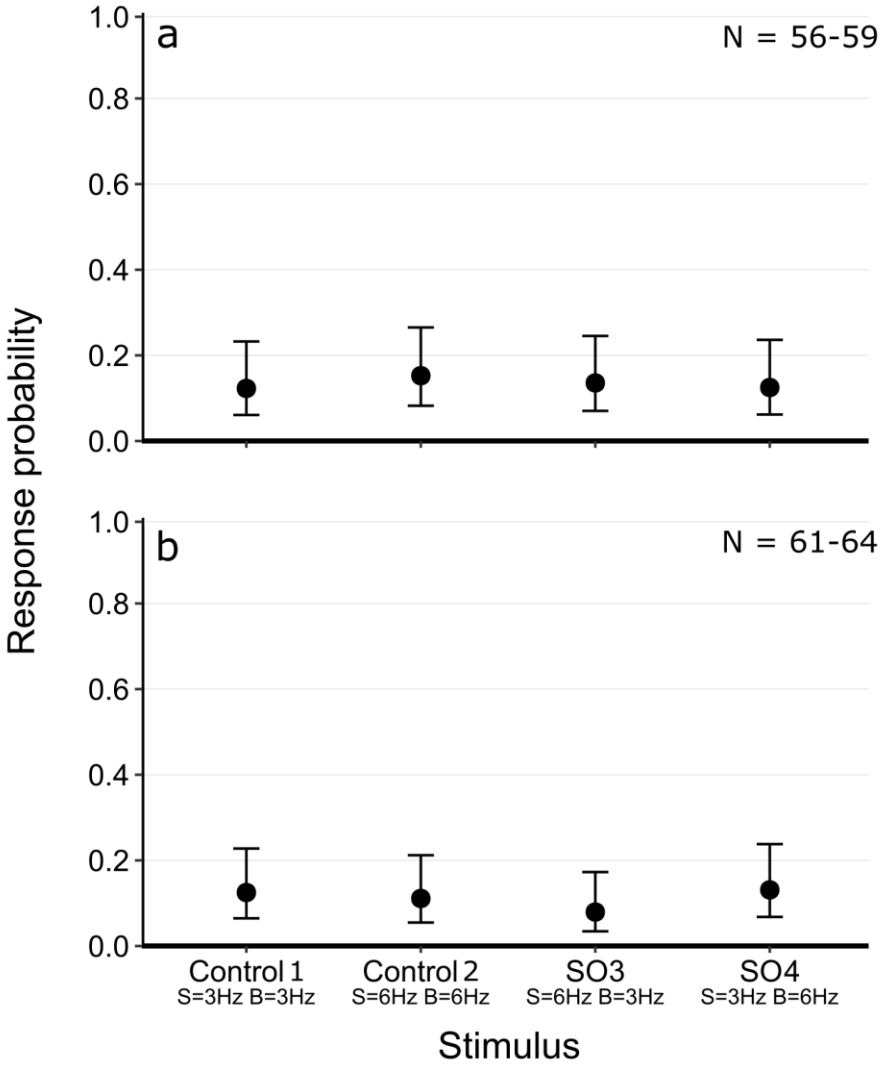

Figure 4.4: Response probability of fiddler crabs to the two controls and two second-order motion (SO3 and SO4) stimuli in the **a)** intensity and **b)** polarization dynamic background experiments. Error bars represent Wilson score intervals calculated using the sample size for each point (N) and the number of responses.

4.4 Discussion

This study is the first to present evidence that a crustacean can see second-order motion. It is also the first to show evidence for the detection of second-order motion in polarization in any species. These findings support those from other studies showing that the detection of second-order motion is not limited to vertebrates (Theobald et al., 2008; Nityananda et al., 2018).

4.4.1 Response to second-order motion generated by flicker

Fiddler crabs are capable of detecting second-order motion generated by visual flicker in both intensity and polarization when viewed against a static background, but not against a dynamic background. In both the intensity and polarization experiment with the static background crabs responded more to SO2 than to SO1 (although this was not statistically significant in the polarization experiment) illustrating the importance of visual flicker as a response criterion for threat detection, in addition to the second-order motion it produced. The importance of flicker may also be demonstrated by the observation that response to SO2 was slightly higher than the response to FO in the intensity experiment. However, this result may also be attributed to the fact that some of the crabs responded to FO by immediately breaking into a sprint rather than freezing, i.e. it elicited the second stage of the anti-predator response (home-run) rather than the first stage (freezing); therefore, although the crab did respond to the stimulus the auto score program would have recorded it as having not responded, resulting in a slightly more conservative estimate of response probability for FO.

A key advantage of flicker as a response criterion is that it can be evaluated by a single ommatidium and thus provides one of the earliest indications of an approaching predator (Smolka et al., 2011, 2013). Given that fiddler crabs readily respond to changes in light intensity detected by one or two ommatidia (Hemmi & Pfeil, 2010; Smolka et al., 2011), it is

possible that the crabs could have been responding to the static change in intensity, or polarization, of one or more individual squares rather than the second-order motion itself. Indeed, in the intensity experiment with the static background there was a significant difference in response probability between the control and FC indicating that the static change in intensity alone was enough to elicit a response even in the absence of motion cues. The finding that crabs were significantly more likely to respond to SO2 (which contained second-order motion cues) than FC (which contained flicker but no second-order motion) does however demonstrate that the crabs were capable of distinguishing between the actual motion of SO2 and the flicker alone. In the polarization experiment with the static background the crabs also responded to SO2 significantly more than FC indicating that crabs can detect and respond to second-order motion in polarization. However, in the absence of second-order motion, polarization flicker was not sufficient to elicit a response. In the crabs' mudflat environment polarization flicker would readily occur in wind induced ripples in pools of water or the sea, so static polarization flicker is likely to be most commonly associated with harmless environmental noise and may therefore not provide a reliable indication of predation threat. The finding that the crabs responded to FC in intensity but not polarization is consistent with the findings from chapter 2 that intensity and polarization information are processed in separate visual channels.

In contrast to the findings from the static background experiments, the experiments that used the dynamic flickering background found no difference in the level of response between the controls and the second-order motion stimuli. While this may seem to contradict the findings of the static background experiments it is worth noting that, even for a human, SO3 and SO4 were reasonably difficult to detect (see supplementary movies S6 and S7; appendix A.8). It is possible that the difference in flicker rate between the background and the stimulus was not large enough for the crabs to distinguish between them. It can also be argued that SO3 and SO4

are less biologically relevant than SO2. For instance, the flicker from the flapping wings of birds such a terns would be viewed against the sky which would not be flickering; this is somewhat similar to SO2 which was viewed against the static background.

4.4.2 Second-order motion in nature

As is the case with intensity and polarization, first- and second-order motion cues are unlikely to occur in isolation in the natural world. It has been suggested that natural scenes contain some features that would preferentially stimulate first-order mechanisms while other features are more likely to stimulate second-order mechanisms (Schofield, 2000). Therefore, sensitivity to both first- and second-order motion can increase the amount of visual information available to an animal. For fiddler crabs one benefit of seeing second-order motion could be predator identification because different avian predators create different flicker signals (Smolka et al., 2011, 2013). For instance, the fluttering wings of terns, a major predator of many fiddler crab species (Land, 1999), produce a strong flicker signal, whilst other birds that commute over the mudflats but do not hunt fiddler crabs, produce a much weaker flicker signal (Smolka et al., 2011, 2013). Since flicker from flapping wings can produce second-order motion (Theobald et al., 2010) it is possible that the presents or absence of second-order motion could be an indicator of predation risk for fiddler crabs helping them to distinguish between predatory and none predatory birds.

4.4.3 Visual processing of second-order motion

In humans, and other mammals, there is evidence for the existence of independent first- and second-order motion processing pathways, the outputs of which combine later in visual processing to form a single value that represents motion direction (Zhou & Baker, 1990; Ledgeway & Smith, 1994; Lu & Sperling, 1995; Smith et al., 1998; Baker, 1999; Schofield &

Georgeson, 1999; Scott-Samuel & Georgeson, 1999). Although it remains uncertain exactly why this would have evolved, there is evidence to suggest that, under conditions of low visual contrast, this method of visual processing means that first- and second-order cues can be combined in a way that enhances perceptual accuracy, although combining these cues has little benefit when visual contrast is high (Smith & Scott-Samuel, 2001). Although research on species other than humans is limited there is some evidence to suggest that processing first- and second-order motion in parallel visual channels is unlikely to be limited to vertebrates alone and may be present in invertebrates such as flies (Theobald et al., 2008; Aptekar et al., 2012; Lee & Nordstrom, 2012). This raises the possibility that second-order cues may also help to enhance perceptual accuracy in other animals including crustaceans. Detecting both first- and second-order cues may be particularly beneficial for crepuscular and nocturnal species which are active when visual contrast within a scene is lower than that during the day. Given that intensity and polarization information are processed separately in independent channels (chapter 2), the discovery that crabs are able to detect second-order motion in polarization poses additional questions regarding how this form of motion is processed.

4.5 Chapter summary

This study is the first to show evidence of the detection of second-order motion in a crustacean and the first to show detection of second-order motion in polarization in any animal. The findings support previous research that found visual flicker to be an important cue for detecting predators and suggest that the presence, or absence, of second-order motion generated by this flicker may be an important indicator of the level of predation risk for fiddler crabs living in a mudflat environment.

Chapter 5

Does circadian cycle affect the intensity and polarization contrast sensitivity of dark adapted ghost crabs?

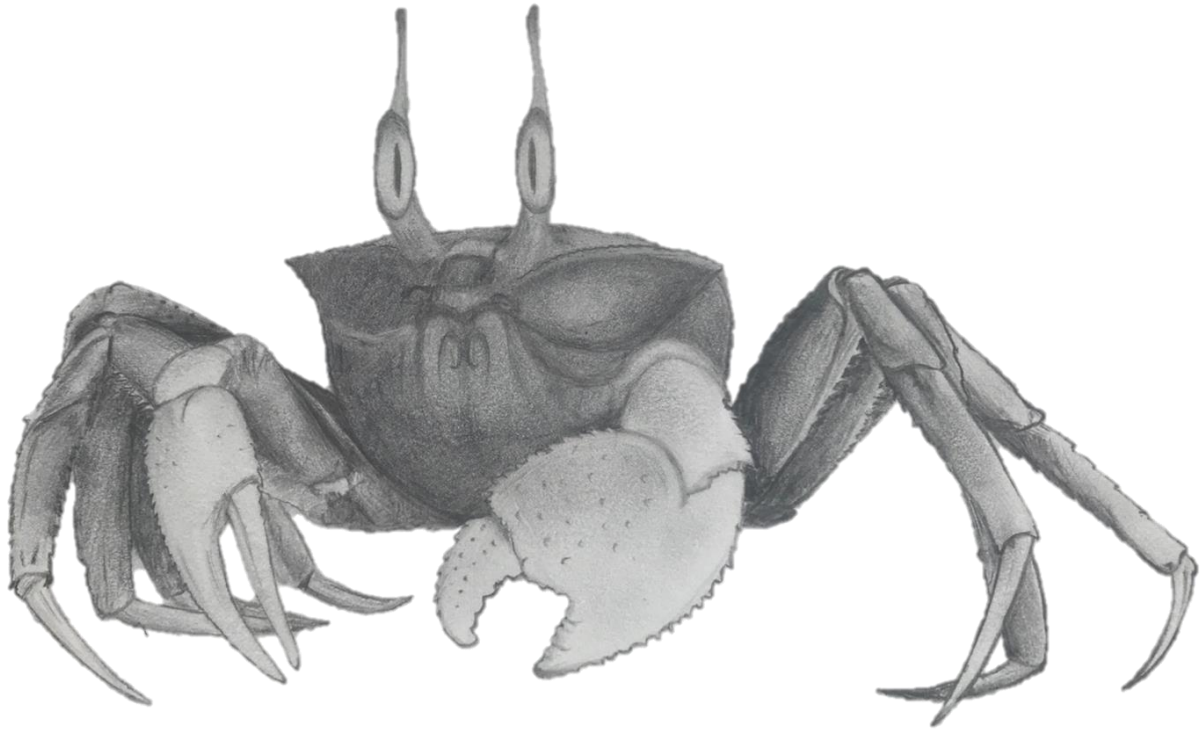

The horn-eyed ghost crab *Ocypode ceratophthalma*
Pencil drawing by Stevie Kennedy-Gold

So far the studies within this thesis have investigated polarization vision in a diurnal fiddler crab under bright daylight conditions. While they are generally considered to be nocturnal, ghost crabs can be active at any time of day and thus offer an exciting opportunity to study the use of polarization vision for object detection at different times of day. The study reported in this caveat chapter aimed to test whether circadian cycle affects the ability of ghost crabs to detect intensity and polarization contrasts at different times of day, and ultimately sort to establish whether ghost crabs could provide a new system for studying polarization vision.

5.1 Introduction

Even at night there is the potential for animals to use polarization vision for a variety of visual tasks as similar polarization cues exist on moonlit nights as during the day despite the intensity of the light being over a million times lower (Gál et al., 2001b; Johnsen et al., 2006; Nilsson, 2009; Warrant & Johnsen, 2013). Some nocturnal and crepuscular species of insect have been shown to detect and use polarization cues at night for navigation (Dacke et al., 1999, 2003a,b, 2011; Greiner et al., 2007; Reid et al., 2011; el Jundi et al., 2015; Freas et al., 2017). For example, crepuscular and nocturnal dung beetles (*Scarabaeus zambesianus* and *Scarabaeus satyrus* respectively) use the polarization pattern of the moonlit sky to orientate and roll their ball of dung in a straight line (Dacke et al., 2003a,b; el Jundi et al., 2015). The accuracy to which *S. satyrus* is able to navigate using the polarization pattern around the crescent moon is equal to that achieved by diurnal species during the day even when the light level is 100 million times dimmer (Dacke et al., 2011).

Compared to vision during daylight, vision in low light presents a challenge because as the number of photons detected by the photoreceptors decreases so does the signal to noise ratio (Lillywhite & Laughlin, 1979; Dubs et al., 1981; Nilsson, 2009; Carroll & Warrant, 2017;

Warrant, 2017). This makes it increasingly difficult to distinguish between two similar objects or between an object and the background. Nonetheless, invertebrates photoreceptors are known to be remarkably sensitive to even single photons (Lillywhite & Laughlin, 1979; Dubs et al., 1981; Laughlin & Lillywhite, 1982; Honkanen et al., 2014). The cockroach *Periplaneta americana* for instance has even been shown to perform an optomotor response when less than one photon is absorbed by each of its photoreceptors every 10 s (Honkanen et al., 2014).

Among decapod crustaceans, the adaptations for vision under low light, as well as under daylight, has been particularly well studied in ghost crabs. Along with many species of crustaceans, ghost crabs exhibit adaptive migration of screening pigments (these can be within the photoreceptors themselves or within pigment cells that surround the photoreceptors) in response to light and dark adaption (Eguchi & Waterman, 1967; Arikawa et al., 1987). The migration of screening pigments is often combined with a corresponding change in the size, and sometimes also shape, of the rhabdom (Nässel & Waterman, 1979; Stowe, 1981; Rosenberg & Langer, 2001). Under natural daylight conditions, the diameter of the rhabdom is small during the day but increases dramatically at dusk by as much as nearly 20-fold before being broken down again before dawn (Nässel & Waterman, 1979). The change in eye morphology and the movement of screening pigments is governed by an interaction between ambient light level and circadian cycle (Nässel & Waterman, 1979; Rosenberg & Langer, 2001). While these changes occur in response to the light adaption state of the eye, the magnitude of the change is primarily controlled by the animal's circadian rhythm (this is particularly true for rhabdom size and shape). Consequently, the greatest visual sensitivity is only achievable at night under low light (Nässel & Waterman, 1979; Stowe, 1981; Toh & Waterman, 1982; Arikawa et al., 1987; Toh, 1987; Rosenberg & Langer, 2001). This means complete dark adaptation is inhibited during the light phase of the day, but, while achievable

at night, will only occur if the light level is low (Nässel & Waterman, 1979; Rosenberg & Langer, 2001). For example, if *Ocypode* species are light-adapted during the night the rhabdom diameter decreases to that of a light-adapted individual during the day. If, on the other hand, the crab is dark-adapted during the day the diameter of the rhabdom increases, but never reaches the size of a dark adapted crab at night (Rosenberg & Langer, 2001). This mean that a crab that is dark adapted during the day will, at least in theory, be less sensitive to light than it would be if it were dark adapted during the night. Sensitivity to polarization contrasts on the other hand should be the same (providing that the microvilli arrangement does not change).

While there is a good understanding of how circadian cycle limits eye sensitivity during the day in ghost crabs, no one has investigated how these restrictions effect intensity and polarization vision in the context of functional tasks such as object detection. Therefore, this study investigated how the intensity and polarization contrast sensitivity of dark adapted ghost crabs (*Ocypode ceratophthalmus*) was affected by the time of day. Specifically, this study aimed to determine if dark adapted crabs were able to detect lower intensity contrasts during the night, than during the day, because of circadian imposed restraints that limit the size of the rhabdom during the day.

5.2 Methods

All experiments took place between 26th July and 25th September 2017. The study consisted of four experiments (two for intensity and two for polarization) conducted under two different ambient light intensities that were comparable to those experienced by the crabs in their natural habitat during twilight in July. Ghost crabs were tested twice in each experiment, once during the day and once during the night. To control for any order effects half of the crabs were first tested during the day while the other half were first tested during the night.

5.2.1 Crab collection and preparation

Ocypode ceratophthalma were collected by hand from different beaches along the north east coast of O'ahu, Hawaii, USA. Crabs were housed separately in clear plastic pots in the lab under natural daylight. A folded strip of kitchen paper was placed in the pot with each crab to provide a substrate for them to walk on and hide under. Crabs were kept for a maximum of five weeks and were fed with shrimp three times a week (Monday, Wednesday and Friday) and regularly provided with fresh sea water. Prior to the experiment a wire harness similar to that used in previous chapters was glued to the crab's carapace. The size (measured across the widest point of the carapace) and sex of each crab was recorded. Each crab was used for up to two experiments before being released. A total of 24 crabs were tested in each experiment.

5.2.2 Selecting the ambient light levels

Spectral irradiance measurements were taken in the field (Chun's reef, O'ahu, Hawaii, USA; 21.6202° N, 158.0850° W), using a spectrometer (USB2000 High Sensitivity, Ocean Optics, Largo, USA), coupled to an optic fibre (QP600-1-UV-VIS, Ocean Optics, Largo, USA) fitted with a cosine corrector (CC-3-UV-S, Ocean Optics, Largo, USA), starting approximately 25 min before sunset and ending 45 mins after sunset on the 23rd July 2017 (Figure 5.1a- coloured lines). Each spectrum was then multiplied by a pigment nomogram (Stavenga et al., 1993) to account for the estimated spectral sensitivity of the R1-7 photoreceptors and the area under the resulting curve (number of photons absorbed) was used as an estimate of the ambient intensity detected by the crabs (Figure 5.1b- coloured points). The peak sensitivity of *O. ceratophthalma*, or indeed any *Ocypode* species, is unknown so a lambda max of 520 nm was used based on that obtained for closely related fiddler crabs (Cronin & Forward, 1988; Jordão et al., 2007).

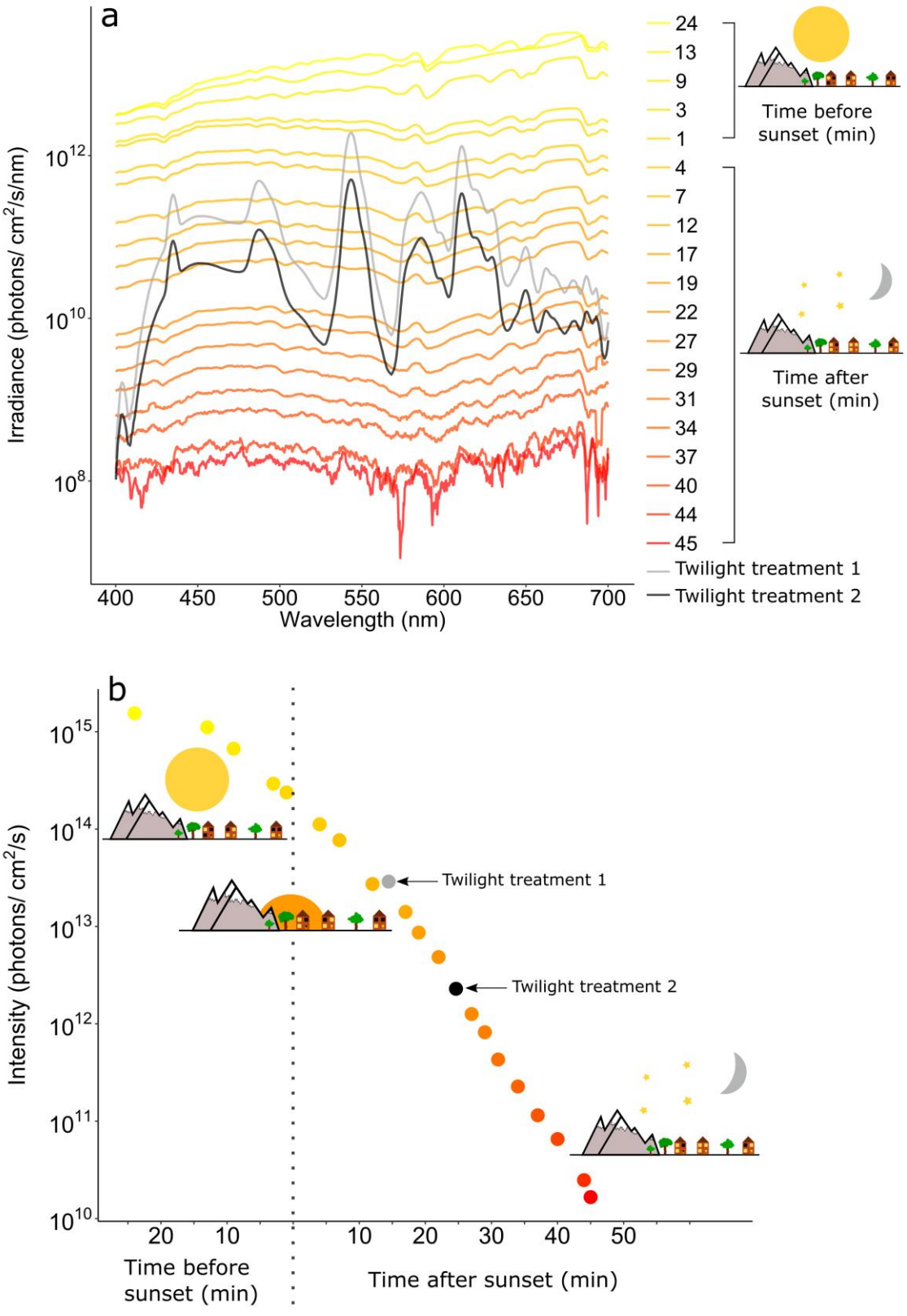

Figure 5.1: Ambient light intensity measured in the field (coloured lines and dots) and in the lab set up (grey and black lines and dots). **a)** Irradiance spectra and **b)** estimated ambient light intensity (calculated from a) measured in the field between approximately 25 min before sunset and 45 mins after sunset and the mean irradiance spectra and intensity of the two twilight treatments in the lab after accounting for the estimated spectral sensitivity of *Ocypode ceratophthalma*.

The crabs were tested under two different ambient light intensities, hereafter referred to as twilight treatments 1 (Figure 5.1- light grey) and 2 (Figure 5.1- dark grey), that differed from one another by one order of magnitude and were comparable to the light intensity recorded approximately 15 min and 25 min after sunset respectively.

5.2.3 Acclimatisation

Before being tested the crabs were dark adapted to twilight treatment 1 in the first set of experiments and to twilight treatment 2 in the second set of experiments for a minimum of two hours. The purpose of this was to ensure that any differences in the crab's contrast sensitivity between day and night were the result of circadian cycle and not because of differences in the ambient light intensity experienced by the crab prior to testing. Acclimatisation began approximately three and a half hours after sunrise for the day treatment and approximately two hours after sunset for the night treatment. For acclimatisation, crabs (within their clear plastic pots) were placed inside a 40 x 40 x 40 cm white photographic tent (LT124, PhotoSEL), (hereafter referred to as the acclimatisation tent, Figure 5.2a and Figure 5.2b), the opening of which was positioned against a modified patterned vertical alignment type liquid crystal display (PVA-LCD) computer monitor (1905FP, Dell, Round Rock, USA) (hereafter referred to as the acclimatisation screen) (see section 5.2.4 for details) that illuminated the inside of the tent. Acclimation took place in a dark room and the acclimatisation screen was the only source of light. Up to six crabs were acclimatised at a time.

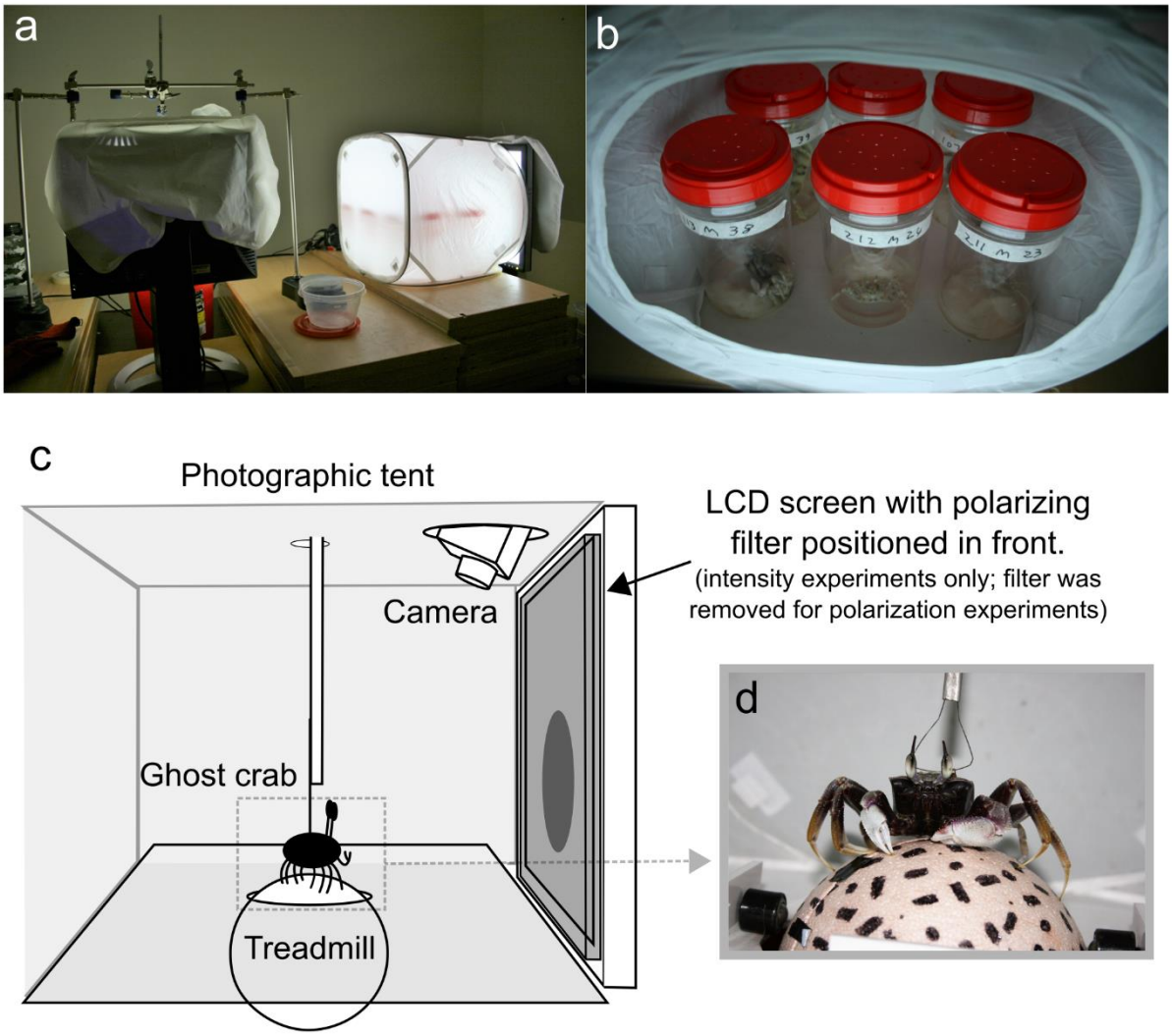

Figure 5.2: Experimental apparatus. **a)** Acclimatisation tent (right) in which crabs were acclimatised to one of the two twilight light intensities for a minimum of two hours before being tested in the experimental tent (left). Note that the photo was taken using along a long exposure time and so the screens appear much brighter than they were in reality. **b)** Ghost crabs were placed in the acclimatisation tent within their plastic containers. **c)** Schematic showing the design of the experimental tent. Crabs were tethered above a treadmill and subjected to looming stimuli of increasing visual contrast in an ascending staircase design. **d)** Photo of a ghost crab positioned on the treadmill.

5.2.4 Experimental setup

The experimental setup was very similar to the acclimatisation stage in that it consisted of a photographic tent (hereafter referred to as the experimental tent), the open side of which was positioned against a modified PVA-LCD screen (experimental screen) that provided illumination (Figure 5.2c). In the centre of the experimental tent was a crab treadmill that was used to test the response of the crabs to a series of looming stimuli in a similar way to that

described in previous chapters. The treadmill was the same as the water-based treadmill used for the field experiment described in section 3.2.2. For the experiment the crabs were tethered above the treadmill in the same way as in previous chapters (Figure 5.2d).

The outer-most polarizing filter had been removed from both the acclimation and experimental LCD screens (in the same way as in chapters 2 and 4) so that they only produced polarization-images in which intensity contrast was substituted for contrast in the DoLP (Foster et al., 2018). The DoLP was controlled by manipulating the RGB value of the image (Figure A.12a and Figure A.12b). The light from the screens was always roughly horizontally polarized within the RGB range used in this study (Figure A.12c and Figure A.12d). For the intensity experiments a polarized filter (#7300, Rosco, London, UK), which was sandwiched between two sheets of 5 mm thick transparent Perspex, was placed in front of both screens so they displayed intensity images. The overall intensity of the screens, and thus the ambient intensity of the acclimatisation and experimental tents, was controlled using neutral density filters (#209 0.3ND and #211 0.9ND, Lee Filter, Andover, UK) positioned between the light source and the LCD panel (Table 5.1).

Table 5.1: The ambient intensity of the acclimatisation and experimental tents was control using neutral density filters (in combination with the polarization filter used for the intensity experiment). The ambient intensity for twilight treatments 1 and 2 differed from one another by one order of magnitude. Intensity is given in photons/cm^2/s.

	Twilight treatment 1		**Twilight treatment 2**	
	Intensity experiment	Polarization experiment	Intensity experiment	Polarization experiment
Polarizing filter	present	absent	present	absent
Neutral density filter	absent	0.3ND	0.9ND	0.9ND
Mean intensity	3.99×10^{13}	1.79×10^{13}	1.32×10^{12}	3.27×10^{12}

For the intensity experiments, a spectrometer (USB2000 High Sensitivity, Ocean Optics, Largo, USA) coupled to an optic fibre (QP600-1-UV-VIS, Ocean Optics, Largo, USA) was used to measure the irradiance values of the experimental screen at each RGB value in twilight treatments 1 and 2. These were used to calculate the Weber contrast of the stimulus/background combinations after accounting for the estimated spectral sensitivity of the R1-7 photoreceptors for *O. ceratophthalma* (refer to section 2.2.2 for details of calculating weber contrast). The polarization properties at each RGB value were measured using the method described in appendix A.1 and the values used to calculate the polarization distance (How & Marshall, 2014) between the stimulus and the background.

5.2.5 Experimental procedure

The experiments were conducted using MATLAB R2016a (MathWorks, 2016) using the Psychophysics Toolbox extensions (Brainard, 1997; Pelli, 1997). Following acclimatisation, each crab was positioned on the treadmill and allowed a minimum of 3 min before starting the experiment. Each stimulus consisted of a looming circle that expanded exponentially from a visual angle of 0° to 20° over 5 s. Upon reaching its full size there was a pause of 2 s before the stimulus disappeared. The study used an ascending staircase design, in which the visual contrast between the stimulus and the background started at zero and gradually increased with each successive stimulus (Table 5.2). The ascending staircase design used in this study was an adaptation of a common psychophysical technique used to behaviourally assess contrast thresholds in animals (Moskowitz & Kitzes, 1966; De Weerd et al., 1990; Treutwein, 1995; García-Pérez, 1998). Crabs were shown up to 23 stimuli in the intensity experiments and up to 18 stimuli in the polarization experiments. In the intensity experiments the stimuli were all darker than the background, and in the polarization experiments the stimuli were all less polarized than the background (which was fully polarized; DoLP = 0.99). Each stimulus

presentation was separated by a random pause that ranged between 30 s to 120 s. All trials were recorded using a Sony HDR-SR11 Handycam which was connected to a separate monitor to allow the experimenter to see the crab. To reduce the amount of time each individual spent on the treadmill, the experiment was ended once the crab had responded to a minimum of two stimuli. Only the most extreme behavioural response, i.e. jumping, was counted as a response while scoring on the fly. In the event that a crab did not respond to a single stimulus the experiment was ended once all of the stimuli had been presented. At the end of each trial, regardless of the number of previous presentations, crabs were shown a maximum contrast loom (i.e. the greatest contrast attainable) that functioned as a positive control.

Table 5.2: Weber contrast (intensity experiments) and polarization distance (polarization experiments) between the background and the looming stimuli for the two ambient light intensities, and the order the stimuli were presented in.

Stimulus order	Intensity experiments (Weber contrast)		Polarization experiments (polarization distance)	
	Twilight 1	Twilight 2	Twilight 1	Twilight 2
1 (negative control)	0	0	0	0
2	-0.027	-0.031	-0.171	-0.171
3	-0.06	-0.064	-0.351	-0.351
4	-0.082	-0.086	-0.513	-0.513
5	-0.109	-0.114	-0.624	-0.624
6	-0.131	-0.138	-0.818	-0.818
7	-0.149	-0.157	-0.942	-0.942
8	-0.171	-0.179	-1.057	-1.057
9	-0.188	-0.198	-1.161	-1.161
10	-0.206	-0.218	-1.264	-1.264
11	-0.228	-0.239	-1.406	-1.406
12	-0.247	-0.257	-1.462	-1.462
13	-0.267	-0.279	-1.571	-1.571
14	-0.286	-0.297	-1.658	-1.658
15	-0.304	-0.315	-1.736	-1.736
16	-0.324	-0.334	-1.834	-1.834
17	-0.343	-0.353	-1.899	-1.899
18	-0.36	-0.372	na	na
19	-0.38	-0.391	na	na
20	-0.396	-0.407	na	na
21	-0.411	-0.424	na	na
22	-0.747	-0.758	na	na
Positive control	-1	-1	-2.233	-2.233

5.2.6 Video scoring

Post hoc blind scoring was carried out in MATLAB R2017a (MathWorks, 2017) using VLC media player v2.2.6 (VideoLan Organization). For each 13 s video (5 s before the start of the loom, 5 s during loom expansion and 3 s after) the time at which the crab displayed one or more of the following behaviours was recorded: started or stopped walking, flinched, jumped, eye twitch, retracted legs and/or claws, and lowered body. These data were used to determine which behaviours were the most reliable proxy for the detection of the stimulus. Based on this, the crabs were recorded as having responded if they jumped, flinched, or lowered their body during a 3 s scoring window (last 3 s of loom expansion) (see appendix A.10). For each crab, the lowest contrast to elicit a response was recorded as the contrast threshold (i.e. the lowest detectable contrast) for that treatment. Crabs that did not respond to a single stimulus (excluding the positive control) were excluded from the main analysis. In addition to the main analysis, the response probability to the negative and positive controls was also compared.

5.2.7 Statistical analysis

All statistical analysis was conducted in R (R Core Team, 2017). The data were analysed using repeated ordinal regression with cumulative link mixed models (CLMM) in the R package ordinal (Christensen, 2015). Contrast threshold was treated as an ordinal variable. The justification for this is that although contrast threshold is technically a continuous variable, in this study it was sampled at discrete ordinal intervals hence the decision to treat it as such in this analysis. In the models, contrast threshold was used as the response variable, and time of day (day or night), ambient light level (twilight 1 or 2), and an interaction between the two were fitted as fixed effects. Crab ID was included as a random effect to control for repeated measures. Model simplification was used to test for significant fixed effects and interactions

whereby models were compared with one another using a likelihood ratio test (LRT) to sequentially remove non-significant interactions and effects.

In addition to the main analysis, McNemar tests, which can account for repeated measures, were used to compare the response probability to the negative and positive controls. A Bonferroni correction was used to control for multiple testing.

5.3 Results

5.3.1 Intensity and polarization contrast thresholds

There was no difference in the intensity contrast threshold of the crabs between day and night (likelihood ratio test: $\chi^2_{(1)} = 1.64$, $P = 0.2$; Figure 5.3a and Figure 5.3b), nor did the threshold differ between the two ambient light intensities (LRT: $\chi^2_{(1)} = 3.64$, $P = 0.057$). Likewise, there was no difference in polarization contrast threshold between day and night (LRT: $\chi^2_{(1)} = 0.84$, $P = 0.359$; Figure 5.3c and Figure 5.3d), nor between the two light intensities (LRT: $\chi^2_{(1)} = 2.53$, $P = 0.112$). Note that in the polarization experiment a high number of crabs did not respond to any of the stimuli and were thus excluded from the analysis.

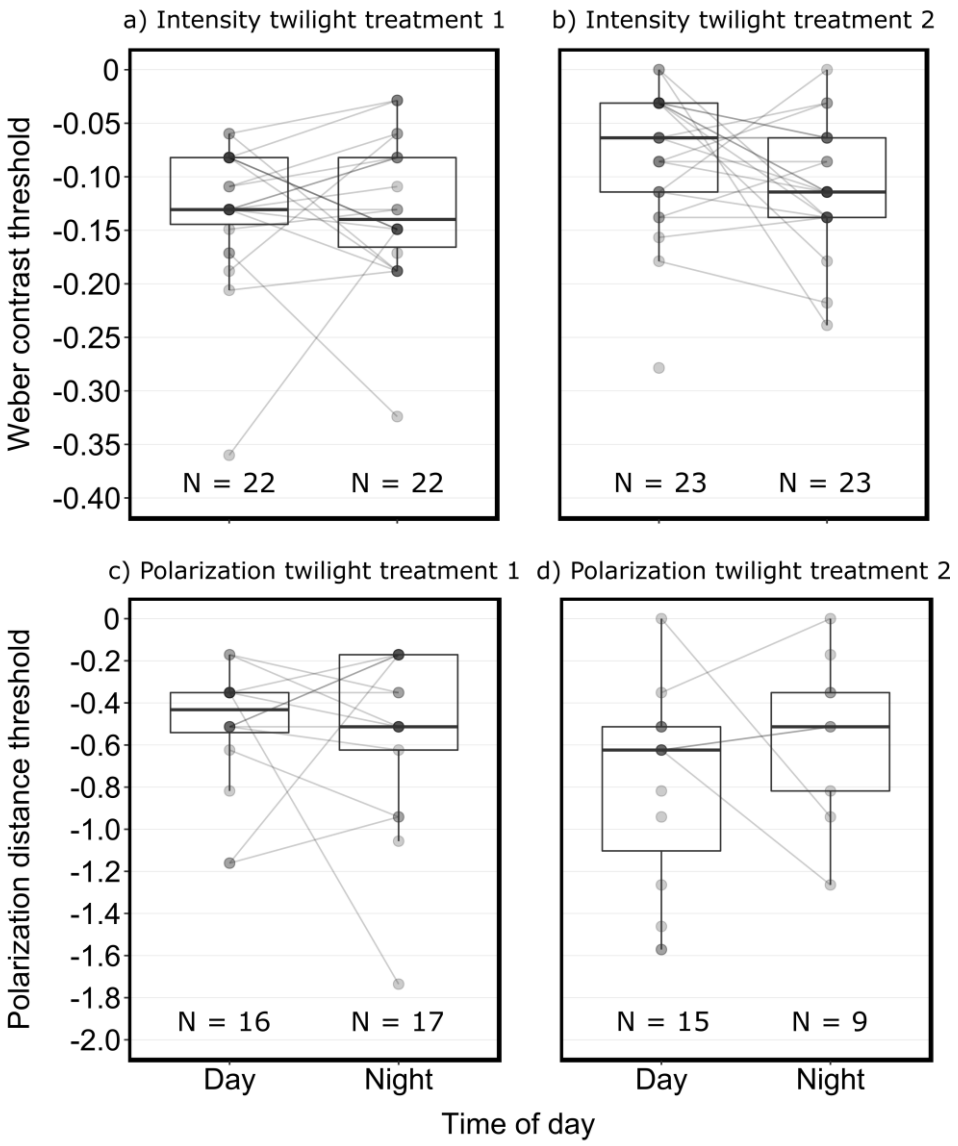

Figure 5.3: Lowest visual contrast that elicited a response from the ghost crabs in the **a-b)** intensity and **c-d)** polarization experiments at different times of day under the two ambient light intensities. The amount of fill in each point indicates the number of individuals that shared the same threshold (i.e. the darker the point the higher the number of crabs that share that contrast value). Lines are used to join points from the same individual. Box plots show medians plus the interquartile range (IQR), whiskers are the lowest and highest values that are within 1.5 times the IQR from the upper and lower quartiles.

5.3.2 Response probability to negative and positive controls

A large proportion of the crabs tested in the polarization experiments failed to respond to any of the presented stimuli (as indicated by the smaller sample sizes shown in Figure 5.3c and Figure 5.3d). This lower than expected response to polarization stimuli is particularly obvious when comparing the crabs' response probability to the negative and positive controls in each

experiment (Figure 5.4). In both intensity experiments response to the maximum contrast positive control was close to 100% (Figure 5.4a and Figure 5.4b). Conversely, in the polarization experiments response probability to the positive control was no different from the level of response to the negative control (Figure 5.4c and Figure 5.4d).

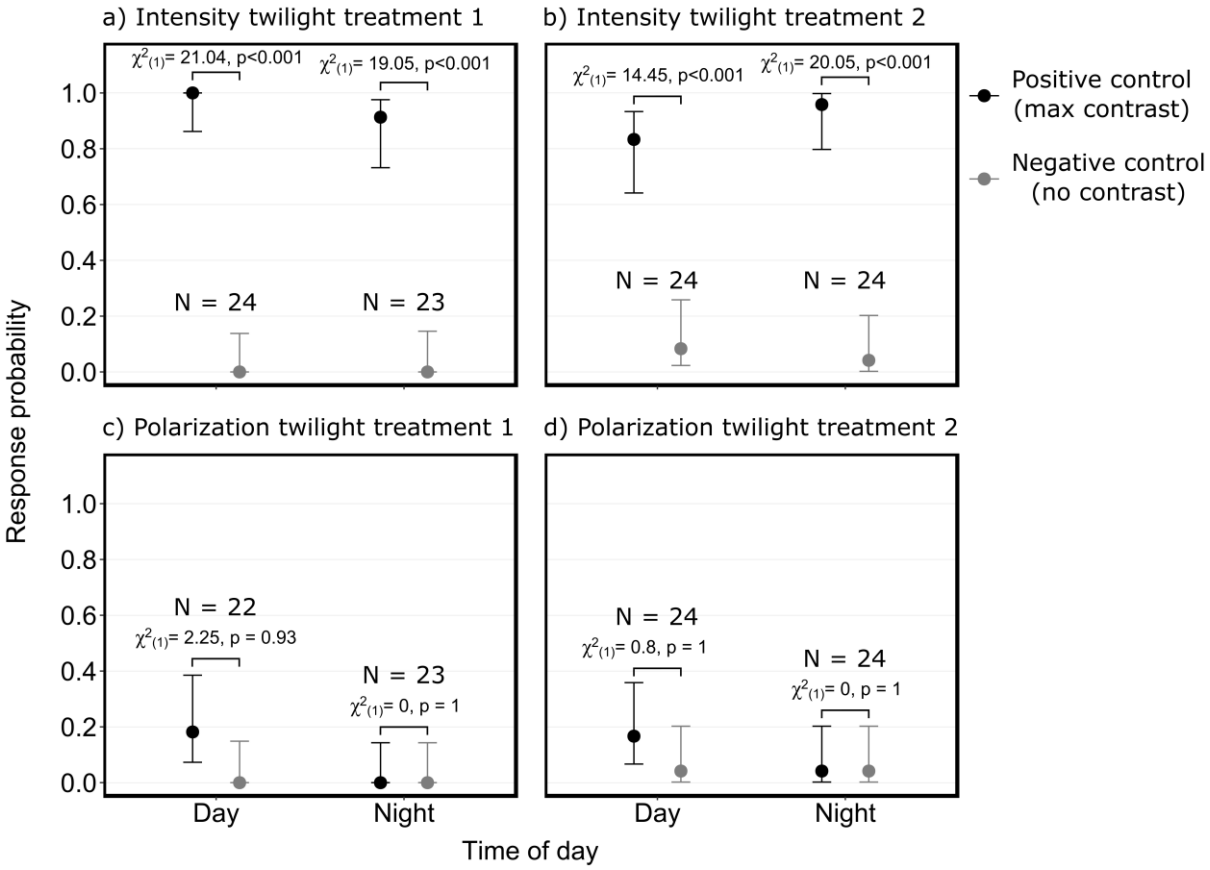

Figure 5.4: Response probabilities of ghost crabs to the positive (maximum contrast) and negative (no contrast) controls in the **a-b)** intensity and **c-d)** polarization experiments at different times of day under the two ambient light intensities. Error bars are Wilson score intervals calculated using the sample size for each point (N) and the number of responses. Significance was determined using McNemar tests. The positive control had a weber contrast of -1 and a polarization contrast, calculated as polarization distance, of -2.2 in the intensity and polarization experiments respectively.

5.4 Discussion

5.4.1 Behavioural response of ghost crabs to looming stimuli

A major caveat of this study, and ultimately the main reason for this being a caveat chapter, was the fact that *O. ceratophthalmus* displayed very few behaviours that constituted a reliable proxy for the detection of the looming stimulus. For instance, based on Figure A.13 - Figure A.16 a walking crab appeared just as likely to 'freeze' due to chance as it was in response to a visual stimulus. In comparison *A. tangeri* tended to show a steady walk on the treadmill and would usually only stop walking and freeze in response to the visual stimulus, thus providing a very reliable proxy for detection of the visual contrast. The only reliable behavioural indication that the ghost crabs had seen a visual stimulus was the jump response, however, not all crabs displayed this response and it was common for the crabs to not show any response to a set of visual stimuli even after they had previously jumped in response to a less contrasting stimulus. As such, there is a high probability of false negatives (type-2 errors) in the results.

5.4.2 Effect of circadian cycle on intensity and polarization contrast sensitivity

Whilst caution must be taken when interpreting the results of this study due to the caveat described above, the results suggest that circadian imposed restraints that limit the size of the rhabdom during the day did not have a negative effect on the ability of dark adapted crabs to detect intensity contrasts during the day. The same result was also found for polarization, although this should be expected given that the detection of polarization contrasts is an opponent process and thus isn't a function of intensity (Bernard & Wehner, 1977; How & Marshall, 2014).

The ambient light levels used in this study were comparable to those experienced naturally during twilight. Therefore, none of the crabs were tested under nocturnal light levels and so in both treatments the crabs would have been at least partially light adapted, and not dark adapted as intended. This has implications for the study because the size of the rhabdoms within light-adapted crabs during the night is the same as that within light-adapted crabs during the day (Rosenberg & Langer, 2001). This is the case even if the crab is kept in the darkness for the first few hours following sunset before being light-adapted (Rosenberg & Langer, 2001). It is therefore possible that there would have been no difference in the size of the crabs' rhabdoms, and consequently their sensitivity, between night and day. In such cases, one would not expect any difference between night and day in regards to the lowest intensity contrast detectable by the crabs under the light levels tested in this study.

Even if the crabs in this study had been dark adapted to much lower light intensities (e.g. moonlight or starlight) it does not necessarily mean that circadian imposed restrictions on the size of the rhabdom during the day would make the eye less sensitive than it would be during the night. This is because morphological adaptations are not the only means by which an animal can increase visual sensitivity. For instance, several insects species are known to use spatial and temporal neural summation, in combination with morphological and optical adaptations, to enable them to see under low light (Greiner et al., 2004a,b; Theobald et al., 2006; Warrant & Dacke, 2011, 2016; Baird et al., 2015; Stöckl et al., 2016). This strategy enables the nocturnal Indian carpenter bee *Xylocopa tranquebarica* and the hawkmoth *Deilephila elpenor* to discriminate coloured stimuli at intensities as low as starlight (Kelber et al., 2002, 2003; Balkenius & Kelber, 2004; Johnsen et al., 2006; Somanathan et al., 2008). While there is some evidence of neural summation in crustaceans (Nilsson & Nilsson, 1981; Moeller & Case, 1995) no study has investigated if it occurs in semi-terrestrial crabs such as *Ocypode*.

5.4.3 Response to polarization contrasts

One finding that brings into question the reliability of the estimations of the lowest polarization contrasts detected by the crabs is the difference in the probability of the crabs responding to the maximum contrast stimulus (positive control) in the polarization experiments compared to in the intensity experiments. In all four polarization treatments there was no significant difference between the response probabilities to the positive and negative controls. While these findings do not support the idea that *O. ceratophthalma* uses polarization vision for target detection, previous studies have shown that ghost crabs can detect polarized stimuli (Schöne & Schöne, 1961; Daumer et al., 1963). This result is more likely to be a reflection of the fact that the ghost crabs were not well suited to the behavioural experiments used in this study. This is supported by the observation that *O. ceratophthalma* responded more reliably to a maximum contrast polarization stimulus during preliminary experiments (personal observations). The lack of response to the maximum contrast stimulus in the main study may have resulted from the fact that, unlike in the aforementioned preliminary experiments, the positive control was always the last stimulus to be presented; i.e. it was only shown to the crabs after they had responded to a certain number of low contrast stimuli, or, if they did not respond to anything, they had seen all of the stimuli. Therefore, it is possible that the low response to the maximum polarization contrast is the result of habituation to the polarization stimuli brought on by the gradual increase in polarization contrast due to the ascending staircase design. Indeed, short term habituation following repeated exposure to the same stimulus has been shown to occur in other species of crabs (Oliva et al., 2007) and habituation was also found in some of the experiments in chapters 2 and 3.

It is also possible that polarization cues may not be as important for ghost crabs as they are for fiddler crabs due to differences in the type of habitat in which these two groups are predominantly found. Unlike fiddler crabs, which are predominantly found on damp intertidal mudflats (Crane, 1975), *O. ceratophthalma* primarily tend to inhabit sandy shores, and often dig burrows and forage well above the high tide mark (Hughes, 1966; Lucrezi & Schlacher, 2014), where polarized reflections are less prevalent because the dry sand reflects less, or no, polarized light. In addition, the predominantly nocturnal lifestyle of ghost crabs further reduces the prevalence of polarization within their environment because polarized reflections of wet areas of sand would be limited to crepuscular periods and nights illuminated by the moon. Consequently, polarization could be a less reliable source of information for ghost crabs than for fiddler crabs and this may explain why they were less likely to respond to the polarization stimuli.

An interesting observation made during this study was that the crabs were often more responsive to sounds made by the experimenter than they were to the visual stimuli. Ghost crabs are known to be highly sensitive to acoustic vibrations transmitted through the air and the substrate (Popper et al., 2001). It is possible that nocturnal ghost crabs may rely on alternative sensory modalities, such as acoustic detection, more than other semi-terrestrial species such as fiddler crabs, which rely more heavily on vision.

5.5 Chapter summary

The results suggest that circadian imposed restraints that limit the size of the rhabdom during the day did not have a negative effect on the ability of crabs to detect intensity, or polarization, contrasts during the day under light intensities comparable to those experienced during twilight. However, the behavioural ecology of *O. ceratophthalma* meant that conducting behavioural

experiments with this species was difficult and consequently the findings of this study are not reliable. As a result of this, the findings of this chapter are not discussed as part of the synopsis in the next chapter.

Chapter 6

Conclusions and future work

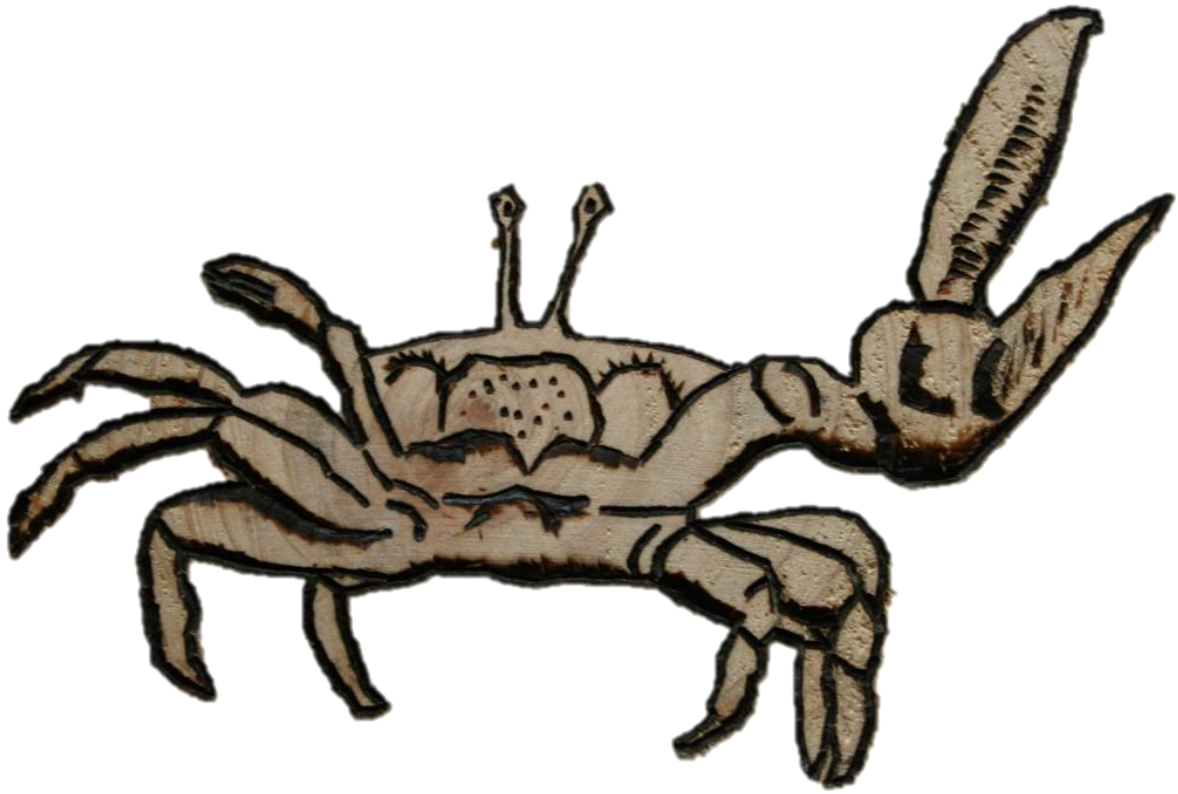

Claw waving display of the fiddler crab *Afruca tangeri*
Wood engraving by Sam Huguet

Our knowledge of the polarization of light and how animals detect and use this valuable source of information has come a long way since Félix Santschi reported the mysterious observation that ants were able to maintain a straight course back to their nest even when the only thing they could see was a patch of unobscured sky (Santschi, 1923). The last few decades in particular have seen numerous breakthroughs in our understanding of polarization vision. The work within this thesis builds upon this understanding by answering several outstanding questions relating to how crabs, and perhaps other crustaceans, process and use polarization information to enhance object detection. As is the nature of science, whilst several questions have been answered, numerous more have taken their place. This chapter provides a brief summary of the main findings that answer some of the questions investigated within this thesis and highlights a few of the new questions that stand out.

6.1 Visual processing of intensity and polarization

The data presented in chapter 2 show that within the visual system of fiddler crabs, intensity and polarization information are processed independently in parallel channels. This discovery demonstrates that crabs, and possibly other crustaceans, do not simply detect polarization as a modulation of the intensity information. Each form of visual information therefore contributes its own measure of visual contrast, which then feeds into processing circuits that mediate visually guided behaviours. In the context of the crab's binary freeze response, intensity and polarization contrasts do not interact in an additive or multiplicative manner to affect response; instead the crab's response depends on whichever contrast is the most salient and above a certain threshold, whether it be intensity or polarization. Since chapter 2 only looked at the crabs initial freeze response, future work should investigate other visually guided behaviours. Different behaviours will be controlled by separate neuronal pathways to those controlling the binary freeze response and so intensity and polarization may be integrated differently. Future

work might also investigate if polarization and intensity information from the R1-7 receptors is integrated with intensity information from the R8 receptor in a possible colour vision pathway.

A secondary finding of chapter 2 was the asymmetric response to polarization in which the crabs were more responsive to looms that were less polarized than the background compared to those that were more polarized. This is analogous to considering ON and OFF responses to intensity (Joesch et al., 2010). Since the experiments in chapter 2 were limited to horizontally polarized stimuli, questions remain regarding whether this same asymmetric response would be observed at other AoPs. Preliminary experiments, similar to the polarization only experiment from chapter 2, except the AoP was vertical instead of horizontal, show that regardless of the AoP, fiddler crabs are always more responsive to looming stimuli that are less polarized than the background, suggesting that it is the DoLP that is important and not the AoP (Martin How, unpublished data). Future work might extend this further to test how the response to horizontally polarized looms on a vertically polarized background compares to the opposite. Future studies of this kind could improve and advance the calculation of polarization distance (How & Marshall, 2014), which has been used throughout this thesis to estimate the discriminability of objects in polarized light. This is especially important given the need for studies on polarization vision to continue to move away from talking about DoP and AoP and instead focus on measures such as polarization distance which reflect the information actually available to the animal.

The discoveries of chapter 2 were made possible by the development of a custom-built intensity-polarization screen that allowed intensity and polarization properties of visual stimuli to be adjusted independently and simultaneously. This novel system, which is outlined in

section 2.2.2 provides a means to present better 'real-world' visual information and can be used by biologists studying the behavioural and sensory ecology of other invertebrates.

6.2 Detection of targets against the sky

Although the data in chapter 3 fell short of conclusively demonstrating that fiddler crabs can use their polarization vision to detect targets against the sky, the findings do suggest that the crab's null points of discrimination have a negative effect on the detection of polarization contrasts against the sky. Despite this, as discussed at the end of chapter 3, natural objects viewed against the sky will always present an intensity contrast, even if the object's colour pattern or illumination conditions means the intensity contrast is inconsistent. Therefore, given that fiddler crabs do not rely exclusively on their polarization vision for object detection, the null points of discrimination are unlikely to have a biologically meaningful effect on the crabs in their natural environment.

Chapter 3 briefly highlighted the need to better understand the actual nature of the information conveyed by polarization and whether the information extracted from polarization cues and signals differs depending on whether the stimulus is detected above or below the visual horizon. For instance, as suggested in section 3.4.4, for objects viewed above a crab's visual horizon, polarization and intensity are likely to convey the same information, i.e. the approach of a potential predator; whereas for objects viewed below the crab's visual horizon, polarization may convey information, such as whether or not a nearby conspecific has its own burrow, that intensity alone does not.

6.3 Detection of second-order motion

The study in chapter 4 is the first to show evidence for the detection of second-order motion in a crustacean and the first to show detection of second-order motion in polarization in any animal. Future research should investigate the ecological importance of detecting second-order motion to better enable the findings of chapter 4 to be put into the context of the crabs in their natural environments. For example, the presence or absence of second-order motion may be an indication of the level of predation risk, although this suggestion currently lacks ecological validation. It would therefore be good for future work to test whether predators such as terns really do generate second-order motion, not only in intensity but also polarization, and how this compares to the motion signature generated by non-predatory species. Future work might also investigate the mechanism by which second-order motion is detected by crabs, and whether there are separate pathways for first- and second-order motion in intensity and polarization.

6.4 Overall conclusions

In the context of threat detection, the vast majority of predators will be viewed as an unpolarized object against a more polarized background. When detectable by the visual system of fiddler crabs (i.e. when the predator is viewed against the mudflats or certain regions of the sky), polarization will provide a reliable source of information in the form of a consistent negative polarization contrast. The same predator would also generate an intensity contrast, however, the polarity of the contrast between not only the predator and the background, but also between different regions of the predator's body, can vary depending on its colour pattern and the illumination conditions and direction. Consequently, on one hand intensity contrast is more reliable than polarization in that it will always be present, but the polarity of the contrast is often inconsistent. On the other hand, while a polarization contrast is not always present or

detectable by the crabs, when it is detectable, a predator will almost always be less polarized than the background, thus the polarization contrast will be more consistent than the intensity information.

Therefore, by processing intensity and polarization in separate, parallel channels, crabs have evolved a system that is able to benefit from the advantages of both intensity and polarization information, whilst simultaneously mitigating the weaknesses of both. If we also consider that in some situations variability in either intensity or polarization may itself provide a valuable source of information (e.g. visual flicker and the generation of second-order motion), it becomes even more evident that, despite having a tiny brain and the constraints of a dipolat visual system, fiddler crabs are nonetheless able to utilise as much of the visual information available to them as they possibly can.

6.5 Closing remarks

Polarization vision entices and excites us because it is a doorway into a secret hidden world. The study of polarization vision not only fuels our imaginations, but it is also a source of inspiration for present and future technologies (Roberts et al., 2014; Shabayek et al., 2014; Wang et al., 2019), including next generation cameras (Garcia et al., 2017; Powell et al., 2018) and applications for human eye health (Temple et al., 2019). Whatever the future of the field has in store, one thing is for certain, humans will continue to be fascinated by a world we can barely see. To paraphrase the quote from Johnsen (2012) that is written at the very start of this thesis, much of the world around us is still hidden, and it will remain that way until one of us learns to look in just the right way.

Appendices

A.1 Measuring polarization using a spectrometer

Measuring the polarization properties of light was an essential technique used throughout this thesis. All of the polarization data presented in this thesis were calculated using Stokes parameters S_0, S_1 and S_2. For the polarization properties of the LCD screens used for the experiments in chapters 2, 4 and 5 the measurements were taken using a spectrometer (QE65000, Ocean Optics, Largo, USA) coupled to a Glan-Thompson polarizer (GTH10M-B, Thorlabs, New Jersey, USA) via an optical fibre (P200-10-UV/Vis, Ocean Optics, Largo, USA). A Gershun tube was used to block off-axis illumination. Four measurements were taken with the transmission axis of the Glan-Thompson polarizer oriented at 0°, 45°, 90° and -45°, where 0° is horizontal. The Stokes parameter S_0, which is the total intensity (I), was calculated as:

$$S_0 = I_{0°} + I_{90°}$$

$$= I_{45°} + I_{-45°}$$

S_1 and S_2 were calculated as:

$$S_1 = I_{0°} - I_{90°}$$

$$S_2 = I_{45°} - I_{-45°}$$

The Stokes parameters S_0, S_1 and S_2 were then used to calculate the degree of linear polarization:

$$DoLP = \frac{\sqrt{S_1^2 + S_2^2}}{S_0}$$

When calculating the angle of polarization there are actually three solutions depending on the signs of S_1 and S_2.

If $S_1 \geq 0$:

$$AoP = \frac{1}{2} \times \tan^{-1}\left(\frac{S_2}{S_1}\right)$$

If $S_1 < 0$ and $S_2 < 0$:

$$AoP = \frac{1}{2} \times \tan^{-1}\left(\frac{S_2}{S_1}\right) - 90$$

If $S_1 < 0$ and $S_2 \geq 0$:

$$AoP = \frac{1}{2} \times \tan^{-1}\left(\frac{S_2}{S_1}\right) + 90$$

Since crabs are insensitive to circularly polarized light (which appears the same as unpolarized light) ellipticity was not measured.

For the photographic polarimetry in chapter 3 the Stokes parameter were calculated using the green channel from the RAW images taken with the polarizing filter orientated at 0°, 45°, 90°, and -45°.

A.2 Alternative methods for calculating Weber contrast

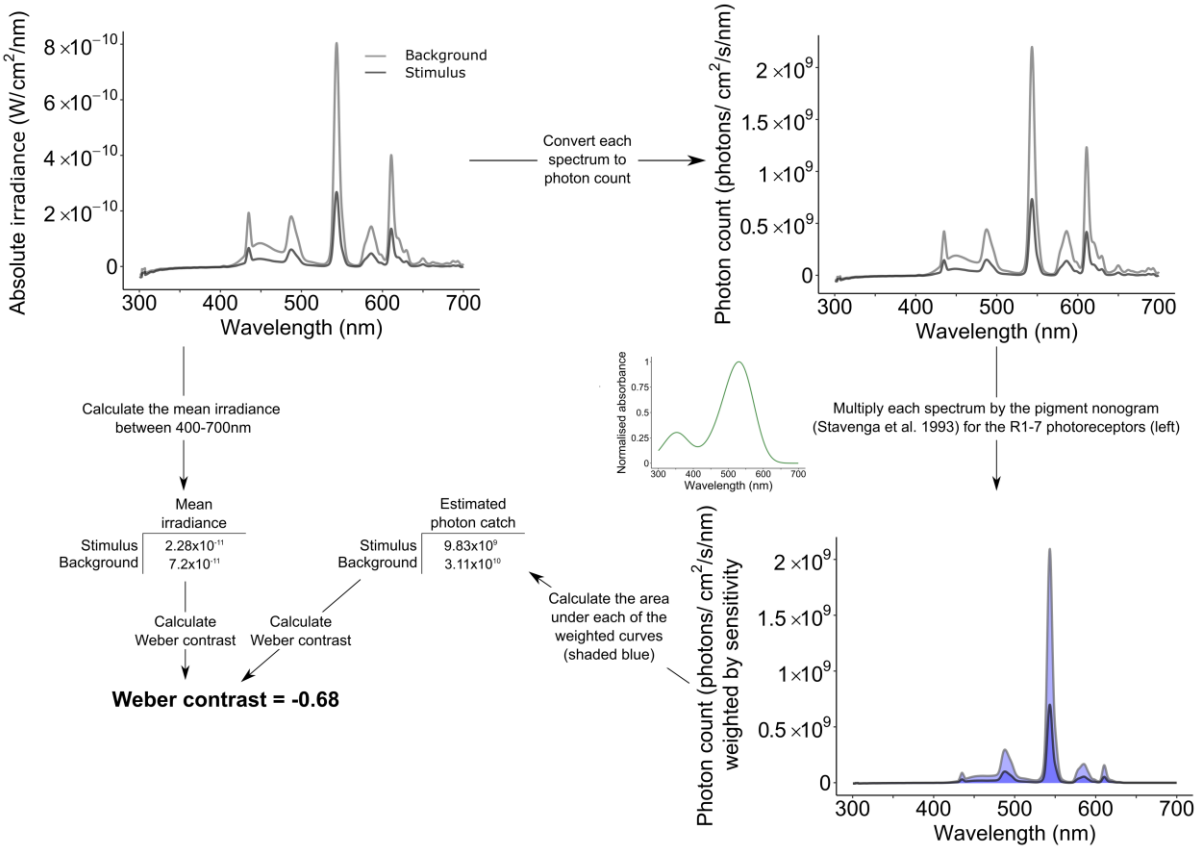

Figure A.1: Schematic showing two alternative methods for calculating Weber contrast between an example stimulus and background presented on an LCD screen. Both methods yield the same weber contrast to two decimal places. Note that this method of estimating photon catch does not account for other factors, many of which are unknown, such as the transmission of light through the ocular media or the effect of screening pigments. Therefore, this method was merely intended to provide the best possible approximation of photon catch given the information available from the literature.

A.3 Polarization video camera

The description of the polarization camera used to take the polarization videos in chapter 2 is taken from the supplementary material that accompanies Smithers et al (2019). The polarization video camera was built by Martin J. How.

Polarization video data for chapter 2 was collected using a custom-built camera system, comprising two usb-controlled cameras (UI-3240CP-NIR-GL, IDS, Obersulm, Germany), a polarization beam-splitter (CCM1-PBS25/M, Thorlabs, Newton, USA) and a lens (Arsat 1:35, 30mm, Kiev Cameras, Ukraine). The two cameras were temporally synchronised using a custom-made master/slave hardware-trigger system and manually controlled exposure settings. All other automatic image processing systems (e.g. gain) were disabled. The two cameras were mounted directly onto two faces of the polarization beamsplitter cube so that one camera received the horizontally polarized component of the visual scene and the other, the vertical (Figure A.2). The wide-angle lens was mounted on the third surface of the beamsplitter cube to counter the reduced field of view caused, i) by lengthening the focal distance from the lens to the camera CCD chip, and ii) by the small dimensions of the camera chip. Horizontal and vertical video frames were then processed using custom-written software (Matlab 2018b, Mathworks, Natick, USA). Images were first registered using a feature-detection technique (function *detectSURFFeatures* from the vision toolbox). Each pixel in horizontal/vertical video frame pairs were then used to calculate a measure of receptor contrast, based on the formulae of Bernard and Wehner (1977) and How and Marshall (2014). False colours were then assigned to the range of possible values of receptor contrast to illustrate the contrast available to the fiddler crab visual system. It should be noted that caution should be taken when calculating the polarization properties of dark objects or areas of a scene because instrument noise in the

measurements can result in significant artefacts and incorrect conclusions about high degrees of polarization when in fact none exist (Tibbs et al., 2018).

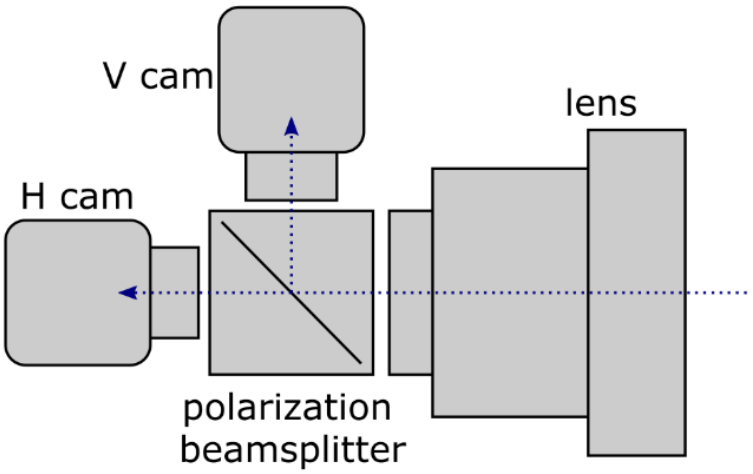

Figure A.2: Top view schematic of the two-channel polarization camera used to capture video of seabirds. H and V cam are USB-controlled cameras detecting horizontal and vertical components of the visual scene filtered by the polarization beamsplitter cube. Blue dotted arrows indicate the path of light through the lens, beamsplitter and camera.

The images in Figure 2.2 and Figure 2.3 were taken at approx. 13:10 and 09:50 respectively on 2nd Nov 2018 at Western-Super-Mare, UK (51.3474° N, 2.9773° W). The elevation and azimuth of the sun were 24° and 184° respectively for Figure 2.2 and 13° and 134° respectively for Figure 2.3. Because the camera was not kept stationary during filming (but instead followed the birds across the sky or the mudflat) accurate data on the filming direction and elevation of the camera at the point the images were taken are not available.

A.4 Intensity-Polarization (IP) response model

The description of the IP response model used in chapters 2 and 3 is taken from the supplementary material that accompanies Smithers et al (2019). The Matlab code for running this model is included in appendix A.11.

The intensity-polarization (IP) response model was used to predict the response of fiddler crabs to combinations of intensity and polarization contrasts based on a single channel or parallel channels model. The full Matlab script is included at the end in appendix A.11 and will be available to download from the supplementary material for Smithers et al (2019). The model simulates a population of 10,000 virtual crabs, assigns them a threshold level of response to positive and negative contrasts in intensity and polarization (based on the experimental data in chapter 2), then estimates the probability of response to combinations of intensity and polarization based on a single channel or a parallel channel integration system. The following steps illustrate how the model is formulated.

Step 1 – Simulate a population of crabs and assign each with a threshold for responding to positive and negative intensity and polarization contrasts. 10,000 normally distributed threshold values were generated for four different situations: negative and positive weber contrasts of -0.0548 (± SD 0.0204) and 0.162 (± 0.0417) and polarization distances of -0.333 (± 0.111) and 0.846 (± 0.374) to approximate the response curves measured in the behavioural experiments (Figure 2.6a and Figure 2.6b). These threshold distributions were derived by fitting sigmoidal curves (using the 'sigm_fit' function in Matlab https://uk.mathworks.com/matlabcentral/fileexchange/42641-sigm_fit) to the negative and positive results in the intensity-only and polarization-only behavioural experiments (Figure 2.6a and Figure 2.6b). The centre for each threshold distribution was derived from the mid-

point of each fitted sigmoidal curve, and the standard deviation was scaled relative to the sigmoidal slope using the relationship,

$$SD = 0.4/slope$$

in order to approximate the slopes observed in the behavioural data. Threshold distributions were generated using the 'normrnd' function in Matlab, which returns an array of random numbers following a normal distribution with a specified peak location and standard deviation. The distribution of response thresholds for both intensity and polarization contrasts is illustrated in Figure A.3 (red shaded areas for negative and green for positive contrasts). In addition to this, type 1 errors (crab responds to a sub-threshold stimulus) and type 2 errors (no response despite an above-threshold stimulus) were simulated by switching the response of 5% of all simulated trials, selected randomly using the 'rand' function in Matlab. This results in a response probability curve across the simulated population which approximates that observed in the experimental data (Figure A.3, black lines).

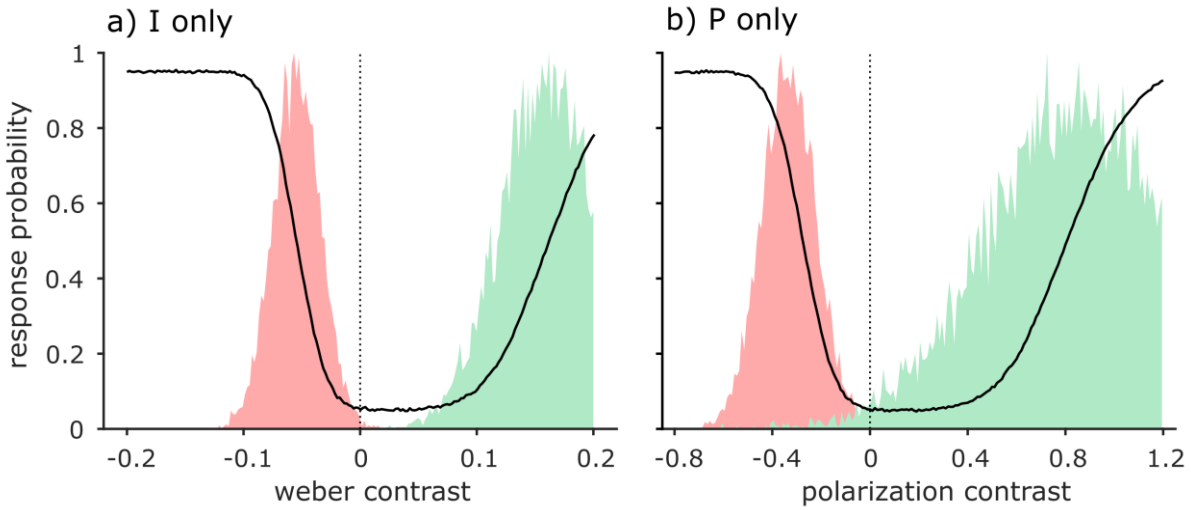

Figure A.3: Illustration of the IP response model in **a)** intensity-only and **b)** polarization-only simulations. Normally distributed response thresholds (red (negative) and green (positive) shaded areas – normalised to y-axis range) approximating those observed in the behavioural experiments were used to simulate the response profile of a population of 10,000 crabs. A random sub-sample of 5% of simulated trials had their response switched to simulate a small chance of type 1 and type 2 error. This resulted in a population-level response curve (black line) that increases either side of the zero contrast value (dotted line).

Step 2 – Combine intensity and polarization contrasts using the single channel and parallel channel models. Combinations of intensity and polarization are processed using one of two methods:

a) *Single channel model*: first the polarization contrast measure is modified by a conversion factor to bring the polarization distance scale approximately equivalent to the weber contrast scale. A conversion factor of 0.17 is used for this example, a value derived by using a least sum-of-squares approach to compare the behavioural response probabilities in Figure 2.6a and Figure 2.6b. The intensity and modified polarization contrasts are then summed and crab response rescored according to the intensity-only thresholds outlined in Figure A.3a. The addition of fixed polarization contrast to a series of intensity contrasts would then result in a sideways shift of the response curve, the direction of which depends on the polarity of the I-P combination (Figure A.4a and Figure 2.5a).

b) *Parallel channels model*: in this case, if either intensity or polarization contrasts are above threshold, then the animal responds. If both are below threshold, then no response is observed. This results in an upwards shift of the response curve (Figure A.4b and Figure 2.5b).

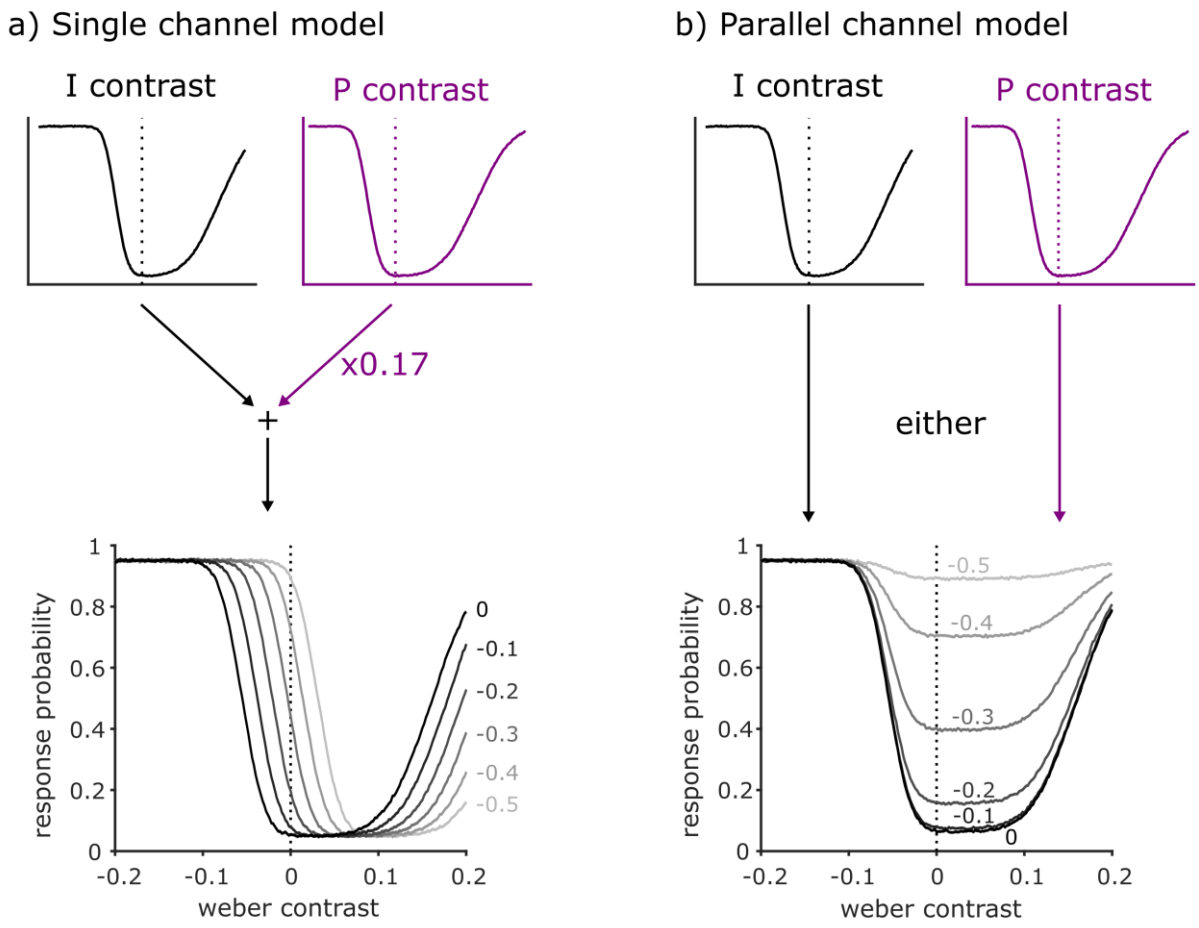

Figure A.4: Combination of intensity and polarization contrasts using the **a)** single and **b)** parallel channel models. For the single channel model (a), I and P contrasts are added together (after scaling the polarization distance measure by a factor of 0.17) to form a single measure of contrast. For the parallel channel model (b), each channel contributes a separate estimate of contrast and responses are elicited if either are above threshold. Bottom two graphs illustrate the effect on response probability of adding five different fixed polarization contrasts (grey lines and values) to a series of intensity contrasts.

A.4.1 Modification of the parallel channel model for chapter 3

The response thresholds for the parallel channel model were based on the results of the behavioural experiments in chapter 2. Since all of the stimuli in these experiments were horizontally polarized, it was necessary to adapt the model so that it could also take into account stimuli with AoP > 45°. Preliminary experiments, similar to the polarization only experiment from chapter 2, except the AoP was vertical instead of horizontal, revealed that regardless of the AoP, fiddler crabs are always more responsive to looming stimuli that are less polarized than the background compared to stimuli that are more polarized than the background (Martin How, unpublished data). Therefore, when calculating the estimated polarization distance between each target and the sky, the polarity of the value was based on whether or not the target was more or less polarized than the background. This made it so that the simulated population of crabs was most responsive to stimuli that were less polarized than the background irrespective of the AoP of either the target or the sky.

A.5 Irradiance measurements taken in Spain

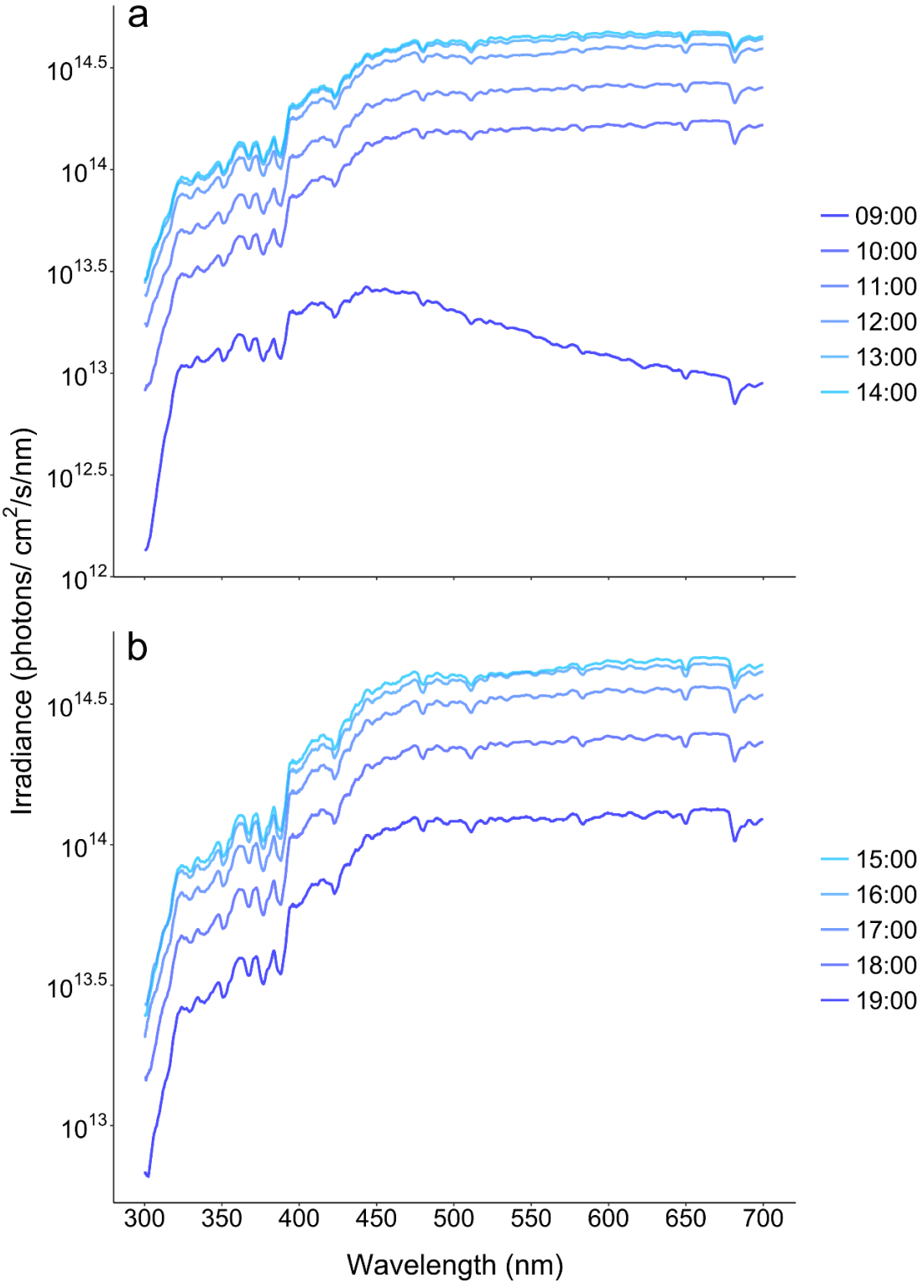

Figure A.5: Irradiance measurements taken on a clear day at the site where the field experiment in chapter 3 was conducted. The measurements from the **a)** morning session were taken on 13th May 2018 while the measurements from the **b)** afternoon session were taken on 16th May 2018. The measurements were taken using a spectrometer (FLAME-S-UV-VIS-ES, Ocean Optics, Largo, USA) coupled to an optical fibre (P200-10-UV/VIS, Ocean Optics, Largo, USA) fitted with a cosine corrector (CC-3-UV-S, Ocean Optics, Largo, USA) that was pointing at the zenith.

A.6 Example polarization photos used to measure polarization properties of the sky and target in chapter 3

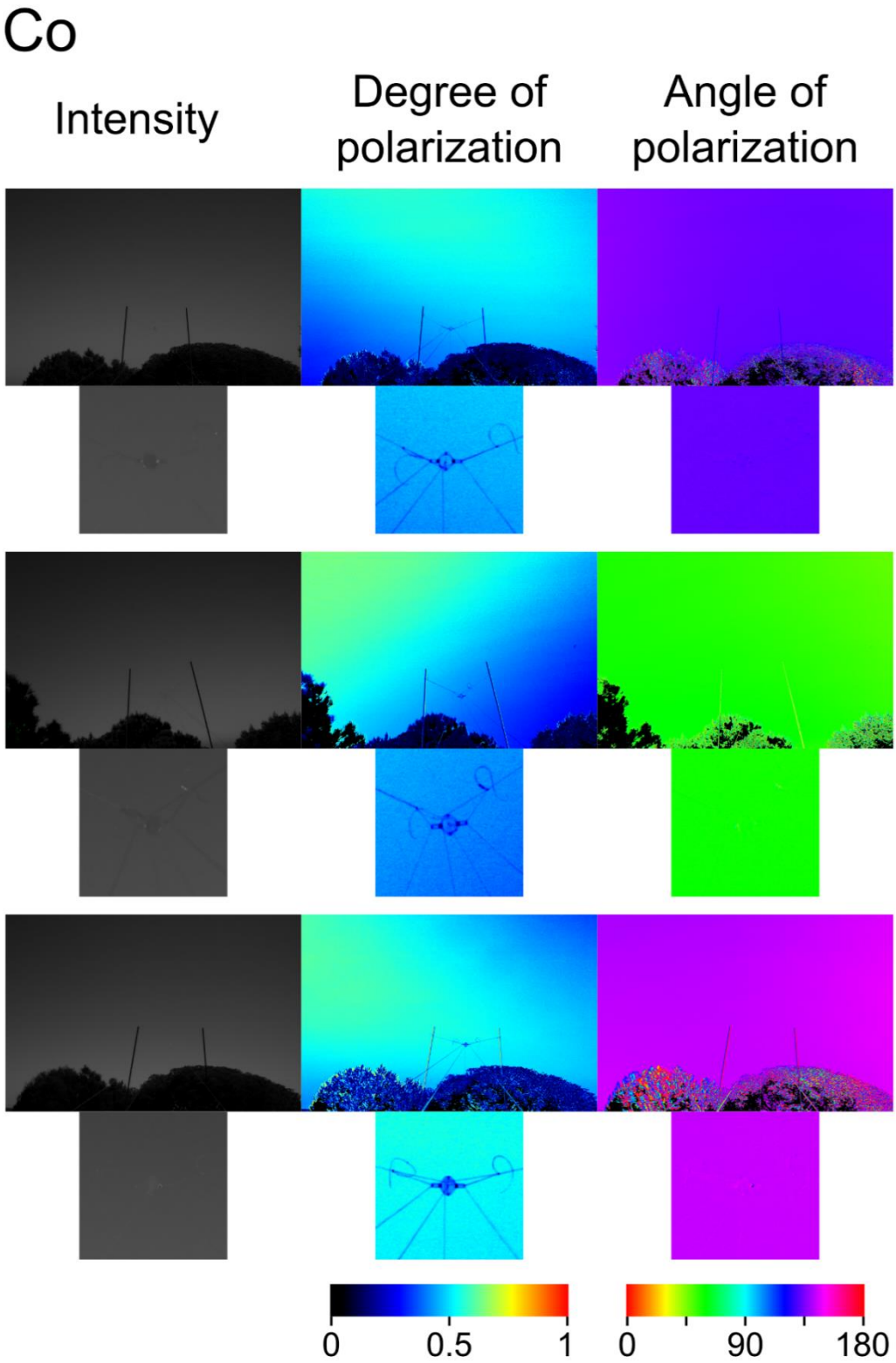

Figure A.6: Examples of polarization images (showing Co) used to measure the DoLP and AoP of the patch of sky the targets were viewed against. Lower image shows a zoomed in view of the Co target. Co = control target (no intensity or polarization contrast).

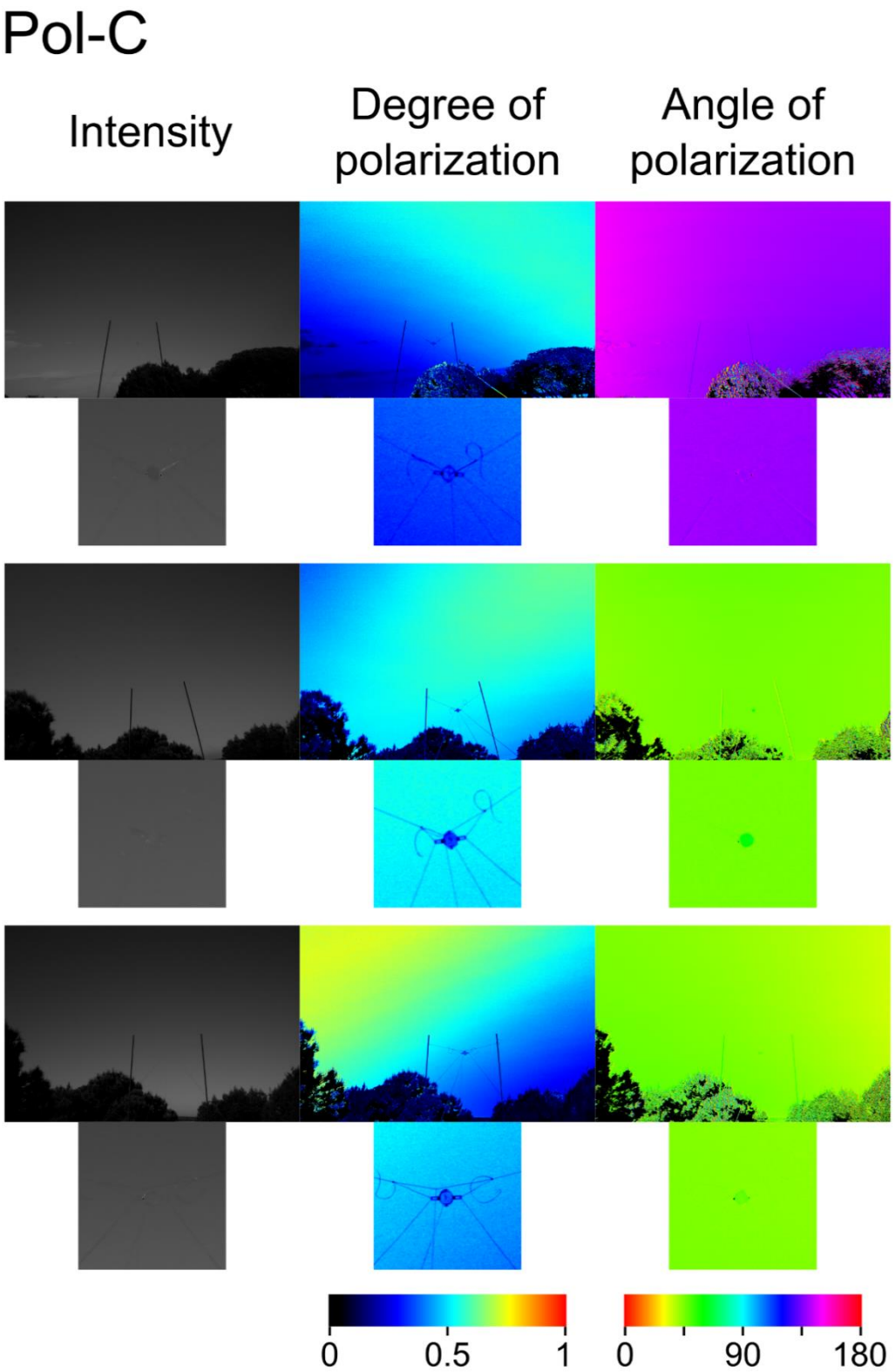

Figure A.7: Examples of polarization images (showing Pol-C) used to measure the DoLP and AoP of the patch of sky the targets were viewed against. Lower image shows a zoomed in view of the Pol-C target. Pol-C = polarization control target; optic axis of the quarter-wave retarder aligned parallel to the AoP of the sky (low polarization contrast).

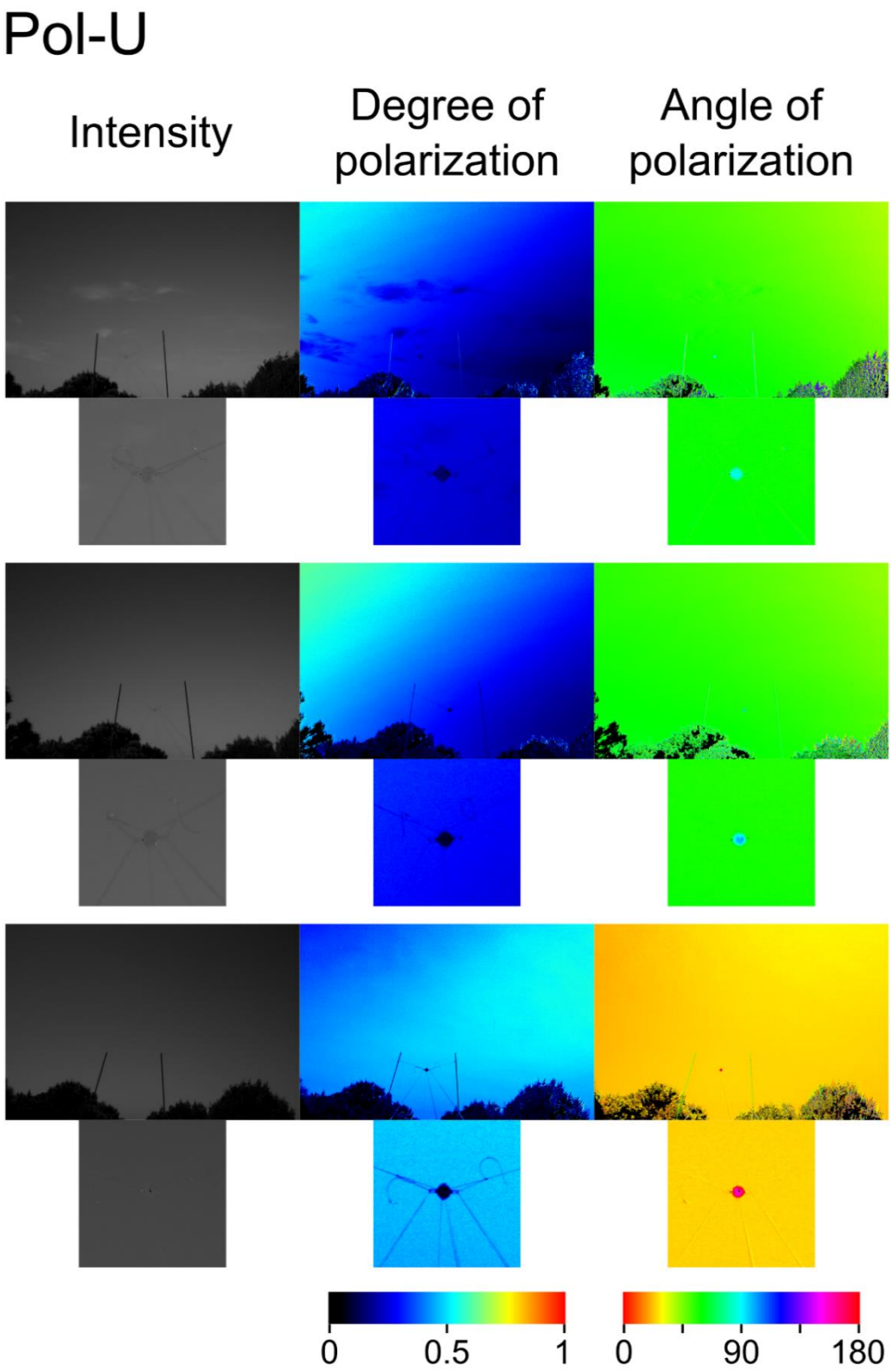

Figure A.8: Examples of polarization images (showing Pol-U) used to measure the DoLP and AoP of the patch of sky the targets were viewed against. Lower image shows a zoomed in view of the Pol-U target. Pol-U = unpolarized target; optic axis of the quarter-wave retarder aligned ±45º to the AoP of the sky (greatest contrast in DoLP).

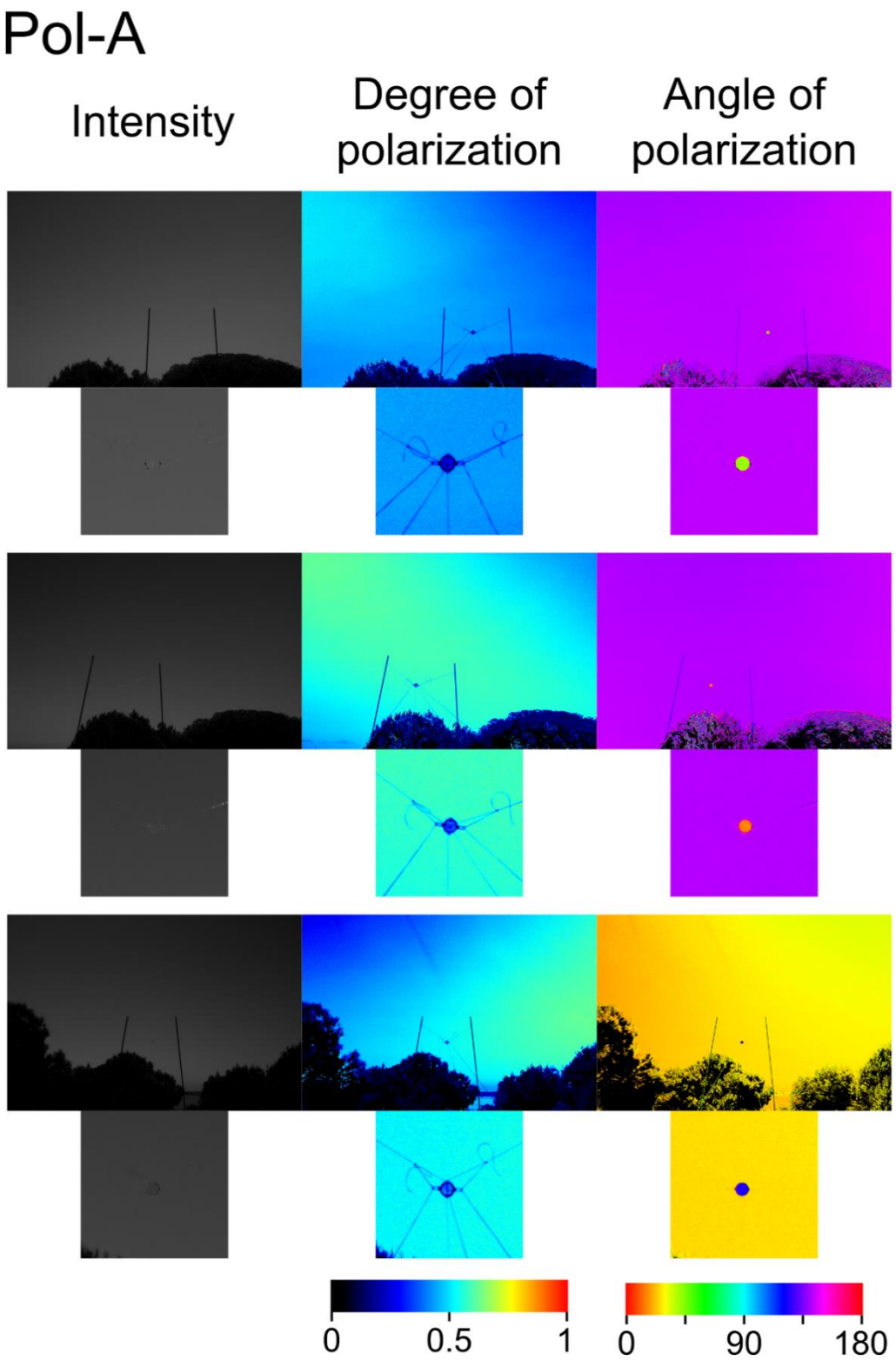

Figure A.9: Examples of polarization images (showing Pol-A) used to measure the DoLP and AoP of the patch of sky the targets were viewed against. Lower image shows a zoomed in view of the Pol-A target. Pol-A = AoP target; optic axis of the half-wave retarder aligned ±45º to the AoP of the sky (greatest contrast in AoP).

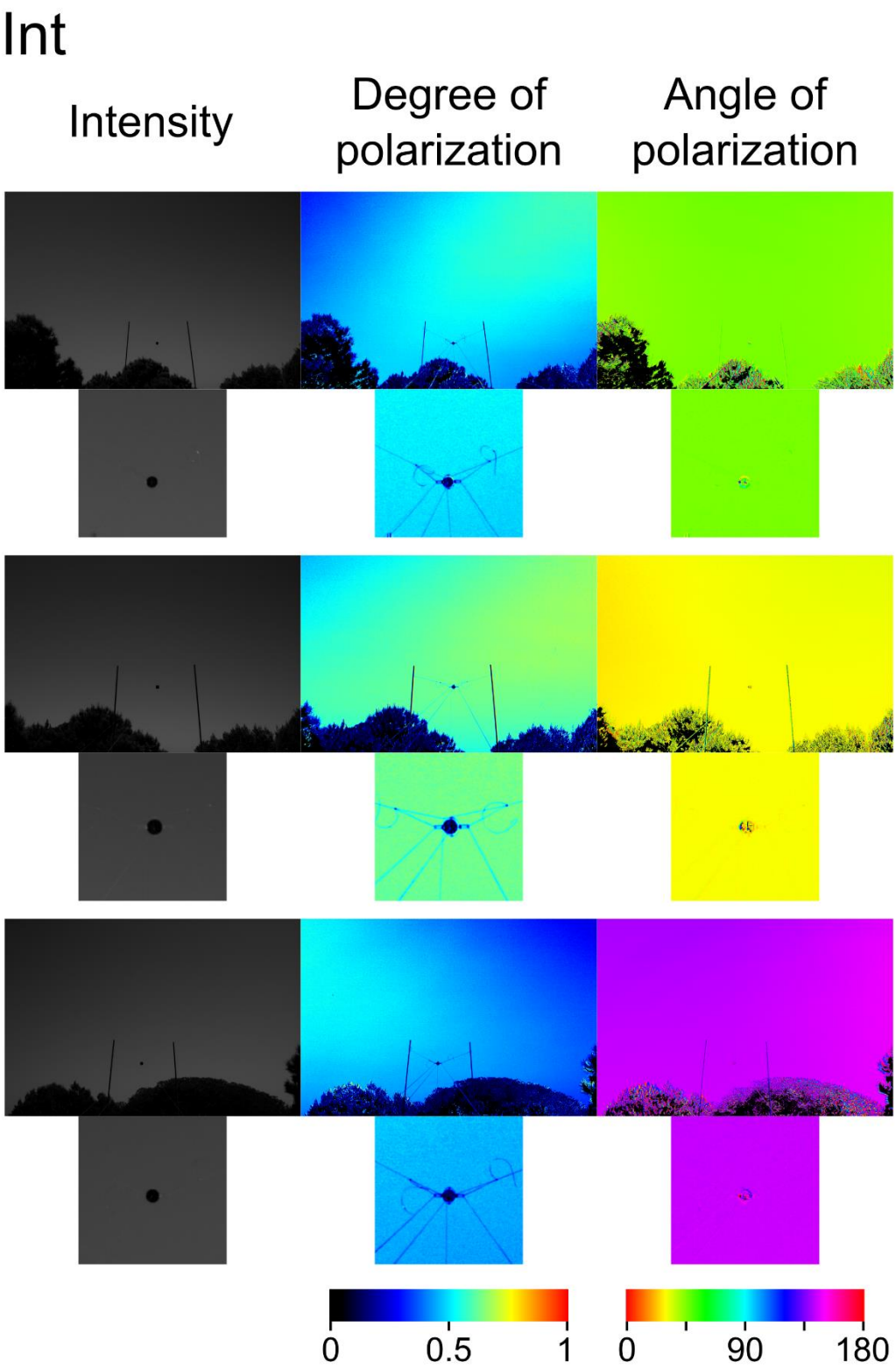

Figure A.10: Examples of polarization images (showing Int) used to measure the DoLP and AoP of the patch of sky the targets were viewed against. Lower image shows a zoomed in view of the Int target. Int = intensity target (greatest intensity contrast).

A.7 Polarization properties of the LCD screen from chapter 4

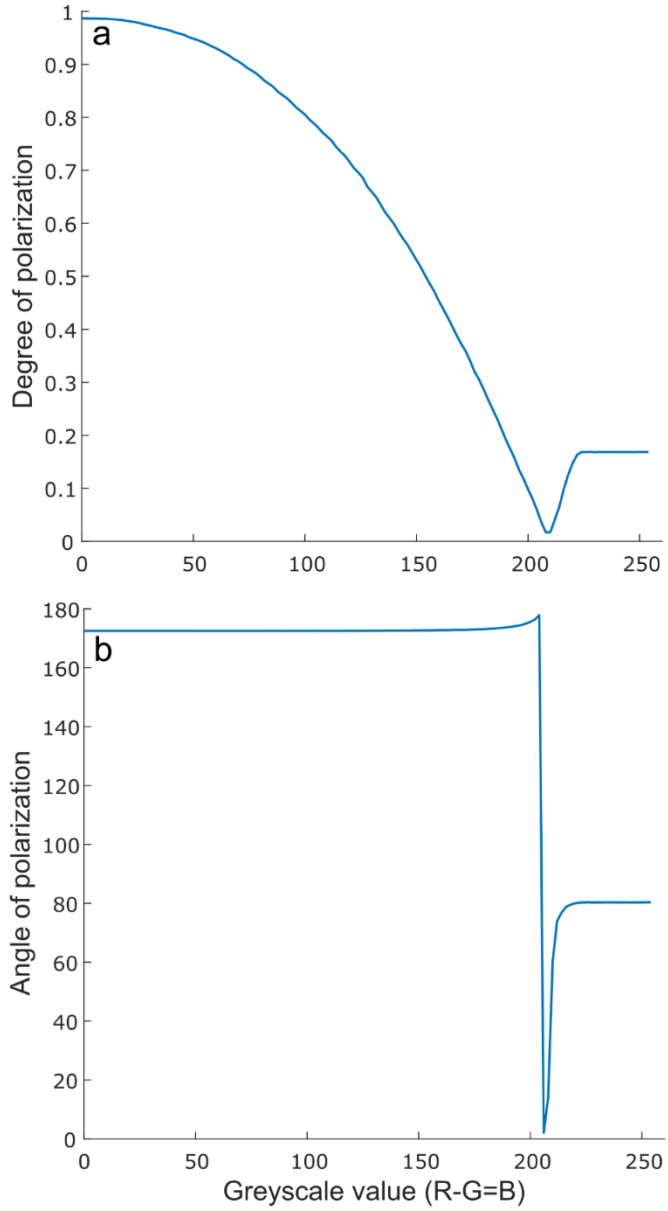

Figure A.11: Polarization properties of the LCD screen used for the polarization second-order motion experiments in chapter 4. **a)** DoLP and **b)** AoP of the screen.

A.8 Supplementary movies for chapter 4

At the time this thesis was submitted the movies referred to in chapter 4 are hosted privately on google drive by Samuel P. Smithers. They are available upon request and via the following link below. Upon publication of the study reported in chapter 4 these movies will be made available within the paper's supplementary material. When viewing this thesis as a PDF, if clicking on the link does not work, try copying and pasting the link into your web browser.

https://drive.google.com/open?id=1CG8sTbQU6I3ia66fz8XpY0nYkdiKCjqC

A.9 Polarization properties of the LCD screens from chapter 5

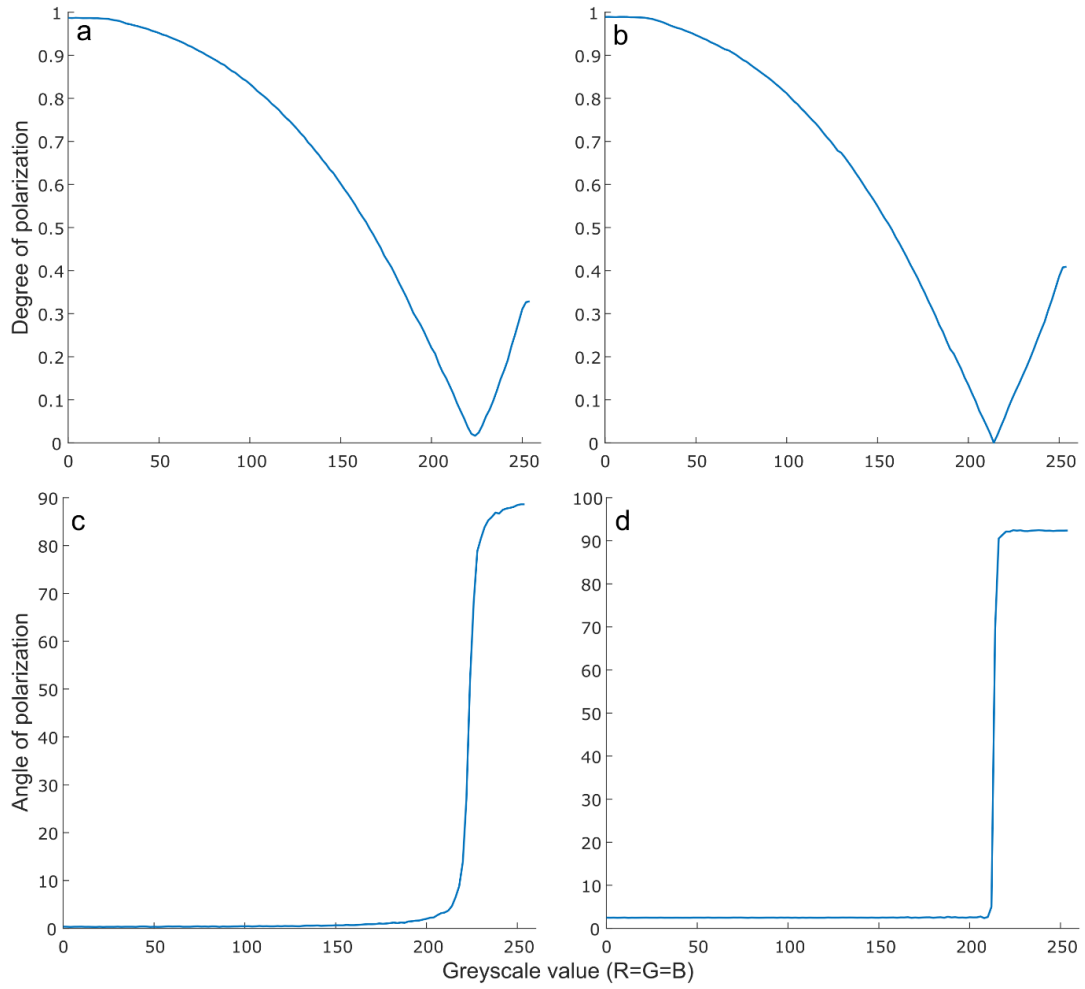

Figure A.12: Polarization properties of the LCD screen used for the experiments in chapter 5. DoLP of **a)** the experimental screen and **b)** the acclimatisation screen. AoP of **c)** the experimental screen and **d)** the acclimatisation screen

A.10 Behavioural response of ghost crabs

For each of the experiments reported in chapter 5 the total number of times that the crabs displayed each of the recorded behaviours was plotted over time (Figure A.13 to Figure A.16). These data were used to establish which of the behaviours only occurred during the presentation of the stimulus and were therefore most likely a response to the detection of the loom. Based on these data and observations made during preliminary experiments the ghost crabs were recorded as having responded if they jumped, flinched or lowered their body during a 3 s scoring window (i.e. the last 3 s of loom expansion (8-10 s)).

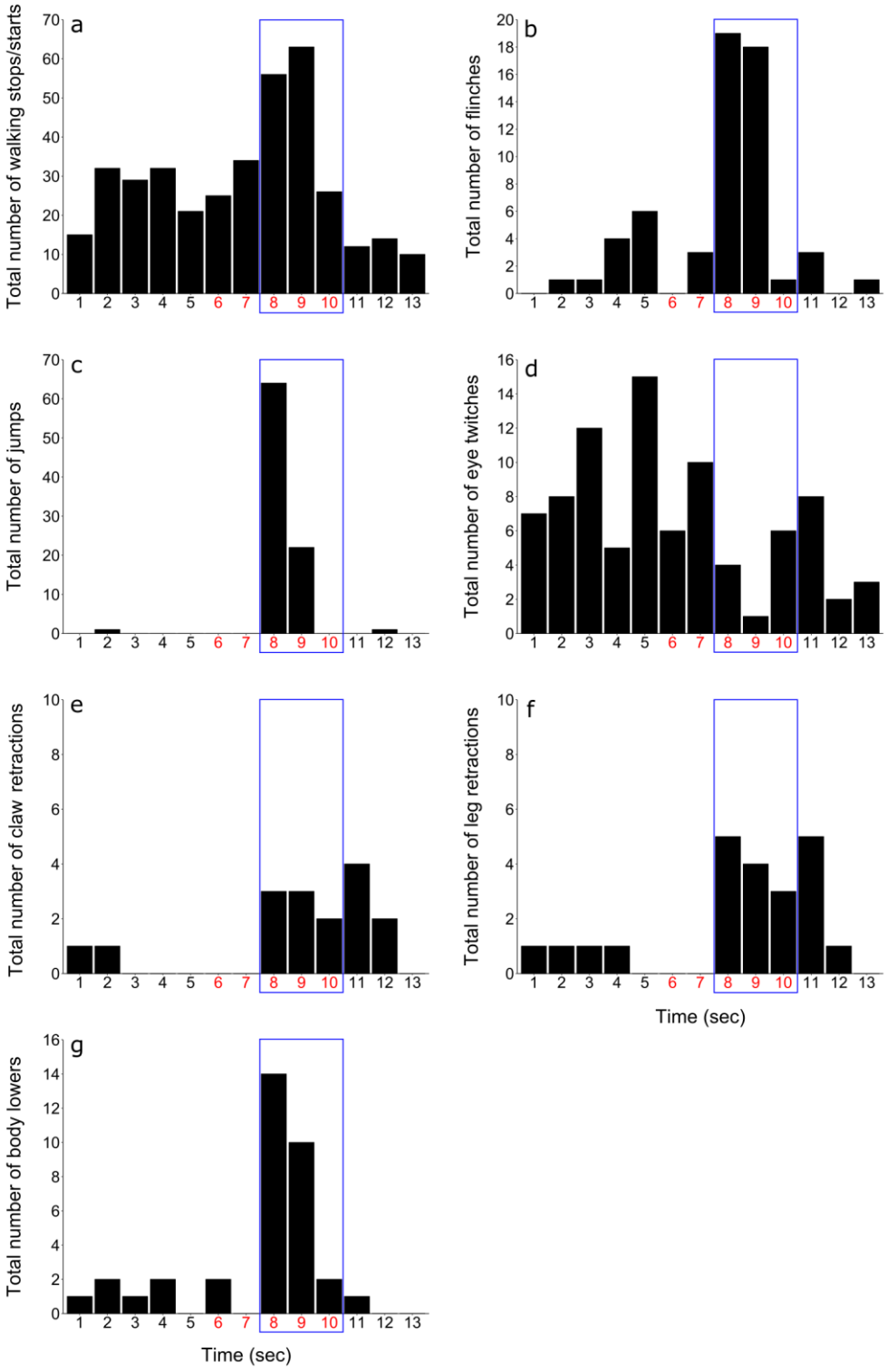

Figure A.13: Total number of times that the crabs **a)** stopped or started walking, **b)** flinched, **c)** jumped, **d)** eye twitched, e) retracted their claws, **f)** retracted their legs, and **g)** lowered their body, over time when tested in the intensity experiment during the day and night in twilight treatment 1. Each video clip was 13 s (five seconds before the start of the loom, five seconds during loom expansion (indicated in red) and three seconds after).The three second scoring window is indicated by the blue box.

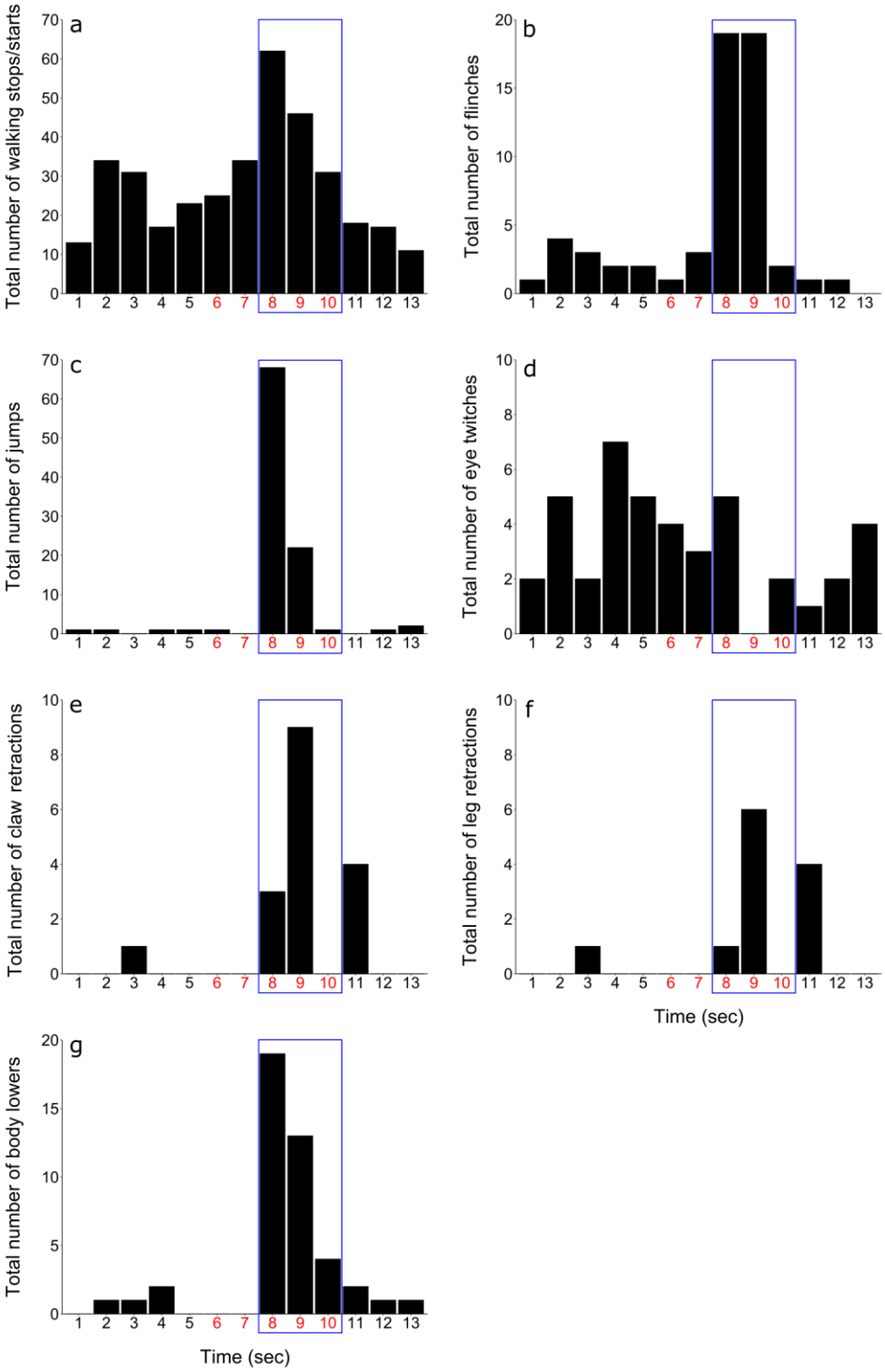

Figure A.14: Total number of times that the crabs **a)** stopped or started walking, **b)** flinched, **c)** jumped, **d)** eye twitched, **e)** retracted their claws, **f)** retracted their legs, and **g)** lowered their body, over time when tested in the intensity experiment during the day and night in twilight treatment 2. Each video clip was 13 s (five seconds before the start of the loom, five seconds during loom expansion (indicated in red) and three seconds after). The three second scoring window is indicated by the blue box.

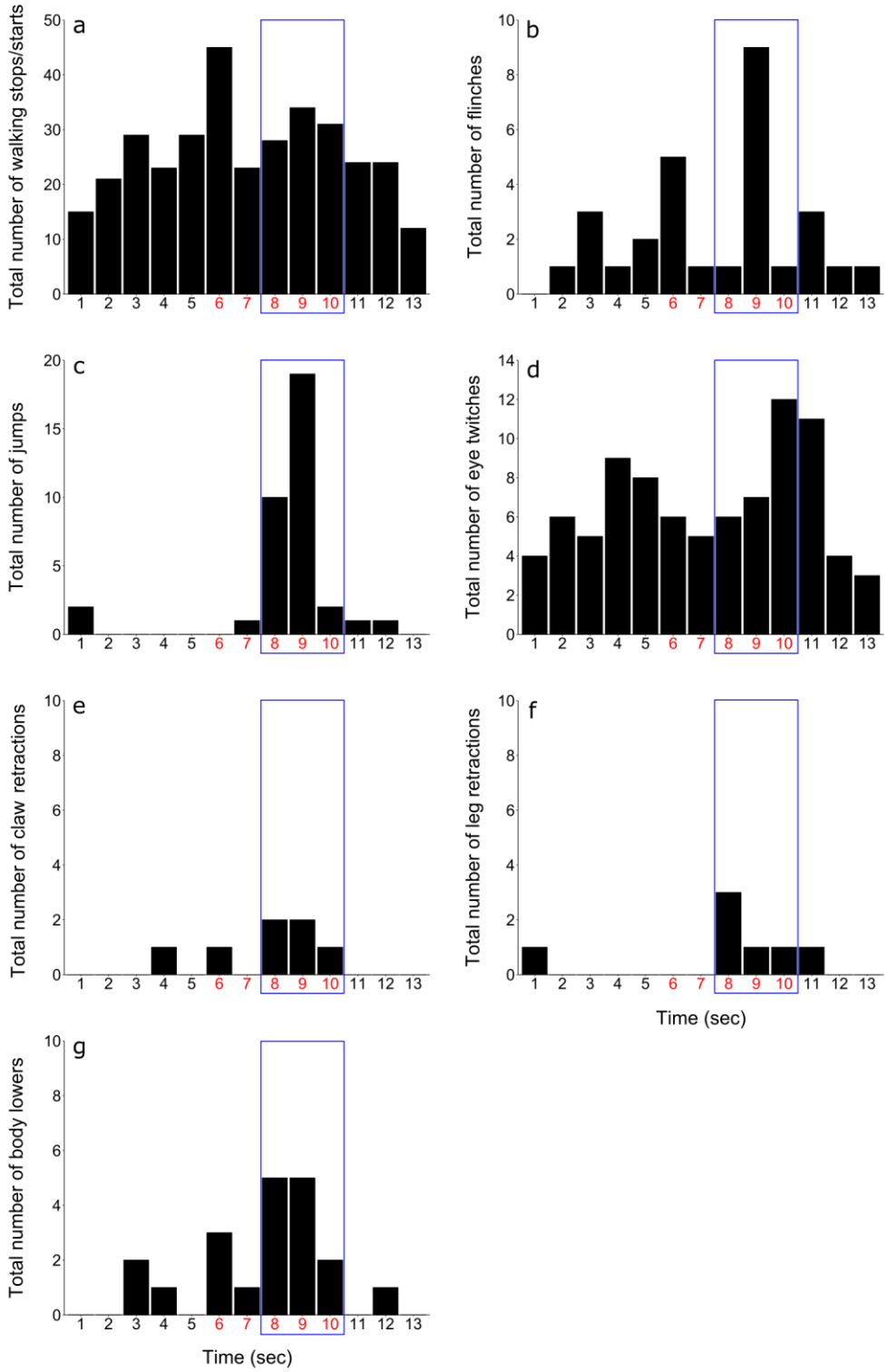

Figure A.15: Total number of times that the crabs **a)** stopped or started walking, **b)** flinched, **c)** jumped, **d)** eye twitched, **e)** retracted their claws, **f)** retracted their legs, and **g)** lowered their body, over time when tested in the polarization experiment during the day and night in twilight treatment 1. Each video clip was 13 s (five seconds before the start of the loom, five seconds during loom expansion (indicated in red) and three seconds after). The three second scoring window is indicated by the blue box.

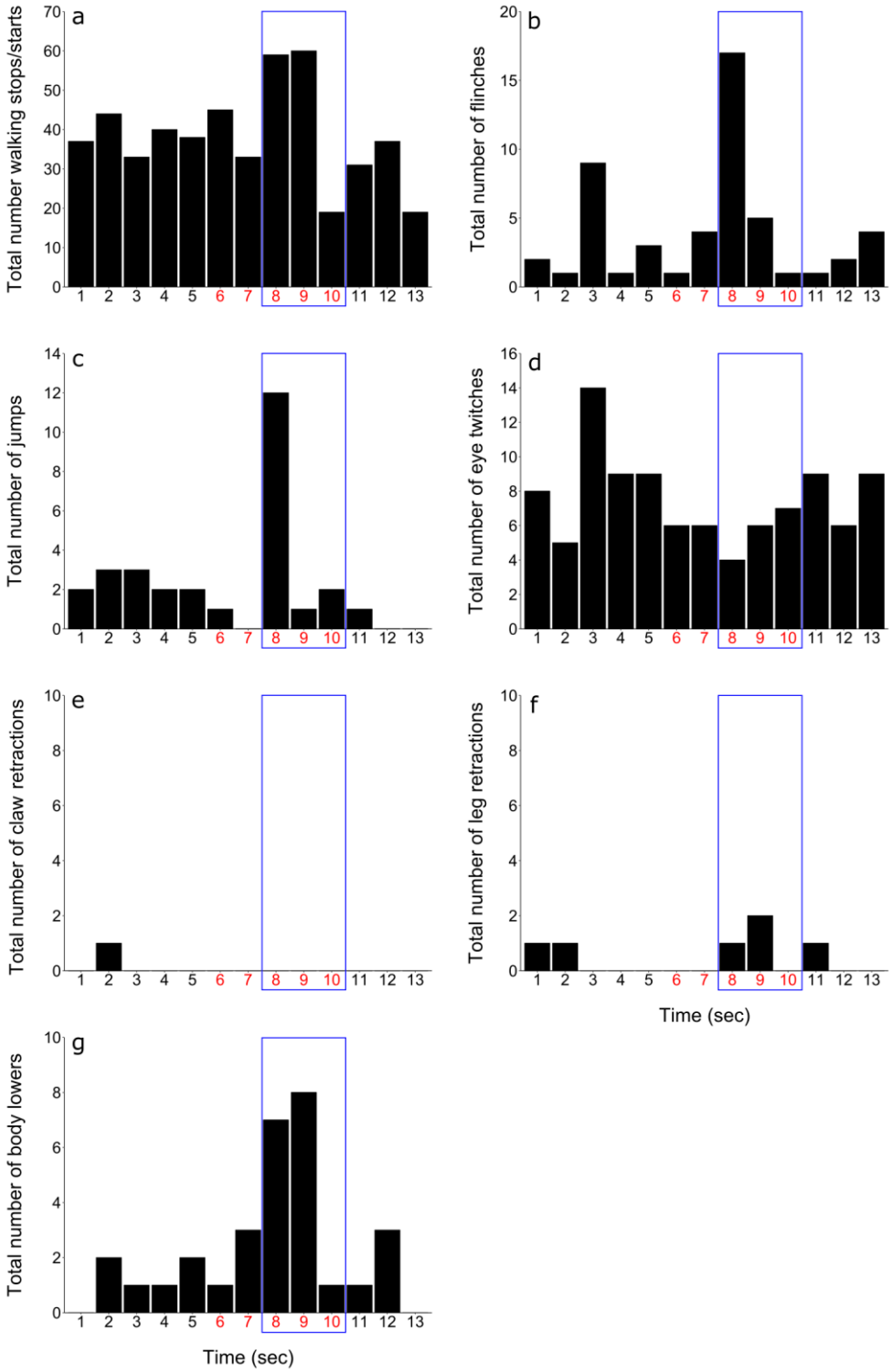

Figure A.16: Total number of times that the crabs **a)** stopped or started walking, **b)** flinched, **c)** jumped, **d)** eye twitched, e) retracted their claws, **f)** retracted their legs, and **g)** lowered their body, over time when tested in the polarization experiment during the day and night in twilight treatment 2. Each video clip was 13 s (five seconds before the start of the loom, five seconds during loom expansion (indicated in red) and three seconds after). The three second scoring window is indicated by the blue box.

A.11 Matlab code for IP model

The Matlab code used to run the IP response model used in chapters 2 and 3, and detailed in appendix A.4 is taken from the supplementary material that accompanies Smithers et al (2019).

```
function IP_fiddlerIPmodel3_methodsfig
% Script to simulate the interaction between intensity and polarization
% contrast for loom-detection behaviour in the fiddler crab Afruca tangeri
% supplementary material for Smithers et al 2019.
%
% Dr Martin J How and Sam P Smithers, University of Bristol, 2019
% Revised May 2019
% m.how@bristol.ac.uk

%% %%%%%%%%%%%%%%%%%%%%%%%%%%%%%%%%%%%%%%%%%%%%%%%%%%%%%%%%%%%%%%%%%%%%%%%%%%%
%Intensity contrast settings set to (approximately) match the behavioural
%data in Smithers et al 2019.

%Intensity contrast range
weber = -0.2:0.002:0.2;
%Negative contrast threshold +-standard deviation [threshold SD]
web_negthresh = [-0.0548 0.0204];
%Positive contrast threshold +-standard deviation [threshold SD]
web_posthresh = [0.162 0.0417];

%% %%%%%%%%%%%%%%%%%%%%%%%%%%%%%%%%%%%%%%%%%%%%%%%%%%%%%%%%%%%%%%%%%%%%%%%%%%%
%Polarization contrast settings

%Polarization contrast range
polop = -0.8:0.01:1.2;
%Negative contrast threshold +-standard deviation [threshold SD]
pol_negthresh = [-0.333 0.111];
%Positive contrast threshold +-standard deviation [threshold SD]
pol_posthresh = [0.846 0.374];

%% %%%%%%%%%%%%%%%%%%%%%%%%%%%%%%%%%%%%%%%%%%%%%%%%%%%%%%%%%%%%%%%%%%%%%%%%%%%
%Other settings

%Weber:polarization ratio - used to calculate the influence of polarization
%contrasts on intensity contrasts in the single channel model
webpolratio = 1/0.172712;
%Number of crabs to simulate
numcrabs = 10000;
%Seed the random number generator
rng('shuffle');

%% %%%%%%%%%%%%%%%%%%%%%%%%%%%%%%%%%%%%%%%%%%%%%%%%%%%%%%%%%%%%%%%%%%%%%%%%%%%
%Response thresholds for each crab in the simulated population
weberthresh(:,1) = ones(numcrabs,1).*web_negthresh(1);%Negative I threshold
weberthresh(:,2) = ones(numcrabs,1).*web_posthresh(1);%Positive I threshold
polthresh(:,1) = ones(numcrabs,1).*pol_negthresh(1);  %Negative P threshold
polthresh(:,2) = ones(numcrabs,1).*pol_posthresh(1);  %Positive P threshold

%% %%%%%%%%%%%%%%%%%%%%%%%%%%%%%%%%%%%%%%%%%%%%%%%%%%%%%%%%%%%%%%%%%%%%%%%%%%%
```

```
%Prepare plot axes
figure(1); clf;
set(gcf,'menubar','figure','color','w','name','Supplementary figure')
ax1=axes; ax2=axes;

%% %%%%%%%%%%%%%%%%%%%%%%%%%%%%%%%%%%%%%%%%%%%%%%%%%%%%%%%%%%%%%%%%%%%%%%%%
%Genearate normally-distributed noise for response thresholds
weberthresh(:,1) = normrnd(weberthresh(:,1),web_negthresh(2)); %Weber -
weberthresh(:,2) = normrnd(weberthresh(:,2),web_posthresh(2)); %Weber +
polthresh(:,1) = normrnd(polthresh(:,1),pol_negthresh(2)); %Polarization -
polthresh(:,2) = normrnd(polthresh(:,2),pol_posthresh(2)); %Polarization +

%% %%%%%%%%%%%%%%%%%%%%%%%%%%%%%%%%%%%%%%%%%%%%%%%%%%%%%%%%%%%%%%%%%%%%%%%%
%Plot simulated response data
weberresp = responsemodel(weber,weberthresh,0,polthresh,webpolratio,...
    'singlechannel');
polresp = responsemodel(0,weberthresh,polop,polthresh,webpolratio,...
    'singlechannel');
axes(ax1); hold on; plot(weber,weberresp./numcrabs,'-r'); hold off;
axes(ax2); hold on; plot(polop,polresp./numcrabs,'-r'); hold off;

%% %%%%%%%%%%%%%%%%%%%%%%%%%%%%%%%%%%%%%%%%%%%%%%%%%%%%%%%%%%%%%%%%%%%%%%%%
%Overlay histogram of noise
for ip=1:2
    for dd=1:2
        if ip==1 && dd==1,  temp=weberthresh(:,1); xx = weber; end
        if ip==1 && dd==2,  temp=weberthresh(:,2); xx = weber;  end
        if ip==2 && dd==1,  temp=polthresh(:,1); xx = polop; end
        if ip==2 && dd==2,  temp=polthresh(:,2); xx = polop;  end
        [N,EDGES] = histcounts(temp,xx);
        X = EDGES(2:end)-(EDGES(2)-EDGES(1))/2;
        if ip==1, axes(ax1);end
        if ip==2, axes(ax2);end
        hold on;
        plot(X,(N./max(N)),':k');
        plot([0 0],[0 1],'--k')
        hold off
    end
end

%% %%%%%%%%%%%%%%%%%%%%%%%%%%%%%%%%%%%%%%%%%%%%%%%%%%%%%%%%%%%%%%%%%%%%%%%%
%Set axis properties
set(ax1,'xlim',[-0.22 0.22],'xtick',[-0.2:0.1:0.2],...
    'ylim',[0 1],'box','off','tickdir','out',...
    'position',[0.1 0.6 0.4 0.35]);
axes(ax1); xlabel('weber contrast');ylabel('response probability');
set(ax2,'xlim',[-0.85 1.25],'xtick',[-0.8:0.4:1.2],...
    'ylim',[0 1],'box','off','tickdir','out',...
    'yticklabel',[],'position',[0.55 0.6 0.4 0.35]);
axes(ax2); xlabel('polarization contrast');


%% %%%%%%%%%%%%%%%%%%%%%%%%%%%%%%%%%%%%%%%%%%%%%%%%%%%%%%%%%%%%%%%%%%%%%%%%
%Run set of simulations for addition of a range of polarization contrasts
polrange = -0.5:0.1:0; %Range of polarization contrasts to be added
%Make axes to plot the results
ax2 = axes; ax3 = axes;
for polval= polrange
    %Run single channel model
    weberrespS = responsemodel(weber,weberthresh,polval,...
```

```
        polthresh,webpolratio,'singlechannel');
    %Run parallel channel model
    weberrespP = responsemodel(weber,weberthresh,polval,...
        polthresh,webpolratio,'parallelchannel');
    %Plot results
    axes(ax2); hold on;
    plot(weber,weberrespS./numcrabs,'-',...
        'color',[-1 -1 -1].*polval.*1.5); hold off
    axes(ax3);hold on;
    plot(weber,weberrespP./numcrabs,'-',...
        'color',[-1 -1 -1].*polval.*1.5); hold off
end

%% %%%%%%%%%%%%%%%%%%%%%%%%%%%%%%%%%%%%%%%%%%%%%%%%%%%%%%%%%%%%%%%%%%%%%%%%%%%
%Final touches to plots
axes(ax2);
hold on; plot([0 0],[0 1],'--k'); hold off; %Zero contrast line
title('single channel model')
xlabel('weber contrast'); ylabel('response probability');
set(ax2,'xlim',[min(weber) max(weber)],...
    'box','off',...
    'tickdir','out',...
    'position',[0.15 0.08 0.34 0.30]);
axes(ax3);
hold on; plot([0 0],[0 1],'--k'); hold off; %Zero contrast line
title('parallel channel model')
xlabel('weber contrast');
set(ax3,'xlim',[min(weber) max(weber)],...
    'box','off',...
    'tickdir','out',...
    'position',[0.6 0.08 0.34 0.30],...
    'yticklabel',[]);

%%%%%%%%%%%%%%%%%%%%%%%%%%%%%%%%%%%%%%%%%%%%%%%%%%%%%%%%%%%%%%%%%%%%%%%%%%%%%%
function resp = responsemodel(weber,weberthresh,pol,polthresh,...
    webpolratio,modeltype)
% Calculates the probability of crabs responding (resp) to combinations of
% intensity and polarization contrasts.
% Required inputs:
%       weber - weber contrast of stimulus
% weberthresh - response threshold of the crabs
%         pol - polarization distance of stimulus from background
%   polthresh - response threshold of the crabs to polarization
% NOTE: weber, weberthresh, pol, and polthresh must all be the same size
% webpolratio - the ratio of effectiveness at eliciting a response between
%               the weber scale and the polarization distance scale (5 for
%               our data). This is used for the singlechannel model
%               calculations
% modeltype - 'singlechannel' or 'parallelchannel'
%  Dr Martin J How and Sam Smithers, University of Bristol, 2018 -
m.how@bristol.ac.uk

switch modeltype
    case 'singlechannel' %Run single channel model
        rlist = weber+(pol./webpolratio)<=weberthresh(:,1) | ...
            weber+(pol./webpolratio)>=weberthresh(:,2);
    case 'parallelchannel' %Run parallel channel model
        rlist1 = weber<=weberthresh(:,1) | weber>=weberthresh(:,2);
        rlist2 = pol<=polthresh(:,1) | pol>=polthresh(:,2);
        rlist = (rlist1+rlist2)>0;
end
```

```
%Add 0.95 response noise to simulate type 1 and type 2 errors
rng('shuffle')
switchlist = rand(size(rlist))>0.95;
%Switch 5% to opposite response
rlist(switchlist) = abs(double(rlist(switchlist)-1));
resp = sum(rlist);
```

Bibliography

Albright JD. (**1992**). Form-cue invarient motion processing in primate visual cortex. *Science* **255**: 1141–1143.

Alkaladi A, How MJ & Zeil J. (**2013**). Systematic variations in microvilli banding patterns along fiddler crab rhabdoms. *Journal of Comparative Physiology A* **199**: 99–113.

Alkaladi A & Zeil J. (**2014**). Functional anatomy of the fiddler crab compound eye (*Uca vomeris*: Ocypodidae, Brachyura, Decapoda). *Journal of Comparative Neurology* **522**: 1264–1283.

Aptekar JW, Shoemaker PA & Frye MA. (**2012**). Figure tracking by flies is supported by parallel visual streams. *Current Biology* **22**: 482–487.

Arikawa K, Kawamata K, Suzuki T & Eguchi E. (**1987**). Daily changes of structure, function and rhodopsin content in the compound eye of the crab *Hemigrapsus sanguineus*. *Journal of Comparative Physiology A* **161**: 161–174.

Bains S. (**1996**). Sunfish shows the way through the fog. *Science* **272**: 653.

Baird E, Byrne MJ, Smolka J, Warrant EJ & Dacke M. (**2012**). The dung beetle dance: an orientation behaviour? *PLoS ONE* **7**: e30211.

Baird E, Fernandez DC, Wcislo WT & Warrant EJ. (**2015**). Flight control and landing precision in the nocturnal bee *Megalopta* is robust to large changes in light intensity. *Frontiers in Physiology* **6**: 305.

Baker CL. (**1999**). Central neural mechanisms for detecting second-order motion. *Current Opinion in Neurobiology* **9**: 461–466.

Balkenius A & Kelber A. (**2004**). Colour constancy in diurnal and nocturnal hawkmoths. *Journal of Experimental Biology* **207**: 3307–3316.

Barros F. (**2001**). Ghost crabs as a tool for rapid assessment of human impacts on exposed sandy beaches. *Biological Conservation* **97**: 399–404.

Basnak MA, Pérez-Schuster V, Hermitte G & Berón de Astrada M. (**2018**). Polarized object detection in crabs: a two-channel system. *Journal of Experimental Biology* **221**: jeb173369.

Bates D, Maechler M, Bolker B & Walker S. (**2015**). Fitting linear mixed-effects models using lme4. *Journal of Statistical Software* **67**: 1–48.

Bech M, Homberg U & Pfeiffer K. (**2014**). Receptive fields of locust brain neurons are matched to polarization patterns of the sky. *Current Biology* **24**: 1–6.

Belušič G, Šporar K & Meglič A. (**2017**). Extreme polarization sensitivity in the retina of the corn borer moth *Ostrinia*. *Journal of Experimental Biology* **220**: 2047–2056.

Bernard GD & Wehner R. (**1977**). Functional similarities between polarization vision and color vision. *Vision Research* **17**: 1019–1028.

Berry M V., Dennis MR & Lee Jr RL. (**2004**). Polarization singularities in the clear sky. *New Journal of Physics* **6**: 162.

Bildstein KL, McDowella SG & Brisbin L. (**1989**). Consequences of sexual dimorphism in sand fiddler crabs, *Uca pugilator*: differential vulnerability to avian predation. *Animal Behaviour* **37**: 133–139.

Blamires S. (**2004**). Habitat preferences of coastal goannas (*Varanus panoptes*): are they exploiters of sea turtle nests at fog bay, Australia? *Copeia* **2**: 370–377.

Brainard DH. (**1997**). The psychophysics toolbox. *Spatial Vision* **10**: 433–6.

Branco JO, Hillesheim JC, Fracasso HAA, Christoffersen ML & Evangelista CL. (**2010**). Bioecology of the ghost crab *Ocypode quadrata* (Fabricius, 1787) (Crustacea: Brachyura) compared with other intertidal crabs in the Southwestern Atlantic. *Journal of Shellfish Research* **29**: 503–512.

Brines ML & Gould JL. (**1982**). Skylight polarization patterns and animal orientation. *Journal of Experimental Biology* **96**: 69–91.

Budelmann BU. (**1995**). Cephalopod sense organs, nerves and the brain: adaptations for high performance and life style. *Marine and Freshwater Behaviour and Physiology* **25**: 13–33.

Calabrese GM, Brady PC, Gruev V & Cummings ME. (**2014**). Polarization signaling in swordtails alters female mate preference. *Proceedings of the National Academy of Sciences* **111**: 13397–13402.

Cameron DA & Pugh EN. (**1991**). Double cones as a basis for a new type of polarization vision in vertebrates. *Nature* **353**: 161–164.

Carroll DCO & Warrant EJ. (**2017**). Vision in dim light: highlights and challenges. *Philosophical Transactions of the Royal Society B* **372**: 20160062.

Cartron L, Josef N, Lerner A, McCusker SD, Darmaillacq AS, Dickel L & Shashar N. (**2013a**). Polarization vision can improve object detection in turbid waters by cuttlefish. *Journal of Experimental Marine Biology and Ecology* **447**: 80–85.

Cartron L, Dickel L, Shashar N & Darmaillacq AS. (**2013b**). Maturation of polarization and luminance contrast sensitivities in cuttlefish (*Sepia officinalis*). *Journal of Experimental Biology* **216**: 2039–2045.

Cavanagh P & Mather G. (**1989**). Motion: the long and short of it. *Spatial Vision* **4**: 103–129.

Caves EM, Brandley NC & Johnsen S. (**2018**). Visual acuity and the evolution of signals. *Trends in Ecology & Evolution* **33**: 358–372.

Caves EM & Johnsen S. (**2017**). AcuityView: an r package for portraying the effects of visual acuity on scenes observed by an animal. *Methods in Ecology and Evolution* **9**: 793–797.

Chiou TH, Mäthger LM, Hanlon RT & Cronin TW. (**2007**). Spectral and spatial properties of polarized light reflections from the arms of squid (*Loligo pealeii*) and cuttlefish (*Sepia officinalis* L .). *Journal of Experimental Biology* **210**: 3624–3635.

Chiou TH, Kleinlogel S, Cronin T, Caldwell R, Loeffler B, Siddiqi A, Goldizen A & Marshall J. (**2008a**). Circular polarization vision in a stomatopod crustacean. *Current Biology* **18**: 429–434.

Chiou TH, Caldwell RL, Hanlon RT & Cronin TW. (**2008b**). Fine structure and optical properties of biological polarizers in crustaceans and cephalopods. In: *Proc. SPIE.*, 697203.

Chiou TH, Marshall NJ, Caldwell RL & Cronin TW. (**2011**). Changes in light-reflecting properties of signalling appendages alter mate choice behaviour in a stomatopod crustacean *Haptosquilla trispinosa*. *Marine and Freshwater Behaviour and Physiology* **44**: 1–11.

Chiou TH, Place AR, Caldwell RL, Marshall NJ & Cronin TW. (**2012**). A novel function for a carotenoid: astaxanthin used as a polarizer for visual signalling in a mantis shrimp. *Journal of Experimental Biology* **215**: 584–589.

Christensen RHB. (**2015**). ordinal - Regression models for ordinal data.

Christy JH. (**1995**). Mimicry, mate choice, and the sensory trap hypothesis. *The American Naturalist* **146**: 171–181.

Chubb C & Sperling G. (**1988**). Drift-balanced random stimuli: a general basis for studying non-Fourier motion perception. *Journal of the Optical Society of America A* **5**: 1986–2007.

Coulson KL. (**1988**). *Polarization and intensity of light in the atmosphere*. Hampton, VA: A. Deepak Publishing.

Crane J. (**1975**). *Fiddler crabs of the world*. Princeton, New Jersey: Princeton University Press.

Cronin TW, Shashar N, Caldwell RL, Marshall J, Cheroske AG & Chiou TH. (**2003**). Polarization vision and its role in biological signaling. *Integrative and comparative biology* **43**: 549–558.

Cronin TW, Warrant EJ & Greiner B. (**2006**). Celestial polarization patterns during twilight. *Applied Optics* **45**: 5582–5589.

Cronin TW, Johnsen S, Marshall NJ & Warrant EJ. (**2014**). Polarization vision. In: *Visual ecology*. Princeton and Oxford: Princeton University Press, 178–205.

Cronin TW. (**2018**). A different view: sensory drive in the polarized-light realm. *Current Zoology* **64**: 513–523.

Cronin TW & Forward RB. (**1988**). The visual pigments of crabs. I. Spectral characteristics. *Journal of Comparative Physiology A* **162**: 463–478.

Cronin TW & Marshall J. (**2011**). Patterns and properties of polarized light in air and water. *Philosophical Transactions of the Royal Society B* **366**: 619–626.

Cronin TW & Shashar N. (**2001**). The linearly polarized light field in clear, tropical marine waters: spatial and temporal variation of light intensity, degree of polarization and e-vector angle. *Journal of Experimental Biology* **204**: 2461–2467.

Dacke M, Nilsson DE, Warrant EJ, Blest AD, Land MF & O'Caroll DC. (**1999**). Built-in polarizers form part of a compass organ in spiders. *Nature* **401**: 470–473.

Dacke M, Doan TA & O'Carroll DC. (**2001**). Polarized light detection in spiders. *Journal of Experimental Biology* **204**: 2481–2490.

Dacke M, Nilsson DE, Scholtz CH, Byrne M & Warrant EJ. (**2003a**). Insect orientation to polarized moonlight. *Nature* **424**: 33.

Dacke M, Nordström P & Scholtz CH. (**2003b**). Twilight orientation to polarised light in the crepuscular dung beetle *Scarabaeus zambesianus*. *Journal of Experimental Biology* **206**: 1535–1543.

Dacke M, Byrne MJ, Baird E, Scholtz CH & Warrant EJ. (**2011**). How dim is dim? Precision of the celestial compass in moonlight and sunlight. *Philosophical transactions of the Royal Society B* **366**: 697–702.

Dacke M, Baird E, Byrne M, Scholtz CH & Warrant EJ. (**2013**). Dung beetles use the Milky Way for orientation. *Current Biology* **23**: 298–300.

Dacke M & el Jundi B. (**2018**). The dung beetle compass. *Current Biology* **28**: R993–R997.

Daly IM, How MJ, Partridge JC, Temple SE, Marshall NJ, Cronin TW & Roberts NW. (**2016**). Dynamic polarization vision in mantis shrimps. *Nature Communications* **7**: 12140.

Daly IM, How MJ, Partridge JC & Roberts NW. (**2017**). The independence of eye movements in a stomatopod crustacean is task dependent. *Journal of Experimental Biology* **220**: 1360–1368.

Daumer K, Jande R & Waterman TH. (**1963**). Orientation of the ghost-crab *Ocypode* in polarized light. *Zeitschrift für vergleichende Physiologie* **47**: 56–76.

Detto T. (**2007**). The fiddler crab *Uca mjoebergi* uses colour vision in mate choice. *Proceedings of the Royal Society B* **274**: 2785–2790.

Detto T & Backwell PRY. (**2009**). The fiddler crab *Uca mjoebergi* uses ultraviolet cues in mate choice but not aggressive interactions. *Animal Behaviour* **78**: 407–411.

Douglas JM, Cronin TW, Chiou TH & Dominy NJ. (**2007**). Light habitats and the role of polarized iridescence in the sensory ecology of neotropical nymphalid butterflies (Lepidoptera: Nymphalidae). *Journal of Experimental Biology* **210**: 788–799.

Dubs A, Laughlin S & Srinivasan M. V. (**1981**). Single photon signals in fly photoreceptors and first order interneurones at behavioral threshold. *The Journal of Physiology* **317**: 317–334.

Duelli P & Wehner R. (**1973**). The spectral sensitivity of polarized light orientation in *Cataglyphis bicolor* (Formicidae, Hymenoptera). *Journal of Comparative Physiology A* **86**: 37–53.

Egri Á, Blahó M, Sándor A, Kriska G, Gyurkovszky M, Farkas R & Horváth G. (**2012**). New kind of polarotaxis governed by degree of polarization: attraction of tabanid flies to differently polarizing host animals and water surfaces. *Naturwissenschaften* **99**: 407–416.

Eguchi E. (**1965**). Rhabdom structure and receptor potentials in single crayfish retinular cells. *Journal of Cellular and Comparative Physiology* **66**: 411–429.

Eguchi E & Waterman TH. (**1967**). Changes in retinal fine structure induced in the crab *Libinia* by light and dark adaptation. *Zeitschrift für Zellforschung und mikroskopische Anatomie* **79**: 209–229.

Eguchi E & Waterman TH. (**1973**). Orthogonal microvillus pattern in the eighth rhabdomere of the rock crab *Grapsus*. *Zeitschrift für Zellforschung und mikroskopische Anatomie* **137**: 145–157.

Endler J. (**1993**). The color of light in forests and its implications. *Ecological Monographs* **63**: 1–27.

Endler J. (**2000**). Evolutionary implications of the interaction between animal signals and the environment. In: Espmark Y, Amundsen T, Rosenqvist G, eds. *Animal Signals: signalling and signal design in animal communication*. Trondheim, Norway: Tapir Academic Press, 11–46.

Ens BJ, Klaassen M & Zwarts L. (**1993**). Flocking and feeding in the fiddler crab (*Uca tangeri*): prey availability as risk-taking behaviour. *Netherlands Journal of Sea Research* **31**: 477–494.

Evangelista C, Kraft P, Dacke M, Labhart T & Srinivasan M V. (**2014**). Honeybee navigation: critically examining the role of the polarization compass. *Philosophical transactions of the Royal Society B* **369**: 20130037.

Fent K. (**1986**). Polarized skylight orientation in the desert ant *Cataglyphis*. *Journal of Comparative Physiology A* **158**: 145–150.

Flamarique IN. (**2019**). Swimming behaviour tunes fish polarization vision to double prey sighting distance. *Scientific Reports* **9**: 944.

Flamarique IN & Hawryshyn CW. (**1997**). Is the use of underwater polarized light by fish restricted to crepuscular time periods? *Vision Research* **37**: 975–989.

Foster JJ, Temple SE, How MJ, Daly IM, Sharkey CR, Wilby D & Roberts NW. (**2018**). Polarization vision: overcoming challenges of working with a property of light we barely see.

The Science of Nature **105**: 27.

Freas CA, Narendra A, Lemesle C & Cheng K. (**2017**). Polarized light use in the nocturnal bull ant, *Myrmecia midas*. *Royal Society Open Science* **4**: 170598.

von Frisch K. (**1949**). Die polarisation des himmelslichts als orientierender faktor bei den tänzen der bienen. *Experientia* **5**: 142–148.

Gagnon YL, Templin RM, How MJ & Marshall NJ. (**2015**). Circularly polarized light as a communication signal in mantis shrimps. *Current Biology* **25**: 3074–3078.

Gál J, Horváth G, Meyer-Rochow VB & Wehner R. (**2001a**). Polarization patterns of the summer sky and its neutral points measured by full-sky imaging polarimetry in Finnish Lapland north of the Arctic Circle. *Proceedings of the Royal Society of London A* **457**: 1385–1399.

Gál J, Horváth G, Barta A & Wehner R. (**2001b**). Polarization of the moonlit clear night sky measured by full-sky imaging polarimetry at full Moon: comparison of the polarization of moonlit and sunlit skies. *Journal of Geophysical Research Atmospheres* **106**: 22647–22653.

Garcia M, Edmiston C, Marinov R, Vail A & Gruev V. (**2017**). Bio-inspired color-polarization imager for real-time in situ imaging. *Optica* **4**: 1263–1271.

García-Pérez MA. (**1998**). Forced-choice staircases with fixed step sizes: asymptotic and small-sample properties. *Vision Research* **38**: 1861–1881.

Glantz RM. (**1996**). Polarization sensitivity in the crayfish optic lobe: peripheral contributions to opponency and directionally selective motion detection. *Journal of Neurophysiology* **76**: 3404–3414.

Glantz RM. (**2001**). Polarization analysis in the crayfish visual system. *Journal of Experimental Biology* **204**: 2383–2390.

Glantz RM & Schroeter JP. (**2006**). Polarization contrast and motion detection. *Journal of Comparative Physiology A* **192**: 905–914.

Glantz RM & Schroeter JP. (**2007**). Orientation by polarized light in the crayfish dorsal light

reflex: behavioral and neurophysiological studies. *Journal of Comparative Physiology A* **193**: 371–384.

Govardovskii VI, Fyhrquist N, Reuter T, Kuzmin DG & Donner K. (**2000**). On search of the visual pigment template. *Visual Neuroscience* **17**: 509–528.

Grable MM, Shashar N, Gilles NL, Chiao CC & Hanlon RT. (**2002**). Cuttlefish body patterns as a behavioral assay to determine polarization perception. *Biological Bulletin* **203**: 232–234.

Greiner B, Ribi WA & Wcislo WT. (**2004a**). Neural organisation in the first optic ganglion of the nocturnal bee *Megalopta genalis*. *Cell and Tissue Research* **318**: 429–437.

Greiner B, Ribi WA & Warrant EJ. (**2004b**). Retinal and optical adaptations for nocturnal vision in the halictid bee *Megalopta genalis*. *Cell and Tissue Research* **316**: 377–390.

Greiner B, Cronin TW, Ribi WA, Wcislo WT & Warrant EJ. (**2007**). Anatomical and physiological evidence for polarisation vision in the nocturnal bee *Megalopta genalis*. *Journal of Comparative Physiology A* **193**: 591–600.

Hafemann DR & Hubbard JI. (**1969**). On the rapid running of ghost crabs (*Ocypode ceratophthalma*). *Journal of Experimental Zoology* **170**: 25–31.

von Haidinger W. (**1844**). Ueber das directe erkennen des polarisirten lichts und der lage der polarisationsebene. *Annalen Der Physik* **LXIII**: 29–39.

Hanlon RT & Mäthger LM. (**2006**). Anatomical basis for camouflaged polarized light communication in squid. *Biology Letters* **2**: 494–496.

Hardie RC. (**2012**). Polarization vision: *Drosophila* enters the arena. *Current Biology* **22**: R12–R14.

Hawryshyn CW & Bolger AE. (**1990**). Spatial orientation of trout to partially polarized light. *Journal of Comparative Physiology A* **167**: 691–697.

Helbig AJ. (**1990**). Depolarization of natural skylight disrupts orientation of an avian nocturnal

migrant. *Experientia* **46**: 1986–1989.

Hemmi JM. (**2005a**). Predator avoidance in fiddler crabs: 2. The visual cues. *Animal Behaviour* **69**: 615–625.

Hemmi JM. (**2005b**). Predator avoidance in fiddler crabs: 1. Escape decisions in relation to the risk of predation. *Animal Behaviour* **69**: 603–614.

Hemmi JM & Pfeil A. (**2010**). A multi-stage anti-predator response increases information on predation risk. *Journal of Experimental Biology* **213**: 1484–1489.

Hemmi JM & Zeil J. (**2003**). Burrow surveillance in fiddler crabs I. Description of behaviour. *Journal of Experimental Biology* **206**: 3935–3950.

Henze MJ & Labhart T. (**2007**). Haze, clouds and limited sky visibility: polarotactic orientation of crickets under difficult stimulus conditions. *Journal of Experimental Biology* **210**: 3266–3276.

Homberg U, Heinze S, Pfeiffer K, Kinoshita M & el Jundi B. (**2011**). Central neural coding of sky polarization in insects. *Philosophical transactions of the Royal Society B* **366**: 680–687.

Honkanen A, Takalo J, Heimonen K, Vahasoyrinki M & Weckstrom M. (**2014**). Cockroach optomotor responses below single photon level. *Journal of Experimental Biology* **217**: 4262–4268.

Horch K, Salmon M & Forward R. (**2002**). Evidence for a two pigment visual system in the fiddler crab, *Uca thayeri*. *Journal of Comparative Physiology A* **188**: 493–499.

Horváth G, Bernáth B, Suhai B, Barta A & Wehner R. (**2002**). First observation of the fourth neutral polarization. *Journal of the Optical Society of America A* **19**: 2085–2099.

Horváth G. (**2014**). *Polarized light and polarization vision in animal sciences*. Springer, Berlin, Heidelberg.

Horváth G & Wehner R. (**1999**). Skylight polarization as perceived by desert ants and measured by video polarimetry. *Journal of Comparative Physiology A* **184**: 1–7.

Hothorn T, Bretz F & Westfall P. (**2008**). Simultaneous inference in general parametric models. *Biometrical Journal* **50**: 346–363.

How MJ, Zeil J & Hemmi JM. (**2009**). Variability of a dynamic visual signal: the fiddler crab claw-waving display. *Journal of Comparative Physiology A* **195**: 55–67.

How MJ, Pignatelli V, Temple SE, Marshall NJ & Hemmi JM. (**2012**). High e-vector acuity in the polarisation vision system of the fiddler crab *Uca vomeris*. *Journal of Experimental Biology* **215**: 2128–2134.

How MJ, Porter ML, Radford AN, Feller KD, Temple SE, Caldwell RL, Marshall NJ, Cronin TW & Roberts NW. (**2014a**). Out of the blue: the evolution of horizontally polarized signals in *Haptosquilla* (Crustacea, Stomatopoda, Protosquillidae). *Journal of Experimental Biology* **217**: 3425–3431.

How MJ, Christy JH, Roberts NW & Marshall NJ. (**2014b**). Null point of discrimination in crustacean polarisation vision. *Journal of Experimental Biology* **217**: 2462–2467.

How MJ, Christy JH, Temple SE, Hemmi JM, Marshall NJ & Roberts NW. (**2015**). Target detection is enhanced by polarization vision in a fiddler crab. *Current Biology* **25**: 3069–3073.

How MJ & Hemmi JM. (**2008a**). Courtship herding in the fiddler crab *Uca elegans*. *Journal of Comparative Physiology A* **194**: 1053–1061.

How MJ & Hemmi JM. (**2008b**). Courtship herding in the fiddler crab *Uca elegans*: tracking control system. *Animal Behaviour* **76**: 1259–1265.

How MJ & Marshall NJ. (**2014**). Polarization distance: a framework for modelling object detection by polarization vision systems. *Proceedings of the Royal Society B* **281**: 20131632.

Hughes DA. (**1966**). Behavioural and ecological investigations of the crab *Ocypode ceratophthalmus* (Crustacea: Ocypodidae). *Journal of Zoology* **150**: 129–143.

Hughes DA. (**1973**). On mating and the "copulation burrows " of crabs of the genus *Ocypode* (Decapoda, Brachyura). *Crustaceana* **24**: 72–76.

Hughes RN & Seed R. (**1995**). Behavioural mechanisms of prey selection in crabs. *Journal of Experimental Marine Biology and Ecology* **193**: 225–238.

Hugie DM. (**2004**). A waiting game between the black bellied plover and its fiddler crab prey. *Animal Behaviour* **67**: 823–831.

Iribarne OO & Martinez MM. (**1999**). Predation on the Southwestern Atlantic fiddler crab (*Uca uruguayensis*) by migratory shorebirds (*Pluvialis dominica*, *P. squatarola*, *Arenaria interpres*, and *Numenius phaeopus*). *Estuaries* **22**: 47.

Jennions MD, Backwell PRY, Murai M & Christy JH. (**2003**). Hiding behaviour in fiddler crabs: how long should prey hide in response to a potential predator? *Animal Behaviour* **66**: 251–257.

Jennions MD & Backwell PRY. (**1996**). Residency and size affect fight duration and outcome in the fiddler crab *Uca annulipes*. *Biological Journal of the Linnean Society* **57**: 293–306.

Joesch M, Schnell B, Raghu SV, Reiff DF & Borst A. (**2010**). ON and OFF pathways in *Drosophila* motion vision. *Nature* **468**: 300–304.

Johnsen S, Kelber A, Warrant E, Sweeney AM, Widder EA, Lee RL & Hernández-andrés J. (**2006**). Crepuscular and nocturnal illumination and its effects on color perception by the nocturnal hawkmoth *Deilephila elpenor*. *Journal of Experimental Biology* **209**: 789–800.

Johnsen S, Marshall NJ & Widder EA. (**2011**). Polarization sensitivity as a contrast enhancer in pelagic predators: lessons from in situ polarization imaging of transparent zooplankton. *Philosophical Transactions of the Royal Society B* **366**: 655–670.

Johnsen S. (**2012**). *The optics of life*. Princeton and Oxford: Princeton University Press.

Jordão JM, Cronin TW & Oliveira RF. (**2007**). Spectral sensitivity of four species of fiddler crabs (*Uca pugnax*, *Uca pugilator*, *Uca vomeris* and *Uca tangeri*) measured by in situ microspectrophotometry. *Journal of Experimental Biology* **210**: 447–453.

el Jundi B, Pfeiffer K & Homberg U. (**2011**). A distinct layer of the medulla integrates sky

compass signals in the brain of an insect. *PLoS ONE* **6**: e27855.

el Jundi B, Pfeiffer K, Heinze S & Homberg U. (**2014a**). Integration of polarization and chromatic cues in the insect sky compass. *Journal of Comparative Physiology A* **200**: 575–589.

el Jundi B, Smolka J, Baird E, Byrne MJ & Dacke M. (**2014b**). Diurnal dung beetles use the intensity gradient and the polarization pattern of the sky for orientation. *Journal of Experimental Biology* **217**: 2422–2429.

el Jundi B, Warrant EJ, Byrne MJ, Khaldy L, Baird E, Smolka J & Dacke M. (**2015**). Neural coding underlying the cue preference for celestial orientation. *Proceedings of the National Academy of Sciences* **112**: 11395–11400.

el Jundi B, Foster JJ, Khaldy L, Byrne MJ, Dacke M & Baird E. (**2016**). A snapshot-based mechanism for celestial orientation. *Current Biology* **26**: 1456–1462.

Kamermans M & Hawryshyn C. (**2011**). Teleost polarization vision: how it might work and what it might be good for. *Philosophical Transactions of the Royal Society B* **366**: 742–756.

Kelber A. (**1999**). Why 'false' colours are seen by butterflies. *Nature* **402**: 251.

Kelber A, Thunell C & Arikawa K. (**2001**). Polarisation-dependent colour vision in *Papilio* butterflies. *Journal of Experimental Biology* **204**: 2469–2480.

Kelber A, Balkenius A & Warrant EJ. (**2002**). Scotopic colour vision in nocturnal hawkmoths. *Nature* **419**: 922–925.

Kelber A, Balkenius A & Warrant EJ. (**2003**). Colour vision in diurnal and nocturnal hawkmoths. *Integrative and Comparative Biology* **43**: 571–579.

Khaldy L, Tocco C, Byrne M, Baird E & Dacke M. (**2019**). Straight-line orientation in the woodland-living beetle *Sisyphus fasciculatus*. *Journal of Comparative Physiology A* **0**: 0.

Kleinlogel S & Marshall NJ. (**2005**). Photoreceptor projection and termination pattern in the lamina of gonodactyloid stomatopods (mantis shrimp). *Cell and Tissue Research* **321**: 273–284.

Koga T, Backwell PRY, Jennions MD & Christy JH. (**1998**). Elevated predation risk changes mating behaviour and courtship in a fiddler crab. *Proceedings of the Royal Society B* **265**: 1385–1390.

Koga T, Backwell PRY, Christy JH, Murai M & Kasuya E. (**2001**). Male-biased predation of a fiddler crab. *Animal Behaviour* **62**: 201–207.

Kriska G, Horváth G & Andrikovics S. (**1998**). Why do mayflies lay their eggs en masse on dry asphalt roads? Water-imitating polarized light reflected from asphalt attracts Ephemeroptera. *Journal of Experimental Biology* **201**: 2273–2286.

Labhart T. (**1988**). Polarization-opponent interneurons in the insect visual system. *Nature* **331**: 435–437.

Labhart T. (**2016**). Can invertebrates see the e-vector of polarization as a separate modality of light? *Journal of Experimental Biology* **219**: 3844–3856.

Land MF. (**1999**). The roles of head movements in the search and capture strategy of a tern (Aves, Laridae). *Journal of Comparative Physiology A* **184**: 265–272.

Land MF & Layne J. (**1995**). The visual control of behavior in fiddler crabs. 1. Resolution, thresholds and the role of the horizon. *Journal of Comparative Physiology A* **177**: 81–90.

Land MF & Nilsson DE. (**2012**). *Animal eyes*. Oxford University Press.

Laughlin S & Lillywhite PG. (**1982**). Intrinsic noise in locust photorecetors. *The Journal of Physiology* **332**: 25–45.

Laughlin S & McGinness S. (**1978**). The structures of dorsal and ventral regions of a dragonfly retina. *Cell and Tissue Research* **188**: 427–447.

Layne J, Land MF & Zeil J. (**1997**). Fiddler crabs use the visual horizon to distinguish predators from conspecifics: a review of the evidence. *Journal of the Marine Biological Association of the United Kingdom* **77**: 43–54.

Layne JE. (**1998**). Retinal location is the key to identifying predators in fiddler crabs (*Uca*

pugilator). *Journal of Experimental Biology* **201**: 2253–2261.

Lebhardt F & Ronacher B. (**2014**). Interactions of the polarization and the sun compass in path integration of desert ants. *Journal of Comparative Physiology A* **200**: 711–720.

Ledgeway T & Smith AT. (**1994**). Evidence for separate motion-detecting mechanisms for first- and second-order motion in human vision. *Vision Research* **34**: 2727–2740.

Lee YJ & Nordstrom K. (**2012**). Higher-order motion sensitivity in fly visual circuits. *Proceedings of the National Academy of Sciences* **109**: 8758–8763.

Leggett LMW. (**1976**). Polarised light-sensitive interneurones in a swimming crab. *Nature* **262**: 709–711.

Lillywhite PG & Laughlin S. (**1979**). Transducer noise in a photoreceptor. *Nature* **277**: 569–572.

Losel R & Homberg I. (**2001**). Anatomy and physiology of neurons with processes in the accessory medulla of the cockroach *Leucophaea* maderae. *Journal of Comparative Neurology* **439**: 193-207

Lu ZL & Sperling G. (**1995**). The functional architecture of human visual motion perception. *Vision research* **35**: 2697–2722.

Lucrezi S & Schlacher TA. (**2009**). Monitoring human impacts on sandy shore ecosystems: a test of ghost crabs (*Ocypode* spp.) as biological indicators on an urban beach. *Environmental Monitoring and Assessment* **152**: 413–424.

Lucrezi S & Schlacher TA. (**2014**). The ecology of ghost crabs. In: Hughes RN, Hughes DJ, Smith IP, eds. *Oceanography and Marine Biology: An Annual Review*. Boca Raton, London, New York: CRC Press, 201–255.

Lythgoe JN & Hemmings CC. (**1967**). Polarized light and underwater vision. *Nature* **213**: 893–894.

Marshall NJ, Land MF, King CA & Cronin TW. (**1991**). The compound eyes of mantis

shrimps (Crustacea, Hoplocarida, Stomatopoda). 1. Compound eye structure: the detection of polarized light. *Philosophical Transactions of the Royal Society B* **334**: 33–56.

Marshall NJ, Kent J & Cronin TW. (**1999**). Visual adaptations in crustaceans: spectral sensitivity in diverse habitats. In: Archer SN, Djamgoz MBA, Loew ER, Partridge JC, Vallerga S, eds. *Mechanisms in the Ecology of Vision*. Springer, 285–327.

Marshall NJ, Powell SB, Cronin TW, Caldwell RL, Johnsen S, Gruev V, Chiou TS, Roberts NW & How MJ. (**2019**). Polarisation signals: a new currency for communication. *Journal of Experimental Biology* **222**: jeb134213.

Marshall NJ & Messenger JB. (**1996**). Colour-blind camouflage. *Nature* **382**: 408–409.

Martin FG & Mote MI. (**1982**). Color receptors in marine crustaceans: a second spectral class of retinular cell in the compound eyes of *Callinectes* and *Carcinus*. *Journal of Comparative Physiology A* **145**: 549–554.

Mäthger LM, Barbosa A, Miner S & Hanlon RT. (**2006**). Color blindness and contrast perception in cuttlefish (*Sepia officinalis*) determined by a visual sensorimotor assay. *Vision Research* **46**: 1746–53.

Mäthger LM, Denton EJ, Marshall NJ & Hanlon RT. (**2009a**). Mechanisms and behavioural functions of structural coloration in cephalopods. *Journal of the Royal Society Interface* **6**: S149–S163.

Mäthger LM, Shashar N & Hanlon RT. (**2009b**). Do cephalopods communicate using polarized light reflections from their skin? *Journal of Experimental Biology* **212**: 2133–2140.

MathWorks. (**2016**). MATLAB R2016b.

MathWorks. (**2017**). MATLAB R2017a.

Medan V, Oliva D & Tomsic D. (**2007**). Characterization of lobula giant neurons responsive to visual stimuli that elicit escape behaviors in the crab *Chasmagnathus*. *Journal of Neurophysiology* **98**: 2414–2428.

Messenger JB, Wilson A. & Hedge A. (**1973**). Some evidence for colour-blindness in Octopus. *Journal of Experimental Biology* **59**: 77–94.

Messenger JB. (**1977**). Evidence that Octopus is colour blind. *Journal of Experimental Biology* **70**: 49–55.

Moeller JF & Case JF. (**1995**). Temporal adaptations in visual systems of deep-sea crustaceans. *Marine Biology* **123**: 47–54.

Moody MF & Parriss JR. (**1961**). The discrimination of polarized light by *Octopus*: a behavioural and morphological study. *Zeitschrift für vergleichende Physiologie* **44**: 268–291.

Moskowitz H & Kitzes L. (**1966**). A comparison of two psychophysical methods using animals. *Journal of the Experimental Analysis of Behavior* **9**: 515–519.

Muheim R, Sjöberg S & Pinzon-Rodriguez A. (**2016**). Polarized light modulates light-dependent magnetic compass orientation in birds. *Proceedings of the National Academy of Sciences*: 201513391.

Munro U & Wiltschko R. (**1993a**). Clock-shift experiments with migratory yellow-faced honeyeaters, *Lichenostomus chrysops* (Meliphagidae), an Australian day migrating bird. *Journal of Experimental Biology* **181**: 233–244.

Munro U & Wiltschko W. (**1993b**). Magnetic compass orientation in the yellow-faced honeyeater, *Lichenostomus chrysops*, a day migrating bird from Australia. *Behavioral Ecology and Sociobiology* **32**: 141–145.

Munro U & Wiltschko R. (**1995**). The role of skylight polarization in the orientation of a day-migrating bird species. *Journal of Comparative Physiology A* **177**: 357–362.

Muramatsu D & Koga T. (**2016**). Fighting with an unreliable weapon: opponent choice and risk avoidance in fiddler crab contests. *Behavioral Ecology and Sociobiology* **70**: 713–724.

Nässel DR & Waterman TH. (**1977**). Golgi EM evidence for visual information channelling in the crayfish lamina ganglionaris. *Brain Research* **130**: 556–563.

Nässel DR & Waterman TH. (**1979**). Massive diurnally modulated photoreceptor membrane turnover in crab light and dark adaptation. *Journal of Comparative Physiology A* **131**: 205–216.

Neves FM & Bemvenuti CE. (**2006**). The ghost crab *Ocypode quadrata* (Fabricius, 1787) as a potential indicator of anthropic impact along the Rio Grande do Sul coast, Brazil. *Biological Conservation* **133**: 431–435.

Nilsson DE. (**2009**). The evolution of eyes and visually guided behaviour. *Philosophical Transactions of the Royal Society B* **364**: 2833–2847.

Nilsson DE & Nilsson HL. (**1981**). A crustacean compound eye adapted for low light intensities (Isopoda). *Journal of Comparative Physiology A* **143**: 503–510.

Nilsson DE & Warrant EJ. (**1999**). Visual discrimination: seeing the third quality of light. *Current Biology* **9**: 535–537.

Nishida S. (**2011**). Advancement of motion psychophysics: Review 2001-2010. *Journal of Vision* **11**: 1–53.

Nityananda V, Tarawneh G, Henriksen S, Umeton D, Simmons A & Read JCA. (**2018**). A novel form of stereo vision in the praying mantis. *Current Biology* **28**: 588–593.

Oliva D, Medan V & Tomsic D. (**2007**). Escape behavior and neuronal responses to looming stimuli in the crab *Chasmagnathus granulatus* (Decapoda: Grapsidae). *Journal of Experimental Biology* **210**: 865–880.

Oliva D & Tomsic D. (**2012**). Visuo-motor transformations involved in the escape response to looming stimuli in the crab *Neohelice* (= *Chasmagnathus*) *granulata*. *Journal of Experimental Biology* **215**: 3488–3500.

Oliva D & Tomsic D. (**2016**). Object approach computation by a giant neuron and its relation with the speed of escape in the crab *Neohelice*. *Journal of Experimental Biology* **219**: 3339–3352.

Orger MB, Smear MC, Anstis SM & Baier H. (**2000**). Perception of fourier and non-fourier motion by larval zebrafish. *Nature Neuroscience* **3**: 1128–1133.

Ortega-Escobar J. (**2017**). Polarized-light vision in spiders. *Trends in Entomology* **13**: 25–34.

Parkyn DC, Austin JD & Hawryshyn CW. (**2003**). Acquisition of polarized-light orientation in salmonids under laboratory conditions. *Animal Behaviour* **65**: 893–904.

Pelli DG. (**1997**). The VideoToolbox software for visual psychophysics: transforming numbers into movies. *Spatial Vision* **10**: 437–442.

Pfeiffer K, Negrello M & Homberg U. (**2011**). Conditional perception under stimulus ambiguity: polarization- and azimuth-sensitive neurons in the locust brain Are inhibited by low degrees of polarization. *Journal of Neurophysiology* **105**: 28–35.

Pignatelli V, Temple SE, Chiou TH, Roberts NW, Collin SP & Marshall NJ. (**2011**). Behavioural relevance of polarization sensitivity as a target detection mechanism in cephalopods and fishes. *Philosophical Transactions of the Royal Society B* **366**: 734–741.

Popper AN, Salmon M & Horch KW. (**2001**). Acoustic detection and communication by decapod crustaceans. *Journal of Comparative Physiology A* **187**: 83–89.

Powell SB, Garnett R, Marshall J, Rizk C & Gruev V. (**2018**). Bioinspired polarization vision enables underwater geolocalization. *Science Advances* **4**: eaao6841.

R Core Team. (**2017**). R: a language and environment for statistical computing.

Rayleigh FRS. (**1899**). XXXIV. On the transmission of light through an atmosphere containing small particles in suspension, and on the origin of the blue of the sky. *The London, Edinburgh, and Dublin Philosophical Magazine and Journal of Science* **47**: 375–384.

Reid SF, Narendra A, Hemmi JM & Zeil J. (**2011**). Polarised skylight and the landmark panorama provide night-active bull ants with compass information during route following. *Journal of Experimental Biology* **214**: 363–370.

Reppert SM, Zhu H & White RH. (**2004**). Polarized light helps monarch butterflies navigate.

Current Biology **14**: 155–158.

La Rivers I. (**1948**). Some Hawaiian ecological notes. *The Wasmann Collector* **7**: 85–110.

Roberts NW, Gleeson HF, Temple SE, Haimberger TJ & Hawryshyn CW. (**2004**). Differences in the optical properties of vertebrate photoreceptor classes leading to axial polarization sensitivity. *Journal of the Optical Society of America A* **21**: 335–345.

Roberts NW, Chiou TH, Marshall NJ & Cronin TW. (**2009**). A biological quarter-wave retarder with excellent achromaticity in the visible wavelength region. *Nature Photonics* **3**: 641–644.

Roberts NW, Porter ML & Cronin TW. (**2011**). The molecular basis of mechanisms underlying polarization vision. *Philosophical Transactions of the Royal Society B* **366**: 627–637.

Roberts NW, How MJ, Porter ML, Temple SE, Caldwell RL, Powell SB, Gruev V, Marshall NJ & Cronin TW. (**2014**). Animal polarization imaging and implications for optical processing. *Proceedings of the IEEE* **102**: 1427–1434.

Roberts NW & Needham MG. (**2007**). A mechanism of polarized light sensitivity in cone photoreceptors of the goldfish *Carassius auratus*. *Biophysical journal* **93**: 3241–3248.

Rosenberg J & Langer H. (**2001**). Ultrastructural changes of rhabdoms of the eyes of *Ocypode* species in relation to different regimes of light and dark adaptation. *Journal of Crustacean Biology* **21**: 345–353.

Sabbah S, Habib-Nayany MF, Dargaei Z, Hauser FE, Kamermans M & Hawryshyn CW. (**2013**). Retinal region of polarization sensitivity switches during ontogeny of rainbow trout. *Journal of Neuroscience* **33**: 7428–7438.

Sabbah S & Shashar N. (**2007**). Light polarization under water near sunrise. *Journal of the Optical Society of America A* **24**: 2049–2056.

Sabra R & Glantz RM. (**1985**). Polarization sensitivity of crayfish photoreceptors is

correlated with their termination sites in the lamina ganglionaris. *Journal of Comparative Physiology A* **156**: 315–318.

Sakura M, Lambrinos D & Labhart T. (**2008**). Polarized skylight navigation in insects: model and electrophysiology of e-vector coding by neurons in the central complex. *Journal of neurophysiology* **99**: 667–682.

Sakura M, Okada R & Aonuma H. (**2012**). Evidence for instantaneous e-vector detection in the honeybee using an associative learning paradigm. *Proceedings of the Royal Society B* **279**: 535–542.

Salmon M & Hyatt GW. (**1979**). The development of acoustic display in the fiddler crab *Uca pugilator*, and its hybrids with *U. panacea*. *Marine behaviour and physiology* **6**: 197–209.

Santer RD, Simmons PJ & Rind FC. (**2005**). Gliding behaviour elicited by lateral looming stimuli in flying locusts. *Journal of Comparative Physiology A* **191**: 61–73.

Santschi F. (**1923**). L'orientation sidérale des fourmis, et quelques considérations sur leurs différentes possibilités d'orientation. *Mémoires de la Société vaudoise des sciences naturelles* **4**: 137–175.

Schlacher TA, Jager R De & Nielsen T. (**2011**). Vegetation and ghost crabs in coastal dunes as indicators of putative stressors from tourism. *Ecological Indicators* **11**: 284–294.

Schneider L & Langer H. (**1969**). Die struktur des rhabdoms im 'doppelauge' des wasserläufers *Gerris lacustris*. *Zeitschrift für Zellforschung und Mikroskopische Anatomie* **99**: 538–559.

Schofield AJ. (**2000**). What does second-order vision see in an image? *Perception* **29**: 1071–1086.

Schofield AJ & Georgeson MA. (**1999**). Sensitivity to modulations of luminance and contrast in visual white noise: Separate mechanisms with similar behaviour. *Vision Research* **39**: 2697–2716.

Schöne H & Schöne H. (**1961**). Eyestalk movements induced by polarized light in the ghost crab, *Ocypode quadrata*. *Science* **134**: 675–676.

Schwind R. (**1984**). Evidence for true polarization vision based on a two-channel analyzer system in the eye of the water bug, *Notonecta glauca*. *Journal of Comparative Physiology A* **154**: 53–57.

Schwind R. (**1999**). *Daphnia pulex* swims towards the most strongly polarized light - a response that leads to 'shore flight'. *Journal of Experimental Biology* **202**: 3631–3635.

Scott-Samuel NE & Georgeson MA. (**1999**). Does early non-linearity account for second-order motion? *Vision research* **39**: 2853–2865.

Shabayek AER, Morel O & Fofi D. (**2014**). Bio-inspired polarization vision techniques for robotics applications. In: Habib MK, ed. *Handbook of research on advancements in robotics and mechatronics*. Hershey PA, USA: IGI Global, 81–117.

Shapley R. (**1990**). Visual sensitivity and parallel retinocortical channels. *Annual Review of Psychology* **41**: 635–658.

Sharkey CR, Partridge JC & Roberts NW. (**2015**). Polarization sensitivity as a visual contrast enhancer in the Emperor dragonfly larva, *Anax imperator*. *Journal of Experimental Biology* **218**: 3399–3405.

Shashar N, Rutledge P & Cronin TW. (**1996**). Polarization vision in cuttlefish - a concealed communication channel? *Journal of Experimental Biology* **199**: 2077–2084.

Shashar N, Hanlon RT & Petz A deM. (**1998**). Polarization vision helps detect transparent prey. *Nature* **393**: 222–223.

Shashar N, Hagan R, Boal JG & Hanlon RT. (**2000**). Cuttlefish use polarization sensitivity in predation on silvery fish. *Vision Research* **40**: 71–75.

Shashar N, Sabbah S & Cronin TW. (**2004**). Transmission of linearly polarized light in seawater: implications for polarization signaling. *Journal of Experimental Biology* **207**: 3619–

3628.

Shashar N, Johnsen S, Lerner A, Sabbah S, Chiao CC, Mathger LM & Hanlon RT. (**2011**). Underwater linear polarization: physical limitations to biological functions. *Philosophical Transactions of the Royal Society B* **366**: 649–654.

Shashar N & Cronin TW. (**1996**). Polarization contrast vision in *Octopus*. *Journal of Experimental Biology* **199**: 999–1004.

Shashar N & Hanlon RT. (**1997**). Squids (*Loligo pealei* and *Euprymna scolopes*) can exhibit polarized light patterns produced by their skin. *Biological Bulletin* **193**: 207–208.

Shih HT, Ng PKL, Davie PJF, Schubart CD, Türkay M, Naderloo R, Jones D & Liu MY. (**2016**). Systematics of the family Ocypodidae Rafinesque , 1815 (Crustacea: Brachyura), based on phylogenetic relationships, with a reorganization of subfamily rankings and a review of the taxonomic status of *Uca* Leach, 1814, sensu lato and its subgenera. *Raffles Bulletin of Zoology* **64**: 139–175.

Smith AT, Greenlee MW, Singh KD, Kraemer FM & Hennig J. (**1998**). The processing of first- and second-order motion in human visual cortex assessed by functional magnetic resonance imaging (fMRI). *The Journal of Neuroscience* **18**: 3816–3830.

Smith AT & Ledgeway T. (**1997**). Separate detection of moving luminance and contrast modulations: fact or artifact? *Vision Research* **37**: 45–62.

Smith AT & Scott-Samuel NE. (**2001**). First-order and second-order signals combine to improve perceptual accuracy. *Optical Society of America* **18**: 2267–2272.

Smithers SP, Roberts NW & How MJ. (**2019**). Parallel processing of polarization and intensity information in fiddler crab vision. *Science Advances* **5**: eaax3572

Smolka J, Zeil J & Hemmi JM. (**2011**). Natural visual cues eliciting predator avoidance in fiddler crabs. *Proceedings of the Royal Society B* **278**: 3584–3592.

Smolka J, Raderschall C & Hemmi JM. (**2013**). Flicker is part of a multi-cue response

criterion in fiddler crab predator avoidance. *Journal of Experimental Biology* **216**: 1219–24.

Smolka J & Hemmi JM. (**2009**). Topography of vision and behaviour. *Journal of Experimental Biology* **212**: 3522–3532.

Somanathan H, Maria R & Warrant EJ. (**2008**). Nocturnal bees learn landmark colours in starlight. *Current Biology* **18**: R996–R997.

Stavenga DG, Smits RP & Hoenderst BJ. (**1993**). Simple exponential functions describing the absorbance bands of visual pigment spectra. *Vision Research* **33**: 1011–1017.

Stewart FJ, Kinoshita M & Arikawa K. (**2019**). Monopolatic motion vision in the butterfly *Papilio xuthus*. *Journal of Experimental Biology* **22**: jeb191957.

Stöckl AL, O'Carroll DC & Warrant EJ. (**2016**). Neural summation in the hawkmoth visual system extends the limits of vision in dim light. *Current Biology* **26**: 821–826.

Stowe S. (**1977**). The retina-lamina projection in the crab *Leptograpsus variegatus*. *Cell and Tissue Research* **185**: 515–525.

Stowe S. (**1981**). Effects of illumination changes on rhabdom synthesis in a crab. *Journal of Comparative Physiology A* **142**: 19–25.

Strausfeld NJ & Nässel DR. (**1981**). Neuroarchitecture serving compound eyes of crustacea and insects. In: Autrum H, ed. *Handbook of sensory physiology. Vol. VII/6B. Vision in invertebrates.* Berlin, Heidelberg, New York: Springer-Verlag, 1–132.

Strutt JW. (**1871**). On the light from the sky, its polarization and colour. *The London, Edinburgh, and Dublin Philosophical Magazine and Journal of Science* **41**: 107–120.

Suhai B & Horváth G. (**2004**). How well does the Rayleigh model describe the E-vector distribution of skylight in clear and cloudy conditions ? A full-sky polarimetric study. *Journal of the Optical Society of America A* **21**: 1669–1676.

Sweeney A, Jiggins C & Johnsen S. (**2003**). Polarized light as a butterfly mating signal. *Nature* **423**: 31–32.

Sztarker J, Strausfeld N, Andrew D & Tomsic D. (**2009**). Neural organization of first optic neuropils in the littoral crab *Hemigrapsus oregonensis* and the semiterrestrial species *Chasmagnathus granulatus*. *Journal of Comparative Neurology* **513**: 129–150.

Talbot CM & Marshall JN. (**2011**). The retinal topography of three species of coleoid cephalopod: significance for perception of polarized light. *Philosophical Transactions of the Royal Society B* **366**: 724–733.

Temizer I, Donovan JC, Baier H & Semmelhack JL. (**2015**). A visual pathway for looming-evoked escape in larval zebrafish. *Current Biology* **25**: 1823–1834.

Temple SE, Pignatelli V, Cook T, How MJ, Chiou TH, Roberts NW & Marshall NJ. (**2012**). High-resolution polarisation vision in a cuttlefish. *Current Biology* **22**: R121–R122.

Temple SE, McGregor JE, Miles C, Graham L, Miller J, Buck J, Scott-Samuel NE & Roberts NW. (**2015**). Perceiving polarization with the naked eye: characterization of human polarization sensitivity. *Proceedings of the Royal Society B* **282**: 20150338.

Temple SE, Roberts NW & Misson GP. (**2019**). Haidinger's brushes elicited at varying degrees of polarization rapidly and easily assesses total macular pigmentation. *Journal of the Optical Society of America A* **36**: 123–131.

Templin RM, How MJ, Roberts NW, Chiou TH & Marshall J. (**2017**). Circularly polarized light detection in stomatopod crustaceans: a comparison of photoreceptors and possible function in six species. *Journal of Experimental Biology* **220**: 3222–3230.

Theobald JC, Greiner B, Wcislo WT & Warrant EJ. (**2006**). Visual summation in night-flying sweat bees: a theoretical study. *Vision Research* **46**: 2298–2309.

Theobald JC, Duistermars BJ, Ringach DL & Frye MA. (**2008**). Flies see second-order motion. *Current Biology* **18**: 464–465.

Theobald JC, Shoemaker PA, Ringach DL & Frye MA. (**2010**). Theta motion processing in fruit flies. *Frontiers in Behavioral Neuroscience* **4**.

Tibbs AB, Daly IM, Bull DR & Roberts NW. (**2018**). Noise creates polarization artefacts. *Bioinspiration and Biomimetics* **13**: 015005.

Toh Y. (**1987**). Diurnal changes of rhabdom structures in the compound eye of the grapsid crab, *Hemigrapsus penicillatus*. *Journal of Electron Microscopy* **36**: 213–223.

Toh Y & Waterman TH. (**1982**). Diurnal changes in compound eye fine structure in the blue crab *Callinectes*. *Journal of Ultrastructure Research* **78**: 40–59.

Tomsic D. (**2016**). Visual motion processing subserving behavior in crabs. *Current Opinion in Neurobiology* **41**: 113–121.

Tomsic D, Sztarker J, Berón de Astrada M, Oliva D & Lanza E. (**2017**). The predator and prey behaviors of crabs: from ecology to neural adaptations. *Journal of Experimental Biology* **220**: 2318–2327.

Treutwein B. (**1995**). Adaptive psychophysical procedures. *Vision Research* **35**: 2503–2522.

Tuthill JC & Johnsen S. (**2006**). Polarization sensitivity in the red swamp crayfish *Procambarus clarkii* enhances the detection of moving transparent objects. *Journal of Experimental Biology* **209**: 1612–6.

VideoLan-Organization. VLC media player.

Wang X, Gao J, Fan Z & Roberts NW. (**2016**). An analytical model for the celestial distribution of polarized light, accounting for polarization singularities, wavelength and atmospheric turbidity. *Journal of Optics* **18**: 065601.

Wang X, Gao J & Roberts NW. (**2019**). Bio-inspired orientation using the polarization pattern in the sky based on artificial neural networks. *Optic Express* **27**: 13681–13693.

Warrant EJ. (**2017**). The remarkable visual capacities of nocturnal insects: vision at the limits with small eyes and tiny brains. *Philosophical transactions of the Royal Society B* **372**: 20160063.

Warrant E & Dacke M. (**2011**). Vision and visual navigation in nocturnal insects. *Annual*

Review of Entomology **56**: 239–254.

Warrant E & Dacke M. (**2016**). Visual navigation in nocturnal insects. *Physiology* **31**: 182–192.

Warrant EJ & Johnsen S. (**2013**). Vision and the light environment. *Current Biology* **23**: R990–R994.

Warren TL, Giraldo YM & Dickinson MH. (**2019**). Celestial navigation in *Drosophila*. *Journal of Experimental Biology* **222**: jeb186148.

Waterman TH. (**1954**). Polarization patterns in submarine illumination. *Science* **120**: 927–932.

Waterman TH. (**1955**). Polarization of scattered sunlight in deep water. *Deep Sea Research* **3**: 426–434.

Waterman TH, Fernández HR & Goldsmith TH. (**1969**). Dichroism of photosensitive pigment in rhabdoms of the crayfish *Orconectes*. *The Journal of general physiology* **54**: 415–32.

Waterman TH. (**1981**). Polarization sensitivity. In: Autrum A, ed. *Handbook of sensory physiology, volume VII/6b*. Berlin: Springer-Verlag, 281–469.

Waterman TH. (**2006**). Reviving a neglected celestial underwater polarization compass for aquatic animals. *Biological Reviews of the Cambridge Philosophical Society* **81**: 111–115.

De Weerd P, Vandenbussche E & Orban GA. (**1990**). Staircase procedure and constant stimuli method in cat psychophysics. *Behavioural Brain Research* **40**: 201–214.

Wehner R. (**1987**). ‘Matched filters’ - neural models of the external world. *Journal of Comparative Physiology A* **161**: 511–531.

Wehner R. (**1989**). The hymenopteran skylight compass: matched filtering and parallel coding. *Journal of Experimental Biology* **85**: 63–85.

Wehner R. (**2001**). Polarization vision - a uniform sensory capacity? *Journal of Experimental*

Biology **204**: 2589–2596.

Wehner R. (**2003**). Desert ant navigation: how miniature brains solve complex tasks. *Journal of Comparative Physiology A* **189**: 579–588.

Wehner R & Müller M. (**2006**). The significance of direct sunlight and polarized skylight in the ant's celestial system of navigation. *Proceedings of the National Academy of Sciences* **103**: 12575–12579.

Wildermuth H. (**1998**). Dragonflies recognize the water of rendezvous and oviposition sites by horizontally polarized light: A behavioural field test. *Naturwissenschaften* **85**: 297–302.

Wolcott TG. (**1978**). Ecological role of ghost crabs, *Ocypode quadrata* (Fabricius) on an ocean beach: scavengers or predators? *Journal of Experimental Marine Biology and Ecology* **31**: 67–82.

Wolff LB. (**1997**). Polarization vision: a new sensory approach to image understanding. *Image and Vision Computing* **15**: 81–93.

Wolfrath B. (**1993**). Observations on the behaviour of the European fiddler crab *Uca tangeri*. *Marine Ecology Progress Series* **100**: 111–118.

Wong BBM, Bibeau C, Bishop KA & Rosenthal GG. (**2005**). Response to perceived predation threat in fiddler crabs: trust thy neighbor as thyself? *Behavioral Ecology and Sociobiology* **58**: 345–350.

Yilmaz M & Meister M. (**2013**). Rapid innate defensive responses of mice to looming visual stimuli. *Current Biology* **23**: 2011–2015.

Zanker JM. (**1996**). Looking at the output of two-dimensional motion detector arrays. *Investigative Ophthalmology & Visual Science* **37**: S743.

Zeil J, Nalbach G & Nalbach HO. (**1986**). Eyes, eye stalks and the visual world of semi-terrestrial crabs. *Journal of Comparative Physiology A* **159**: 801–811.

Zeil J & Al-Mutairi M. (**1996**). The variation of resolution and of ommatidial dimensions in

the compound eyes of the fiddler crab *Uca lactea annulipes* (Ocypodidae, Brachyura, Decapoda). *Journal of Experimental Biology* **199**: 1569–1577.

Zeil J & Hemmi JM. (**2006**). The visual ecology of fiddler crabs. *Journal of Comparative Physiology A* **192**: 1–25.

Zeil J & Hofmann M. (**2001**). Signals from 'crabworld': cuticular reflections in a fiddler crab colony. *Journal of Experimental Biology* **204**: 2561–2569.

Zhou YX & Baker CL. (**1990**). A processing stream in mammalian visual cortex neurons for non-fourier responses. *Science* **261**: 98–101.

Zwarts L. (**1985**). The winter exploitation of fiddler crabs *Uca tangeri* by waders in Guinea-Bissau. *Ardea* **73**: 3–12.